Proceedings of the 4th International Conference on Civil Engineering for Sustainable Development (ICCESD2017), 9~11 February 2017, KUET, Khulna, Bangladesh (ISBN-978-984-34-3502-6)

ASSESSMENT OF MORPHODYNAMIC CHARACTERISTICS OF DUDHKUMAR RIVER USING MULTI-TEMPORAL SATELLITE IMAGES

Probir Kumar Pal[1], Afeefa Rahman[2], Anika Yunus[3]

[1]Graduate Student, Department of Water Resources Engineering (WRE), Bangladesh university of Engineering and Technology (BUET), Bangladesh
[2]Lecturer, Department of Water Resources Engineering (WRE), Bangladesh university of Engineering and Technology (BUET), Bangladesh, email: afeefa@wre.buet.ac.bd
[3]Associate Professor, Department of Water Resources Engineering (WRE), Bangladesh university of Engineering and Technology (BUET), Bangladesh

ABSTRACT

Dudhkumar River flows from upstream of India Border at Bhurungamari to the confluence with Brahmaputra River at Noonkhawa of Kurigram Sadar having a stretch of 64 km. Due to onrush of water from upstream in monsoon, erosion by the Dudhkumar River takes a serious turn, threatening collapse of Sonahat Bridge in Bhurungamari, embankment on its right bank, dykes and several dwelling houses in recent years establishing the river as a destructive one. Thus study aiming at computing the long and short term bankline shifting along the river is of great significance. To attain the objectives, images of Landsat MSS and TM acquired from the year 1973 to 2015 have been used to investigate the riverbank migration pattern, accretion-erosion and change in width of Dudhkumar River. For short term analysis, migration rates are calculated from one Landsat image to the next. For long term analysis, the migration rates are calculated based on the difference between the 1973 image as the reference and subsequent images. From the short-term analysis, the mean erosion and accretion rate estimated as 128 m/y and 194 m/y on the left bank, and 141 and 176 m/y on the right bank indicating the accretion rate as greater than the erosion rate. Erosion rate has been found as greater in right bank rather than left bank and accretion rate is much more in left bank than the right bank. Due to high discharge, maximum erosion and accretion have been found as 349 m/y and 410 m/y respectively at left bank in 2013-2015 indicating the bank protection measures as vulnerable. Results also reveal that the erosion-accretion rate is higher in short-term analysis. The analysis divulged that the Dudhkumar River is a highly meandering river with several critical sections where the river has been suffering enormously with erosion problem and shifting. The present study also identifies steadfast evidence on the dynamic fluvio-geomorphology of Dudhkumar River depicting urge for execution of erosion control schemes.

Keywords: *Dudhkumar River, Bankline shifting, Erosion-accretion, Morpho-dynamics, LANDSAT*

1. INTRODUCTION

The country Bangladesh is occupied with a network of about 405 rivers mostly alluvial in nature, spreading all over the country out of which 57 are transboundary (BWDB, 2011). Riverbank erosion is one of the most unpredictable and critical disaster that takes into account the quantity of rainfall, soil structure, river morphology, topography of river and adjacent areas and effect of floods. Alluvial river possesses problems of sediment erosion-deposition attached with it letting Dudhkumar as no exception and leading the problems of flood, erosion and drainage congestion in the Brahmaputra basin as momentous (Sarkar et.al, 2011). Riverbank erosion has important implications for short and long term channel adjustment, development of meanders, sediment dynamics of the river catchment, riparian land loss and downstream sedimentation problems (Lawler et al., 1997). Being alluvial in nature, floodplains of Bangladeshi rivers are predominantly formed of flood-borne sediments while their bank materials consist mostly of fine-grained cohesive sediments (Azuma et al., 2007). In such alluvial rivers, through continuous erosion accretion processes, the channels frequently change its meandering pattern from reach to reach (Kammu et al., 2008). On the

other hand development works such as, bank protection measures like embankment; dam and bridge may also cause local morphological changes of river affecting the ultimate sediment balance of the river. Thus fluvial channel form and its dynamics over the period of time have been a major interest of study in fluvial geomorphology. (Nabi et. al.,2016). Therefore, a better understanding on morphological changes of alluvial rivers, particularly bank shifting, channel migration due to erosion and accretion processes as well as techniques to detect resultant pattern would be useful for effective planning and management of the alluvial environments.

Temporal satellite remote sensing data of a river having unstable banks can be analyzed in GIS for identification of river bank erosion as well as patches of embankment vulnerable to breaching, upholding the remote sensing approach in study of river morphology. Baki et al. (2012) studied on river bank migration and island dynamics of braided Jamuna River using LANDSAT images. Khan et al. (2014) studied on river bank erosion of Jamuna River by using GIS and Remote Sensing Technology. Hossain et al. (2012) assessed morphological changes of Ganges River. Afrose (2012) analyzed morphological changes of Teesta River. Takagi et al. (2007) analyzed the spatial and temporal changes in the channels of Brahmaputra. Sarker and Thorne (2006) examined the morphological response of major river systems of Bangladesh due to the Assam earthquake. No systematic study and research has been done for defining the morphological characteristics of Dudhkumar River, but this river discharge influence the extreme north western region of Bangladesh significantly. Being an important water course for the northern region of Bangladesh, some recent studies have been conducted on the Dudhkumar River. Hossain (2010) conducted an investigation to determine the In-stream Flow Requirement (IFR) of the Dudhkumar River. In this study the author applied three methods of the hydrological approach and according to demand-availability scenario the author has considered IFR calculated by mean annual flow method. Asad et al. (2013) by using Gumbel's and Powell's method analyzed a flood frequency model. Zaman (2017) studied on morphological changes of the Dudhkumar River due to the proposed road bridge at Paikerchara union of Bhurungamari upazila under Kurigram district using HEC-RAS. Due to river bank erosion a large number of people losses their homes, agricultural lands, resources and become homeless resulting in extreme poverty in the country but there is still lack of sufficient erosion management plan. In this study, understanding the predicament of river Dudhkumar in particular, efforts have been ensued to study the bank line shifting and the rate of erosion-accretion of the river Dudhkumar which may contribute to the development projects and bolstering existing bank protection measures.

1.1 Study Area

A map of the study area focusing the catchment of Dudhkumar river is shown in Figure 1. Dudhkumar River is located in the north-east corner of the North-West region of Bangladesh originating in the Himalayan foot hills in Bhutan and flowing through south-easterly direction from the foot hills through India to its outfall into the Brahmaputra River in Bangladesh (BWDB, 2010). The river enters in Bangladesh near Shilkhuri of Bhurungamari Upazila in Kurigram district (Haque, 2008). The river possesses a length of 220 km having the catchment as around 5,800 km^2 out of which about 240 km^2 is within Bangladesh. About 96% of the catchment area of Dudhkumar lies outside Bangladesh (JICA, 1990; Pakistan Techno Consult, 1969). In Bangladesh the river travels a distance of about 51 km having average slope of 10 cm/km in the south to south-easterly direction to meet with the Brahmaputra River at Noonkhawa. Within Bangladesh, there are several small rivers that drain into the Dudhkumar River, notably Satkura dara, Phulkumar river, Girai khal, Dikdari dara and Santashi khal.

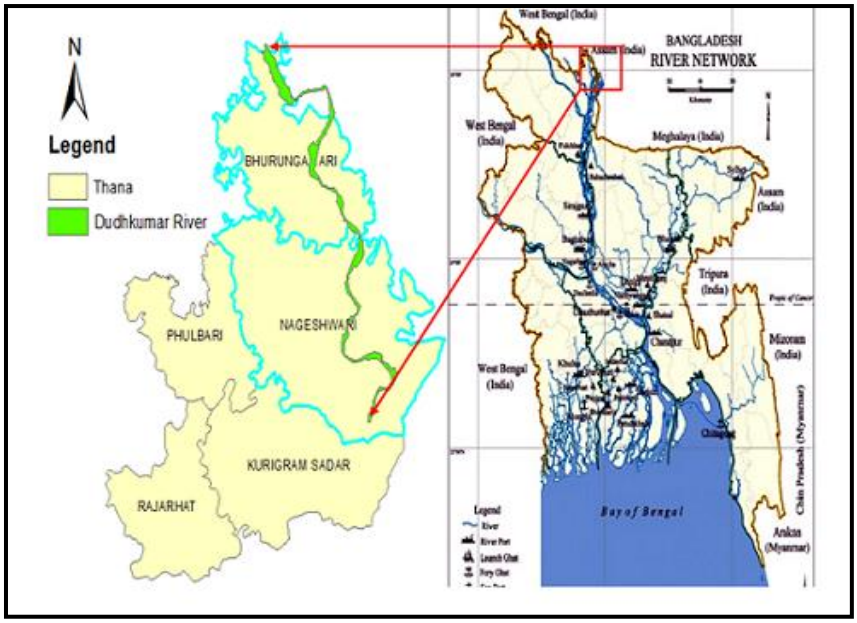

Figure1: Map of the study area showing Dudhkumar river

Dudhkumar is a semi braided river and morphologically highly dynamic. Being a semi braided river, it is associated with the development of loops. Sometimes channels move quite fast and consequent abandonment of meander loop through cut off. Such natural cut off can occur frequently within 1-2 years (HCL et. al. 2009). The sediment size, d_{50}, at Pateswari and Tangonmari have been found as 0.21 mm and 0.16 mm respectively (HCL et al. 2009). The. Average cross sectional area of the river is about 1506 m^2 (BWDB, 2010).Average width of the river at high and low water level is about 284.24m and 225.34m respectively (BWDB, 2010). This high slope makes Dudhkumar a flashy type during monsoon when onrush of surface runoff cause flooding to the flood plain of the river causing bank erosion and destruction of houses and settlement of the people living on the river banks. For the present study, full reach of Dudhkumar having length of 64 km has been considered.

1.2 Data Collection

Landsat satellite images are collected from USGS earth explorer website covering the whole of Dudhkumar River in Bangladesh from 1973 to 2015 for this study and processed thereby as discussed in methodology segment. Hydrological data including discharge and water level of Dudhkumar River at the Pateswari gauging station was collected from Bangladesh Water Development Board (BWDB).Table 1 shows the list of satellite image data with their band numbers and acquisition dates.

Table-1: Satellite images used for this study

Satellite Data	Acquisition Date	Brand Number
Landsat-MSS (80 m x 80 m)	21 February 1973	2, 3, 4
	8 December 1987	3, 4, 5
	19 January 1989	3, 4, 5
	06 March 1991	3, 4, 5
	08 December 1993	3, 4, 5
	28 January 1995	1, 3, 4
	01 November 1997	2, 4, 5
Landsat-TM (30 m x 30 m)	23 December 1999	1, 3, 4
	20 December 2001	3, 4, 5
	18 January 2003	1, 4, 5

07 December 2005	1, 2, 3
18 February 2007	1, 2, 3
04 December 2009	1, 2, 3
08 December 2011	1, 2, 3
21 December 2013	5, 6, 7
11 November 2015	1, 2, 3

2. METHODOLOGY

To conduct the analyses, Landsat satellite images are collected from USGS earth explorer website covering the whole of Dudhkumar River in Bangladesh from the year 1973 to 2015. All the images were collected during the dry season (January to March) except the year 1997 image which was acquired in early November as during dry season, vegetation cover and other ground conditions, particularly the water level, are relatively consistent from year to year which is essential for assessing the inter-year change of erosion and accretion of the River. In addition, during dry season the chances of getting a relatively cloud free atmosphere is a bit higher and the planform generally shows the boundary and pattern of channels within the braid belt clearly. Based on available flow data, time from November to May have been considered as the low flow month and June to October as the high flow month. Initially, each image was projected onto a plane, rotated, rescaled, and geo-referenced using a 1997 Landsat image mosaic of Bangladesh which itself was geo-referenced using SPOT photo maps of 1:5000 scale and produced from multi-spectral SPOT images. The geo-referencing of a satellite image consists of identifying ground control points (GCPs) on the image that correspond to GCPs on the 1997 image mosaic. Each raw satellite image was re-sampled using the nearest neighbor algorithm, and transformed into the WGS 1984 UTM zone 45N projection and coordinate system of the following specifications (ISPAN, 1992): (1) Ellipsoid = Everest 1830, (2) Projection = Transverse Mercator, (3) Central meridian = 900E, (4) False easting = 500,000 m, and (5) False northing = 2,000,000 m. After geometric correction, each satellite image was classified to different land use types using an un-supervised, statistical classification technique, an artificial neural network, that group pixels into distinguishable classes. Three broad land cover classes are identified: water, sand and land (including cultivated/vegetated land). Lastly, from each digitally classified image a map is produced showing river channels, sandbars and a land use class that includes all cultivated and vegetated areas (EGIS, 2002) using the available images during the dry season of 1973, 1987, 1989, 1991, 1993, 1995, 1997, 1999, 2001, 2003, 2005, 2007, 2009, 2011, 2013 & 2015. To quantify changes in river bank locations that have occurred between any two images using Arc View, a total of 80 cross-sections at 0.5 km intervals along the 51 km long study reach of the Dudhkumar River were drawn and coordinates of all intersection points between the banklines and cross-section lines determined Figure 2.

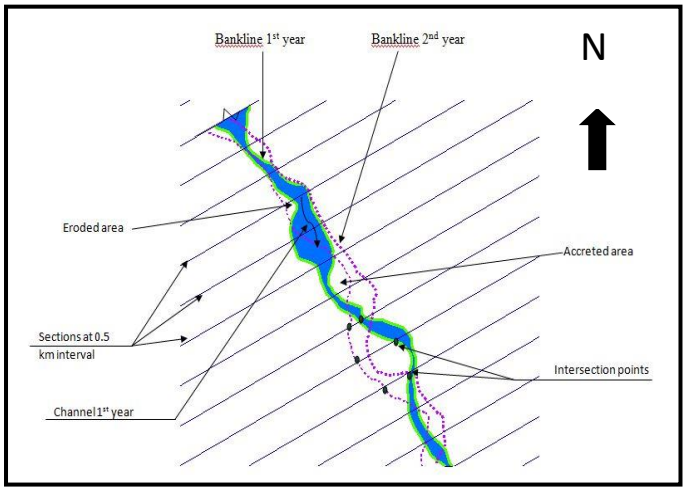

Figure 2: A schematic diagram showing how shifting of the riverbanks from 1987 to 1989 was computed. Sections are taken at 0.5 km intervals along the 51 km valley length of the Dudhkumar River.

Usually, the sections used to measure the banklines shifting are set to be at 90˚ to the axis of the channel (Baki and Gan, 2012). However, for a channel undergoing meandering and erosion, the channel tends to change its flow direction frequently year after year, and so it will be difficult to use sections at 90˚ to the axis of the channel to predict the bank line shifting (Baki and Gan, 2012). In other words, for the Dudhkumar River subjected to frequent and significant erosion/accretion, if we were to set the cross-sections at 90˚ to the axis of the channel, the locations of the cross-sections would shift from year to year. To avoid such a problem, we set the river cross-sections at 90˚ to the valley direction. By so doing, based on changes to the cross-sections detected from the satellite images, we would be able to consistently track temporal changes to left and the right banklines.

3. ANALYSES AND RESULTS

3.1 Analysis on Flow of Dudhkumar River

The discharge and water level data of Dudhkumar River at the Pateswari gauging station was collected from Bangladesh Water Development Board (BWDB). The water level in the river was very low in late February, March and April; very high in June to October where water level varies from 20.00 mPWD to 33.42 mPWD (IWM, 2009).Hydrology of the catchment area of Dudhkumar river is mainly governed by rainfall runoff and cross boundary flows through the river. The mean annual rainfall gradually decreases from 3000 mm in the north to 1800 mm in the south, with an average annual rainfall of 2700 mm (DPM et al., 2005). From available record and data it is found that flows in the Dudhkumar river at Pateswari during the dry season (November to May) comes down to an average of 159 m^3/s and during the monsoon season (June to October) the average flow is about 897 m^3/s. Based on the data available from BWDB, the maximum and minimum discharge is found to be 9250 m^3/s and 52.30 m^3/s that occurred on 6th October, 1968 and 18thApril, 1992 respectively.Flow and stage discharge hydrographs of Dudhkumar river at Pateswari for the period of 1968 to 2007 have been shown in Figure 3.

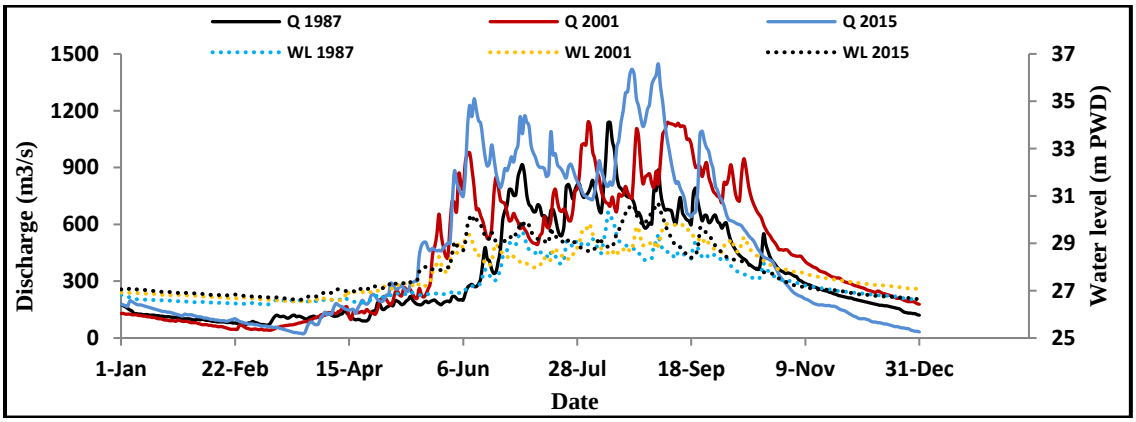

Figure 3: Variation in flow and water level at Pateswari of Dudhkumar River

3.2 Analysis on bank line shifting of study reach

To get an overall picture of the erosion and accretion patterns of Dudhkumar River over two time periods, 1973-1987 (14 years) and 1973-2015 (43 years), the maps of riverbank erosion and accretion are overlapped in ArcGIS. Next, the rates of bank movement as a function of distance along the river for both the left and the right banks for both time periods are plotted in Figure 4 (a) and (b) respectively. These figures show a considerable movement of the bank lines resulted from accretion indicating riverward movement of banks as well as erosion which depicts the landward movement of the banks for both the time periods. For the short term analysis between 1973 and 1987, bankline shifting rates varied from less than a m per year to several hundred meters per year, as is evident in high standard deviations shown in Table 2.For 1973 to 1987, maximum accretion and erosion rate in left bank were 260 m/y in Bhurungamari and 200 m/y in Pateswari sub-district respectively, while the corresponding rates for the right bank were 180 m/y and 200 m/y

respectively in Pateswari. On a whole, right bank of the Dudhkumar River has experienced more accretion rather than erosion highlighting the existence of bank protection measures. For the long term analysis between 1973 to 2015, bankline shifting rates varied below more or less hundred meter per year, as is evident in lower standard deviations. For the time range, maximum accretion and erosion rate in left bank were 100m/y and 40 m/y in downstream reach while the corresponding rates for the right bank were 45 m/y and 100 m/y respectively at downstream of Dudhkumar river.Figure 4(a) also shows that accretion occurred in large areas, especially at the upstream reach of the river at 7 km from the upstream point along the left bank where as considerable erosion at left bank occurred at 29km from upstream.In case of right bank both the maximum erosion and accretion occurred at 29 km from upstream. During the long term period raging from year 1973 to 2015, both the maximum accretion occurred at 28.5 km from upstream and erosion at 23 km from the upstream point in case of left bank. On the right bank, almost the full reach. Accretion appeared in small areas upto 28 km from the upstream on the right bank which could be because of the building of erosion control structures.

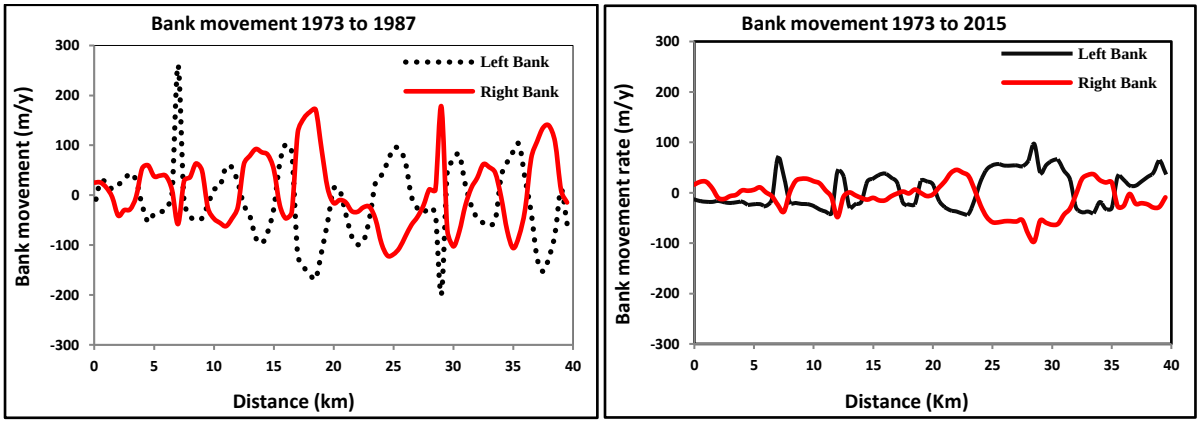

(a) (b)

Figure-4: Bank movement rate along the Dudhkumar River (length means distance from the northern most point of the river) for both the left and the right banks, between (a) 1973 and 1987, and (b) 1973 and 2015

3.3 Short-Term, Inter-Annual Changes to River Banks

The average bank erosion and accretion rates for the left and the right banks of the Dudhkumar River at inter-annual intervals (2 years) are listed in columns 1-4 of Table 1. Even though it will be ideal to have regular satellite images acquired on an annual basis but may not always be possible in practice. The mean short-term erosion rate on the left bank is 128 m/y and that on the right bank is 141 m/y (Table 2) and the mean short-term accretion rate on the left bank is 194 m/y and that on the right bank is 176 m/y.The maximum erosion rate recorded in the left bank of about 349 m/y occurred between 2013 and 2015, while in the right bank the maximum erosion rate of about 263 m/y occurred between 1999 and 2001. The range of erosion rate (maximum-minimum) in the left bank is 300 m/y while that of the right bank is 308 m/y (Table 2). The corresponding mean (range) of accretion rate on the left bank is 194 (357 m/y) and that on the right bank is 176 (250 m/y). Therefore, the left bank experienced a net accretion of about 66 m and higher range of accretion (357 m/y) than erosion rates (300 m/y), while the right bank experienced a net accretion of about 35 m, but range of erosion (308 m/y) is higher than accretion rates (250 m/y). In the left bank the maximum accretion rate of 410 m/y recorded occurred between 2013 and 2015, while in right bank the maximum accretion rate recorded was 318 m/y that occurred between 1993 and 1995. Figure 5a and b depict the short-term bank migration due to erosion-accretion in Dudhkumar River. For short-term changes, the correlation between bank erosion/accretion rates and annual discharges varies from about 0.15 to 0.57 as shown in Figure 6.

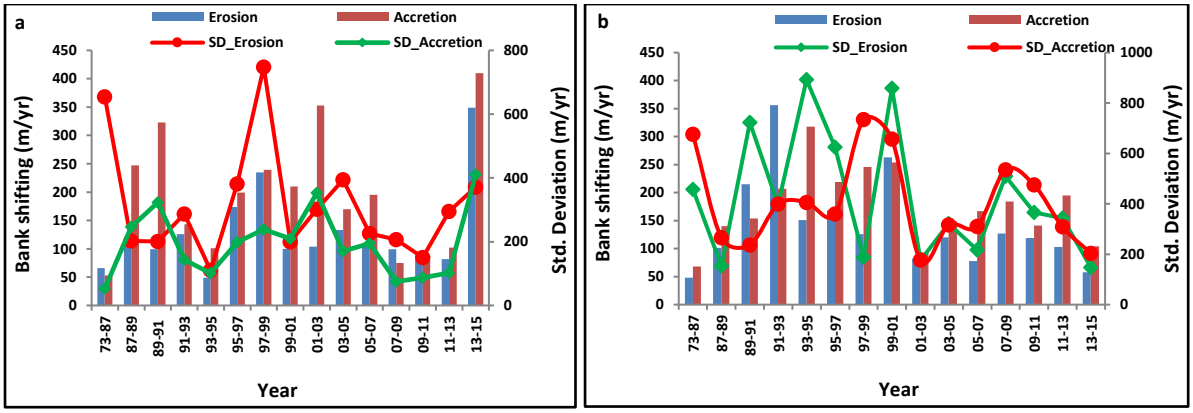

Figure 5: Short-term bank migration due to erosion-accretion in Dudhkumar River (a) left bank (b) right bank.

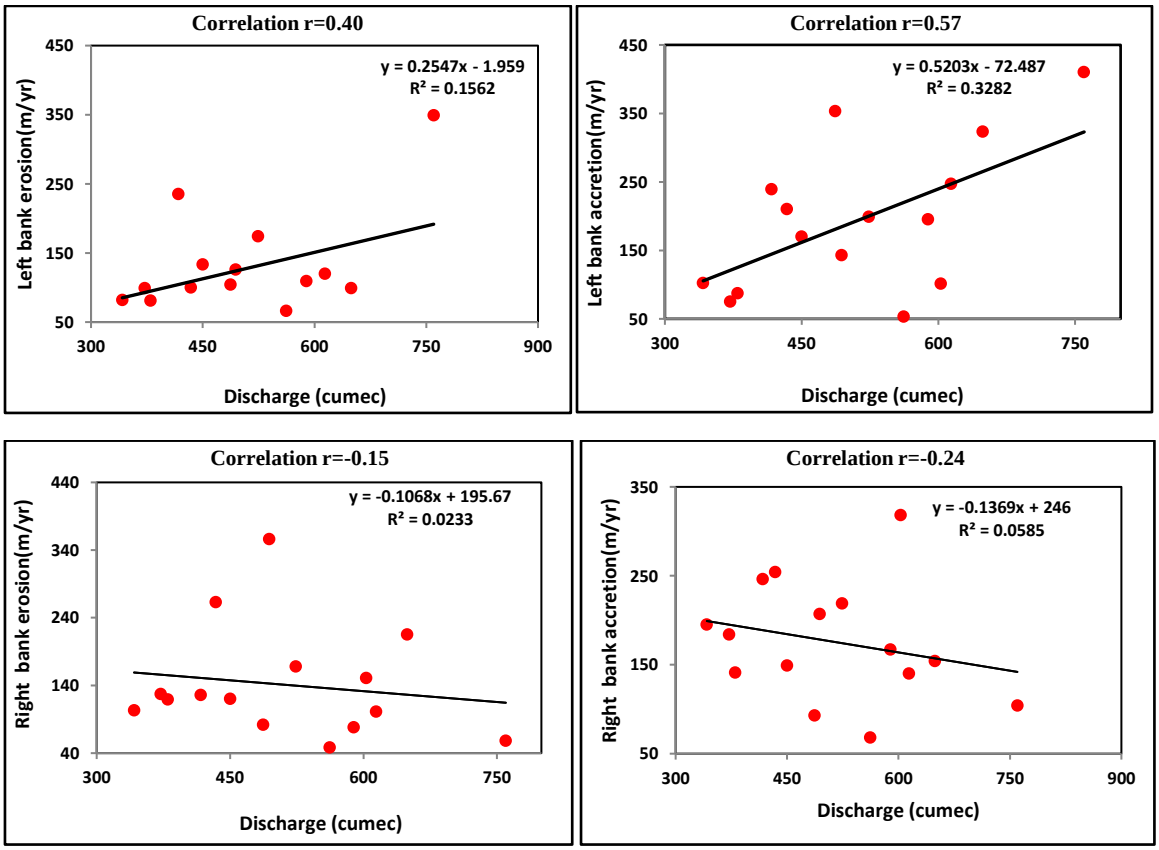

Figure-6: The short-term regression relationships between annual discharge and banks erosion/accretion rates (a) left bank erosion, (b) left bank accretion, (c) right bank erosion, (d) right bank accretion.

Table 2: The inter-annual short-term and long-term riverbank migration rates (erosion and accretion) of the left and right banks of Dudhkumar River

Year	Short-term riverbank migration				Year	Long-term riverbank migration			
	Left bank shifting average rate (m/y)		Right bank shifting average rate (m/y)			Left bank shifting average rate (m/y)		Right bank shifting average rate (m/y)	
Column	Erosion 1	Accretion 2	Erosion 3	Accretion 4		Erosion 5	Accretion 6	Erosion 7	Accretion 8
73-87	66	53	48	68	**73-87**	66	53	48	68
87-89	120	247	101	140	**73-91**	44	48	43	46
89-91	99	323	215	154	**73-95**	37	43	44	31
91-93	126	143	356	207	**73-99**	32	34	35	31
93-95	49	101	151	318	**73-03**	30	32	29	25
95-97	174	199	168	219	**73-07**	24	39	30	24
97-99	235	239	126	246	**73-11**	24	36	28	20
99-01	100	210	263	254	**73-15**	26	41	29	19
01-03	104	353	82	93					
03-05	133	170	120	149					
05-07	109	195	78	167					
07-09	99	75	127	184					
09-11	81	87	119	141					
11-13	82	102	103	195					
13-15	349	410	58	104					

3.4 Long-Term Changes to River Banks

The long-term bank erosion and accretion rates of Dudhkumar for its left and right banks are listed in columns 5-8 of Table 2. The mean (range) erosion rates of the left bank is 35 (42) m/y, while that of the right bank is 36 (20) m/y, respectively (Table 3). As expected, the long-term erosion rate is considerably less than that of the short-term erosion rate for both banks are 35 and 36 m/y shown in Table 3, Similarly, the mean long-term accretion rate for both banks over 43 years are 41 and 33 m/y, respectively, which are considerably less than the short-term accretion rate for left and right banks (194 and 176 m/y). For long-term changes, the correlation between bank erosion/accretion rates and annual discharges varied between 0.01 and 0.44 which are weaker than the corresponding correlations of short-term changes. From a long-term perspective, because of averaging the effects of erosion deposition, the overall bank line shifting rates tend to decrease as the time span considered increases, even though from year to year, annual rates of erosion and accretion can vary significantly partly because of the climatic and hydrologic variability of the Dudhkumar River.

Table 3: Summary statistics of inter-annual short-term and long-term riverbank migration rates (erosion and accretion) of the left and right banks of the Dudhkumar River

Short-term riverbank migration					Long-term riverbank migration			
	Left bank shifting average rate (m/y)		Right bank shifting average rate (m/y)		Left bank shifting average rate (m/y)		Right bank shifting average rate (m/y)	
Column	Erosion 1	Accretion 2	Erosion 3	Accretion 4	Erosion 5	Accretion 6	Erosion 7	Accretion 8
Mean	128	194	141	176	35	41	36	33
Standard Deviation	74	104	80	65	14	7	8	16
CV	0.58	0.54	0.57	0.37	0.40	0.17	0.22	0.48
Range	300	357	308	250	42	52	20	49
$r^{(i,j)a}$	$0.65^{1,2}$	$-0.16^{1,3}$	$0.52^{3,4}$	$-0.27^{2,4}$	$0.83^{5,6}$	$0.88^{5,7}$	$0.87^{7,8}$	$0.82^{6,8}$

$r^{(i,j)a}$ = Correlation between columns i and j.

3.5 Analysis on Total Area of Erosion and Accretion

Area of riverbank changes of the Dudhkumar due to erosion and accretion for 1973 to 2015 are presented in Table 4 and Figure 7, respectively. Figure 7 shows a high spatial variability of erosion and accretion on both sides of the riverbank. From Table 4, it can be seen that erosion rate (ha/y) gradually increased from 1973-2007 and then decreased during 2007-2015 on the left and right bank. It also seen that maximum erosion occur at left bank rather than right bank (2295 ha and 2213 ha). During 1987-1997 erosion rate maximum (229.5 ha/yr) at left bank and 1997-2007 erosion rate maximum (221.3 ha/yr) at right bank but maximum accreted area (rate) found 2440 ha (244 ha/yr) in 1997-2007 at left bank. So, left bank faced greater erosion-accretion rather than right bank.

Table 4: Erosion-accretion along the Dudhkumar River for four study periods

Duration	**Location**	**Erosion**		**Accretion**	
1973-1987 (14 years)		**Total (ha)**	**Rate (ha/yr)**	**Total (ha)**	**Rate (ha/yr)**
	Left Bank	2248	160.57	1146	81.86
	Right Bank	1395	99.64	1991	142.21
1987-1997 (10 years)	**Left Bank**	2295	229.50	1103	110.30
	Right Bank	2084	208.40	941	94.10
1997-2007 (10 years)	**Left Bank**	1408	140.80	2440	244
	Right Bank	2213	221.30	1442	144.20
2007-2015 (8 years)	**Left Bank**	816	102	752	94
	Right Bank	941	117.63	687	85.88

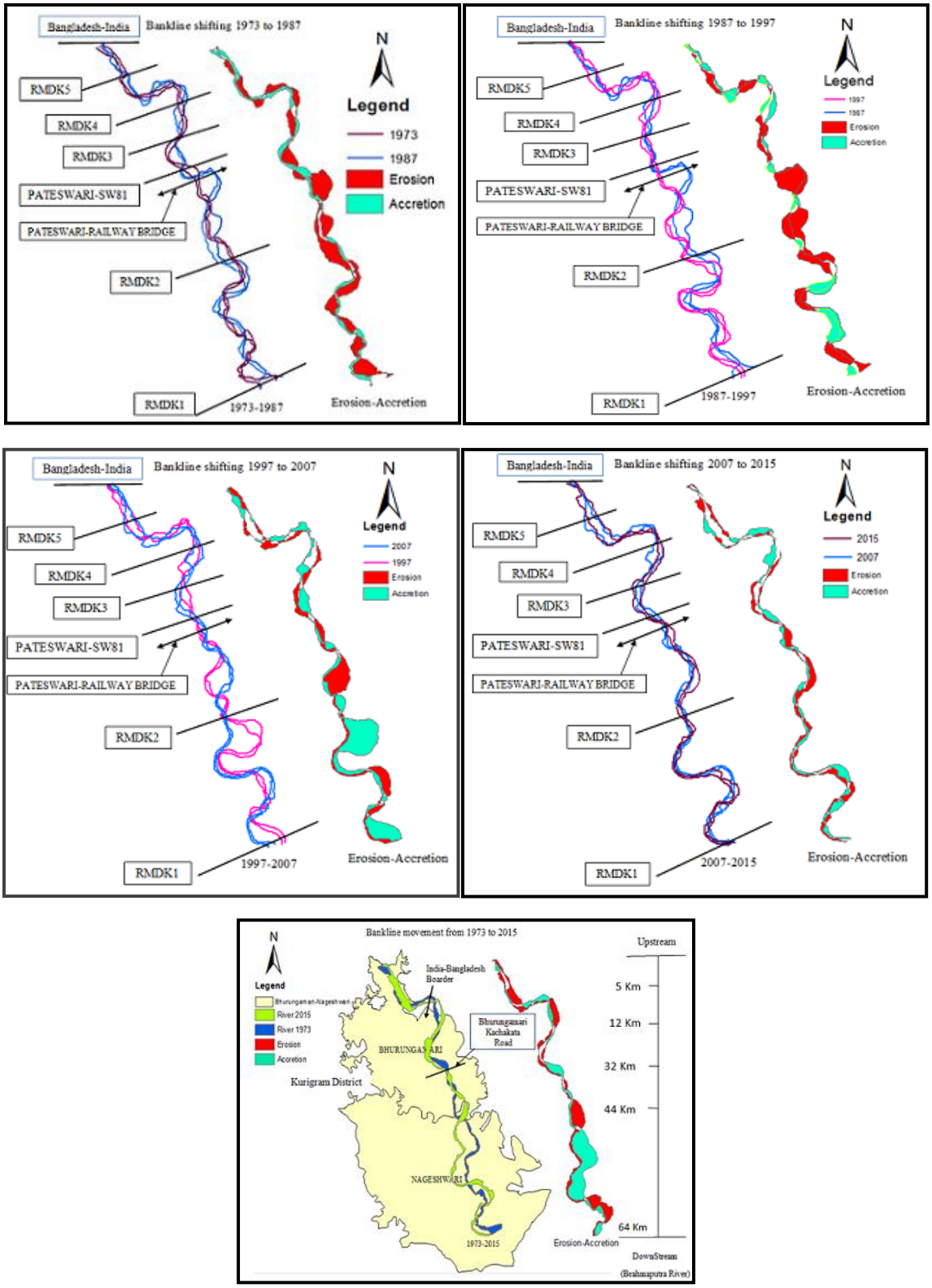

Figure 7: River bank shifting along the Dudhkumar River for different time ranges

3.6 Analysis on Riverbank Shifting Verses River Width

Over 43 years (1973-2015), the average width of the Dudhkumar River was about 595 m, and the minimum (maximum) width was 87(4520) m in 2001 (1991) as summarized in Table 5. The rate of change of the river width peaked in about 1993 which can be shown from the Figure 8(a). From the short-term analysis, the average ratio of erosion and accretion rates to

the river width is 0.22, 0.33 at the left bank and 0.24, 0.30 at the right bank, respectively. From the long-term analysis, the average ratio of erosion and accretion rates to the river width is 0.059, 0.065 at the left bank and 0.06, 0.055 at the right bank, respectively. Again because of the time averaging effect, the ratios for the long-term analysis are smaller than that of short-term analysis.

Table 5: Changes in the Dudhkumar River channel width for 1973-2015

Year	Maximum width (m)	Minimum width (m)	Average width (m)
1973	3005	117	458
1987	2738	91	532
1989	1374	115	377
1991	1968	87	332
1993	3918	500	883
1995	2129	100	477
1997	2266	108	517
1999	2579	164	674
2001	4520	104	752
2003	1807	118	509
2005	3620	110	586
2007	2155	88	478
2009	3517	139	621
2011	2990	90	688
2013	3401	143	737
2015	1792	116	727

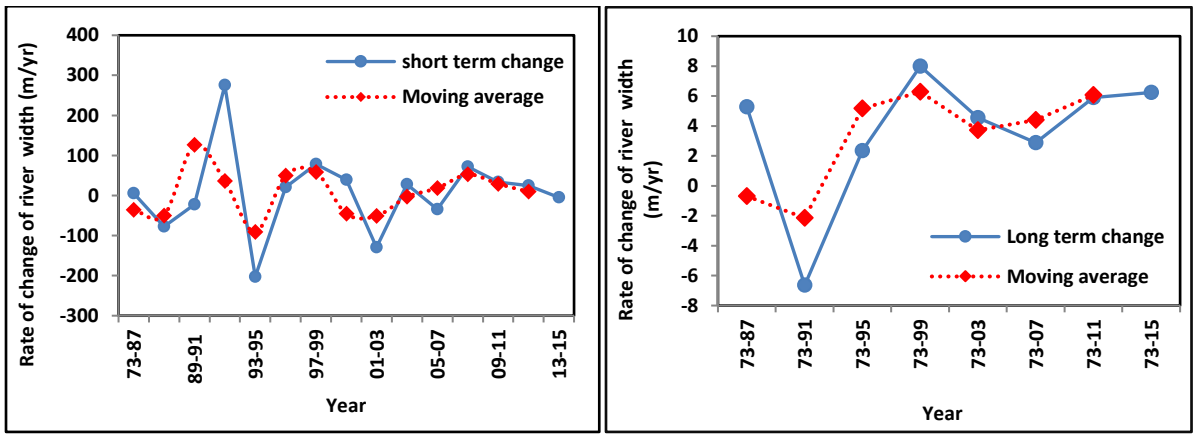

Figure 8: Change of width of Dudhkumar River (a) short term (b) Long term

3.7 Results Summary

The Dudhkumar is a meandering river with many oxbow bends. Over the years, under the combined impact of erosion, accretion, and human interventions, the Dudhkumar River within Bangladesh has experienced significant hydro-morphological changes. Through the analysis of fifteen satellite images of Landsat MSS and TM collected between 1973 and 2015, results on the short-term and the long-term riverbank migrations of Dudhkumar River in Bangladesh can be summarized as below:

- From the short-term analysis, the mean erosion and accretion rates estimated are 128 and 194 m/y on the left bank, and 141 and 176 m/y on the right bank. From the long-term analysis, the average erosion and accretion rates are 35 and 41 m/y on the left bank, 36 and 33 m/y on the right bank.The migration results of both banks indicate a very dynamic form of erosion and accretion processes leading to channel shifting in the Dudhkumar

River. The right bank experienced more erosion than the left bank; and the long term migration rate is smaller than the short-term counterpart for both banks probably because of human interventions such as construction of bank protection structures and the time averaging effect of erosion and accretion.

- The average erosion rate estimated from Landsat images over 43 years for the short and long-terms analysis of the Dudhkumar River are 135 m/y and 36 m/y, respectively, which are much higher than the bank erosion rate of 18 m/y estimated from the global erosion relationship of Van de Wiel (2003), probably because of its highly erodible bank materials. The long-term shifting of river banks due to erosion/accretion and the rate of change of channel width (widening/narrowing) may not necessarily follow the general morphological principle of river migration. For the short-term, only erosion rate for the right bank and accretion rate for the left bank follow this principle.

4. CONCLUSION

The present work on morphodynamic analyses of Dudhkumar river using remote sensing and GIS based approach with multi-date satellite data has revealed sharp changes in fluvial land form of the river in recent years resulting in considerable inhabited land loss.It is observed that in general the river has eroded both the banks throughout its course except at a few sites where banks are well defined as the river is constricted due to presence of dykes at some places of right bank. River adjustment processes that affected fluvial system of the river Dudhkumar include forcing functions like channel degradation and aggradations, lateral river migration, widening or narrowing, avulsion, changes in the quantity and character of the sediment load at spatial and temporal scale, intensely powerful monsoon regime, recurring earthquakes and adverse impact of anthropogenic factors. This study proves the utility and application of satellite remote sensing which allows a retrospective, synoptic viewing of large regions and so provides the opportunity for a spatially and temporally detailed assessment of changes in river channel erosion/deposition. This study has further demonstrated how the use of GIS has been expedient in organization of geo-spatial databases and facilitation of channel position mapping and measurement. The present study identified locations affected by of bank erosion accretion and the bankline shifting and indicated the urgent need to protect the river banks employing afforestation measures and other strategies. Therefore, it is necessary to incorporate geomorphic changes in formulating flood management programmes.

REFERENCES

Afrose, S., 2012. “Morphological Analysis of Teesta River”, B. Sc. Engineering Thesis, Department of Water Resources Engineering, BUET.

Asad., 2013. “A Flood frequency Modeling using Gumbel’s and Powell’s method for Dudhkumar River” B. Sc Engineering Thesis, Depsrtment of Civil Engineering, Stamford University Bangladesh, Dhaka 1217, Bangladesh.

Azuma, R., Sekiguchi, H., Ono, T., 2007. In: Studies of High-resolution Morphodynamics with Special Reference to River Bank Erosion vol. 50(C). Annuals of Disaster Prevention Research Institute, Kyoto University, Japan, pp. 199-209.

Baki, A.B.M., Gan, T.Y., 2012. Riverbank migration and island dynamics of the braided Jamuna River of the Ganges Brahmaputra basin using multi-temporal Landsat images. Quaternary International 263, 146-161.

BWDB, (2011). Rivers of Bangladesh, Bangladesh Water Development Board, August.

Hossain, M.A., Gan, T.Y., Baki, A.B.M., 2013. Assessing morphological changes of Ganges River using satellite images. Quaternary International 304, 142-155.

Hossain, M.J., 2010. “Assessment of Instream Flow Requirement for Dudhkumar River”, M. Sc. Thesis. Department of Water resources Engineering, BUET.

Kammu, M., Lu, X.X., Rasphone, A., Sarkkula, J., Koponen, J., 2008. Riverbank changes along the Mekong River: remote sensing detection in the VientianeNong Khai area. Quaternary International 186, 100-112.

Khan., 2014. “A study on River Bank Erosion of Jamuna River using GIS and Remote Sensing Technology.” Volume-II, M. Sc. Thesis. Department of Water resources Engineering, BUET.

Lawler, D.M., Couperthwaite, J., bull, L.J. and Harris, N.M., 1997, Bank Erosion Events andProcesses in the Upper Severn Basin, *Hydrology and Earth System Sciences,* 1(3): 523-534.

Nabi et.al (2016), " Historical Bankline Shifting Since 1760s: A GIS and Remote Sensing Based Case Study of Meghna River Plate of Rennell’s Atlas", International Journal of Scientific and Research Publications, Volume 6, Issue 12, December 2016, ISSN 2250-3153, P-473-483.

Sarkar et.al, "RS-GIS Based Assessment of River Dynamics of Brahmaputra River in India", Journal of Water Resource and Protection, 2012, 4, 63-72, http://dx.doi.org/10.4236/jwarp.2012.42008 Published Online February 2012 (http://www.SciRP.org/journal/jwarp)

Sarker, M.H., Thorne, C.R., 2006. Morphological response of the BrahmaputraPadma Lower Meghna river system to the Assam earthquake of 1950. In: Sambrook Smith, G.H., Best, J., Bristow, C.S., Petts, G.E. (Eds.), Braided Rivers: Process, Deposits, Ecology and Management. International Association of Sedimentologists Special Publication 36. Blackwell, London, pp. 289-310.

Takagi, T., Oguchi, T., Matsumoto, J., Grossman, M.J., Sarker, M.H., Matin, M.A., 2007. Channel braiding and stability of the Brahmaputra River, Bangladesh, since 1967: GIS and remote sensing analyses. Geomorphology 85, 294-305.

Zaman, M., 2017. “Morphological changes of the Dudhkumer River by using HEC-RAS”, B.Sc. Engineering Thesis, Department of Water Resources, BUET.

SIMULATION OF FLOW AND SALINITY IN RUPSHA-PASSUR RIVER SYSTEM

Shihab Hossain Saran[1], Afeefa Rahman[2*] and Dr. Anika Yunus[3]

[1]Undergraduate Student, Department of Water Resources Engineering (WRE), Bangladesh University of Engineering and Technology (BUET), Email:saranshihab@gmail.com

[2]Lecturer, Department of Water Resources Engineering (WRE), Bangladesh University of Engineering and Technology (BUET), Email:afeefa@wre.buet.ac.bd

[3]Associate Professor, Department of Water Resources Engineering (WRE), Bangladesh University of Engineering and Technology (BUET), Email:anikayunus@wre.buet.ac.bd

ABSTRACT

Surface water salinity in the Gorai River and in its associated river network has been increasing due to low flow from the Ganges River and siltation of Gorai River mouth upholding it as a great concern for the entire south western region of Bangladesh. Rupsha-Passur river system,the major river system associating the Gorai river flows through Khulna, Chalna, Batiaghata, Rampal, Dacope and Mongla upazilla. Being tidal in nature saline water intrudes into the river system from the Bay of Bengal during stronger spring tide but at following neap tide, salinity is not totally flushed out due to low flow availability at upstream. Thus analysis on the dry period flow and salinity characteristics of the Rupsha-Passur river system is momentous. The study has been carried out on a hydrodynamic and salinity modeling in HEC-RAS to assess the variables that governed the flow and amount of salt in the river system. From the results of hydrodynamic and salinity model it has been observed that the maximum flow occurs during the month of August in both the Rupsha and Passur river. The discharges in Khulna, Bhatiaghata, Rampal, Dacope and Mongla Upazillas have been obtained as 2405 m³/s in 23rd August, 3145 m3/s in 27th August, 3689.65 m³/s in 22nd August, 5824 m³/s in29th August and 7688 m³/s in 19th August for the year 2014 respectively. The maximum salinity concentration of these Upazillas are 7703.96 ppm in 28th May, 3630 ppm in 28th June, 3396 ppm in 30th June, 3630 ppm in 19th May and 13049 ppm in 6th June respectively. Analyses results reveal that the peak value of surface water salinity reaches its maximum in late March or early April. On many occasions the maximum salinity of Chalna exceeded the concentration at Mongla although Mongla is 17 km downstream of Chalna which occurred due to high saline water mixing from the Sibsa River. The study is expected to support long term assessment that may affect the sundarbans as a result of changes in the flow from upstream due to the water abstraction activity for domestic and irrigation water supply.

Keywords: *Hydrodynamic modeling, Salinity, Rupsha-Passur, HEC-RAS*

1. INTRODUCTION

Water is a critical resource for life and essential for economic success and sound ecosystems in an environmentally friendly society. Of the world's water about 97.5 % exists as saline water in the oceans and seas. Only 2.5 % exists as fresh water and 99 % of this is trapped in glaciers and ice caps. Water is required for domestic consumption, sanitary use, industrial use, hydroelectric power generation, agriculture, irrigation and protection of the ecology and ecosystems. Bangladesh is a low-lying, riverine country located in South Asia with a largely marshy jungle coastline of 710 km (441 mi) on the northern littoral of the Bay of Bengal, formed by a delta plain at the confluence of the Ganges (Padma), Brahmaputra (Jamuna), Meghna Rivers and their tributaries (BWDB,2012). The flow of the Ganges in Bangladesh reduced significantly due to withdrawal of water in the upstream at the Farakka Barrage. India commissioned the Farakka Barrage in West Bengal in 1975 to divert 40,000 cusec water of the Ganges River into the Bhagirathi-Hooghly Rivers for flushing silt and improve navigability of Kolkata Port connected to the Bay of Bengal on the south (BWDB,

2012). The reduction of dry season flow in the Ganges has led to various water quality related, ecological, hydrological and hydraulic problems in south-western zone of Bangladesh. The main impact of reduced low flow values has been the drop in hydraulic head of the Ganges River system and the consequent increase in salinity in the rivers of the south-western part of the country (Rahman and Ahsan, 2001). The coastal areas of Bangladesh have already been facing salinity problem which is expected to be exacerbated by climate change and sea level rise, as sea level rise is causing unusual increase in the height of tidal water. In dry season, when the flows of upstream water reduce drastically, the saline water goes up to 240 kilometres inside the country and reaches to Magura district. Presently around 31 Upazilla of Jessore, Satkhira, Khulna, Narail, Bagerhat and Gopalganj districts are facing severe salinity problem. Agricultural activities as well as cropping intensities in those Upazilla have been changing; as a result farmers cannot grow multiple crops in a year (Shamsuddoha and Chowdhury, 2007). Most of the lands remain fallow in the dry season (January–May) because of soil salinity and the lack of good-quality irrigation water (Mondal, 1997). In general, soil salinity is believed to be mainly responsible for low land use as well as cropping intensity in the area (Rahman and Ahsan, 2001). Salinity levels increased in the Sundarbans when intake-mouths of the Mathabhanga, Kobadak and other rivers that used to bring fresh water from the Ganges to the south were silted up and thus lost their connection with the Ganges. Therefore the increased salinity and alkalinity have damaged vegetation, agricultural cropping pattern and changed the landscapes in the Sundarbans region. A salinity level of 10 ppt (parts per thousand) in the water inundating the shores of the canals and the rivers of the Sundarbans area have led to the "top dying;" a disease of the prevalent native Sundari trees (Hoque et al., 2006). World Bank study predicted a 1 m sea level rise at the end of the century which might affect 17.5% of total land mass of the country (World Bank, 2000).

Saltwater intrusion is the movement of saline water into freshwater aquifers, which can lead to contamination of drinking water sources and other consequences. The huge freshwater outflow from the Ganges, the Jamuna and the Meghna induce a large zone of brackish water in the coastal region of Bangladesh. The general ocean currents in the Bay show a clockwise circulation of water in the dry season and anti-clockwise circulation in the wet season (Rahman, 2006). Bangladesh is likely to be one of the most vulnerable countries in the world to salinity problem. In monsoon, soil gets enough water and soil salinity decreases as rain water dilutes the concentration of salt in the soil. In post-monsoon, soil salinity starts to increase because of lower rainfall and higher evaporation of moisture from soil surface. Increasing soil salinity continues up to pre-monsoon when soil becomes water stressed (Uddin, 2012). Climate change is an important issue now-a-days. The anticipated sea level rise would produce salinity impacts in three fronts: surface water, groundwater and soil. Increased soil salinity due to climate change would significantly reduce food grain production (Uddin, 2011). IWM, 2013 carried out a study of salinity zoning map for coastal zone of Bangladesh. A comprehensive assessment on salinity and storm surge was carried out through extensive and continuous salinity measurement and field investigation under this study with the following specific objectives:

(a) To set up the flow model of Rupsha-Passur River and calibration and validation of the flow model.

(b) To set up water quality model and perform water quality simulation of Rupsha-Passur river with HEC-RAS.

(c) To develop different flow scenarios and examine the impact of flow availability on salinity for the developed hypothetical flow scenarios.

1.1 Study area

The Rupsha River is a river in southwestern Bangladesh. It forms from the confluence of Bhairab and Atrai river and flows into the Passur river being affected by tide throughout the entire reach. Figure 1 shows the Rupsha-Passur river system focusing the study area. The

river Rupsha flows by the side of Khulna and connects to the Bay of Bengal through Passur River at Mongla. Near Chalna the Rupsha River changes its name to Passur River and flows to the Bay of Bengal. The average width of this river is about 486 meter and the maximum and minimum width is about 650 meter and 322 meter respectively. It is a meandering and perennial river. Passur River is a significant river in the Sundarbans area as an extension of Rupsha River. The river Rupsha flows further south and rename as Passur near Chalna and falls into the Bay of Bengal. The maximum flow of the Gorai-Madhumati ultimately passes through the Rupsha-Passur river system. The Passur is placed after the Meghna in size in the Deltaic region. The river is joined by Mongla canal at about 32 km south from Chalna. Flowing further south the river meets the Shibsa at about 32 km north from its mouth and debouches into the sea keeping its original name Passur (BWDB, 2012).The river is very deep and navigable throughout the year and large marine ships can easily enter Mongla Sea Port through it. The Passur is an important river route through which Khulna-Barisal steamboats and other vessels ply. The total length of Passur is about 104 km. The maximum and minimum width of this river is about 2112 meter and 690 meter respectively. The average width of the river is about 1164 meter. Passur River is a meandering and perennial river and highly affected by tides (BWDB, 2012).

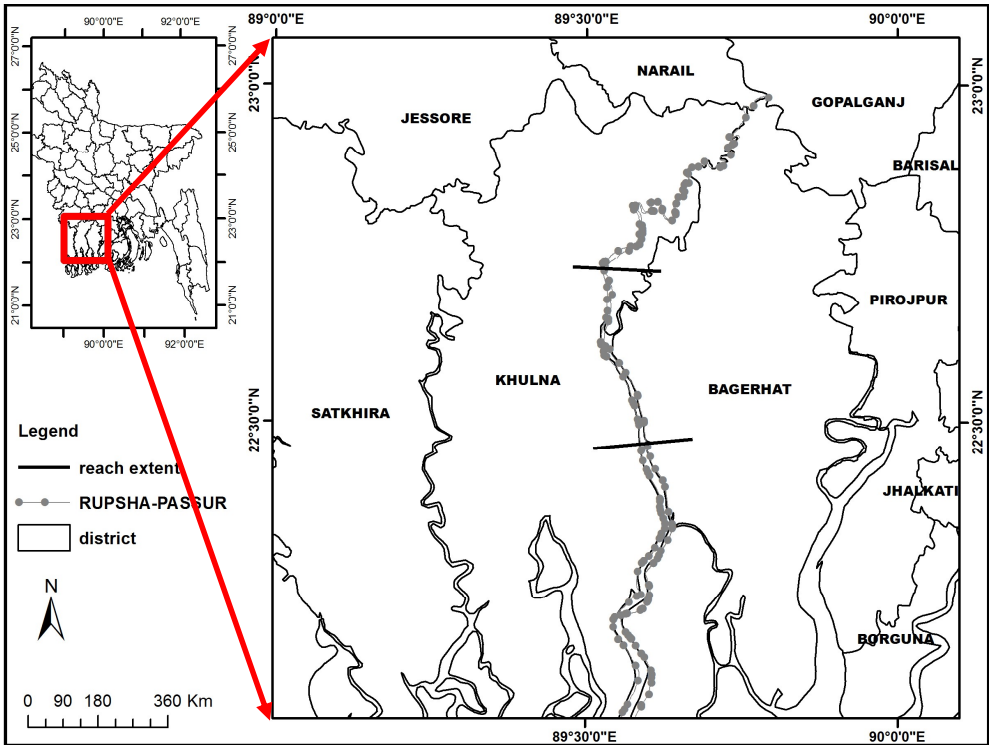

Figure 1: Location of the study area of Rupsha-Passur river.

2. METHODOLOGY

2.1. Data Collection and Model Setup

For the development of hydrodynamic and salinity model of Rupsha-Passur River data on bathymetry, discharge, stage hydrograph and salinity concentration at different stations have been collected from relevant sources. The selected reach of the river is about 70 km long having 14 cross sections (8 of Rupsha & 6 of Passur River) starting near Khulna and ending at Mongla. At Kamarkhali Transit flow is divided into two parts, one part enters into Nabaganga River and the other into Madhumati River. It has been assumed that 70% of discharge of Kamarkhali Transit (SW101) enters into Nabaganga river which later flows

through the Rupsha-Passur river. Stage hydrograph at the downstream of the river system near Mongla (SW 244) is going to be used as the downstream boundary and stage hydrograph at Chalna (SW 243) was used for calibration and validation. As Rupsha-Passur river is a tidal river so there is two high tides and two low tides within a day period. Salinity data at Khulna (SW 241) and Mongla (SW244) have been collected for the year 2014 to be used as upstream and downstream boundaries and data at Chalna (SW 243) is going to be used for calibration of salinity model of Rupsha-Passur river system.

2.2. Calibration and Validation of Hydrodynamic and Salinity Model

The water level data for the month of April 2014 at Khulna(SW241) and Chalna(SW243) along the Rupsha-Passur river system have been used for calibration using the Manning's roughness coefficient, 'n' as calibration parameter. After several trials, manning's roughness co-efficient, n=0.01 provides with the good match between the observed and simulated water level values and optimum value of the coefficient of determination. Figure 2 shows the comparison and correlation between observed and simulated water levels during the month of April for the manning's roughness, n= 0.01 at Khulna. The best value of R^2=0.9302 has been found for n=0.01 as shown in figure. Validation results at locations Khulna and Chalna compliment the calibration results. Calibration of salinity model has been done for different dispersion co-efficient for the month January, February and March near Chalna (SW 243). The best value of R^2 has been found for D=15 m^2/s. Validation results obtained from the model support the calibration outputs.

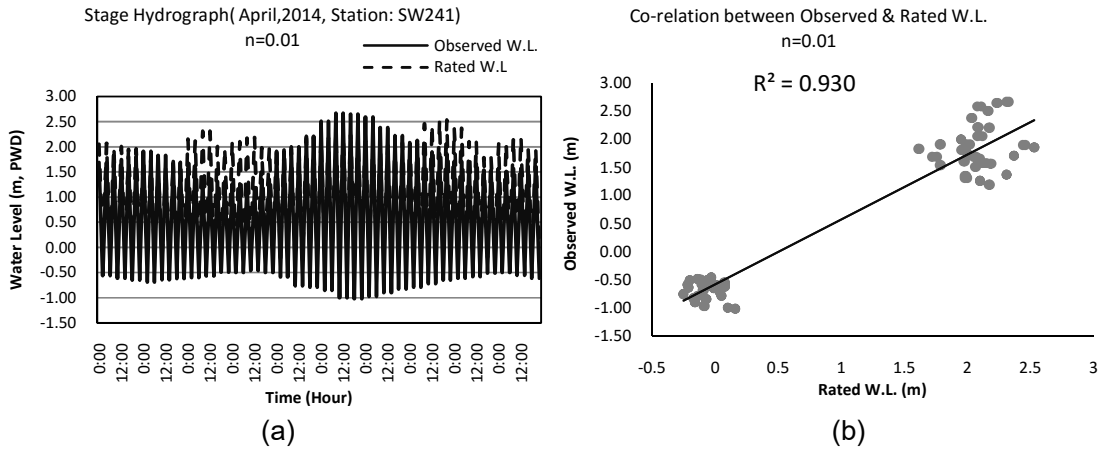

(a) (b)

Figure 2: (a) Calibration Hydrograph for manning's n= 0.010 (b) Regression analysis for manning's n= 0.01 near Khulna (SW 241)

3. ANALYSIS AND RESULTS

3.1. Analysis on Discharge, Water Level and Velocity for different flow scenarios

Rupsha-Passur river system flows through the Khulna and Mongla district of Bangladesh. The discharge and water level have been assessed at these two locations along the reach of Rupsha-Passur River system. Flow scenarios with 15%, 40% increase and 15%, 40% decrease have been obtained at the upstream boundary condition. Figure 3 shows the different flow scenarios that are to be used as upstream boundary condition to predict the hydrodynamic condition and water quality. Using the variable flow scenarios hydrodynamic assessment has been made at specified location along the Rupsha-Passur River system. Table 1 shows the discharge, velocity and water level variation with different flow scenarios at Khulna.

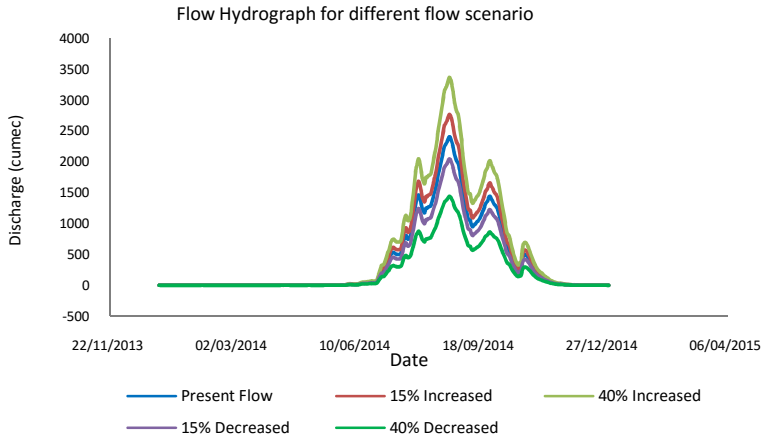

Figure 3: Flow hydrographs for different flow scenarios

From the Table 1, some important points have been found:

(1) The flow is high for the month July, August and September. During the month June and October, the flow is moderate but after this month the flow decreases drastically. The flow is very low for the month January, February, March, April and May. So, it can be said that during the pre-monsoon and post-monsoon period the river gets a little amount of flow at this region and it affects the climatic condition of this region.
(2) The velocity found to be maximum on 31 August. If the discharge is increased by 15% & 40% during monsoon period the velocity is also increased by 11% and 28% respectively
(3) If the velocity is decreased by 15% and 40% during the monsoon period the velocity is also decreased by 8% and 25% respectively.
(4) During the pre-monsoon and post-monsoon period the velocity variation is very negligible for different flow scenarios.
(5) In this region the river is affected by tides. So the water level variation is very little due to the change of discharge. During high tides the water level increases and during low tides the water level decreases.

Table1: Velocity, Discharge and Water Level for different flow scenarios at Khulna

Location Khulna	Parameter	Jan 1	Jan 31	Feb 28	Mar 31	April 30	May 31	June 30	July 31	Aug 31	Sep 30	Oct 31	Nov 30	Dec 31
Present Flow	Velocity (m/s)	0.20	0.16	0.19	0.17	0.17	0.15	0.27	0.68	0.79	0.64	0.26	0.16	0.14
	Discharge (m^3/s)	497	386	455	420	431	381	687	1805	2319	1707	676	417	366
	Water level (m)	1.78	1.54	1.83	1.64	2.05	1.88	2.34	2.35	2.53	2.39	2.26	2.15	1.81
15% Increased	Velocity (m/s)	0.20	0.16	0.19	0.15	0.18	0.15	0.28	0.75	0.93	0.71	0.27	0.16	0.16
	Discharge (m^3/s)	497	386	455	376	456	381	721	2006	2601	1893	715	418	399
	Water level (m)	2.02	1.53	1.83	1.79	2.27	1.88	2.35	2.36	2.53	2.40	2.26	2.15	1.99
40% Increased	Velocity (m/s)	0.20	0.17	0.19	0.17	0.18	0.15	0.30	0.87	1.09	0.82	0.30	0.16	0.16
	Discharge (m^3/s)	497	411	455	420	458	383	776	2340	3071	2200	782.5	420	399
	Water level (m)	2.02	1.55	1.83	1.64	2.29	1.88	2.35	2.36	2.55	2.40	2.26	2.15	1.99
15% Decreased	Velocity (m/s)	0.20	0.16	0.19	0.17	0.17	0.15	0.25	0.61	0.74	0.58	0.24	0.16	0.14
	Discharge (m^3/s)	497	385	455	412	430	380	654	1603	2037	1524	636	416	365
	Water level (m)	2.02	1.53	1.83	1.61	2.05	1.88	2.34	2.35	2.52	2.39	2.26	2.15	1.80
40% Decreased	Velocity (m/s)	0.18	0.16	0.19	0.15	0.16	0.15	0.23	0.48	0.57	0.46	0.22	0.16	0.14
	Discharge (m^3/s)	439	384	454	378	402	379	599	1267	1562	1216	569	414	365
	Water level (m)	1.78	1.53	1.83	1.80	1.77	1.88	2.34	2.35	2.52	2.39	2.26	2.15	1.80

Table 2 shows the discharge, velocity and water level variation with different flow scenarios at Mongla.

From the table 2, it can be seen that:
(1) In this region discharge is increased round the year because the river is affected by tides. During high tides, sea water flows into the upstream and during low tide it again falls into the sea.
(2) The river is affected by tides. So the water level variation is very little due to the change of discharge. During high tides the water level increases and during low tides the water level decreases.
(3) During the monsoon period the velocity is increased by 3% and 8% for the increased flow of 15% and 40% respectively. For the 15% and 40% decreased discharge the velocity of flow is decreased by 2.5% and 8% respectively.
(4) The variation of velocity in Baghaerhat district is less than that of in Khulna district for different flow scenarios.

Table 2: Velocity, Discharge and Water Level for different flow scenarios at Mongla

Location Mongla	Parameter	Jan 1	Jan 31	Feb 28	Mar 31	April 30	May 31	June 30	July 31	Aug 31	Sep 30	Oct 31	Nov 30	Dec 31
Present Flow	Velocity (m/s)	0.91	0.71	0.87	0.79	0.73	0.61	0.82	1.00	0.96	1.01	0.68	0.65	0.60
	Discharge(m^3/s)	3476	2805	3311	3040	3106	2715	3564	4482	4752	4490	3179	2942	2631
	Water level (m)	2.02	1.63	1.94	1.73	2.15	1.97	2.45	2.45	2.62	2.50	2.35	2.25	1.90
15% Increased	Velocity (m/s)	0.91	0.71	0.87	0.79	0.73	0.61	0.83	1.03	1.01	1.05	0.69	0.65	0.60
	Discharge(m^3/s)	3477	2805	3311	3040	3106	2716	3594	4654	5003	4651	3215	2943	2631
	Water level (m)	2.02	1.63	1.94	1.73	2.15	1.97	2.45	2.46	2.62	2.50	2.35	2.25	1.90
40% Increased	Velocity (m/s)	0.91	0.71	0.87	0.79	0.73	0.64	0.84	1.09	1.09	1.10	0.70	0.65	0.65
	Discharge(m^3/s)	3477	2805	3311	3040	3106	2846	3643	4950	5415	4917	3277	2944	2874
	Water level (m)	2.02	1.63	1.94	1.73	2.15	2.07	2.45	2.46	2.62	2.50	2.35	2.25	2.08
15% Decreased	Velocity (m/s)	0.91	0.71	0.87	0.79	0.73	0.61	0.82	0.96	0.92	0.98	0.68	0.65	0.60
	Discharge(m^3/s)	3476	2805	3311	3040	3106	2714	3534	4305	4498	4332	3142	2940	2631
	Water level (m)	2.02	1.63	1.94	1.73	2.15	1.97	2.45	2.45	2.61	2.50	2.35	2.25	1.90
40% Decreased	Velocity (m/s)	0.83	0.71	0.87	0.78	0.73	0.61	0.80	0.90	0.83	0.93	0.66	0.65	0.60
	Discharge(m^3/s)	3199	2805	3296	3002	3105	2713	3484	3997	4056	4068	3080	2939	2631
	Water level (m)	1.90	1.63	1.93	1.72	2.15	1.97	2.45	2.45	2.62	2.50	2.35	2.25	1.90

3.2 Comparative Analysis of Hydrodynamic Parameters

3.2.1 Discharge:

In the figure 4 it has been seen that discharge is generally high during the monsoon period. But in Mongla discharge is greater than that of in Khulna district. This is because Mongla is situated at the downstream of the reach which is very near to the sea. So during the high tide, sea water flows into the upstream. So the discharge is increased in this region. During the pre-monsoon and post-monsoon period the discharge is very low.

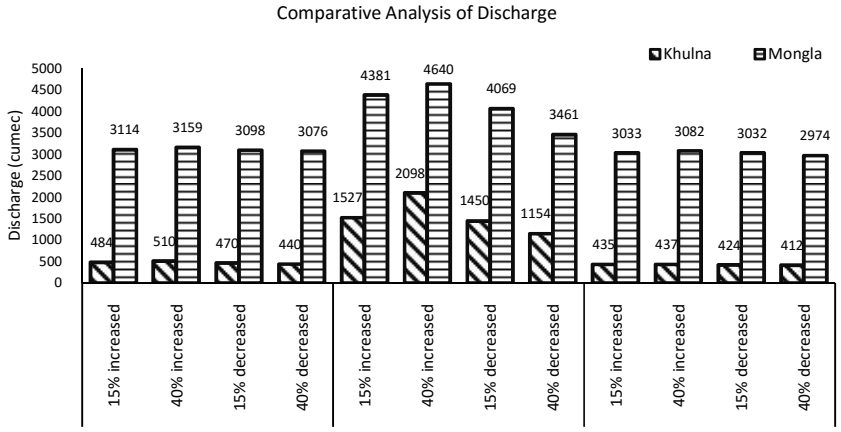

Figure 4: Comparative analysis of discharge between Khulna and Mongla.

3.2.2 Water Level:

In the figure 5, water level has been taken into account during high tide only. So there is little variation with water level in Khulna and Mongla. Water level is high during monsoon period but in pre-monsoon and post-monsoon period water level is lower than monsoon period. During this time water level difference in Khulna and Mongla is very little. Because during these period upstream flow is very little and sea water flow into the upstream during high tide has a great effect.

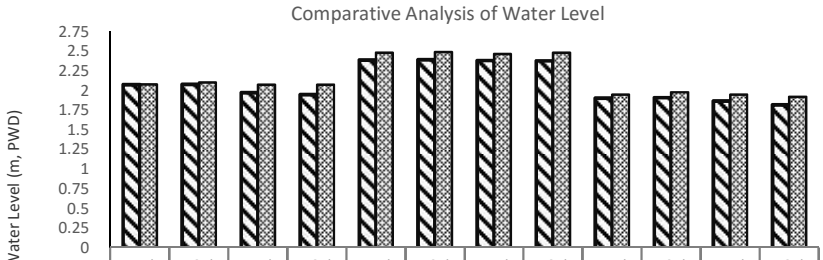

	15% increased	40% increased	15% decreased	40% decreased	15% increased	40% increased	15% decreased	40% decreased	15% increased	40% increased	15% decreased	40% decreased
	Pre-monsoon				Monsoon				Post-monsoon			
Khulna	2.073	2.08	1.97	1.948	2.388	2.393	2.38	2.379	1.904	1.908	1.866	1.818
Mongla	2.08	2.101	2.075	2.073	2.48	2.49	2.465	2.481	1.95	1.98	1.948	1.922

Figure 5: Comparative analysis of water level between Khulna and Mongla

3.2.3 Velocity:

From figure 6 it can be said that velocity is increased during monsoon period as there is greater amount of availability of discharge during this season. During monsoon for the 15% increased flow the velocity in Mongla will be greater than that of in Khulna by 43%. For the 40% increased flow the velocity in Mongla will be greater than in Khulna by 30%. During the pre-monsoon period the velocity in Mongla will be about 4 times than the velocity in Khulna for the 15% and 40% increased flow. During the post-monsoon period the velocity in Mongla also will be about 4 times than the velocity in Khulna for the 15% and 40% increased flow. During the pre-monsoon and post-monsoon period the difference of velocity between Khulna and Mongla is very high because during the period in Khulna region the upstream flow is very low but in Mongla region sea water intrusion occurs during high tides it falls into the sea during low tide.

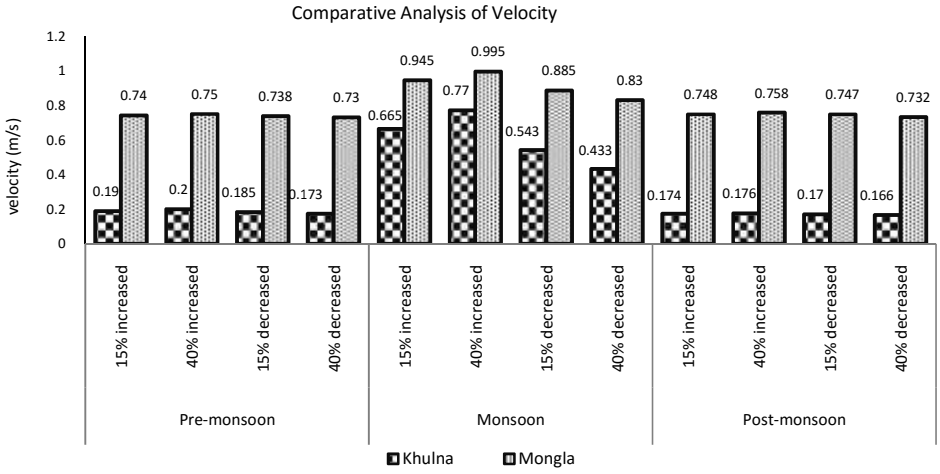

Figure 6: Comparative analysis of velocity between Khulna and Mongla

3.3 Local flow field under different scenarios

To assess the local flow field under different flow scenarios, velocity distributions at different locations along the reach of Rupsha-Passur river system have been represented for the maximum and minimum flow day of observed flow for the year 2014. The velocity distribution for maximum and minimum flow near Khulna and Mongla has been shown in figure 7 and figure 8 respectively. The maximum velocity near Khulna is about 0.8 m/s and minimum velocity tends to zero m/s. On the other hand the maximum velocity near Mongla is about 2 m/s and minimum velocity is about 0.8 m/s. The velocity decreases towards the banks of the rivers.

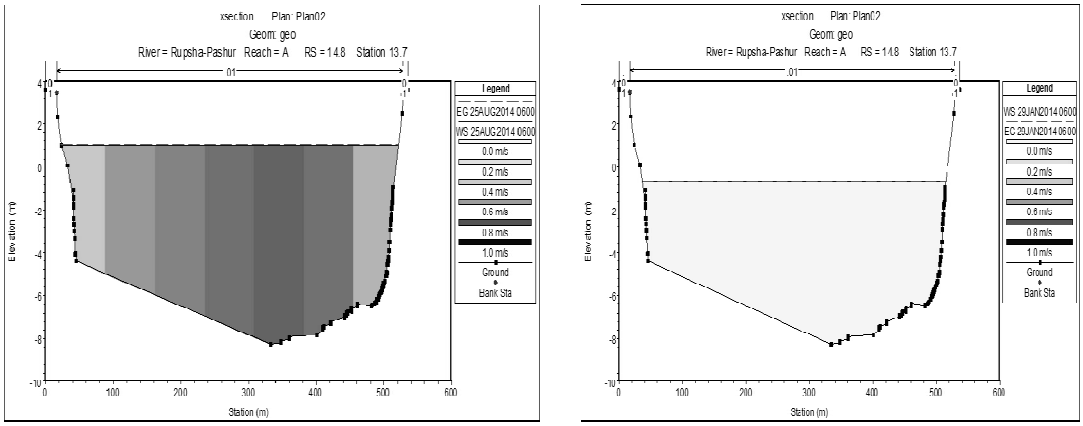

Figure 7: Maximum and minimum velocity distributions for the observed flow of 2014 near Khulna (a) the maximum velocity (b) the minimum velocity

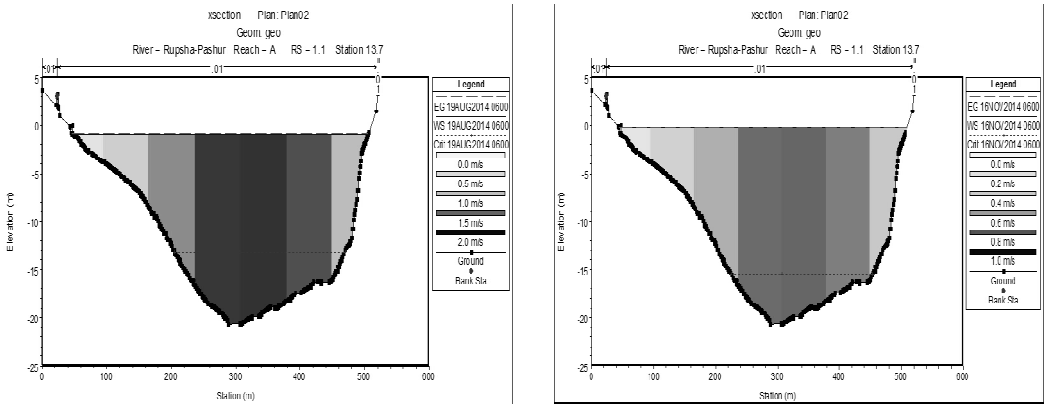

Figure 8: Maximum and minimum velocity distributions for the observed flow in 2014 (a) the maximum velocity (b) the minimum velocity

3.4 Water Quality Analysis

Water quality analysis has been performed for different flow scenarios to examine the effect of salinity at different locations during different seasons. Water quality analysis has been performed to examine the effect of salinity in Khulna and Mongla during different seasons. In Mongla during the pre-monsoon period the salinity is about 13 ppt for the present flow. During the monsoon period the salinity is about 3.5 ppt for the present flow and during post-monsoon period the salinity is about 7 ppt. In Khulna during the pre-monsoon period the salinity is about 3 ppt for the present flow. During the post monsoon and monsoon period salinity variation is not remarkable. Figure 9 shows the variation of salinity over the months for the year of 2014.

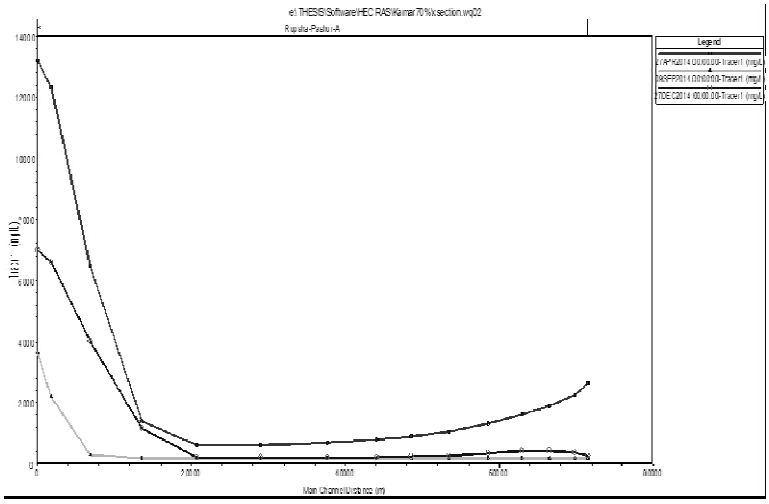

Figure 9: Salinity simulation for the present flow 2014

3.4.1. Analysis on Discharge, Water Level and Velocity for different flow scenarios

From the table 3 it has been seen that:
(1) During April, May, June, July the salinity concentration is very high in Khulna district. But the salinity concentration is moderate for the month January, February, March and low for the month August, September, October, November and December.
(2) The maximum salinity concentration has been observed in 30 June. During this time if the flow is increased by 15% and 40% then the salinity will be decreased by 10% and 24%

respectively but if the flow is decreased by 15% and 40% the salinity will be increased by 40% and 45% respectively. So it will be very alarming at this region if the current flow is decreased.
(3) The minimum salinity concentration is observed in 31 August.
(4) During the pre-monsoon season the salinity concentration becomes greater than 10 ppt which is very harmful for agriculture and environment at this region. And if the present flow is somehow decreased this scenario will be worsened.

Table-3: Salinity Concentration for different flow scenarios at Khulna

Location Khulna	Parameter	Jan 1	Jan 31	Feb 28	Mar 31	April 30	May 31	June 30	July 31	Aug 31	Sep 30	Oct 31	Nov 30	Dec 31
Present Flow	Salinity (ppt)	2.65	2.49	2.83	3.89	5.25	7.32	13.09	6.47	0.85	0.94	1.04	1.08	1.47
15% Increased	Salinity (ppt)	2.65	2.46	2.81	3.84	5.20	7.26	11.75	6.41	0.85	0.94	1.03	1.07	1.45
40% Increased	Salinity (ppt)	2.65	2.46	2.79	3.81	5.15	6.81	10.03	6.40	0.84	0.94	1.03	1.06	1.45
15% Decreased	Salinity (ppt)	2.75	2.49	2.86	4.05	5.39	7.52	18.49	6.68	0.92	0.95	1.05	1.07	1.49
40% Decreased	Salinity (ppt)	2.80	2.55	2.87	4.06	5.48	7.88	19.02	6.95	1.06	0.97	1.05	1.08	1.55

From the table 4, it has been observed that:
(1) The maximum salinity concentration has been observed in 30 June. During this time if the flow is increased by 15% and 40% then the salinity will be decreased by 0.5% and 35% respectively but if the flow is decreased by 15% and 40% the salinity will be increased by 4% and 18% respectively. So it will be very alarming at this region if the current flow is decreased.
(2) During the pre-monsoon and post-monsoon period salinity concentration in this region is greater than that of in Khulna district. This is because Mongla is at downstream of the reach with respect to Khulna district. So during high tide, sea water intrusion is very high in Mongla.
(3) The minimum concentration of salinity has been observed in 31 August. This is because during this time the river gets maximum flow. So this increased flow retards the sea water intrusion.

Table-4: Salinity Concentration for different flow scenarios at Mongla

Location Mongla	Parameter	Jan 1	Jan 31	Feb 28	Mar 31	April 30	May 31	June 30	July 31	Aug 31	Sep 30	Oct 31	Nov 30	Dec 31
Present Flow	Salinity (ppt)	8.16	5.10	5.5	12.6	14.50	12.1	16.3	8.03	1.03	1.13	1.24	8.54	7.95
15% Increased	Salinity (ppt)	8.15	4.93	5.4	7.49	12.49	11.8	16.3	7.93	1.02	1.13	1.2	8.19	7.77
40% Increased	Salinity (ppt)	8.14	4.92	4.8	7.11	8.21	11.4	10.5	5.82	0.99	1.12	1.23	5.58	7.21
15% Decreased	Salinity (ppt)	8.16	5.37	5.9	13.3	18.28	13.2	16.9	8.47	1.08	1.14	1.25	8.68	8.75
40% Decreased	Salinity (ppt)	9.53	6.29	6.9	15.5	21.38	16.4	22.5	10.3	1.44	1.34	1.65	10.80	12.8

3.4.2 Comparative Analysis of Salinity between Khulna and Mongla

In the figure 10 it can be seen that for the extreme scenario (15% & 40% decreased flow) the salinity in Mongla is above 15 ppt and in Khulna above 8 ppt during the pre-monsoon season. But if flow is increased by 40% the salinity is about 7 ppt in Mongla and 6 ppt in Khulna during the pre-monsoon season. But during the monsoon period the salinity is about 3 ppt both in Khulna and Mongla. During the post-monsoon period the salinity again increases in Mongla and it becomes above 6 ppt. But in Khulna the salinity remains below 2 ppt. For 15% decreased flow the salinity in Mongla is greater than that of in Khulna by 45% during the pre-monsoon season. For 40% decreased flow the salinity in Mongla is greater than that of in Khulna by 49% during the pre-monsoon season.

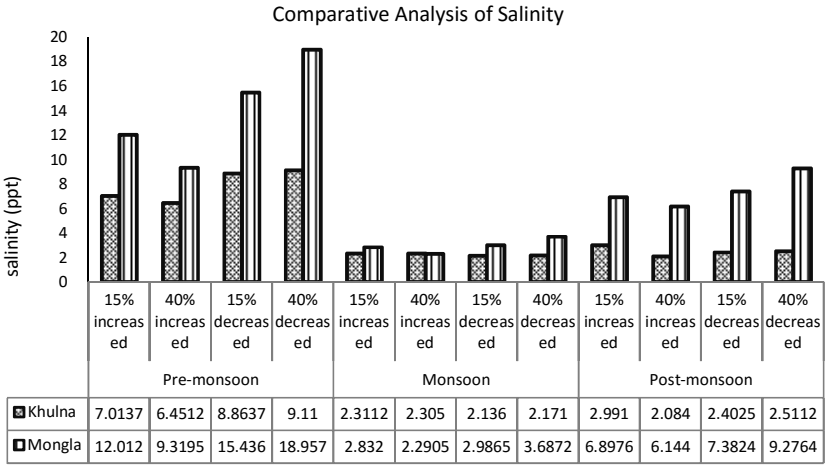

	15% increased	40% increased	15% decreased	40% decreased	15% increased	40% increased	15% decreased	40% decreased	15% increased	40% increased	15% decreased	40% decreased
	Pre-monsoon				Monsoon				Post-monsoon			
Khulna	7.0137	6.4512	8.8637	9.11	2.3112	2.305	2.136	2.171	2.991	2.084	2.4025	2.5112
Mongla	12.012	9.3195	15.436	18.957	2.832	2.2905	2.9865	3.6872	6.8976	6.144	7.3824	9.2764

Figure-10: Comparative analysis of salinity concentration between Khulna and Mongla

5. CONCLUSIONS AND RECOMMENDATIONS

In this study, an attempt was performed to analyze the trend of variables of Rupsha-Passur River and assess its present flow and salinity condition. From the study, the following conclusions and recommendations can be drawn:

From hydrodynamic and water quality analysis, it was seen that these rivers get very little flow during the pre-monsoon and post-monsoon period. As a result during these periods the salinity remains very high due to increased intrusion of saline water. To prevent the intrusion of saline water the discharge must be increased during pre-monsoon and post-monsoon periods. The maximum salinity occurs in March, April, May and June, during the dry period. During this period the water cannot be used for irrigation and drinking purposes. The salinity intrusion zone has been increased during this time. This study is limited to the impact of Rupsha-Passur river discharge only. For better result, its branch channels and other sources of fresh water should be considered. Sea level rise should be taken into account to perform this study so that the salinity scenarios can be understood more accurately.

REFERENCES:

BWDB, “Ganges Barrage Study Project (Feasibility Report –Main Report)”, September, 2012.

BWDB, “Rivers of Bangladesh”, Bangladesh Water Development Board (BWDB), August, 2011.

Hoque A., Sarkar M.S.K.A , Khan S.A.K.U., Moral M.A.H and Khurram A.K.M., "Present Status of Salinity Rise in Sundarbans Area and its Effect on Sundari (Heritiera fomes) Species," Research Journal of Agriculture and Biological Sciences, 2(3), pp. 115-121,2006.

IWM, “Union-wise Flood Mapping for Flood-Prone Areas, storm surge an salinity zoning map for coastal zone (baseline condition) and modeled scenarios following climate change of the same refereeing to the baseline milestone events to facilitate Community Risk Assessment (CRA) having climate sensitive decision”, Revised Final Report, 2013.

Mondal M.K., "Management of soil and water resources for higher productivity of the coastal saline rice lands of Bangladesh," University of the Philippines, Los Banos, Philippines,1997.

Rahman M. and Ahsan M., "Salinity constraints and agricultural productivity in coastal saline area of Bangladesh", 2001

Rahman M.M. and Bhattacharya A. K., “Salinity Intrusion and its Management Aspects in Bangladesh”, Journal of Environmental Hydrology, The Electronic Journal of the International Association for Environmental Hydrology, Volume 14, Paper 14, , On the World Wide Web,October 2006

Shamsuddoha M. and Chowdhury R. K., "Climate Change Impact and Disaster Vulnerabilities in the Coastal Areas of Bangladesh," Coast Trust, p. 32, 2007

Technology,2015.

Uddin M.S. , Khan M.S. I., Talukdar M.M.R., Hossain M. I. and Ullah M.H. (December, 2011), “Climate Change and Salinity in Bangladesh: Constraints and Management Strategy for Crop Production”, Rajshahi University journal of environmental science, Vol.: 1, 13-20, ISSN 2227-1015, December 2011.

Uddin M.S. , Khan M.S.I., Talukdar M.M.R., Hossain M.I. and Ullah M.H., “Seasonal Variation of Soil Salinity In Coastal Areas of Bangladesh”, International Journal of Environmental Science, Management and Engineering Research Vol. 1 (4), pp. 172-178, Available online at http://www.ijesmer.com, 2012.

World Bank, Bangladesh: Climate Change & Sustainable Development. Report No. 21104 BD, Dhaka,2000.http://wwwwds.worldbank.org/external/default/WDSContentServer/WDSP/IB/2001/04/13/000094946_01033105302920/Rendered/PDF/multi0page.pdf

Proceedings of the 4th International Conference on Civil Engineering for Sustainable Development (ICCESD 2018), 9~11 February 2018, KUET, Khulna, Bangladesh (ISBN-978-984-34-3502-6)

IMPACT ASSESSMENT OF KHAN JAHAN ALI BRIDGE ON RUPSHA RIVER

Md. Mahfuzur Rahman[1] and Kh. Md. Shafiul Islam[2]

[1] Student, Khulna University of Engineering & Technology, Bangladesh, e-mail: sheemul.48@gmail.com
[2] Professor, Khulna University of Engineering & Technology/Department of Civil Engineering, Bangladesh, e-mail: khmsislam@yahoo.com

ABSTRACT

In this study, the impact of the Khan Jahan Ali Bridge (in Khulna, Bangladesh) on the Rupsha River was assessed. The amount of flow path of the river occupied by the bridge pier was calculated about 15.75%. Since the River is a tidal river, the flow is unsteady for which discharge is changed frequently. To calculate the discharge of this river, the river flow velocity data (current meter readings) was collected at a certain date (November 19, 2013) from Bangladesh Water Development Board (BWDB), Khulna. From this data, the river discharge was calculated as 4047 m3/s using area velocity method. To assess the impact of the bridge on the river geometry, the cross section of the river at 2km and 7km upstream of the bridge was collected from BWDB, Dhaka and the data of water level (1978-2013) were collected at 7km upstream of the bridge from BWDB, Khulna. It was observed that from 2003 the maximum water level was rising and the minimum water level initially increased and thereafter decreased (2009-2013) after the construction of the bridge (2004-2008). It was seen that at 2km u/s of the bridge, scouring has occurred at the right bank and deposition was occurred at the left bank from the very beginning of the construction of the bridge. On the other hand, at 7km u/s of the bridge, scouring has occurred at both banks from the very beginning of the construction of the bridge and then the river bed level was increased for both banks.

Keywords: *Khan Jahan Ali Bridge, Rupsha River, river discharge, river geometry, water level*

1. INTRODUCTION

Bangladesh is located in a delta region facing the Bay of Bengal in South Asia and its territory is divided by many rivers. The Rupsa River is a major river in southwestern Bangladesh and a distributary of the Ganges. Its entire length is affected by tides. It flows by the side of Khulna and connects to the Bay of Bengal through the Pasur River at Mongla channel. Khan Jahan Ali Bridge was constructed over the river Rupsha at Labonchara in the Khulna city. It is also known as the Rupsha Bridge. The Port of Mongla, the second biggest port in Bangladesh in terms of cargo handling tonnage, is located approximately 40km south from the largest city in the southwest region Khulna.

At the beginning of the 2000s, a ferry service was used for river crossing at the Rupsha River and this was a major factor in preventing the smooth flow of traffic to the port. As a bridge over the Rupsha River would enable land transport from the Capital city Dhaka to Mongla Port via the Jamuna Bridge and the Paksey Bridge, it was expected that this would improve the convenience of the port. This is the background to the plan for a bridge over the Rupsha River.

The purpose of bridge construction is to ensure and facilitate the communication over the flow of waterways conveniently. The construction of bridge may require placement of bridge piers in the channel or floodplain of natural waterways. However, these structures have detrimental effects on the hydrology and morphology of the adjacent area of the streams as the waterway is constricted. Piers will obstruct the flow and cause an increase in water levels upstream of the bridge (Biswas, 2010). A significant amount of waterways is occupied by

bridge pier in the Rupsha River. In this study, impact assessment of the Khan Jahan Ali Bridge on the Rupsha River was investigated.

2. METHODOLOGY

The main concern of this study is to analyze the effect of bridge on stream flow, water level and channel geometry. To accomplish the objectives of this study, the water level data and cross section data at two points of upstream of the bridge were collected. The river discharge was measured by area velocity method. The collected data was then analyzed and from the output of the analysis the effects of the bridge on river water level and geometry were obtained. The steps in this study are shown in below:

- Selection of study area.
- Collection of historical data.
- Data analysis.
- Comparison of conditions before and after construction of the bridge.
- Conclusion.

2.1 Study Area

The Rupsha-Pasur River System (RS) is one of the biggest and important river systems in the Sundarbans estuarine ecosystem. It is the largest fresh water supplier into this mangrove forest. In Khulna of Bangladesh, the Rupsha-Bhairab is a major tidal river system flowing on the east of the city. Khan Jahan Ali Bridge was constructed over the river Rupsha at Labonchara. The study area covers the river flow from 7 km upstream to the Khan Jahan Ali Bridge.

The construction was started on 30 May 2001 and inaugurated on the 21st May 2005. The Length of the bridge is 1,360m while the width is 16.65m. At bridge section the river width is 476 m. The bridge has 7 spans on 8 piers and 5 piers are on the river with 15m width of each pier. About 15.75% flow-path is occupied by bridge pier. There are special security measures in the 8 piers of the bridge. According to the Project manager, the piers are well fortified to prevent any errant watercraft to hit the piers. This is the first protection system installation in any bridge in the country. Seismic prevention has also been set in the bridge which is 80m above the sea level. The vast infrastructure of the bridge is built on the concrete beneath 70m to 72m in the 50ft. deep the Rupsha River (Kobayashi, 2011). Figure 1 shows the satellite view of the Khan Jahan Ali Bridge and Figure 2 shows the basement of Bridge pier.

Figure 1: Satellite view of the Khan Jahan Ali Bridge

Figure 2: Basement of Bridge pier

2.2 Data Collection

To accomplish this study water level, velocity and cross-section data of the Rupsha River were collected. Data were collected from Bangladesh Water Development Board (BWDB), Khulna and Dhaka. Water level and current meter data were collected for the Station 241 (Station Name: Rupsha-Pasur), which is situated about 7 km upstream from the bridge. The water level data were collected from BWDB, Khulna. The data length varied from 1978 to 2013 i.e. 35 years. The cross-section data at 2 km & 7 km u/s of the bridge for the year 1995, 2002, 2006 and 2009 were collected from BWDB, Dhaka. Current meter readings on 19.11.2013 at Station 241 were collected from BWDB, Khulna. Table 1 shows the information for the collected data types. The value of water level data represents how much the river is lower or upper with respect to sea level. The maximum water level data are collected generally in the month of August to November and the minimum water level data are collected from January to April.

Table 1: List of collected data

Data Type	Data Period	Data Length	Location
Maximum &Minimum Water Level	1978-1995 & 2010-2013	19 years	Station 241
Daily Water Level	1995-2010	16 years	
Cross-Section (two points)	May 1995	8 nos.	2 km & 7 km u/s of the bridge
	May 2002		
	April 2006		
	January 2009		
Current meter readings	19.11.2013	1	Station 241

3. DATA ANALYSIS

3.1 Water Level Comparison

The maximum and minimum water level data for the Station 241 are calculated. Table 2 shows the maximum and minimum Water Level at 7 km upstream of the Rupsha bridge (Station ID-241).

Table 2: Maximum and minimum water level at u/s of the Rupsha Bridge (Station No. 241)

	Maximum Water Level		Minimum Water Level	
Year	**Date**	**Value (m PWD)**	**Date**	**Value (m PWD)**
1978	September	2.72	March	-0.64
1979	August	2.76	February	-0.62
1980	August	2.76	March	-0.65
1981	August	2.79	March	-0.64
1982	September	2.79	March	-0.67
1983	September	2.92	February	-0.65
1984	August	3.28	February	-0.59
1985	August	3.00	April	-0.92
1986	August	2.94	February	-0.72
1987	8-9-1987	3.12	2-3-1987	-0.73
1988	28-8-1988	3.41	19-3-1988	-0.59
1989	17-9-89	2.90	9-2-1989	-0.45
1990	22-8-90	3.15	12-3-1990	-0.59
1991	12-9-1991	3.15	18-3-1991	-0.74
1992	30-8-1992	3.10	20-2-1992	-0.72
1993	18-9-1993	3.25	9-3-1993	-0.72
1994	23-8-1994	3.22	27-4-1994	-0.67
1995	28-8-1995	3.15	18-3-1995	-0.73
1996	31-8-1996	3.25	22-1-1996	-0.82
1997	19-8-1997	3.21	10-3-1997	-0.76
1998	7-9-1998	3.46	31-1-1998	-0.75
1999	14-7-1999	3.44	19-7-1999	-0.62
2000	2-8-2000	3.26	21-3-2000	-1.47
2001	18-9-2001	3.24	10-3-2001	-0.71
2002	13-8-2002	3.27	27-3-2002	-0.70
2003	8-10-2003	3.98	21-3-2003	-0.69
2004	19-9-2004	3.34	1-3-2004	-0.15
2005	28-6-2005	3.74	6-2-2005	-0.01
2006	12-6-2006	3.19	1-3-2006	-0.04
2007	20-6-2007	3.55	27-4-2007	-0.07
2008	19-9-2008	3.22	21-2-2008	-0.08
2009	25-8-2009	3.2	20-3-2009	-0.47
2010	7-11-2010	4.14	2-3-2010	-1.23
2011	25-11-2011	3.92	20-2-2011	-1.20
2012	18-9-2012	3.42	11-3-2012	-1.12
2013	22-8-2013	3.75	29-3-2013	-0.96

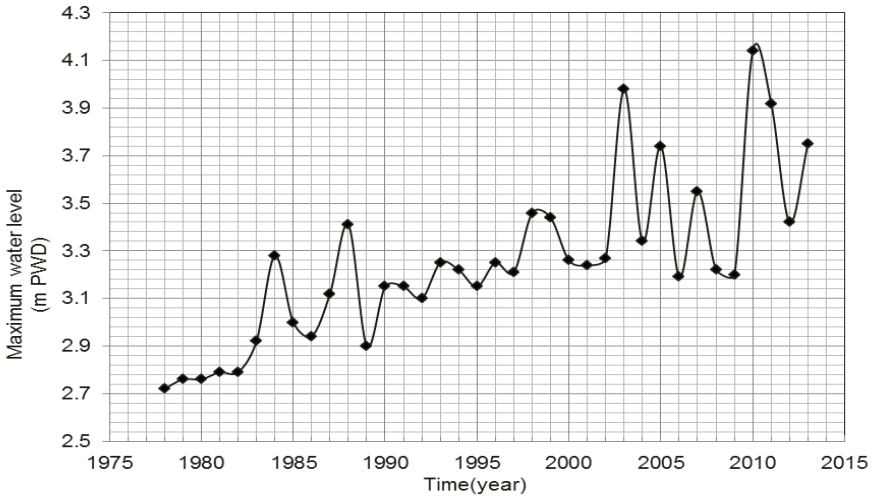

Figure 3: Maximum water level (m PWD) variation with respect to time (year)

Figures 3 and 4 show the maximum and minimum water level (m PWD) variation respectively for the station-241 (near to bridge). The construction of the bridge was started in 2001 and finished in 2005. It is observed from the Figure 3 that from 2003 the water level is rising than the previous time. From the Figure 4, it is seen that the minimum water level initially has increased after the construction of the bridge (2004-2008) and thereafter decreased (2009-2013).

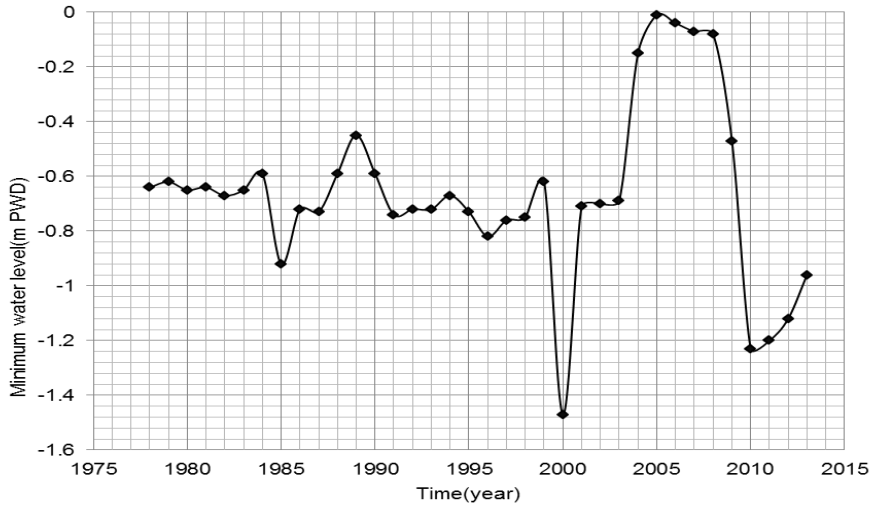

Figure 4: Minimum water level (m PWD) variation with respect to time (year)

3.2 Discharge of Rupsha River at U/S of the Khan Jahan Ali Bridge

Table 3: Discharge calculation by area velocity method (November 19, 2013)

Vertical	Distance from left edge (m)	Average Width (m)	Depth d (m)	Current meter reading N (Rev/sec)	Velocity V (m/s)	Segmental Discharge ΔQ (m^3/sec)
	0	9.40	0			0
	4.70	9.40	2.19	0.34	0.09	2.00
	10.85	9.40	7.68	1.20	0.32	23.66
	13.20	9.40	7.41	1.16	0.31	22.04
	24.74	9.40	7.68	1.20	0.32	23.66
	37.28	9.40	7.93	1.24	0.33	25.22
	41.61	9.40	8.23	1.29	0.35	27.15
	47.08	9.40	8.93	1.40	0.38	31.92
	50.24	9.40	9.30	1.45	0.39	34.60
	55.57	9.40	10.21	1.60	0.43	41.66
I	65.00	9.40	10.52	1.64	0.44	44.21
	70.15	9.40	10.97	1.71	0.46	48.05
	77.36	9.40	11.13	1.74	0.47	49.45
	80.36	9.40	12.01	1.88	0.51	57.54
	87.20	9.40	11.68	1.83	0.49	54.43
	92.54	9.40	11.13	1.74	0.47	49.45
	101.15	9.40	11.77	1.84	0.49	55.27
	106.42	9.40	12.80	2.00	0.54	65.31
	108.77	9.40	12.90	2.02	0.54	66.33
	120.08	9.40	13.47	2.11	0.57	72.30
	122.40	9.40	13.96	2.18	0.59	77.63
	128.56	9.40	13.75	2.15	0.58	75.32
	136.45	9.40	14.48	4.86	1.11	151.37
	142.94	9.40	14.39	4.83	1.10	149.51
	150.78	9.40	14.64	4.92	1.12	154.72
	156.25	9.40	14.54	4.88	1.11	152.62
	165.31	9.40	14.78	4.96	1.13	157.68
II	172.32	9.40	15.18	5.10	1.16	166.28
	178.48	9.40	15.85	5.32	1.21	181.20
	183.03	9.40	15.00	5.04	1.15	162.38
	191.53	9.40	14.70	4.94	1.12	155.98
	199.47	9.40	14.91	5.01	1.14	160.45
	206.01	9.40	15.09	5.07	1.15	164.32
	213.77	9.40	15.33	5.15	1.17	169.56
	232.99	9.40	15.58	5.23	1.19	175.11
	245.28	9.40	16.19	5.44	1.24	189.01
	252.83	9.40	15.55	2.39	0.64	94.44
	262.92	9.40	15.55	2.39	0.64	94.44
	270.62	9.40	15.55	2.39	0.64	94.44
	282.78	9.40	15.03	2.31	0.62	88.26
	294.42	9.40	14.72	2.26	0.61	84.67
	304.35	9.40	14.85	2.28	0.61	86.16
	309.80	9.40	15.09	2.32	0.62	88.96
III	322.14	9.40	14.33	2.20	0.59	80.26
	335.60	9.40	13.11	2.01	0.54	67.23
	348.41	9.40	7.47	1.14	0.31	21.98
	358.96	9.40	3.60	0.55	0.15	5.20
	373.90	9.40	1.98	0.30	0.08	2.99
	395.32	9.40	0			0
					Total=	4046.70 m^3/sec

In the tidal river like Rupsha, the authority (BWDB) does not measure the river discharge regularly. To calculate the discharge of this river, the river flow velocity data (current meter readings) is collected at a certain date (November 19, 2013). From this data, the river discharge is calculated using area velocity method as 4047 m^3/s. Table 3 shows the discharge calculation by area velocity method (Subramanya, 2013). To calculate the velocity along verticals, following calibration equations are used. The equation 1, 2 and 3 are formulated by the authority (BWDB).

$$Vertical - I : V = 0.26257N + 0.01707 m/\sec \quad (1)$$
$$Vertical - II : V = 0.22600N + 0.01251 m/\sec \quad (2)$$
$$Vertical - III : V = 0.26805N + 0.00532 m/\sec \quad (3)$$

3.3 Change in River Cross-Section

The river cross-section data at two points (2 and 7 km u/s of the Rupsha Bridge) were collected for four different times i.e. at May 1995, May 2002, April 2006 and January 2009. From this data, cross-sections of the river were plotted.

Cross-section at 2km u/s of the bridge:

Figures 5 to 8 show the cross-sections which were taken 2km apart from u/s of the bridge in May 1995, May 2002, April 2006 and January 2009 respectively. The alignment of the river is almost straight at 2 km and 7km u/s of the bridge. It is seen from the Figures 5 and 6 that the depth is increased at right bank, whereas decreased at left bank. It clearly indicates that the scouring is occurred at the right bank and deposition is occurred at the left bank from very beginning of the construction of the bridge.

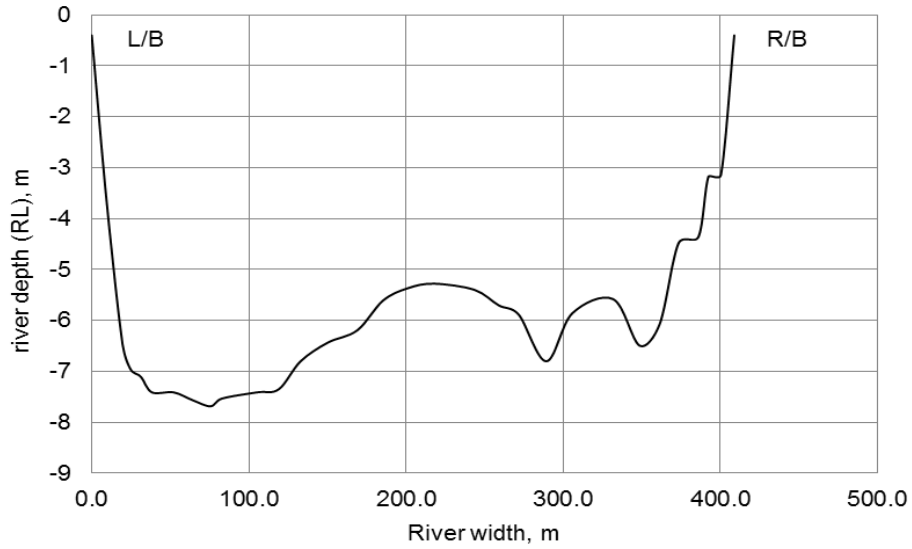

Figure 5: Cross-section at 2 km u/s from the bridge (at May, 1995)

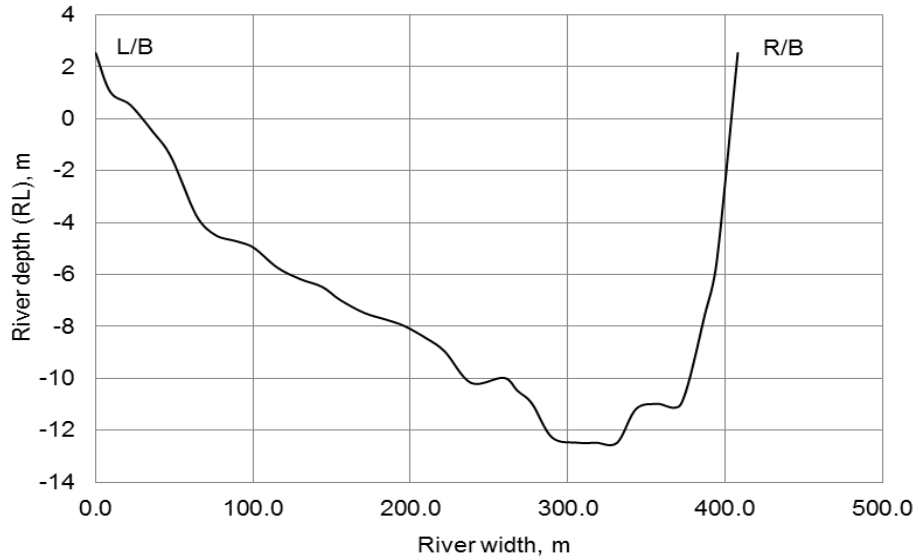

Figure 6: Cross-section at 2 km u/s from the bridge (at May, 2002)

Figures 7 and 8 show the cross-sections of the river which were taken at 2km u/s of the bridge and those were after completion of the bridge construction. It is seen that the left bank is slightly eroded after the construction but the right bank remain almost same. Hence, it is concluded that the river cross section has been changed due to the construction of the bridge at 2km u/s of the bridge.

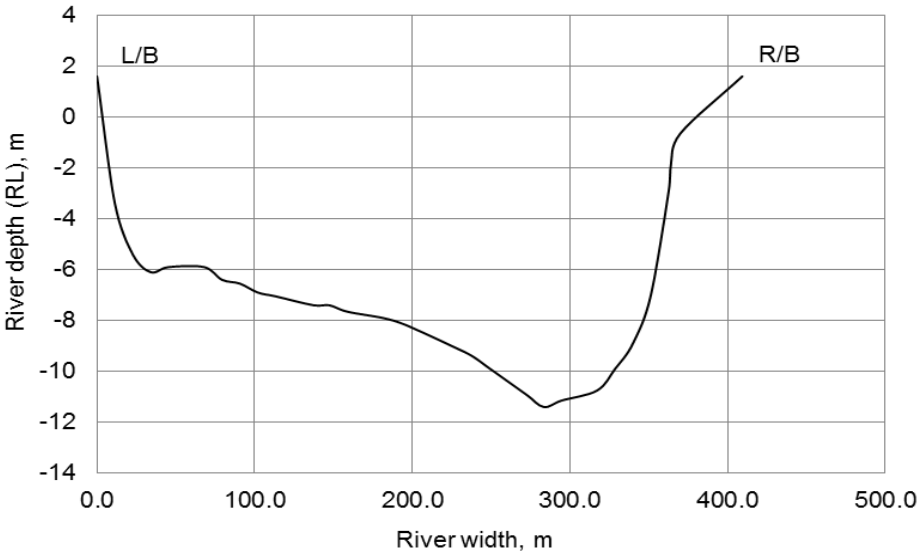

Figure 7: Cross-section at 2 km u/s from the bridge (at April, 2006)

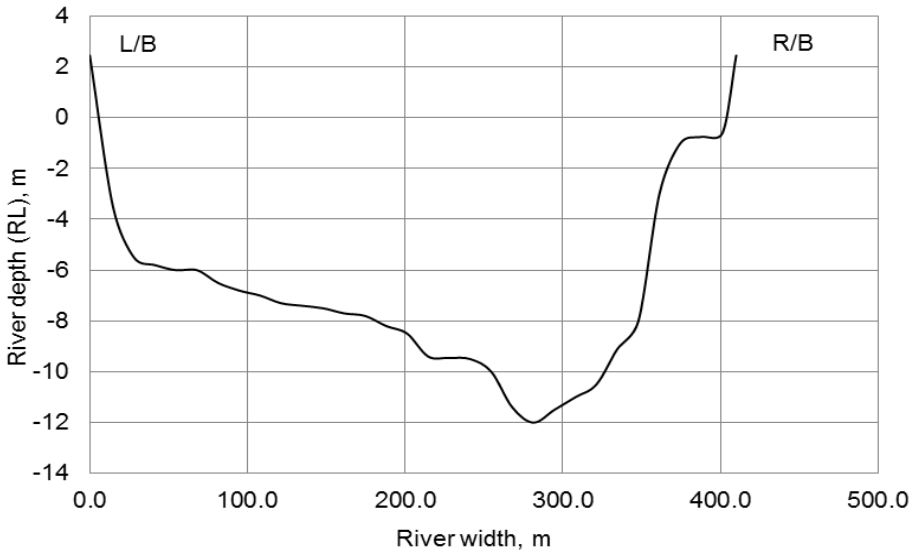

Figure 8: Cross-section at 2 km u/s from the bridge (at January, 2009)

Cross-section at 7km u/s of the bridge:

Figures 9 to 12 show the cross-sections at 7km u/s of the bridge in May 1995, May 2002, April 2006 and January 2009, respectively. It is seen from the Figure 9 and 10 that the depths are increased at both banks in which increasing rate is higher for the left bank. It clearly indicates that the scouring is occurred at both banks from very beginning of the construction of the bridge.

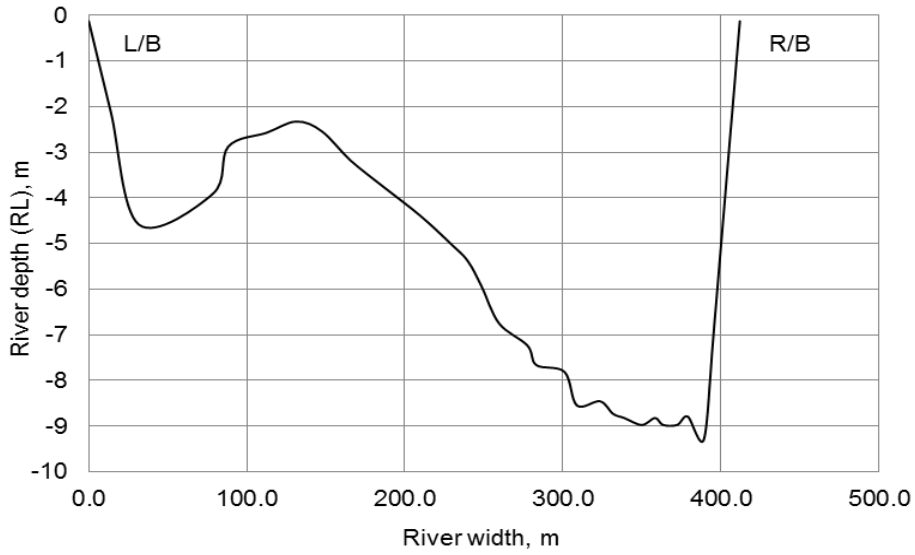

Figure 9: Cross-section at 7 km u/s from the bridge (at May, 1995)

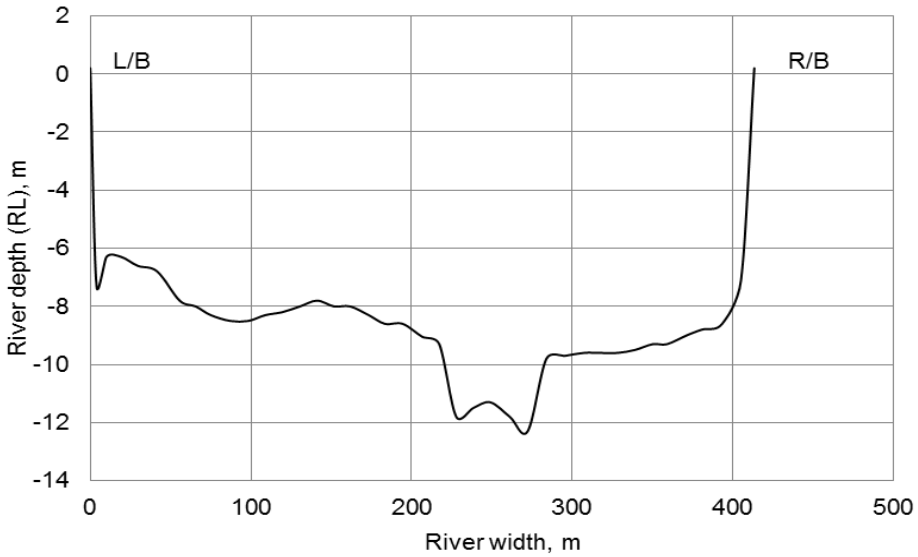

Figure 10: Cross-section at 7 km u/s from the bridge (at May, 2002)

Figures 11 and 12 show the cross-section of the river at 7km u/s of the bridge after completion of the bridge. It is seen that the river bed level increases for both banks in which increasing rate is higher at the right bank that clearly indicates that deposition has been happened. Hence, it is concluded that the river cross section has been changed due to the construction of the bridge at 7km u/s of the bridge.

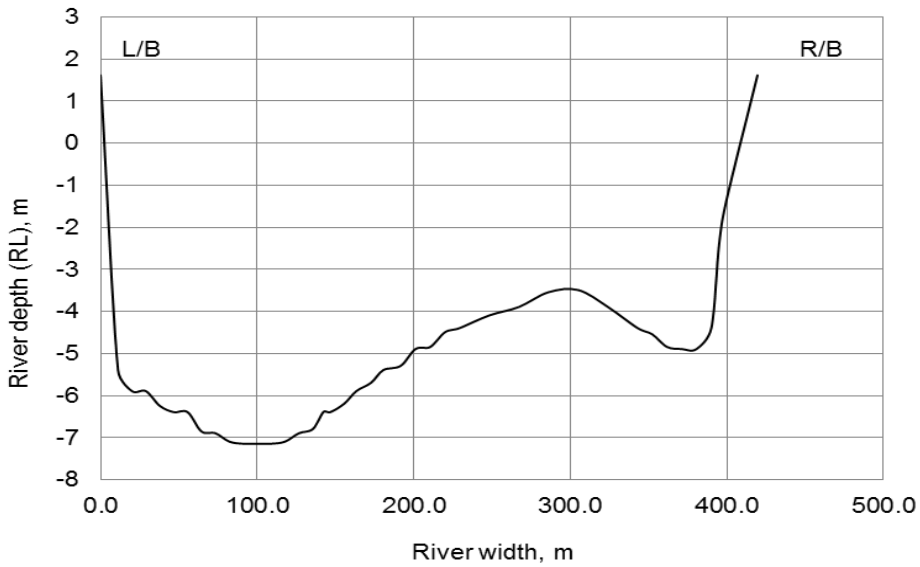

Figure 11: Cross-section at 7 km u/s from the bridge (at April, 2006)

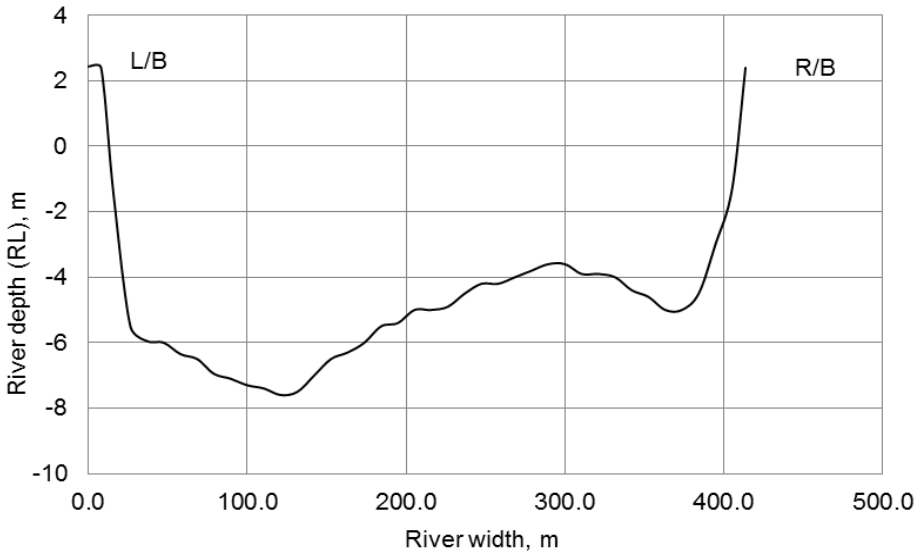

Figure 12: Cross-section at 7 km u/s from the bridge (at January, 2009)

4. CONCLUSIONS

The main purpose of this study was to assess the impact of the Khan Jahan Ali Bridge on water level, stream flow and channel geometry of the Rupsha River. It was calculated that about 15.75% flow path was obstructed by bridge pier. It was observed that from 2003 the maximum water level was rising than the previous time and the minimum water level initially increased after the construction of the bridge and then decreased. It was seen that near the bridge, the scouring was occurred at the right bank and deposition was occurred at the left bank from very beginning of the construction of the bridge. On the other hand, at far distance from the bridge, the scouring was occurred at both banks from very beginning of the construction of the bridge. It is concluded that the water level both minimum and maximum is rising as well as the river geometry is also changed after the construction of the bridge.

ACKNOWLEDGEMENTS

I would like to express my sincere thanks and appreciation to Dr. Kh. Md. Shafiul Islam, Professor, Department of Civil Engineering, KUET and to all the interviewers who helped to conduct in the data collection process.

REFERENCES

Bangladesh Water Development Board, (2012). *Processing & Flood Forecasting Circle*, Dhaka.

Biswas, S.K., (2010). Effect of bridge pier on waterways constriction: A case study using 2D Mathematical modeling, *IABSE-JSCE Joint Conference on Advances in Bridge Engineering-II,* August 8-10, 2010, Dhaka, Bangladesh. 370-376.

Kobayashi, N., (2011). Ex-Post Evaluation of Japanese ODA Loan, *Rupsha Bridge Construction Project,* 1-13.

Subramanya, K., (2013). *Engineering Hydrology* (3rd ed., pp. 109-111). New Delhi, India: Tata McGraw-Hill.

Proceedings of the 4th International Conference on Civil Engineering for Sustainable Development (ICCESD2018), 9~11 February 2018, KUET, Khulna, Bangladesh (ISBN-978-984-34-3502-6)

SPATIAL LOCATION OF SUITABLE PLACES FOR WATER DISTRIBUTION FACILITIES IN KHULNA CITY, BANGLADESH: APPLICATION OF GIS

Md. Nazmul Haque[1] and Md. Mustafa Saroar[2]

[1]Department of Urban and Regional Planning, Khulna University Engineering & Technology, Khulna-9203, Bangladesh, e-mail: nhaque.kuet13@gmail.com
[2]Professor, Department of Urban and Regional Planning, Khulna University Engineering & Technology, Khulna-9203, Bangladesh.

ABSTRACT

This study helps to find suitable location for water distribution facilities in Khulna city. For adopting the objective this research determined the demand of water supply system in Khulna city and planning of sufficient water supply and distribution location using GIS technique. Three main indicators are selected: (i) Flow Accumulation, (ii) Population density and (iii) Slope of Khulna city for suitability analysis. An increasing demand of water due to population growth and agriculture so proper distribution network system badly needed. Application of GIS in this project will help to planning a sufficient water distribution network. It has been carried out by developing various administrative information in GIS environment. Planning and designing in respective sectors like water distribution network, information of land use and population data has been carried out by using Arc GIS Software. The research suggests that only 2% area within Ward no. 12 & partially 24 are highly suitable for water distribution facilities.

Keywords: *Water supply, Distribution network, Reservoir.*

1. INTRODUCTION

The research will fulfil the agenda to find suitable location for water distribution facilities in Khulna city. Khulna is a low-lying city which has developed in a linear pattern alongside the bhairab and Rupsha Rivers in south western Bangladesh. Khulna is the country's third largest city in Bangladesh and has been known as an industrial city with a port. The whole city area is only 2.5 meters above the mean sea level. Khulna has a history of about one hundred years **(**Islam and Karim, 2006). A large amount of money is invested around the world to provide water supply facilities. Even an enormous population of the world is suffering by inadequate water supply system. Approximately 80% to 85% of the cost of a total water supply system is contributed toward water transmission and the water distribution network (Goulter,1992.) The city is surrounded by lots of industry nevertheless it has plenty of importance for its geographical, political, historical, and financial reasons. The scarcity of water has been increased gradually owing to increasing resettlement from the surrounding districts, for rapid urbanization and industrialization but lack of parallel growth in necessary water supply infrastructure (Islam and Karim, 2006)**.** It is geographic information system (GIS) that is been used for analyzing the data both spatial and attribute. It is convenient to sort out the suitable data from a vast amount of data set using GIS. Geographic information system helps us to analyze all types of data for any purposes.The multi criteria analysis is one of them. The multi criteria analysis helps to find out the suitable places for a desired query.

The outcome of the study shows the demand of the water supply system in Khulna city, existing distribution network of water in the city is not able to distribute sufficient amount of water to every houses in the city. So this study helps to finding suitable location for water distribution to reduce the problem of water supply system as well as minimize the cost. There are 56 production wells and 12000 hand tube wells in Khulna city. The average depth

of the tube well is 270m (IWM, 2011). There are some limitations which should be overcome by this study such as not enough attribute information about existing water distribution system, there is a little provision of criteria for water distribution are found with respect of Bangladesh, so some standards are taken from different country requirement for water distribution properly.

2. LITERATURE REVIEW

For finding suitable location of water distribution system, the existing water distribution system of Khulna city must be known. Existing condition shows that Khulna city water supply system entirely depends on groundwater source. The population of Khulna city is increasing day by day and thus increasing water demand. To meet the future water demand in Khulna city the provision of extension of groundwater development is very limited. Therefore, to fulfil the future water demand it is very essential to find suitable location for water distribution system.

Table 1: Basic Demographic Information

Ward	Pop 2001	Pop 2009	Pop 2010	Pop 2015	Pop 2020	Area(sq.km)
Ward-1	20311	25230	25730	28420	31370	2.227856
Ward-2	18815	23370	23830	26320	29060	2.179358
Ward-3	23016	28590	29150	32200	35550	3.657733
Ward-4	14299	17760	18110	20010	22080	2.034172
Ward-5	15314	19020	19400	21430	23650	0.775361
Ward-6	20995	26080	26590	29370	32430	2.159462
Ward-7	14808	18390	18760	20720	22870	0.471743
Ward-8	18545	23030	23490	25950	28640	0.943937
Ward-9	34614	42990	43850	48430	53460	3.540127
Ward-10	18518	23000	23460	25910	28600	0.809781
Ward-11	19398	24090	24570	27140	29960	0.364905
Ward-12	52036	64630	65910	72800	80370	0.659046
Ward-13	19959	24790	25280	27920	30830	1.119565
Ward-14	26444	32840	33500	37000	40840	2.691663
Ward-15	25724	31950	32580	35990	39730	1.659229
Ward-16	35881	44570	45450	50200	55420	2.253474
Ward-17	30352	37700	38450	42470	46880	2.298736
Ward-18	16765	20820	21240	23460	25890	1.617838
Ward-19	26321	32690	33340	36830	40650	0.492191
Ward-20	22539	27990	28550	31530	34810	0.499665
Ward-21	24984	31030	31650	34950	38590	1.725098
Ward-22	21633	26870	27400	30270	33410	0.825691
Ward-23	18332	22770	23220	25650	28310	0.510105
Ward-24	42959	53360	54420	60100	66350	1.678222
Ward-25	27106	33670	34340	37920	41860	0.762184
Ward-26	18087	22470	22910	25310	27930	0.664920
Ward-27	31489	39110	39890	44060	48630	0.811904
Ward-28	22404	27830	28380	31350	34600	0.735918
Ward-29	20431	25380	25880	28580	31550	0.659339
Ward-30	35827	44500	45380	50130	55330	1.320933
Ward-31	32592	40480	41290	45580	50350	3.902639

Table 1 shows the population wise data of KCC and the area of each ward. Demand of safe water of the people should increase with the increase of population. As a general rule, a goal must be: S M A R T

(Specific – measurable – attainable – relevant – time-bound)

The aim of the study is to identify the suitable location for the water distribution system in Khulna city, Bangladesh. Through investigation by GIS and decision making process is done.

3. MATERIALS AND METHODS

3.1 Study Area

Khulna city was selected as the study area. Khulna is a low-lying city which has developed in a linear pattern alongside the Bhairab and Rupsha Rivers in south western Bangladesh.

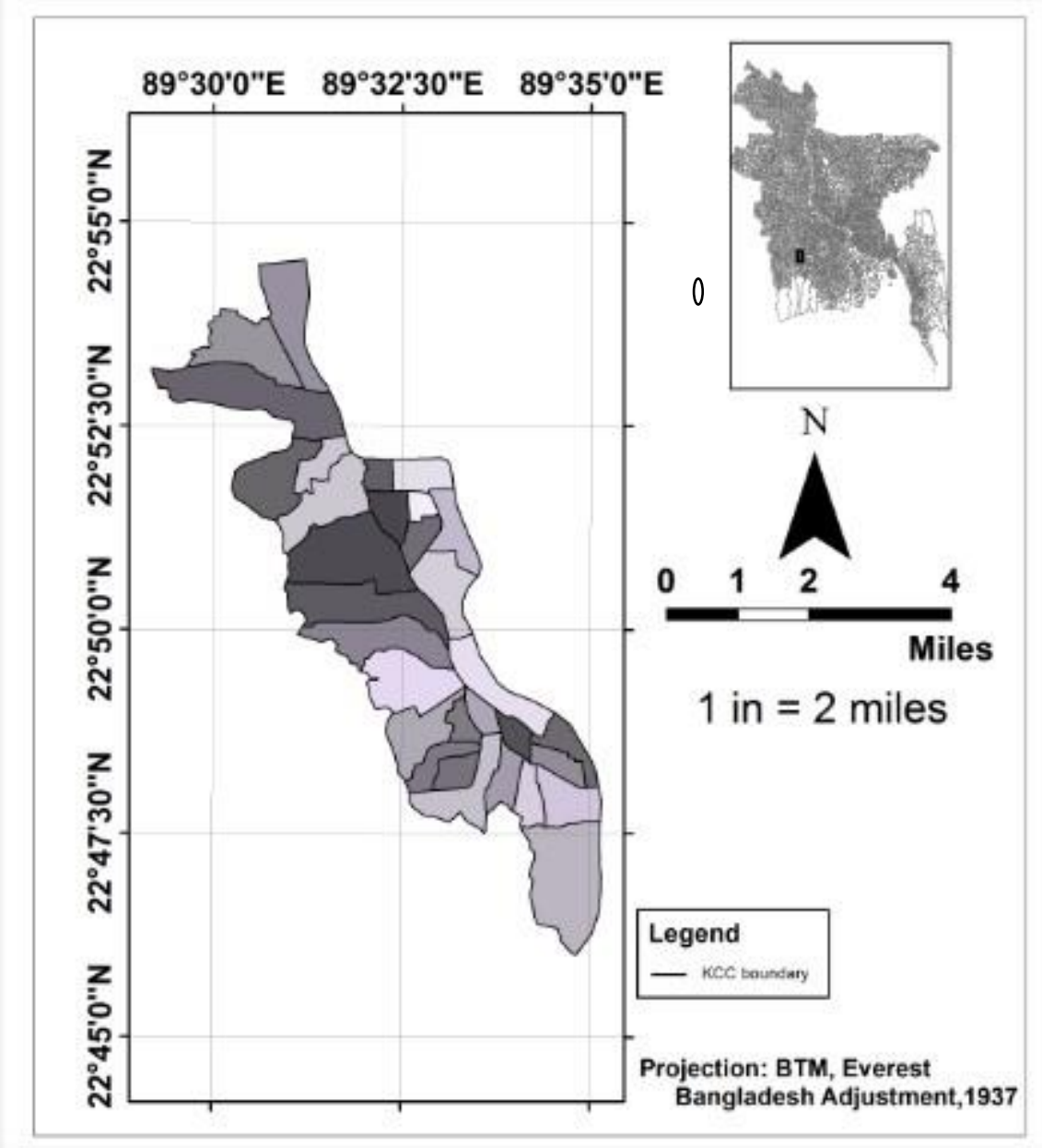

Figure 1: Study Area (KCC), Author 2017

Khulna is the country's third largest city in Bangladesh and has been known as an industrial city with a port. The whole city area is only 2.5 meters above the mean sea level. Khulna has a history of about one hundred years(Islam and Karim, 2006).

Khulna was declared a municipality in 1884, became a railway link in 1985, district headquarters in 1961, and a city corporation in 1984. The linkages of Khulna city with other towns and growth centers can make it a most important city.

3.2 Criteria Selection

The criteria standards are taken from the GIS analysis of KCC boundary and spatial data. The divisions of the classes are randomly taken on the basis of the data by analysing the highest and the lowest value are observed from the study

Table 2: Criteria Selection

Criteria	**Suitability classes**		
	Highly suitable (3)	Moderately suitable (2)	Less suitable (1)
Flow accumulation	3227 to 6453	851 to 3227	0 to 851
Population	4146 to 6089	2183 to 4146	230 to 2183
Slope (mm)	2440 to 3660	1220 to 2440	0 to 1220

Source: Expert opinion Survey, 2017

Here the suitability classes are classified on the basis of Author's calculation from the data collected. Three equal interval value are taken to identify the classes. For weighing the criteria's (%) of influence also setting up on the basis of expert opinion survey that what (%) may be given for each factor.

Table 3: Weight of Criteria's

Criteria	**(%) influences**
Flow accumulation	20%
Population	50%
Slope	30%

Source: Expert opinion Survey, 2017

As the influence of population is very high in any spatial planning, the value of % influences are high than any other Criteria. Here the influences are taken randomly on the basis of traditional thoughts.

3.3 Ranking

The ranking are done here on the basis of preliminary investigation where 1 shows the least important, 2 shows moderate important and 3 shows the most important class. At last the suitable locations are selected for the proposed water distribution. Expert opinion survey was done to get the sequence of ranking of the suitability.

4. RESULTS AND DISCUSSION

In this section there are different types of DEM are used for the analysis of the suitable location for water distribution. Three types of map are produced to identify the most suitable location for each criteria. From the map the most suitable, less suitable and the moderately suitable sapatial location are marked and further investigation are done to select the overall suitable place for water distribution facilities in Khulna city. Then the zonal districts was calculated from the map to determime the percentage of each portion.

4.1 Population Map

Here the population concentration map was generated by using the spatial and attribute data. The map shown that the maximum and minimum concentration of population 72800 and 20010 respectively. The most suitable ward is 24 and partially 12 for performing the concentrated population density in Khulna city. So, this places should be marked to

introduce new water distribution stations to serve the defeciency need of resedential people as Nirala (Wrad 24) is a high class residential area. It is known that where the resedence are higher the need of water is incresing. If the location of the distribution facilites are very close to the densed area or over popuated area it would be more acceptable.

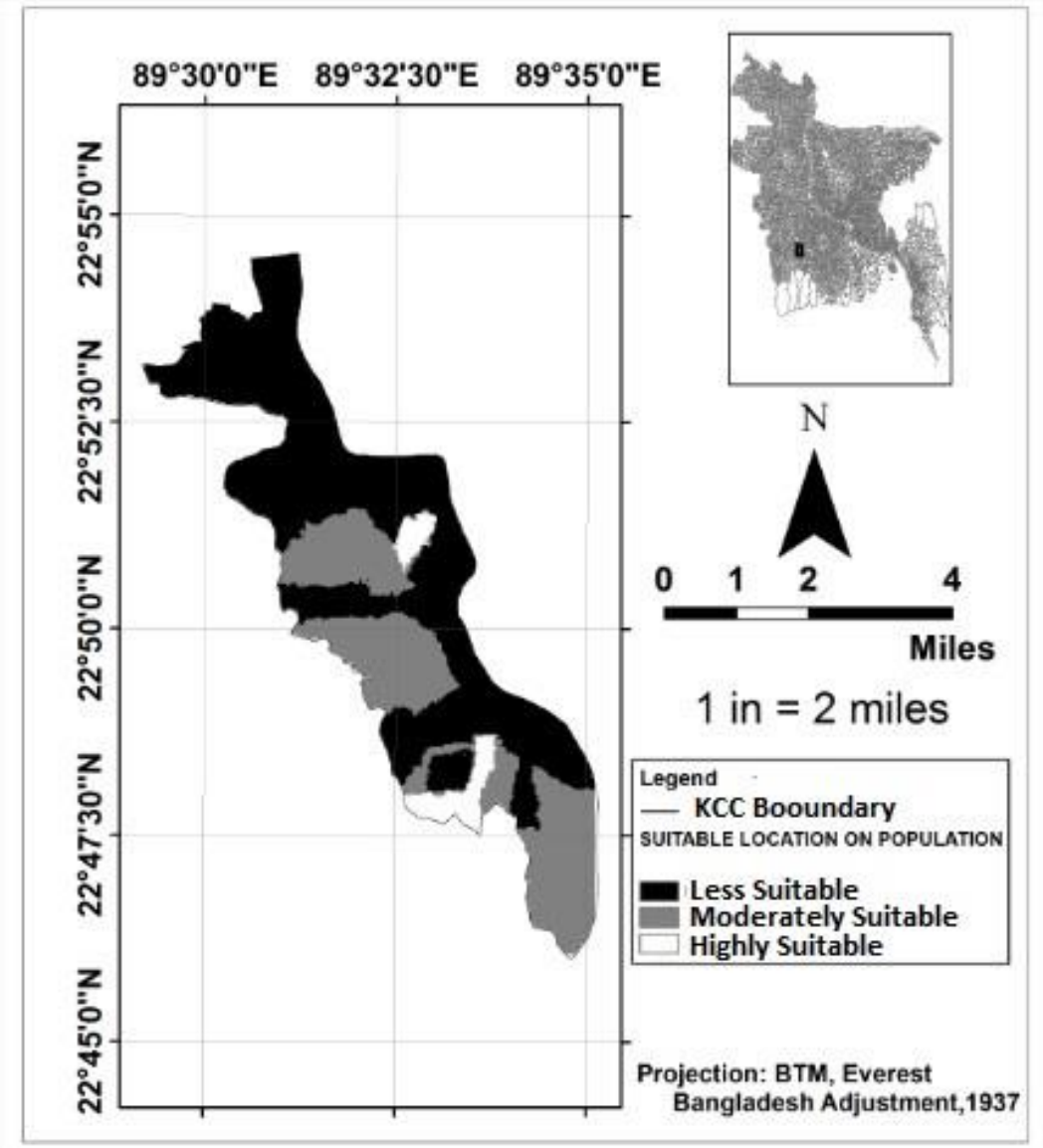

Figure 2: Suitable location on Population Density; Author, 2017

4.2 Flow Direction Map

The flow map shows linear movement between places. As such, they are popular maps to represent migrations, commodity flows, traffic patterns and water movement. Flow maps may be used to show both qualitative data (e.g., connections) and quantitative data (e.g., magnitudes). In qualitative flow mapping, the symbols are of uniform width and typically are arrows. In quantitative flow mapping, the line symbol selected and alters its width based on the data values.When employing this technique, flow lines should be symbolized so they are distinct from the background base map. Use arrows if the direction of the flow is important. Using lines instead of arrows implies that the direction occurs in both directions. Also, place small lines on top of large lines when they overlap.

In the following figure 3 the black coloured area indicates that this areas are less suitable for flow accumulation capacity since the elevation of the area is too high so new water distribution facilities may be established in any other place of white coloured. Generally it is

known that the higher elevation may use to store the water so that water can easily distributed to the locality. The map also indicates that flow of water may prevail much in white portion to other section so it can be easily said that these areas are most suitable to establish new water distribution facilities.

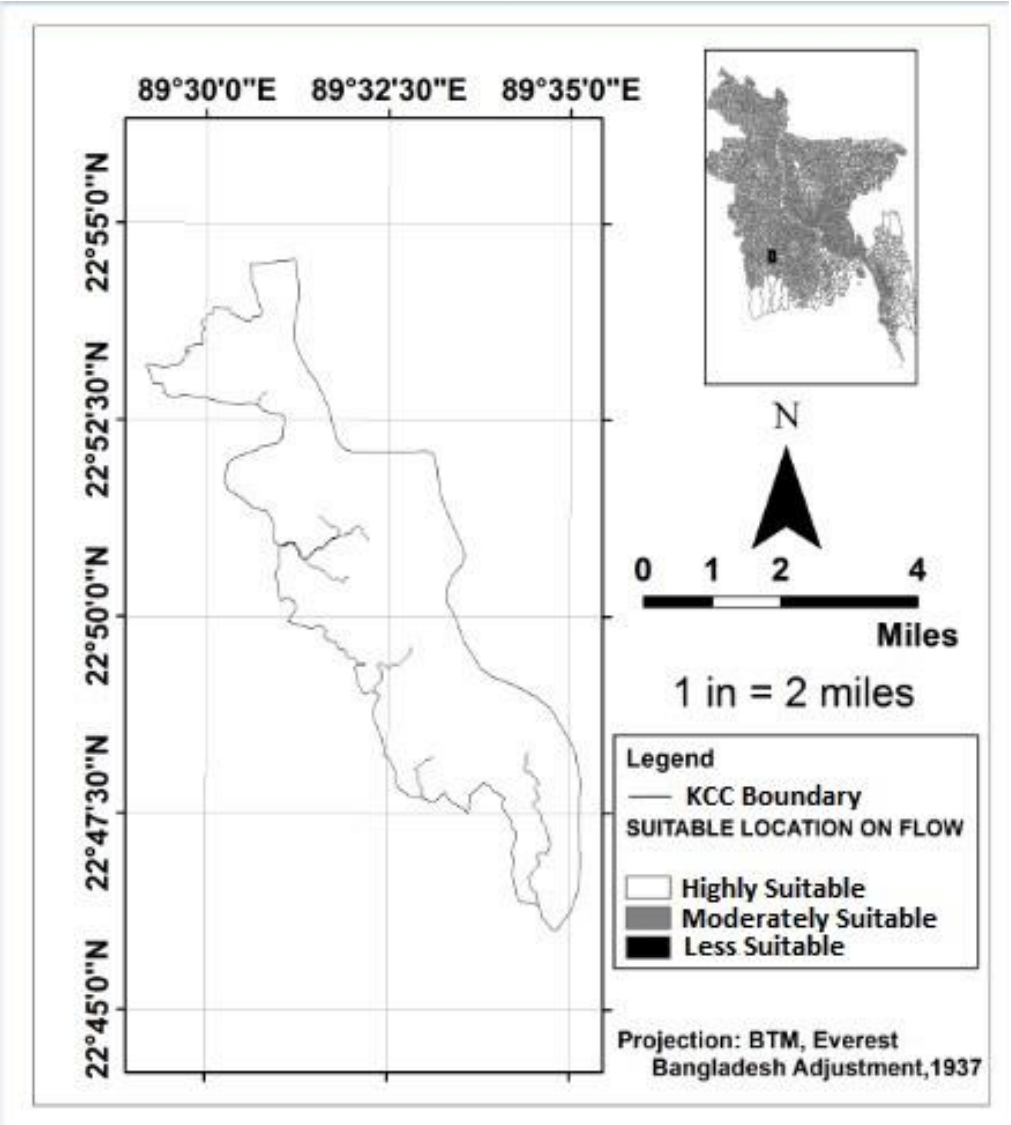

Figure 3: Suitable location onFlow direction; Author, 2017

4.3 Slope Showing Map

Slope is the measure of steepness or the degree of inclination of a feature relative to the horizontal plane. Gradient, grade, incline and pitch are used interchangeably with slope. Slope is typically expressed as a percentage, an angle, or a ratio. To find the slope of a feature, the horizontal distance (run) as well as the vertical distance (rise) between two points on a line parallel to the feature need to be determined. The slope is obtained by dividing the rise over run. Multiply this ratio by 100 to express slope as a percentage.

The highest slope of the area is about 4.70 where the lowest is about – 4.48. Here the less suitable location on the basis of population density shows the highly suitable location for slope identity. So there is a near for introducing a common map where all criteria's should be judged on different influences

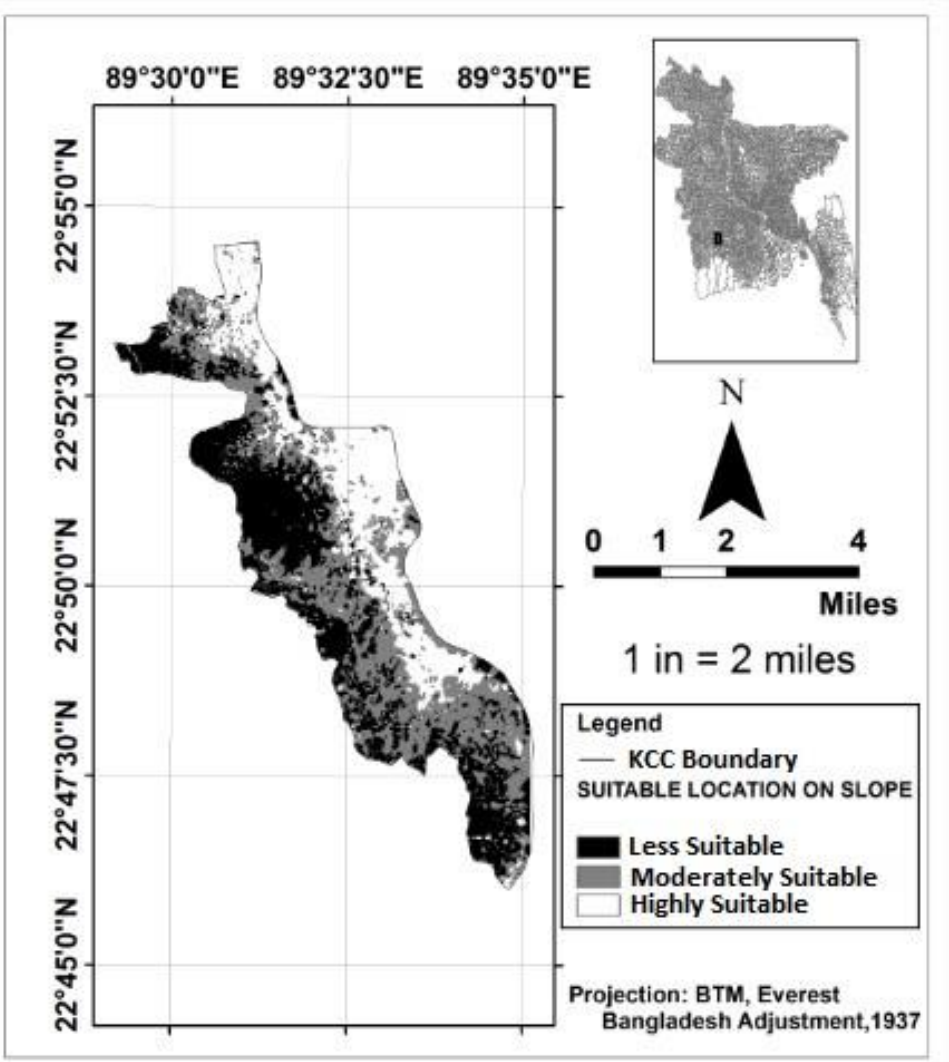

Figure 4: Suitable location onSlope; Author, 2017

4.4 Weighted Overlay Analysis

The three factors used in this weighted overlay analysis, Reclassify from Flow accumulation population concentration, and slope map. Weighted overlay analysis enables factors to be combined and weighted to solve multi-decision problems in this case selecting suitable site for water distribution. The three factors were loaded in the weighted overlay tool by setting the evaluation scale to 1 to 10 to 1 to agree with the reclassification of input to 3 interval classes. These classes were ranked as the high, moderate and less suitable location for siting water distribution. The factors were assigned percentage of influence with Euclidean distance from the slope, flow accumulation and the population concentration and here 30, 20 and 50 percentages was used for the flow accumulation, population concentration and slope respectively. The suitability map was produced from the input as shown in the figure 5 below.

Euclidean distance tools describe each cell's relationship to a source or a set of sources based on the straight-line distance. Second tool is Reclassify .It reclassifies the values in a raster. Here the output of Euclidean distance is reclassify base on established Criteria. Output of reclassify have 3 value one is Less suitable, second is Moderately suitable and other is Highly suitable.

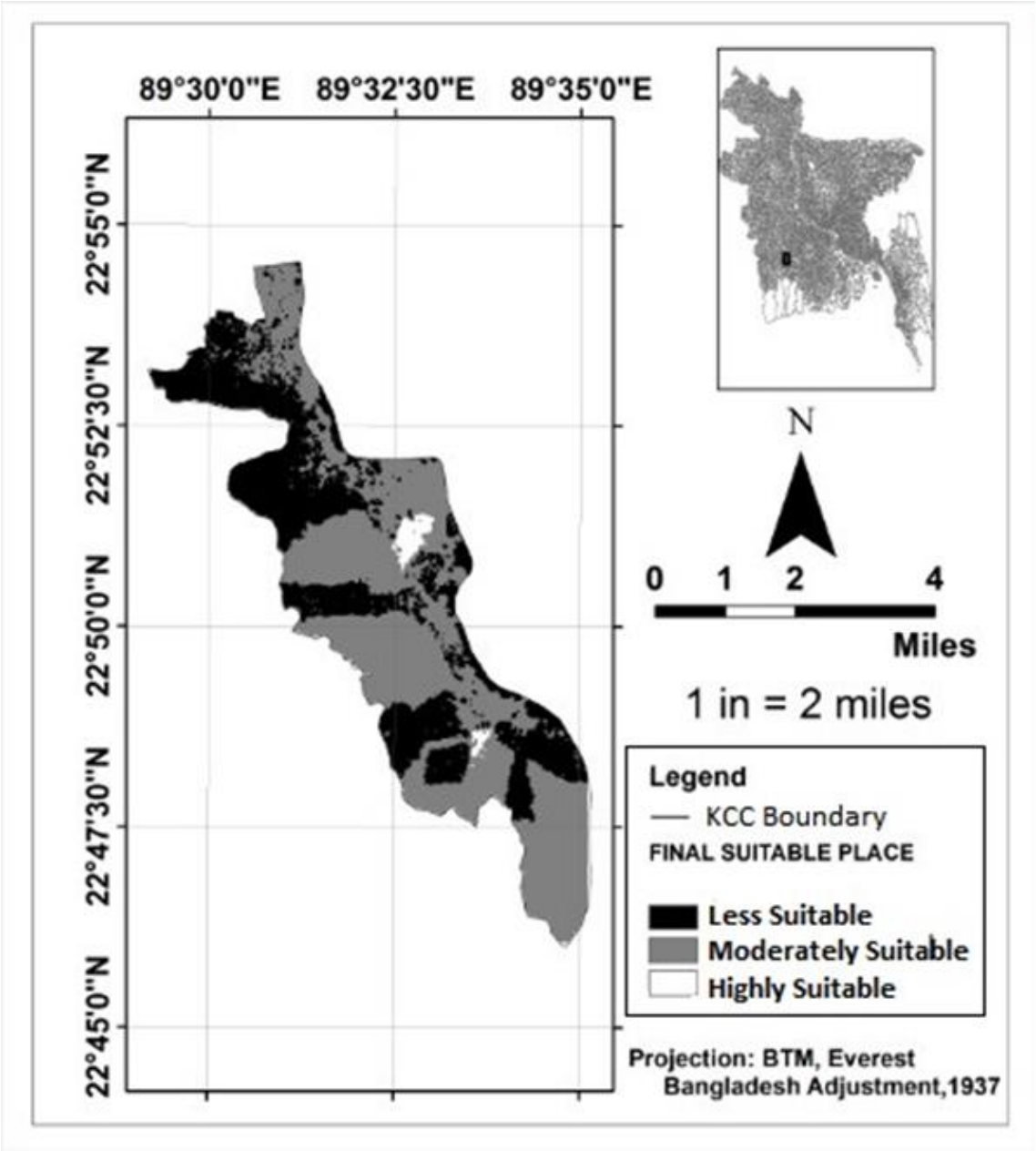

Figure 3: Suitable location for water distribution facilities, Author 2017

5. CONCLUSIONS

The map indicates that black coloured area stands for the less suitable location. That means the water distribution facilities may not give there as the density of population is low as well as low elevated area and flow direction is also not satisfactory.The grey coloured area shows the moderately suitable location for the purpose. Finally the white area is the most suitable for the project area to provide water distribution facilities as the all conditions are satisfied the criteria's. The research suggests that only 2% area within ward no. 12 & partially 24 are highly suitable for water distribution facilities.This kind of study gives knowledge about which involved with their use in each component and be demanding that those components work together, both initially and into the future.

ACKNOWLEDGEMENTS

Special thanks to Md. Esraz-Ul-Zannat, Assistant Professor and Tanmoy Chakraborty, Lecturer, Department of Urban and Regional Planning, KUET for their cooperation and valuable comments on this research.

REFERENCES

Eastman, R J (2006). Idrisi Andes: Guide to GIS and image processing. Clark Labs, Clark University, Worcester,USA.

Estoque, R C & Murayama, Y (2010). Suitability analysis for beekeeping sites in La union, Philippines, using GIS & MCE techniques. Research Journal of AppliedSciences, 5, 242 – 253.

Goulter, I. C. (May, 1992.). Systems analysis in water-distribution network design: from theory to practice3. Journal of Water Resources Planning and Management.

IWM. (2011). Preparing the Khulna Water Supply Project. Khulna: 7385-BAN, Final report TA.

Karim, Islam. (2006). Small Scale Private Real Estate Business- challenges to the sustainable urbanization: a case study of Khulna city. Khulna University.

Study Report on ―Groundwater Resources and Hydro-Geological Investigations in and around Khulna City", FINAL REPORT-Volume-1, Municipal Services Project, LGED, Khulna, May 2005.

Proceedings of the 4th International Conference on Civil Engineering for Sustainable Development (ICCESD 2018), 9~11 February 2018, KUET, Khulna, Bangladesh (ISBN-978-984-34-3502-6)

WATER PRICING IN FOUR SLUMS OF BARISAL CITY CORPORATION: AN ANALYSIS

Muhammad M Rahaman[1] and Md S Khan [2]

[1] Professor, Department of Civil Engineering, University of Asia pacific, Bangladesh, e-mail: rahamanmm@gmail.com
[2]Graduated student, Department of Civil Engineering, University of Asia pacific, Bangladesh, e-mail: khanmdshafim@gmail.com

ABSTRACT

Nowadays, getting quality water has become very expensive for many developing countries. Despite being a riverine country, it has become a major challenge for Bangladesh to provide quality water at a reasonable price to the citizens. That is why an analysis is necessary to find out the current water pricing of Barisal City Corporation and to compare it with other cities around the world. This paper attempts to find out the current water pricing and affordability in four selected slums of Barishal City Corporation (BCC), i.e. Stadium Colony slum, Vatar Khal slum, Palaspur Guchchogram slum and Namar Char Slum. The aim of the paper is to generate a deeper understanding of the water pricing problems and to recommend some alternatives to improve the situation in the slums of BCC. A field survey has been performed in January 2017 that involves semi structured questionnaire survey and focused group discussions with slums dwellers and different stakeholders. It is found that the slums dwellers who are using the legal connection from Barisal City Corporation water supply system are paying around 40 to 80 times more than the people living in apartment complexes at Barishal City Corporation. Even slum dwellers are paying much more than the residents of many developed countries in the world. According to the chapter 1 of Bangladesh Water Act 2013, access to water for drinking and domestic uses is being considered as basic right to all citizens specially for poor and disadvantaged group of the society. For this reason an income sensetive affordable water pricing is necessary to in the slums in the Barishal City Cooporation where poor segment of the society resides. Water pricing can also play an effective role in acheiving sustainable development goals related to water.

Keywords: *water pricing; slum dwellers; Barisal City Corporation; affordability*

1. INTRODUCTION

Water is the most versatile of all elements. Every living organism in the world needs water to survive. The percentage of water in human body is approximately 70% by weight. The human brain is made up of 95% water. According to research every adults uses around 80-100 gallons of water daily (Perlman, 2016).

From the begging of human era water is being considered as a symbol of devotion and purity. Most of the cities have been established based on availability and access to water (WWAP, 2016). But water scarcity has become one of the major problems of the 21st century (Griffin, 2001). Scientists declared that there is enough fresh water on the planet for seven billons people but it is not distributed evenly and too much of it is being wasted, polluted or unsustainably managed (Mekkonen and Hoekstra, 2016). Mekkonen and Hoekstra (2016) found that four billion people or two-thirds of the global population are facing water scarcity at least 1 month of the year. Around half of those people live in Asia.

For this reason, ensuring affordable water pricing has become a urgent need for the society.. Bangladesh is not an exception. The major cities of Bangladesh are facing the challenge to provide affordable quality water to its residents especially in the slum areas (cf. Rahman and

Ahmed, 2016; UN-Habitat, 2003). This study focuses on the current water pricing in the slum areas of one of the major cities of Bangladesh, Barishal City Corporation.

The objectives of this study are as follows

- To find out the water pricing in four selected slums of Barishal City Corporation (BCC);
- To find out what percentage of income the slum dwellers are spending for water;
- To compare the water pricing in selected slums of BCC with other cities in the world.

2. METHODOLOGY

In Barisal City Corporation, there are around 137 slums with a population of 38,736. Among these 137 slums, this study focused on four major slums namely Stadium Colony Slum, Vatar Khal Slum, Palaspur Guchchhogram Slum and Namar Char Slum.

For the study a questionnaire survey has been conducted on January 2017 at Barisal City Corporation. Data have been collected through focus group discussions with the slums dwellers in the study area. Secondary data has been collected from journal articles, books, relevant databases and government and non-governmental organizations.

3. ANALYSIS AND RESULTS

3.1 Water pricing in the selected slums

The selected study slums are located near the main river of Barisal, namely, Kirtankhola. These four slums consists of total of 3151 households with 10458 residents. Table 1 presents the basic information about the study area.

Table 1: Basic information about the study area

Survey Area	Household	Population	Sources of water
Stadium colony Slum	756	1588	tube well and river water
Vatar Khal Slum	346	1206	tube well, river and BCC connection water
Palaspur G.Gram Slum	1898	7116	tube well, river and BCC connection water
Namar Char Slum	151	549	tube well and river water

(Source: BBS, 2014)

In the slums of Barisal City Corporation, the availability and affordability of legal connection is out of reach of the slum dwellers. The slum dwellers mainly rely on tube well water as well as river water for their daily drinking and domestic needs. It is observed that Barisal City Corporation (BCC) does not supply water to its resident in quantity basis. BCC charges BDT 200 (0.75 inch pipe diameter) per month for a residential connection with a onetime installation cost of BDT 6900. In this circumstance, the apartment complex residents install a single connection line for the whole building where almost 10-20 families reside. On the other hand, the slum dwellers take a connection line for 2-5 families, which generate a huge discrimination in terms of money spent for water in between the people of apartment complex and the slum dwellers

The slum dwellers of BCC are suffering a lot due to lack of water. They do not get clean and safe water in most of the cases. From the field survey, it is found that people from the apartment complex spend only 1.7 BDT for 1000 litres water and the slum dwellers of Vatarkhal and Palaspur Guchchhogram spend around 40.42 BDT and 78.6 BDT. By discussing with the slum dwellers, it is found that they are willing to take the connection from BCC but the installation cost and monthly cost is very high for them. Table 2 shows the current water pricing and residents' willing to pay for (1000 litres water) in selected slums in

Barisal City Corporation. And table 3 shows the percentage of income spent for water in selected slums in Barisal City Corporation.

Table 2: Current price and Resident's willing to pay for (1000 litres water) different slums in BCC

Name of slums	Current water price (BDT/1000 litres)	Resident's willingness to pay (BDT/1000 litres)
Stadium colony Slum	0	69.04
Vatar Khal Slum (legal)	40.42	24.73
Vatar Khal Slum (illegal)	0	50.86
Palaspur G.Gram Slum (legal)	78.6	38.22
Palaspur G.Gram Slum (illegal)	0	32.7
Namar Char Slum	0	55.3

It is quite surprising that the slum dwellers are spending high amount of their income percentage for water rather than the residents of apartment complex.

Table 3: Income percentage spent for water at different slums in BCC

Stadium colony Slum	Vatar Khal Slum		Palaspur G.Gram Slum		Namar Char Slum
	Legal	Illegal	Legal	illegal	
0%	1.64%	0%	1.24%	0%	0%

3.2 Water pricing in different cities

The cost of supplying water varies significantly between western and developing nations, but prices are rising all around the world (Rahaman and Varis, 2005). Africa and Asia have the highest rate of urbanization and the continued growth of cities has not kept up with the increase in population. This has put even more pressure on the existing water supply and it leaves many people, particularly those in the slums, without access to safe drinking water. Among 160 million people of Bangladesh, around 4 million people do not have safe water and 2.2 million of them living in slums. According to Census of Slum Areas and Floating Population 2014, 97.25% slum dwellers in BCC use tubewell water and only 2.39% people use the tap water from BCC (BCC, 2016).

In figure 1, a comparison of water tariffs in Dhaka Water Supply and Sanitation Authority (Dhaka WASA), Barisal City Corporation and the four selected slums in BCC are shown. It reveals that the slum dwellers in the study area of BCC are paying a very high amount (around 40 to 80 times) for water in comparison to the city dwellers residing in apartment complex of BCC. This is an injustice to the slums dwellers considering their economic condition. This discrimination is happening because BCC do not have quantity based water supply system. This system needs to be improved for bringing a proper balance between the slum dwellers and the residents of apartment complex.

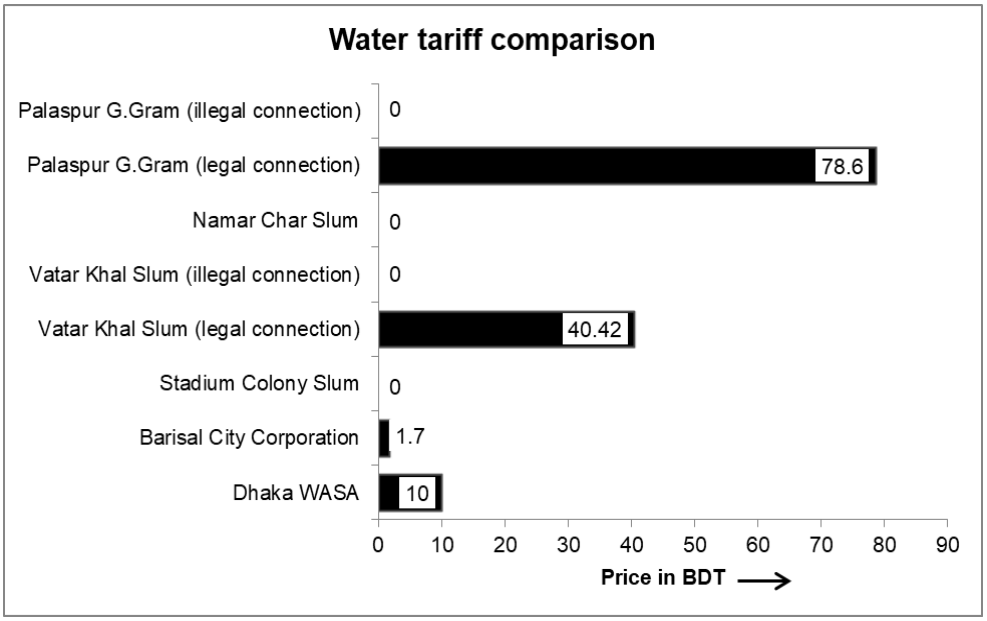

Figure 1: Water tariff per 100 litres in different slums and cities
Source: Rahman and Ahmed, 2016

Rahaman and Ahmed (2016) conducted a similar study in three slums of Dhaka City, namely, Koral slum, Godown slum and Tejgaon Slum. Figure 2 shows the water pricing n the selected slums of BCC and three slums in Dhaka. The water pricing in Palashpur Guchchhogram Slum of Barisal City Corporation is around BDT 78.6. Only slum dwellers in Korail slum of Dhaka are paying higher than that amount.

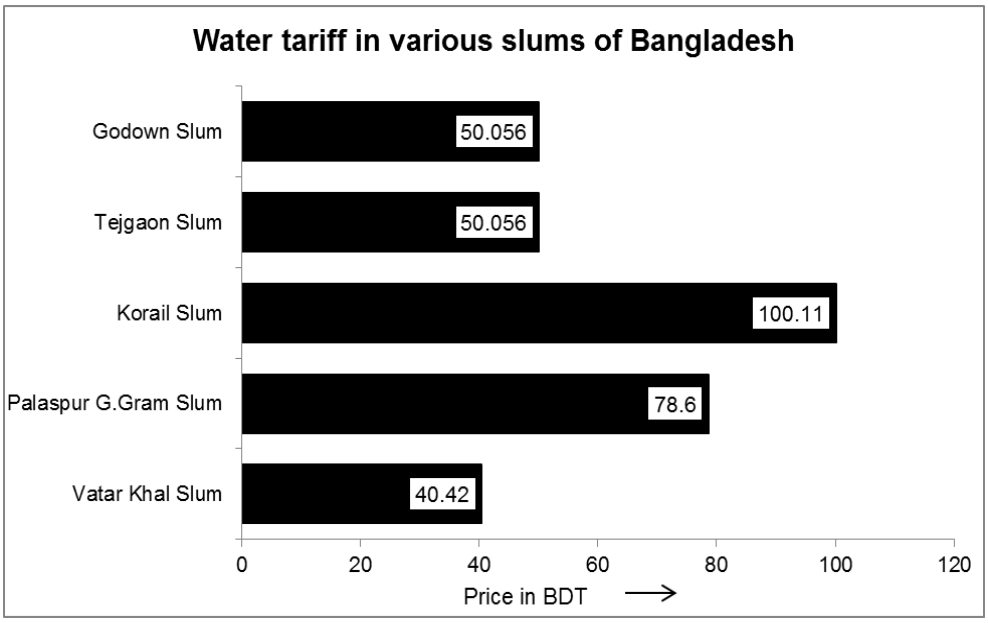

Figure 2: Water tariffs in selected slums of Dhaka City and Barishal City
Source: Rahaman and Ahmed (2016)

Figure 3 provides a graphical representation of water pricing around the world and in the selected slums of BCC. Figure 3 shows that the slum dwellers of Barisal City Corporation are paying higher amount of money for water in comparison to many developed western countries.

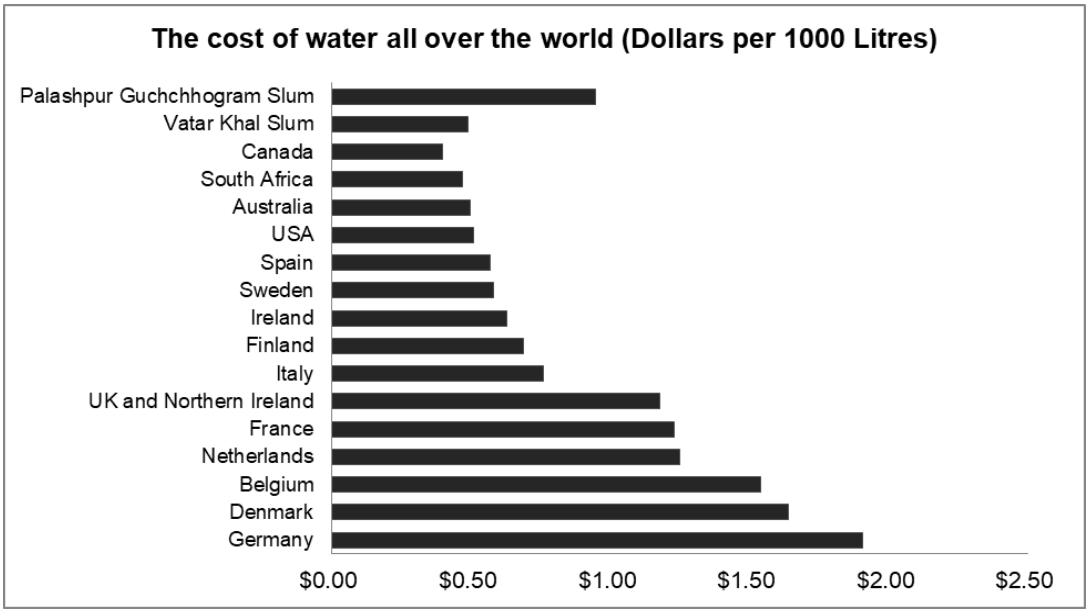

Figure 3: Water pricing per 1000 litres in selected countries
Source: Rahaman and Ahmed, 2016

In most of the developed countries, the price of 1000 litres water is below 1 USD which is maximum 0.1% of their income (Rahaman and Ahmed, 2016; Olmstead et al, 2007), but residents in the selected slums of BCC are paying almost same or higher then those countries. Table 4 shows the water pricing in different countries around the world and in the selected slums in BCC.

Table 4: Water pricing (1000 L) in selected countries

Country	Price (USD)	Price (Bdt)
Germany	$1.91	158.8165
Denmark	$1.64	136.366
Belgium	$1.54	128.051
Netherlands	$1.25	103.9375
France	$1.23	102.2745
Uk And Northern Ireland	$1.18	98.117
Italy	$0.76	63.194
Finland	$0.69	57.3735
Ireland	$0.63	52.3845
Sweden	$0.58	48.227
Spain	$0.57	47.3955
Usa	$0.51	42.4065
Australia	$0.50	41.575
South Africa	$0.47	39.0805
Canada	$0.40	33.26
Dhaka Wasa	$0.12	9.978
Barisal City Corporation	$0.02	1.663
Vatar Khal Slum	$0.49	40.7435
Palashpur Guchchhogram Slum	$0.95	78.9925

Source: Rahaman and Ahmed, 2016

4. CONCLUSIONS

This study analysed the current water pricing in four selected slums of Barishal City Corporations, i.e. Stadium Colony slum, Vatar Khal slum, Palaspur Guchchogram slum and Namar Char slum.

From this study, it is found that people residing in the apartment complex with legal connection from Barishal City Corporation spend only 1.7 BDT for 1000 litres of water and the slum dwellers of Vatarkhal and Palaspur Guchchhogram slums spend around 40.42 BDT and 78.6 BDT respectively, for the same amount of water. In addition to that, the slum dwellers are spending a higher percentage of income for water than people living in apartment complex in BCC. It is quite surprising that the slum dwellers with the legal connection of water from BCC are spending a very high amount for 1000 litres water even more than many developed countries (see Figure 3). This is a clear injustice to the slum dwellers considering their economic condition.

Still, slum dwellers in the four selected slums without having legal connections from BCC, are willing to take the legal connections of water from BCC. But they could not get the connections, as the installation cost is very high. Their willingness to be connected with BCC water supply system is due to the fact that the water quality from the illegal tube wells and river water is unsafe and unreliable. Collecting water from tube wells and river requires lots of efforts and it is not possible to have access to those sources all the time. If Barisal City Corporation provides water connections with low installation cost and price water on quantity basis; the slums dwellers in the selected slums will have access to better quality of water with an affordable price.

5. RECOMMENDATIONS

On the basis of the analysis on water pricing in four slums of Barisal City Corporation, following steps could improve the accessibility of quality water by slums dwellers in the study area:

- Since slum dwellers live in an illegal space in Barisal city, BCC can build a separate water supply system for the slum dwellers;
- Considering the poor economic condition of slum dwellers, BCC can provide connection with negligible installation cost and with a monthly rate based on water quantity;
- A treatment plant can be established to maintain the water quality, as the current quality of BCC is not good enough;
- Slum dwellers' not connected BCC water supply networks are collecting water from different unsafe water sources like tube wells and river. So BCC should ensure that the existing tube wells and surface water sources are safe.

ACKNOWLEDGEMENTS

Authors would like to appreciate the financial assistance of the Department of Civil Engineering, University of Asia Pacific, Dhaka, Bangladesh. Special thanks are due to Tariqul Islam and Mahadi Hasan Rabby for participating in the field study.

REFERENCES

Barisal City Corporation, (2016). Barisal City at a Glance: Barisal City Corporation. [online] Available at: http://barisalcity.gov.bd/ [Accessed 21 Nov. 2016].

Griffin, R. C. (2001). Effective Water Pricing. *JAWRA Journal of the American Water Resources Association*, *37*(5), 1335–1347.

Mekkonen, M. M., & Hoekstra, A. Y. (2016). Four billion people facing severe water scarcity. *Science Advances*, *2*(2), e1500323–e1500323.

Olmstead, S. M., Michael Hanemann, W., & Stavins, R. N. (2007). Water demand under alternative price structures. *Journal of Environmental Economics and Management*, *54*(2), 181–198.

Perlman, H. U. (2016). The USGS Water Science School: All about water!. [online] Water.usgs.gov. Available at: https://water.usgs.gov/edu/ [Accessed 21 Nov. 2016].

Perspectives for Rational Use of Water Resources in the Mediterranean Region, 57–68.

Rahaman, M.M. & Ahmed, T.S. (2016). Affordable Water Pricing for Slums Dwellers in Dhaka Metropolitan Area: The Case of Three Slums. *Journal of Water Resource Engineering and Management*. 2016; 3(1): 15–33p.

Rahaman, M.M. & Varis, O. (2005) Integrated Water Resources Management: Evolution, Prospects and Future Challenges, *Sustainability: Science, Practice and Policy* (USA), 1(1): 15-21.

UN-Habitat. (2003). *The Challenge of Slums - Global Report on Human Settlements*. *Earthscan Publications on behalf of UN-Habitat*.

WWAP (2016). The United Nations World Water Development Report 2016: Facts and Figures. United Nations, New York.

Proceedings of the 4th International Conference on Civil Engineering for Sustainable Development (ICCESD 2018), 9~11 February 2018, KUET, Khulna, Bangladesh (ISBN-978-984-34-3502-6)

IS THE PROPENSITY OF INCREASING THE RICE PRODUCTION A SUSTAINABLE APPROACH? AN ANALYSIS

M K Shehab[1] and Muhammad M Rahaman[2]

[1] Research Assistant, Department of Civil Engineering, University of Asia Pacific, Bangladesh, e-mail: k.shehabce@gmail.com
[2] Professor, Department of Civil Engineering, University of Asia Pacific, Bangladesh, e-mail: rahamanmm@gmail.com

ABSTRACT

Rice production signifies the single largest land use for food production on the earth where Asia accounts for 90% of the world's rice production and consumption. Demand pressure for food will, however, remain significant in low-income countries that comprise the bulk of Asian populations, because of high population growth rates. India, Bangladesh, and Pakistan are the three foremost rice producing countries in South Asia. With the implantation of high yielding crop varieties, farm mechanization, application of numerous types of chemical fertilizers and pesticides, food production has raised remarkably. During, 1961-2014, 314.20%, 262.65%, and 193.89% of rice production were increased by Pakistan, Bangladesh, and India respectively. Maintaining self-sufficiency in production to fulfil the increasing food demand is the prime objective of these countries. However, water consumption rate to produce per kg of rice is much higher compared with other crops. Besides, climate change has an adverse impact on the productivity of rice production. High water demand for rice production and inadequate availability of surface water in the non-monsoon period, continually increase the pressure on groundwater. The research reveals the overall scenario of the rice field in India, Bangladesh, and Pakistan by considering the water consumption, agricultural land use, and production patterns of rice during 1961-2014. AQUASTAT and FAOSTAT databases of Food and Agriculture Organization are used as the data sources for the study.

Keywords: *Land use, water consumption, production patterns, rice*

1. INTRODUCTION

Hunger is one of the most challenging issues in the 21st century. Even though Africa is represented as the heart of hunger, a large volume of hungry people lives in Asia (HN, 2017). As the developing nation, South Asia faces this challenge comparatively high. 281 million people who are not getting adequate food and nutrition live in South Asia (SDGs, 2017). Besides projection revealed that the global population would be increased by 50% compared to the present and demand for food will be doubled within 2050 (Tilman et al., 2002). Moreover, the pressure of the food demand will significant for developing nations due to the high growth of population. Increasing food production to fulfil the food demand will be one of the major challenges for sustainable development.

Considering the land area and population size, India, Pakistan, and Bangladesh are three dominating countries in South Asia (FAO, 2017). The annual rate of population increase in India, Pakistan, and Bangladesh are 1.1%, 2.0%, and 1.1% respectively (WDI, 2017). Agriculture is the most dominant sector of economics where a significant part of the population in the South Asian region lives in rural area and depends on agriculture for livelihoods. In 2016, Agriculture contributes around 17.35%, 14.77%, and 25.23% of GDP in India, Pakistan, and Bangladesh (WDI, 2017). It is abundantly clear that future growth of agricultural sector holds the key to livelihoods and food security, elimination of poverty, increasing the growth and sustainable progress of economy in each of the nations.

Target 2.1 of the United Nations Sustainable Development Goals aims to end hunger and assure access by all people, in particular, the poor and people in vulnerable circumstances, including children, to safe, nutritious and sufficient food all year round by 2030 (SDGs, 2017). Large and growing population in SAARC countries creates more demand for food and places greater stress on limited resources. More productive crops need to be produced to fulfill this growing food demand. Besides, the SAARC countries currently depend heavily on the production of India, Pakistan, Bangladesh, and Nepal for the supply of balanced food (Sahu, 2010). People of this region largely depend on high water consuming crops such as rice because of their food habit.

Rice is the second most demanding crop in the world (Nguyen & Ferrero, 2006; Kuenzer & Knauer, 2013) and it is the staple food for more than half of world's population (Roy et al., 2014) especially for the South Asian people (Singh, 2009). Besides, South Asia is the second largest rice producing region in the world. In 2003, South Asia used almost 37.5% global area for rice production and contributed 32% of global rice production (IRRI, 2016). India, Bangladesh, Nepal, and Pakistan contribute to 38.35% of world rice harvested area (Sahu, 2010). Moreover, rice production has gone through historical changes during 1980 to 2011 as it is increased three-fold (Roy et al., 2014). However, India has the largest rice cultivated area and is the leading rice producing country in the world next to China (Zhang et al., 2016). In addition, India produces 20% of global rice production as well (IRRI, 2017).

Furthermore, rice is a major crop in India and the staple food of most Indians. Rice covers 24% of the total cultivated area in India and contributes 40% of total grain production (Bishwajit et al., 2013). Eventually, 65% of the total population in India depends on rice (Rahaman et al., 2016). After the 'Green Revolution', planting high yield varieties and high uses of agrochemicals result to increase rice production in India during the recent years (Janaiah et al., 2006). 41.50% of rice production has increased in India during 1990-2012 (FAOSTAT, 2017; Rahaman & Shehab, 2017).

As an agricultural country, agriculture is a primary source of economy in Bangladesh, and rice plays a significant role (Roy et al. 2014). Bangladesh is the third largest rice producer in South Asia and sixth largest rice producer in the world. 75.4% of total population in Bangladesh entirely depend on rice production for their livelihoods (Majumder et al., 2016). Besides, rice covers 70% of the total cultivated area in Bangladesh (Karim et al., 2012; Majumder et al., 2016; Hossain et al., 2006). Rice cultivation produced enormous employment opportunities which employ around 65% of total labor force (Roy et al., 2013). Additionally, rice contributes 10% of the total GDP in Bangladesh (Roy et al., 2013). In fact, 95% of cereal production in Bangladesh is covered by rice (Karim et al., 2012). Moreover, Bangladesh is in the fourth position in the world considering the per capita rice consumption (Majumder et al., 2016). Bangladesh has increased rice production about three-fold during 1970 to 2009 (Ahmad et al., 2014). Expansion of using high yield crop, fertilizer, and pesticide, rice production has increased remarkably (Hossain et al., 2006; Roy et al., 2014). Besides, the groundwater-based irrigation system is the key to boost the rice production in recent years (Ahmad et al., 2014).

One-third of the country's population is currently living in poverty and malnutrition is challenging issue in Pakistan (Hussain et al., 2009). Besides, the economy of Pakistan mainly depends on agriculture. It accounted 20% of the national GDP in 2012 and employed 45% of total labor force in 2008 (Akhter et al., 2017; Zhu et al., 2013). Pakistan is the eleventh largest rice producing country in the world and rice is the second largest demanding crop in Pakistan. In addition, Pakistan is well-recognized worldwide for exporting rice (Akhter et al., 2017). Moreover, it covers 10% of the total cultivated area in Pakistan (Bashir et al., 2007).

International Water Management Institute (IWMI) indicates that there will be a need for 17% more irrigation water to feed the world population by 2025, at the same time near about 2 billion people of the world will have to face absolute water scarcity during this period (Sahu, 2010). Mitigating the shortage of water can be solved by making efficient use of water in agriculture globally (Prasad et al., 2006). Approximately 70% of total global freshwater withdrawal fulfills the agricultural water demand and more than 90% of its consumptive use (Watto & Mugera, 2016; Rahman et al., 2010). The irrigated area represents less than 20% of the global cropland, but it contributes more than 40% of the global food production (Watto & Mugera, 2016). One of the significant factors affecting agricultural production around the world is irrigation water (Arfanuzzaman & Ahmad, 2016). Groundwater is considered as a hidden resource which has been recognized as an essential element of the water resources system. Due to increasing use of groundwater for irrigation and consequently higher extraction rates, groundwater resources are rapidly dwindling in many parts of the world. Currently, groundwater is used for about 38% of all global irrigation supply and about 50% in South Asia (Shrestha et al., 2014). To fulfil the growing demand, irrigation by using groundwater is a key to increase the crop production in recent decades (Ahmad et al., 2014).

Projection stated that rice demand in the world would be increased 571.9 million tonnes in 2001 to 777.1 million tonnes in 2030 due to the continuous growth of population (Nguyen & Ferrero, 2006). Acquiring self-sufficiency to secure the food supply locally is the prime goal of those developing countries in South Asia (Ahmad et al., 2014). Besides, the significance of self-sufficiency and effective policies for food security have raised after the world food crisis in 2007-2008 (Mainuddin & Kirby, 2015; Hussain et al., 2009). However, rice is a high water consuming crop compared to the other common producing crop in South Asia (WFN, 2017). Besides. India, Pakistan, and Bangladesh mostly depend on groundwater for irrigation. Due to the lack of implementation of advanced technology for irrigation, most of the developing countries have low irrigation efficiency. So the propensity of increasing rice production to achieve self-sufficiency with sustainable agricultural practices is now a challenging issue for all rice producing country.

With this in mind, this study aims to reveal the overall scenario of available water resources and production pattern of rice in India, Pakistan, and Bangladesh during 1961-2014 so that proper steps could be taken to shorten the challenges to cope with water and land deficiency and to secure long-term regional food security.

2. METHODOLOGY

The data has been analysed based on specific parameters stated by AQUASTAT and FAOSTAT database of Food and Agricultural Organization, (i.e., land use, water resources, water use, harvested area of rice and rice production) to explain the changes in the rice production and the availability of water resources in India, Pakistan, and Bangladesh that have occurred during 1961-2014. Secondary data has been collected from various international, governmental and local organizations as well as published articles, books, documents, and reports.

3. ANALYSIS AND RESULTS

3.1 Agricultural land use

Among all the county in South Asia, India is in the leading position considering the land use for agriculture. India uses 169.36 million hectares of land for agriculture in 2014 followed by Pakistan and Bangladesh (FAO, 2017; Figure 1). Besides, India uses 51.52% of total land for agriculture in 2014 (FAO, 2017; Figure 1). The agricultural land use remains almost constant in India in recent past (1961-2014). Pakistan is the second largest country in South

Asia who uses over 31.25 million hectares of land for agriculture in 2014 (FAO, 2017; Figure 2). Besides, 39.26% of total land is used for cultivation in Pakistan which is comparatively low in amount (FAO, 2017; Figure 2). Moreover, Figure 2 reveals that the agricultural land was fluctuating over the recent past.

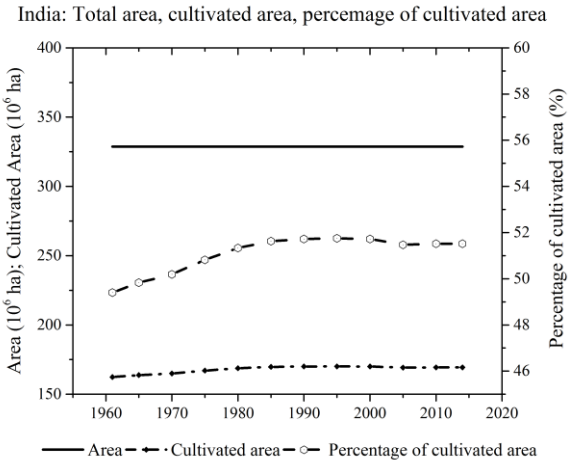

Figure 1: Total area, cultivated area, and percentage of cultivated area in India.

Source: FAO, 2017

Bangladesh is in the fourth position in South Asia considering the total land size (FAO, 2017). 8.50 million hectares of land is for agricultural practice in Bangladesh in 2014 (FAO, 2017; Figure 3). Being a small country compared to India and Pakistan, Bangladesh uses the highest percentage of land for agricultural practices. 57.57% of total land is used for cultivation in Bangladesh in 2014 (FAO, 2017; Figure 3). However, in recent years, the cultivated area in Bangladesh is gradually decreasing which is an alarming issue for Bangladesh. Moreover, In Bangladesh, almost 6.52% of agricultural land is decreased during 1985-2014.

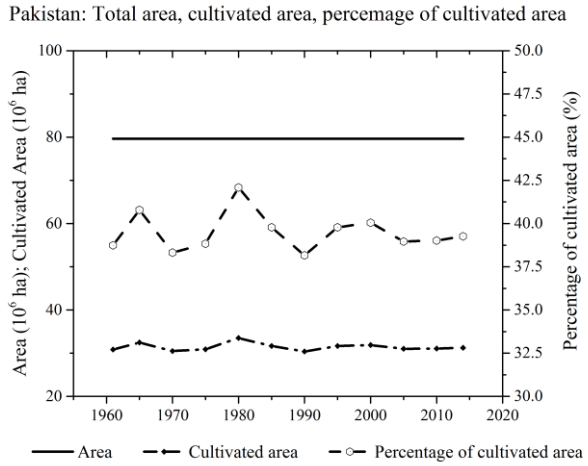

Figure 2: Total area, cultivated area, and percentage of cultivated area in Pakistan.
Source: FAO, 2017

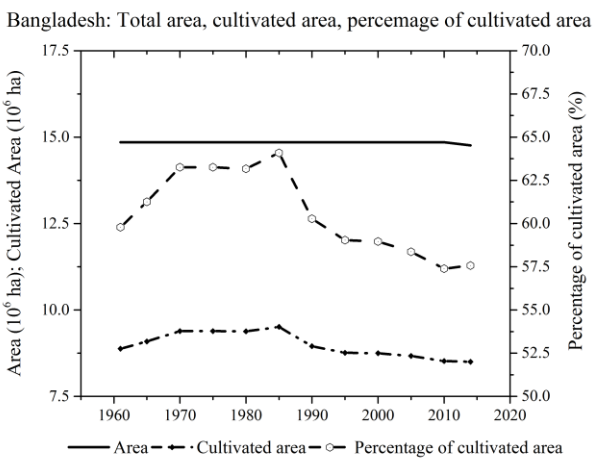

Figure 3: Total area, cultivated area, and percentage of cultivated area in Bangladesh.
Source: FAO, 2017

Irrigation potential means that the area of land which is potentially irrigable. In 2013, irrigation potential area in India, Bangladesh, and Pakistan were 139.5 million hectares, 6.93 million hectares, and 21.3 million hectares respectively (FAO, 2017).

3.2 Available water resources and water uses

India has a typical monsoon climate where the annual average rainfall over the country is around 1083 mm (FAO, 2017), but it varies significantly from place to place. The intensity of rainfall is relatively low in northwest part of India. The annual average rainfall in Pakistan is 494 mm (FAO, 2017). Bangladesh has the monsoon climate with significant fluctuations in rainfall throughout the country. The annual average precipitation is 2666 mm per year (FAO, 2017) which is the highest value among the South Asian countries. 80% of the total rainfall occurs during the monsoon season, and the intensity of the rainfall is relatively high in northeast compared to the northwest part of Bangladesh.

Table 1: Water resources in India, Pakistan, and Bangladesh.

Parameters	Unit	India	Pakistan	Bangladesh
Total renewable surface water	10^9 m^3/year	1869	239.2	1206
Total renewable groundwater		432	55	21.12
Total renewable water resources		1911	246.80	1227

Source: FAO, 2017

Total renewable surface water is the sum of the internal renewable surface water resources and the total external renewable surface water resources (Climpag, 2017). Similarly, total renewable groundwater is the sum of the internal renewable groundwater resources and the total external renewable groundwater resources (Climpag, 2017). India has the highest amount of total renewable surface water in South Asia which is 1869 billion m^3 per year (FAO, 2017; Table 1). Besides, the total renewable surface water in Bangladesh and Pakistan are 1206 billion m^3 and 239.2 billion m^3 respectively (FAO, 2017; Table 1). Moreover, considering the total renewable groundwater, India is in the top position among the South Asian countries. India has 432 billion m^3 the total renewable groundwater followed by Pakistan and Bangladesh (FAO, 2017; Table 1).

Table 2: Water withdrawal in India, Pakistan, and Bangladesh (2008-2012)

Parameters	Unit	India	Pakistan	Bangladesh
Agricultural water withdrawal	10^9 m^3/year	688	172.4	31.5
Industrial water withdrawal		17	1.4	0.77
municipal water withdrawal		56	9.65	3.6
Total water withdrawal		761	183.5	35.87
Surface water withdrawal		396.50	121.90	7.39
Groundwater withdrawal		251	61.60	28.48

Source: FAO, 2017

Total water withdrawal is the quantity of water withdrawn for agricultural, industrial and municipal purposes annually. Agricultural water withdrawal is the annual quantity of self-supplied water withdrawn for irrigation, livestock and aquaculture purposes. India uses the highest amount of water compared to Pakistan and Bangladesh (Table 2). During 2008-2012, the total water withdrawal in India was 761 billion m^3 per year (FAO, 2017; Table 2) among which 90.41% of total water withdrawal was used for agricultural uses. Besides, 94.68% of agricultural water use is increased in India in between 1973-2012. Moreover, in 2008-2012, the total surface water withdrawal in India was 396.50 billion m^3 per year (FAO, 2017; Table 2) which represents 52.10% of total water withdrawal.

The total water withdrawal in Pakistan was 183.5 billion m^3 during 2008-2012 (FAO, 2017; Table 2) where 93.95% of water was used for agriculture. 14.70% of agricultural water use was increased in Pakistan in between 1973-2012. Furthermore, the total surface water withdrawal in Pakistan in 2008-2012 was 121.90 billion m^3 per year which was 66.43% of total water withdrawal. Although the dependency on surface water is significant, the volume of groundwater uses has already crossed the recharge limit. In 2008-2012, the total groundwater withdrawal in Pakistan was 61.60 billion m^3 per year where the total renewable groundwater was 55 billion m^3 per year (FAO, 2017; Tables 1, 2). The consequence of overuse of groundwater is alarming where the groundwater table is lowering in Pakistan which is now a significant concern for sustainable development.

During 2008-2012, the volume of total water withdrawal in Bangladesh was 35.87 billion m^3 per year. 31.5 billion m^3 of water was used for agricultural practices in Bangladesh during 2008-2012 which is 87.82% of total water withdrawal. Bangladesh used 7.39 billion m^3 of surface water in 2008-2012 (FAO, 2017; Table 2) where it used only 0.61% of renewable surface water potential. Moreover, the dependency on groundwater is huge in Bangladesh compared to India and Pakistan. Groundwater contributes 79.40% of total water withdrawal in Bangladesh. Same as Pakistan, the quantity of using groundwater which was 28.48 billion m^3 per year in Bangladesh has exceeded the recharge rate of 21.12 billion m^3 per year (FAO, 2017; Tables 1, 2). Excessive use of groundwater results to fall of groundwater table and increases salt contamination which are serious concern for both Pakistan and Bangladesh (Rahaman et al., 2016).

3.3 Production pattern of rice

Considering the rice harvested area and production, India is in the second position all over the world (Zhang et al., 2016). Besides, India is the top rice producer in South Asia and used

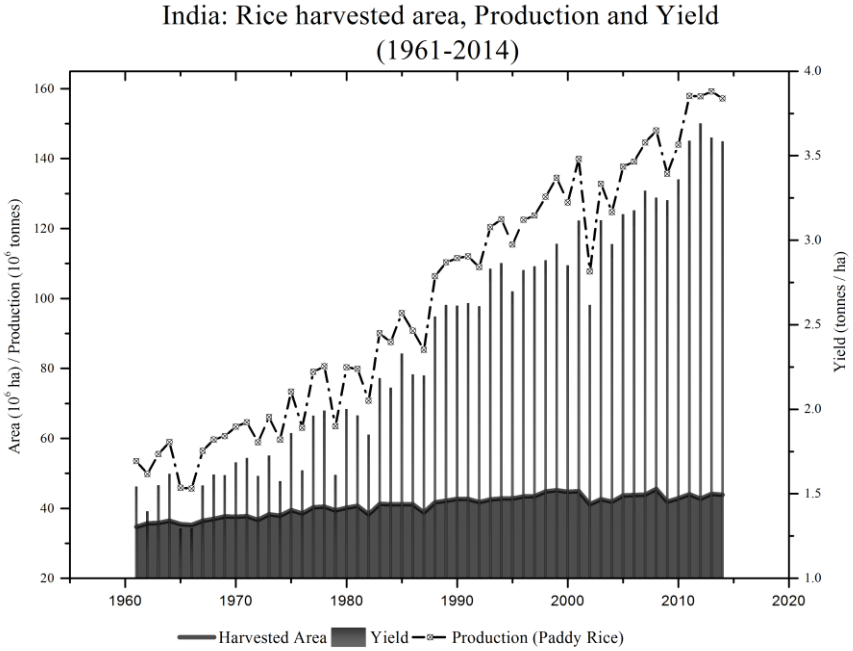

Figure 4: India: Rice harvested area, production and yield during 1961-2014.

Source: FAOSTAT, 2017

over 43.85 million hectares of land for rice production and produced 157.20 million tonnes of rice (paddy rice) in 2014 (FAOSTAT, 2017; Figure 4). During 1961-2014, 26.40% of rice harvested area was increased by India (FAOSTAT, 2017). After the 'Green Revolution',

expansion of cultivating high yield varieties crop results to increase the rice production in India in past decades (Auffhammer et al., 2012). During 1961-2014, 193.89% of rice production has increased in India. The government of India emphasis on cultivating hybrid rice for increasing rice production to fulfill growing food demand. Besides, a study revealed that rice planting area is increasing at a rate of 0.27 million hectares per year in India (Zhang et al., 2016). Moreover, the yield of rice production in India was 3.58 tonnes per hectares. Figure 4 represents the production pattern of rice in India during 1961-2014.

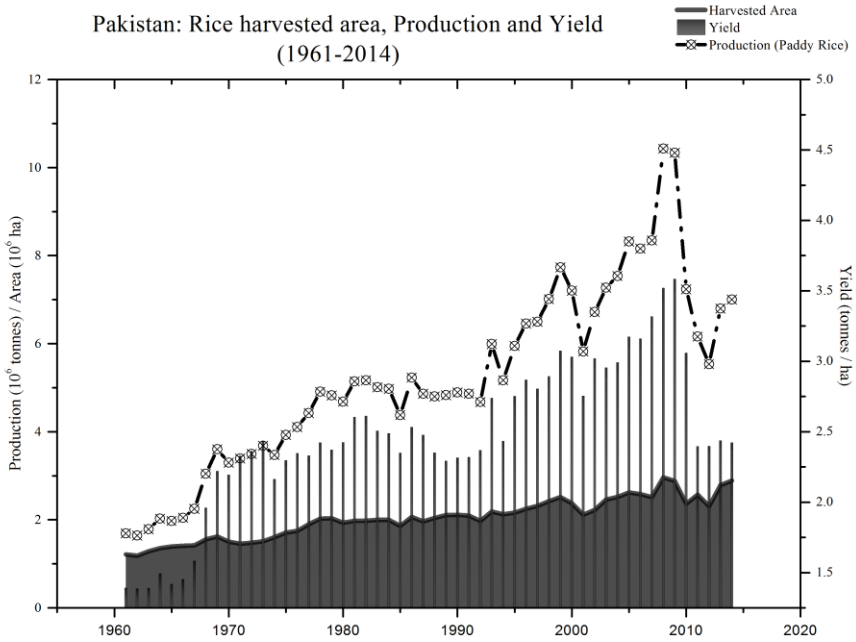

Figure 5: Pakistan: Rice harvested area, production and yield during 1961-2014.

Source: FAOSTAT, 2017

Pakistan is another dominating rice producing country where rice is the second largest demanding food. In 2014, 2.89 million hectares of land was used for rice cultivation, and the production amount was 7 million tonnes (FAOSTAT, 2017). 138.84% of rice harvested area and 314.20% of rice production were increased in Pakistan during 1961-2014. Pakistan is well known for exporting 'Basmati' rice all over the world (Bashir et al., 2007). In 2013, Pakistan extorts 3.8 million tonnes of rice (FAOSTAT, 2017). Additionally, the rate of exporting rice in Pakistan is gradually increasing. The yield of rice production in Pakistan was 2.42 tonnes per hectares in 2014 (FAOSTAT, 2017). The productivity of rice production is relatively low compared to India and Bangladesh. Figure 5 shows the production pattern of rice in Pakistan during 1961-2014.

Bangladesh is the fourth leading rice producing country in the world and second largest rice producer among the South Asian countries. In 2014, 11.32 million hectares of land was used for rice cultivation in Bangladesh (FAOSTAT, 2017). Besides, Bangladesh produced 52.32 million tonnes of rice in 2014 (FAOSTAT, 2017). As rice is the staple food in Bangladesh, achieving self-sufficiency is the prime goal of Bangladesh. Promoting the cultivation of high yield varieties and fertilizers by the governmental and nongovernmental organization helped to increase rice production in recent years. During 1961-2014, 33.49% of rice harvested area and 262.65% of rice production were increased in Bangladesh. In fact, the yield of rice production in Bangladesh was 4.62 tonnes per ha in 2014 which is the highest value among the South Asian countries (FAOSTAT, 2017). Figure 6 shows the productivity of rice and the production amount is gradually increasing over the years. Besides, the groundwater based irrigation system is the key to boost the rice production in Bangladesh.

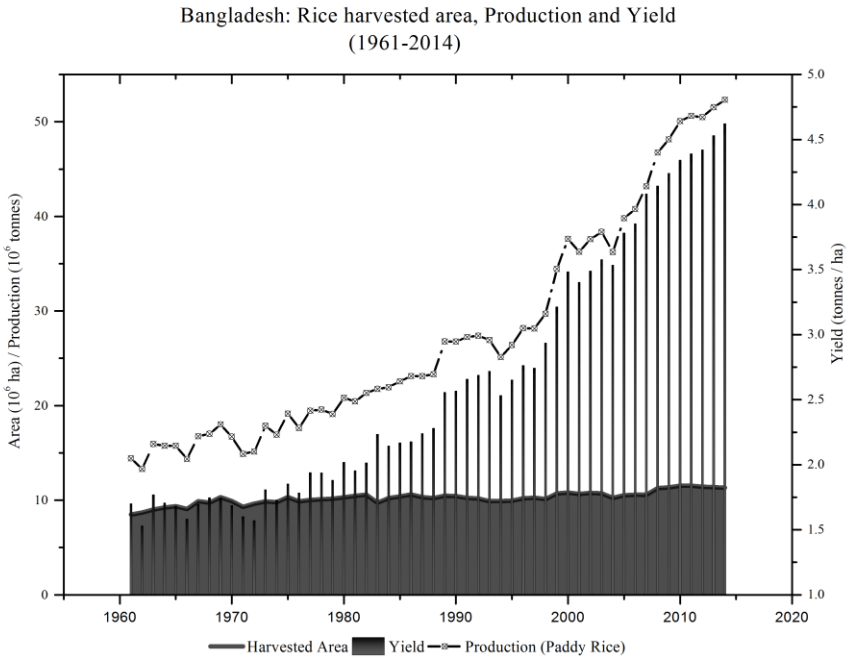

Figure 6: Bangladesh: Rice harvested area, production and yield during 1961-2014.

Source: FAOSTAT, 2017

4. CONCLUSIONS

Being the highly populated countries, India, Pakistan, and Bangladesh are the leading water consuming countries in South Asia. By using limited land and water resources, it is now a great challenge to fulfil the growing food demand. However, the agricultural practice remains almost constant in India. Meanwhile, high population growth and increasing urbanization caused to decrease the land use for agriculture in Bangladesh in recent past. Almost 6.52% of agricultural land is decreased during 1985-2014. The water demand for irrigation put stress on limited water resources. Although Pakistan and India depend on the source of surface water to fulfil more than 50% of their consumptive and non-consumptive demands, the dependency on groundwater is increasing at an alarming rate. On the other hand, Bangladesh significantly depends on groundwater to fulfil the growing water demand.

Moreover, amount of groundwater abstraction has already exceeded the rechargeable amount in Pakistan and Bangladesh that contributed to fall of groundwater table and increase in salt contamination that are serious concerns for both countries. Promoting long-term loans with low interest by the government and expansion of using local made diesel engines caused to increase the number of tube wells as well as uses of groundwater in Pakistan. In consequence, the irrigated area under surface water is decreasing in Pakistan in recent years. Similarly, in Bangladesh, the dependency on groundwater is increasing due to eliminating import duties on diesel pumps and allow importing agricultural equipment without a permit since 1983 (Rahaman et al., 2016). In addition, more than 94% of surface water in Bangladesh originates from upstream countries and inadequate surface water in the non-monsoon season results to increase groundwater uses in Bangladesh (Rahaman, 2009).

Rice is the most demanding crop and high water consuming crop. The historical changes in rice production in India, Bangladesh, Pakistan are occurred by the expansion of cultivating high yield varieties where groundwater was the primary key. As malnutrition is a notable challenge for India, Pakistan, and Bangladesh, increasing rice production by sustainably using limited water resources could minimize the hunger issue.

India, Pakistan and Bangladesh should enhance their tendency of trading products among themselves, which will allow each of them to achieve food sufficiency. Each country should give priority to produce the least water consuming crops such as potato and vegetables especially during non-monsoon months which will help to reduce the pressure on limited water and land resources. Besides, conjunctive use of surface and groundwater for irrigation and rainwater harvesting could be a way to minimize the stress on groundwater. Reducing use of groundwater and increasing irrigation efficiencies should be encouraged. The increase of surface water for irrigation during non-monsoon months should be ensured through transboundary water cooperation among the countries sharing international river basins.

ACKNOWLEDGEMENTS

The excellent support from the Department of Civil Engineering, University of Asia Pacific, and its staff is greatly appreciated.

REFERENCES

Ahmad, M. D., Kirby, M., Islam, M. S., Hossain, M. J., & Islam, M. M. (2014). Groundwater use for irrigation and its productivity: Status and opportunities for crop intensification for Food Security in Bangladesh. *Water Resources Management*, 28, 1415-1429.

Akhter, M., Ali, M., Haider, Z., Mahmood, A., & Saleem, U. (2017). Comparison of yield and water productivity of rice (Oryza sativa L.) hybrids in response to transplanting dates and crop maturity durations in irrigated environment. *Irrigation & Drainage Systems Engineering*, 6(1), 180.

Arfanuzzaman, M. & Ahmad, Q. K. (2016), Assessing the regional food insecurity in Bangladesh due to irrigation water shortage in the Teesta catchment area, Water Policy, 18 (2), 304–317.

Auffhammer M, Ramanathan V, Vincent JR (2012) Climate change, the monsoon, and rice yield in India. *Climatic Change* 111 (2), 411–424.

Bashir, K., Khan, N. M., Rasheed, S., & Salim, M. (2007). Indica rice varietal development in Pakistan: an overview. *Paddy and Water Environment*, 5, 73–81.

Bishwajit, G., Sarker, S., Kpoghomou, M. A., Gao, H., Jun, L., Yin, D. & Ghosh, S. (2013), Selfsufficiency in rice and food security: A South Asian perspective. *Agriculture & Food Security*, 2(10).

Climpag (2017). Climate Impact on Agriculture, Food and Agriculture Organization. (http://www.fao.org/nr/climpag/nri/nrilist_en.asp)

FAO (2017). AQUASTAT database, Food and Agricultural Organization of United Nations. (http://www.fao.org/nr/water/aquastat/data/query/index.html?lang=en.)

FAOSTAT (2017). Database for food and agriculture, Food and Agricultural Organization of United Nations. (http://faostat.fao.org/site/291/default.aspx)

Hossain, M., Bose, M. L., & Mustafi, B. A. A. (2006). Adoption and productivity impact of modern rice varieties in Bangladesh. *The Developing Economies*, XLIV-2, 149–166.

Hunger Notes (HN) (2017). World Hunger Education Service, Washington, D.C. 20017. (http://www.worldhunger.org/)

Hussain, I., Mudasser, M., Hanjra, M. A., Amrasinghe, U., & Molden, D. (2009). Improving wheat productivity in Pakistan: econometric analysis using panel data from Chaj in the upper Indus Basin. *Water International*, 29 (2), 189–200.

IRRI (2016), Rice in South Asia, The International Rice Research Institute, Los Baños, Philippines. (http://irri.org/rice-today/rice-in-south-asia)

IRRI (2017). Rice in India. The International Rice Research Institute, Los Baños, Philippines. (http://india.irri.org/)

Janaiah, A., Hossain, M., & Otsuka, K. (2006). Productivity impact of the modern varieties of rice in India. The Developing Economies, XLIV-2, 190–207.

Karim, M. R., Ishikawa, M., Ikeda, M., & Islam, M. T. (2012). Climate change model predicts 33% rice yield decrease in 2100 in Bangladesh. *Agronomy for Sustainable Development*, 32, 821–830.

Kuenzer, C., & Knauer, K. (2013). Remote sensing of rice crop areas. International Journal of Remote Sensing, 34, 2101-2139.

Mainuddin, M., & Kirby, M. (2015). National food security in Bangladesh to 2050. *Food Security*, 7 (3), 633–646.

Majumder, S., Bala, B. K., Arshad, F. M., & Haque, M. A. (2016). Food security through increasing technical efficiency and reducing postharvest losses of rice production systems in Bangladesh. Food Security, 8 (2), 361–374.

Nguyen, N. V., & Ferrero, A. (2006). Meeting the challenges of global rice production. Paddy and Water Environment, 4, 1-9.

Prasad, A.S., Umamahesh, N.V. & Viswanath, G.K. (2006), Optimal Irrigation Planning under Water Scarcity. Journal of Irrigation and Drainage Engineering, 132 (3), 228-237.

Rahaman, M. M. (2009). Integrated Ganges basin management: conflict and hope for regional development. *Water Policy*, 11, 168–190.

Rahaman, M. M., & Shehab, M. K. (2017). *Water consumption, land use and production patterns of rice, wheat and potato in South Asia during 1988-2012*. Manuscript submitted for publication.

Rahaman, M. M., Shehab, M. K., & Islam, A. (2016). *Total production and water consumption of major crops in South Asia during 1988-2013*. Proceedings of Conference on Water Security and Climate Change: Challenges and Opportunities in Asia, Asian Institute of Technology, Bangkok, Thailand, November 29 –December 1, 2016.

Rahman, M. M., Rahman, M. R. & Asaduzzaman, M. (2010), Establishment of dams and embankments on frontier river of north east part of India: impact on north-western region of Bangladesh, Journal of Science Foundation, 8(1&2), 1-12.

Roy, R., Chan, N. W., & Rainis, R. (2014). Rice farming sustainability assessment in Bangladesh. Sustainability Science, 9, 31-44.

Sahu, P. K. (2010), Forecasting Production of Major Food Crops in Four Major SAARC Countries, *International Journal of Statistical Sciences*, 10, 71-92.

Shrestha, S., Adhikari, S., Babel, M. S., Perret, S. R. & Dhakal, S. (2014), Evaluation of groundwater based irrigation systems using a water–energy–food nexus approach: a case study from Southeast Nepal, Journal of Applied Water Engineering and Research, 3 (2), 53-66.

Singh, M. P. (2009). *Rice Productivity in India under Variable Climates*. Country report presented at MARCO Symposium 2009: Challenges for Agro-environmental Research in Monsoon Asia, Tsukuba, Japan, October 5–7.

Sustainable Development Goals (SDGs) (2017), United Nations SDGs, New York: United Nation. (http://www.un.org/sustainabledevelopment/hunger/)

Tilman, D., Cassman, K. G., Matson, P. A., Naylor, R., & Polasky, S. (2002). Agricultural sustainability and intensive production practices, *Nature*, 418, 671-677.

Water Footprint Network (WFN) (2017). Water Footprint Network, International Water House, The Netherlands. (http://waterfootprint.org/en/)

Watto, M. A., & Mugera, A. W. (2016). Irrigation water demand and implications for groundwater pricing in Pakistan. *Water Policy*, 18(4), 565–585.

World Development Indictors (WDI) (2017). World Development Indicators. World Bank, United States. (http://www.worldbank.org/.)

Zhang, G., Xiao, X., Biradar, C. M., Dong, J., Qin, Y., Menarguez, M. A., Zhou, Y., Zhang, Y., Jin, C., Wang, J., Doughty, R. B., Ding, M., & Moore, B. (2016). Spatiotemporal patterns of paddy rice croplands in China and India from 2000 to 2015. *Science of The Total Environment*, 579, 82-92.

Zhu, T., Ringler, C., Iqbal, M. M., Sulser, T. B., & Goheer, M. A. (2013). Climate change impacts and adaptation options for water and food in Pakistan: scenario analysis using an integrated global water and food projections model. *Water International*, 38, 651–669.

Proceedings of the 4th International Conference on Civil Engineering for Sustainable Development (ICCESD 2018), 9~11 February 2018, KUET, Khulna, Bangladesh (ISBN-978-984-34-3502-6)

EFFECT OF LAND USE ON WATER QUALITY OF THE TURAG RIVER

Md. Rafiu Zaman[1], Md. Mahmud Hossain[2], Abu Saeed Md. Noman[3] and Mohammad Shahedur Rahman[4]

[1] M.Sc. Student, Islamic University of Technology, Bangladesh, e-mail: rafiucee@iut-dhaka.edu
[2] M. Sc. Student, Islamic University of Technology, Bangladesh, e-mail: mahmud31@iut-dhaka.edu
[3] Graduate Student, Islamic University of Technology, Bangladesh, e-mail: noman.iut@gmail.com
[4] Former PhD Candidate, Dalhousie University, Canada, e-mail: msr@iut-dhaka.edu

ABSTRACT

Considerable research has been carried out to establish relationship between land use patterns and water quality in developed countries. In Bangladesh, research has been conducted in waste effluent effects on water quality with the surrounding environment. But very few research works have been done concerning land use effects on water sources though limited control on land use pattern makes river water more vulnerable to use. The purpose of this study is to identify water quality of the Turag River coming from residential/ industrial/ agricultural areas and to determine the impact of land use on water quality. As northern part of Dhaka city consists of a number of industries, Turag River is the water body receiving most of the agricultural, urban, industrial wastes. In the study, forty-five water samples in three different river depths were collected from five different points of the river based on the type of land use. Water samples were collected in the winter season to show a worse scenario. In laboratory, five basic water quality parameters- pH, Colour, Turbidity, Total Dissolved Solid, and Biochemical Oxygen Demand -were considered. A generalized survey was conducted around the sample collection sites to get a clear conception about the land use. The findings of the study show that only few of the test results are fitting in the existing standards. Besides Industrial pollutions, municipal point source of pollution had a great effect on the water quality. Quality of water deteriorates with the increase of land use.

Keywords: *Water Quality, Land Use, Turag River*

1 INTRODUCTION

Water is the most inevitable natural requisite to sustain life for plants and animals as well as human beings (Nwankwoala & Nwagbogwu, 2012). Water quality is important as a health and development issue at a national, religion and local level. Despite its necessity, water pollution is most crucial issue of the present world (Fakayode, 2005). For reducing water pollution, it is considered as the first priority to save fresh water resources from the pollutants. To accomplish this purpose, water quality testing is an essential part of environmental monitoring. These test basically includes Biochemical Oxygen Demand (BOD), Chemical oxygen demand (COD), E.coli test, TDS, Turbidity, Odor, pH, Iron concentration of water and Hardness of water (Tariquzzaman et al., 2016). Poor water quality affects not only aquatic life but also the surrounding ecosystem.

Land use has been considered not only as a local environmental issue, but also as a force of global importance (Foley et al. 2005). The need for providing food, fiber, water, and shelter to more than six billion people changes the conditions of forests, farmlands, waterways, and air. Global croplands, pastures, plantations, and urban areas have expanded with losses of biodiversity.

Since the late of 1970s, the influence of land use on water quality has been a major concern (Lee et al, 2009; Tran et al., 2010; Rothwell et al., 2010). Researchers started to analyze the correlation between land use and water quality mostly after the 90s (Johnson et al., 1997). Water quality assessment techniques was introduced to make these studies much

convenient than before (Griffith, 2002; Ierodiaconou et al., 2005; Rothwell et al., 2010). The relationship between land use patterns and water quality explains the variations of river water quality in a water resource conservation and ecosystem management (Woli et al., 2004; Li et al., 2009). Besides, considerable water pollution is caused by various kinds of land use and practices such as rapid urbanization, growth of population, industrial and agricultural activities (Ngoye & Machiwa, 2004). Generally, agricultural land use has identified a strong command on the nutrient parameters in river water (Pieterse et al., 2003; Ngoye & Machiwa, 2004; Woli et al., 2004). Furthermore, industrial and urban land uses are associated with organic pollution, nutrients and heavy metals and other pollutants in the river water (Ferrier et al., 2001; Li et al., 2009).

In Bangladesh, Pasha et al. (2012) performed a study to assess the water quality of the Turag River situated at Gazipur and to identify the impact of industrial and domestic wastes on water quality. Domestic wastes have a significant effect on water quality associated with surrounding sanitation system. Islam et al. (2012) investigated solid waste and industrial effluents effect on water quality of the Turag River. The results of the study showed that the upstream water was neutral with comparatively high dissolved oxygen, but low values of other parameters. Besides that, solid wastes and industrial effluents being discharged into the river have considerable negative effects on the water quality of the river water and as such, the water was not good for human purposes and for other uses. So, a deep understanding is required concerning the relationship between land use effects and water quality in developing countries like Bangladesh. The purpose of this study is to identify water quality of the Turag River coming from residential/ industrial/ agricultural areas and to determine the impact of land use on water quality. The specific objectives are assessment of the present water quality of the Turag River in various points, comparison of various water quality parameters of the Turag River with the existing standards and finally studying the impact of various types of waste- domestic, industrial and agricultural- on the water quality of the Turag River.

2. STUDY AREA AND METHODOLOGY

Overall Study Area and Methodology involves selection of suitable water sample collection sites (Section 2.1), water quality parameter selection (Section 2.2), Sampling and analysis of Turag River water (Section 2.3), Survey data collection and analysis (Section 2.4) to find out the relationship between land use and water quality of Turag River.

2.1 Study Area

Dhaka is the most densely populated cities of Bangladesh having population of more than 15 million. Northern side of the city consists of numerous industries located in Tongi. As Turag River flows marking the edge of the city, water body of the river receives most of the agricultural, urban and industrial wastes. Over the last few decades, the river has undergone tremendous chemical and biological changes as a result of increasing human interferences. For the execution of the research, ten sites were primarily chosen from maps based on the probable dumping zone of domestic and industrial waste. After three rounds of reconnaissance, five sites (Table 1 & Figure 1) were finally selected based on odour and visible properties of water of the Turag River. Tongi Bridge was the base point of the research area.

Table 1: Location of the Sites of Turag River

Site No.	Name of the Location	Longitude	Latitude
A	Nagda Bridge, Pubail	23.917112	90.467734
B	Tongi Bridge, Tongi	23.882053	90.404182
C	Gudara Ghat, Tongi	23.897993	90.385506

D	Diabari, Uttara	23.883274	90.357300
E	Rustompur Bridge, Savar	23.878545	90.352000

Figure 1: Location of the Sites

2.2 Water Quality Parameters

Five water quality parameters were selected based on the testing apparatus availability and environmental importance for measuring sampling water quality.

2.2.1 pH

pH is a measure of the acidic or alkaline condition of water. It may be expressed as the hydrogen ion concentration, or more precisely the hydrogen ion activity. A controlled value of pH is desired in water supplies (coagulation, disinfection, water softening and corrosion control), sewage treatment and chemical process plants. For the Study, HACK pH meter was used. The pH scale ranges from 0 to 14. A pH value of 7 is neutral, less than 7 is acidic and greater than 7 is basic.

2.2.2 Turbidity

Turbidity is a measure of water clarity. A turbidity test will measure the decrease in the passage of light through a water sample based on the amount of floating materials in the water. Turbidity is caused by suspended materials which absorb and scatter light. Turbidity is a useful indicator of water quality changes. HANNA turbidity meter was used in the research to find the parameter.

2.2.3 Colour

Water is coloured to some extent due to the presence of various impurities i.e., iron and manganese in association with organic matter from decaying vegetation. Apparent colour is seen in the presence of suspended matter, whereas true colour is derived only from dissolved inorganic and organic matters. To measure this parameter, HACH Spectrophotometer was used for the study.

2.2.4 Total Dissolved Solid (TDS)

Total Solids (TS) are the total of all solids in a water sample. They include the Total Suspended Solids (TSS) and Total Dissolved Solids (TDS). Total Suspended Solids (TSS) is the amount of solids in a water sample retained by a filter. Total Dissolved Solids (TDS) are those solids that pass through a filter with a pore size of 2.0 micron or smaller. They are said to be non-filterable. After filtration, the filtrate (liquid) is dried and the remaining residue is weighed and calculated as mg/L of Total Dissolved Solids.

Total solids measurement can be useful as an indicator of the effects of runoff from construction, agricultural practices, logging activities, sewage treatment plant discharges and other sources. The most important aspect of TDS with respect to drinking water quality is its effect on taste. The palatability of drinking water with a TDS level less than 600 mg/L is generally considered to be good. Drinking water supplies with TDS levels greater than 1200 mg/L are unpalatable to most consumers.

2.2.5 Biochemical Oxygen Demand (BOD)

Biochemical Oxygen Demand (BOD) determination is a chemical procedure for determining the amount of dissolved organic matter to occur under standard condition at a standardized time and temperature. Usually, the time is taken as 5 days and the temperature is 20^0C. This is important parameter to assess the pollution of surface waters and ground waters where contamination occurred due to disposal of domestic of domestic and industrial effluents. Drinking water usually has a BOD of less than 1 mg/L. But, when BOD value reaches 5 mg/L, the water is doubtful in purity. HACH BODTrak was used in the study.

2.3 Sampling and Analysis of Water Sample

Almost 80% of the annual average rainfall of 1854 millimeters (73.0 in) occurs during the monsoon season which lasts from May till the end of September. So the pollutants get diluted during rainy season. So water samples were being collected in the winter season (January-March) to show a worse scenario than that for the rainy season. In the study, 45 water samples of different river depths (1.5, 3, 4.5 feet) were collected from five different points of the Turag River. Different river depths are to investigate the water quality changes. In laboratory, five basic water quality parameters- pH, Colour, Turbidity, Total Dissolved Solid, and Biochemical Oxygen Demand -were measured for each water sample. Finally, the values were compared with existing water quality standard to find out the water quality of the Turag River.

2.4 Survey Data Collection and Relationship with Water Quality

A survey was conducted near the selected five points to get some hand to hand data on the land uses around the selected points. Types of waste- agricultural, industrial, domestic-generated in the surrounding points, Type of land use which generates the wastes were the main concern of the survey. The survey wants to focus on how water quality changes with land use. The main causes of the site wastes were also identified. Finally, the relationship between water quality and land use was developed.

3. ANALYSIS AND RESULTS

The results obtained following the outlined methodology are organized into three sub-sections of which Section 3.1 is water sample data analysis and comparing with existing drinking water quality standard for Bangladesh, Section 3.2 is summarizing the survey data and Section 3.3 is to identify the relationship between water quality and land use of the Turag River.

3.1 Water Sample Data Analysis and Existing Water Standard

Table 2 illustrates water quality parameter data- pH, Turbidity in FTU, Colour in Pt/Co, TDS in mg/L, BOD_5 in mg/L- in three different depths (1.5 feet, 3 feet, 4.5 feet) for five selected locations (Section 2.1) of Turag River. Figure 2 shows the average water parameter values for each depth and site as three water sample was collected for each section.

Table 2: Water Quality Parameters Data for Turag River

Site	Depth in feet	Sample No	pH	Turbidity (FTU)	Colour (Pt/Co)	TDS (mg/L)	BOD_5 (mg/L)
A	1.5	AD1_01	7.66	112	496	1150	23
		AD1_02	7.66	112	496	1150.5	23
		AD1_03	7.67	110	496	1149.3	23
	3	AD2_01	7.67	108	492	1147.4	22
		AD2_02	7.68	107	491	1147	21
		AD2_03	7.68	107.1	492	1147.4	21
	4.5	AD3_01	7.7	105	488	1145.9	20
		AD3_02	7.7	106.3	488	1146	21
		AD3_03	7.7	106	487	1146.7	20
B	1.5	BD1_01	7.49	110	403	872.5	24
		BD1_02	7.51	109	402	872	22
		BD1_03	7.5	106	402	871.9	24
	3	BD2_01	7.52	103.2	400	870	23
		BD2_02	7.53	103	401	870	23
		BD2_03	7.52	104	400	871.1	23
	4.5	BD3_01	7.53	100.7	395	871	21
		BD3_02	7.53	100	396	869.5	21
		BD3_03	7.53	100	395	869.4	20
C	1.5	CD1_01	7.91	97	251	1600	31
		CD1_02	7.92	97	250	1600.2	30
		CD1_03	7.91	98.9	250	1601	30
	3	CD2_01	7.94	94.1	250	1597	30
		CD2_02	7.93	92.8	250	1598	29
		CD2_03	7.93	92	249	1596	28
	4.5	CD3_01	7.93	90	247	1596	27
		CD3_02	7.95	90.5	247	1596.8	27
		CD3_03	7.95	90.6	246	1595.3	28
D	1.5	DD1_01	7.04	41.3	324	629	19
		DD1_02	7.04	40.9	324	628.6	18
		DD1_03	7.04	41.1	325	628	18
	3	DD2_01	7.07	40.6	323	628	16
		DD2_02	7.08	39.9	321	627.1	15
		DD2_03	7.07	40	321	627.7	16
	4.5	DD3_01	7.1	39.2	321	626	14
		DD3_02	7.11	39.7	320	626	15
		DD3_03	7.11	38.6	319	626.9	15

E	1.5	ED1_01	7.1	33.7	387	746	17
		ED1_02	7.1	33.7	385	745	18
		ED1_03	7.12	32.9	387	745.9	17
	3	ED2_01	7.15	30.5	385	745	18
		ED2_02	7.15	30.6	382	744	18
		ED2_03	7.16	30	384	744.8	17
	4.5	ED3_01	7.17	28.9	381	744	15
		ED3_02	7.17	28	381	743	16
		ED3_03	7.18	28.6	380	743.2	16

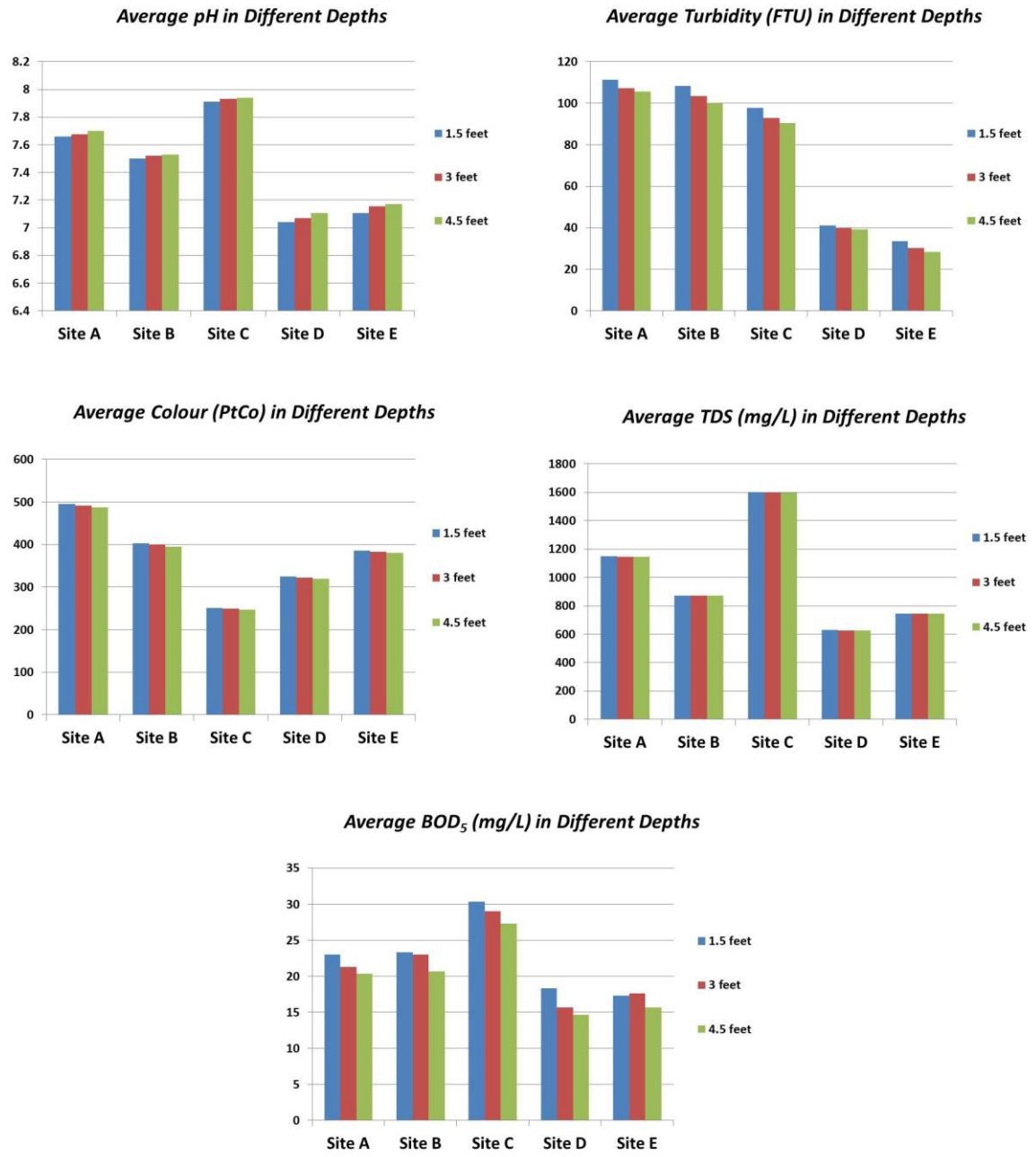

Figure 2: Average Water Quality Parameters Data

Average pH values range for Site-A in depths was in between 7.65 to 7.7 which is slightly alkaline (>7). Besides, Turbidity and Colour average values in all depths were considerably higher than existing drinking water standard (Table 3). Higher colour value means water in yellowish colour. Turbidity is related to suspended matter of water and therefore high turbidity values (1149.93, 1147.26, 1146.2 mg/L) of Site-A demonstrate high number of suspended particles in Turag water. As BOD levels are high (23, 21.33, and 20.33), Dissolved Oxygen (DO) levels decrease because available oxygen in water is being consumed by the bacteria.

Table 3: Drinking Water Quality Existing Standard in Bangladesh (Source: ECR)

Experiment Name	Standard for Drinking Water	Standards for inland surface water
pH	6.5-8.5	6.5-8.5
Turbidity (FTU)	10	--
Colour (Pt/Co)	15	--
TDS (mg/L)	1000	--
BOD_5 (mg/L)	0.2	6

Site-B had pH values slightly higher than neutral level (7.0). Turbidity and Colour test values were mostly similar to Site-A. Though Turbidity and pH values of this site were within standard limit (<1000 mg/L and 6.5 to 8.5), other water quality measurement like BOD, Colour, TDS obtained much higher values than expected. Thus, Site-B river water is not suitable for drinking and recreational activities. Site C showed slightly higher pH values (7.91, 7.93, and 7.94) than other sites. Total Dissolved Solids (TDS) is mainly related to the presence of numerous kinds of minerals like ammonia, nitrite, nitrate, phosphate, alkalis, sulphates and metallic ions which consist of both colloidal and dissolved solids in water. Therefore, higher TDS value in Site-C (>1500 mg/L) indicates the presence of minerals in river water. Since TDS value was the highest, BOD achieved higher value in the Site-C than other sites.

Site-D showed low BOD values (18.33, 15.66, and 14.66) as TDS represented much lower values than Site-C. Besides, turbidity value is considerably lower than other zones but not low enough to satisfy water standard limit. Consequently, pH values were close to neutral (7.04, 7.07, and 7.1). Site-E water exhibited similar water condition to Site-D as pH values were slightly higher and other parameter values are mostly parallel.

Changes in water quality have been found in different depths. Water quality in 3 feet below from river water level is slightly better than 1.5 feet. Similar pattern has been also applicable for depth 4.5 feet. For proper demonstration, water needs to collected from as higher river depths as possible. Therefore, from Table-2, water quality may increase with collected river water depths.

3.2 Summarizing Survey Data

Generalized Survey was conducted to identify major purposes of land use on the selected five sites. Land use is related to the surrounding environment, benefits and social economic condition. In the study, type of waste in river water depends on surrounding environment and land use.

Site-A waste is mainly agricultural. The area around site A is in under cultivation of rice mainly. Approximately 500000 m^2 area is under cultivation for only four months. 10-20 kilograms of fertilizer is used in 3643 m^2 land thrice in cultivation time. In total for cultivation, around 6 tons of fertilizers are used. The main ingredients of these fertilizers are Nitrogen (N), Potassium (K), Zinc (Zn) and Gypsum (CaSO4.2H2O). Though Potassium (K) is applied, its quantity is very less.

Markets cover at 180000 m^2 area at Site-B. Waste produced in the market is dumped in the Turag River. Waste is mostly industrial and domestic (organic).

There are at least two markets, one hospital, two steel/ aluminum mills, one pharmaceutical company in Site-C which contribute in the waste dumped in the Turag River. Around 5,000 m^3 domestic wastes are dumped. Besides, eight vans, each approximately of 1.7344069 m^3 volume, dump waste at Site-C all the year round. Values of environmental parameters at site of Gudara Ghat has topped in most of the experiment due to the type of waste present there as well as the waste brought by the stream. A university, a hospital, and two big and several other small slums, various kinds of industries are situated in the adjacent area of Turag between Tongi Bridge (Site-B) and Gudara Ghat (Site-C).

Site-D and Site-E mainly contain the flow from upstream which combines with another flow of the Turag River. A very small area is cultivated only in the dry season which remains under water for the most part of the year. The waste dumped at Diabari (Site-D) and Rustompur Bridge (Site-E) is mainly industrial. In addition, Site-E has a market covering a small area of the site. Table 4 illustrates the major type of wastes that are dumped in Turag River.

Table 4: Major Waste Type in Sites

Site	Types of Water Use					
	Agricultural	**Market**	**Industrial**	**Household**	**Hospital**	**Institution**
A	✓					
B		✓	✓	✓		
C	✓		✓	✓	✓	✓
D	✓		✓			
E	✓	✓	✓			

3.3 Relationship between Land Use and Water Quality of Turag River

The main purpose of purpose of the study is to find out the relationship between land use and water quality. Water quality of five different sites on the Turag River in different depths was tremendously poor (Section 3.1). Due to urbanization, numerous type of waste has been dumped on the river (Section 3.2).

Site-A mainly contains agricultural waste. Due to various kinds of fertilizer use, water of Site-A obtains high pH, TDS and Turbidity values. Increased sediment loads create more suspended particles that increase turbidity level. Factors affecting the phytoplankton distribution are water temperature, TDS, alkalinity and dissolved oxygen. Runoff from agricultural land increase BOD level which can be harmful for aquatic animals. Different ingredients in fertilizer deteriorate colour of river water. Alongside agricultural waste, industrial and household wastes also contribute to the river water pollution. Domestic and industrial wastes in the Site-B deteriorate water quality by adding substances in water. Due to heavy metal concentration, Site-B average pH values were lower than Site-A. Effluents discharged without treatment in river are responsible for turbidity, colour, and TDS increment. Furthermore, anthropogenic impacts generated through domestic waste directly affect watershed hydrology and reduce water quality.

At Site-C, waste is mixture of agriculture, industrial, domestic and hospital. Thus water quality of Site-C was the worse. Due to water stream, turbidity value may be reduced but this does not mean improving water quality. High pH, TDS and BOD values illustrate increasing water pollution tendency (7.91, 1600, 30). The findings clearly indicate that water is

polluted because of discharge of sewage and other anthropogenic activity. Diabari (Site-D) mostly carries agricultural and industrial wastes. Water at this site was less pH values than Site-A probably because of the acidic nature of the main ingredients of the fertilizers. The main noticeable point is that due to less waste, Site-D river water quality was slightly better than Site-C, Site-A and Site-B.

Site-E contains agricultural, market and industrial waste. Agricultural waste amount was less than Site-A and Site-C. Following this, Site-E water quality parameter values are less than those sites. Finally, findings of the study clearly suggest relationships between land use and water quality. Water quality decreases with increasing land use for different purposes.

4. CONCLUSION

The Turag River becomes a crucial resource to approximately two million people. The major concern is that only a few of the test results are fitting in the existing standards while the others are way off the chart. It is clear from the values from the test and observational survey results that the pollution is escalating rapidly day by day. Numerous industries and land uses developing along the banks of the Turag River cause more pollution and encroachment on river bank. Thus, it can be concluded that the water of this river may exhibit serious threat to the surrounding biological ecosystem. However, some water quality parameters may not be at critical pollution level, the condition of the river side due to urbanization and industrialization may cause severe pollutions. Land use which is a major variable of development of the socio-economic condition, is taking its toll on the water quality of Turag in case of Gazipur. Quality of water deteriorates with the increase and density of land use. In the meantime, the pollution level of the Turag has not yet gone above treatability and the river has not been under the massive grasp of encroachment. Therefore, recovery process of the river needs to be started immediately. Local organizations, residents and provincial, federal departments all should involve in the restoration of the River ecosystem. Discharge of industrial effluents near the surface water as well as domestic waste from residential areas should be decreased and establishment of sewage treatment plants is needed to monitor the region human settlements. A further recommendation is the organization of educational programs to provide proper information to people in the local area about waste water management and soil conservation methods. Some work has already begun in these areas, especially in terms of wastewater management, but much work is required to encourage the use of land management practices in the areas.

REFERENCES

Fakayode, S.O. (2005). Impact of industrial effluents on water quality of the receiving Alaro River in Ibadan, Nigeria*. Ajeam-Ragee*, 10, 1-13.

Ferrier R. C., Jenkins A., Wright R. F., Schöpp W. & Barth H. (2001). Assessment of recovery of European surface waters from acidification, 1970–2000: Introduction to the Special Issue. *Hydrology and Earth System Sciences,* 5, 274-282.

Foley J.A., DeFries R., Asner G.P., Barford C., Bonan G., Carpenter S.R., Chapin F.S., Coe M.T., Daily G.C., Gibbs H.K., Helkowski J.H., Holloway T., Howard E.A., Kucharik C.J., Monfreda C., Patz J.A., Prentice I.C., Ramankutty N. & Snyder P.K. (2005). Global Consequences of Land Use. *Science*, 309, 570-574.

Griffith J.A. (2002). Geographic techniques and recent applications of remote sensing to landscape-water quality studies. *Water Air Soil Pollut*, 138, 181–197.

Ierodiaconou D., Laurenson L., Leblanc M., Stagnitti F., Duff G., Salzman S. & Versace V. (2005). The consequences of land use change on nutrient exports: a regional scale assessment in south-west Victoria, Australia. *J Environ Manage*, 74, 305–316.

Islam M.S., Tusher T.R., Mustafa M. & Mahmud S. (2012). Effects of Solid Waste and Industrial Effluents on Water Quality of Turag River at Konabari Industrial Area, Gazipur, Bangladesh. *Environ. Sci. & Natural Resources*, 5(2), 213 – 218.

Johnson L.B., Richards C., Host G. & Arthur J.W. (1997). Landscape influences on water chemistry in Midwest stream ecosystems. *Freshwater Biology*, 37, 193–208.

Lee T.M., Haag K.H., Metz P.A. & Sacks L.A. (2009). Comparative hydrology, water quality, and ecology of selected natural and augmented freshwater wetlands in West-Central Florida. *US Geological Survey Professional Paper 1758.*

Li S., Gu S., Tan X. & Zhang Q. (2009). Water quality in the upper Han River basin, China: The impacts of land use/land cover in riparian buffer zone. *Journal of Hazardous Materials*, 165, 317–324.

Ngoye E. & Machiwa J. (2004). The influence of land use patterns in the Ruvu river watershed on water quality in the river system. *Phys Chem Earth*, 29, 1161–1166.

Nwankwoala, H.O. & Nwagbogwu, C.N. (2012). Characteristics and quality assessment of groundwater in parts of Akure, South-Western Nigeria. *Journal of Environmental Science and Water Resources*, 1(4), 67-73.

Pasha M.M., Aziz H. M., Asif M.H. & Shahriar S. (2012). A study on the impact of domestic and industrial waste on water quality of Turag River. *ICETCES*, Sylhet, Bangladesh.

Pieterse N.M., Bleuten W., Jacks G. & Jorgensen, S.E. (2003). Contribution of point sources and diffuse sources to nitrogen and phosphorus loads in lowland river tributaries. *J. Hydrol.,* 271, 213-225.

Rothwell J.J., Dise N.B., Taylor K.G., Allott T.E.H., Scholefield P., Davies H. & Neal C. (2010). Predicting river water quality across North West England using catchment characteristics. *J. Hydrol.*, 395 (3–4), 153–162.

Tariquzzaman S.M., Nishu S., Saeed T.F. & Reday R.A. (2016). Water quality and EIA of simple Hatirjheel Lake. *Proceedings of the 3rd International Conference on Civil Engineering for Sustainable Development*, KUET, Khulna, Bangladesh, ISBN: 978-984-34-0265-3.

Tran C.P., Bode R.W., Smith A.J. & Kleppel G.S. (2010). Land-use proximity as a basis for assessing stream water quality in New York State (USA). *Ecological Indicators*, 10, 727–733.

Woli K.P., Nagumo T., Kuramochi K. & Hatano R. (2004). Evaluating river water quality through land use analysis and N budget approaches in livestock farming areas. *Sci Total Environ*, 329, 61–74.

Proceedings of the 4th International Conference on Civil Engineering for Sustainable Development (ICCESD 2018), 9~11 February 2018, KUET, Khulna, Bangladesh (ISBN-978-984-34-3502-6)

RISK ASSESSMENT FOR URBAN WATER SUPPLY IN A DEVELOPING COUNTRY: A CASE STUDY OF DHAKA CITY

S.M. Anik Rahman[1], Md. Mahmud Hossain[2], Md. Rabiul Hasan[3], Shakil Ahmed[4] and Md. Rafiu Zaman[5]

[1] M.Sc. Student, Islamic University of Technology, Bangladesh, e-mail: iut.anikrahman@gmail.com
[2] M.Sc. Student, Islamic University of Technology, Bangladesh, e-mail: mahmud31@iut-dhaka.edu
[3] Graduate Student, Islamic University of Technology, Bangladesh, e-mail: mdrabiulhasan@gmail.com
[4] Doctoral Student and Research Assistant, West Virginia University, USA, e-mail: skahmed@mix.wvu.edu
[5] M.Sc. Student, Islamic University of Technology, Bangladesh, e-mail: rafiucee@iut-dhaka.edu

ABSTRACT

Traditional approach to water quality and safety management has mostly relied on the testing of drinking water either at the point of its treatment works or at selected points within the distribution system. But risk assessment approaches are required for developing countries like Bangladesh to upgrade water supply and sanitation services which can reduce vulnerability of people being affected by water borne diseases. The main purpose of the study is to show spatial variation of major leakages of distribution pipes in different water supply zones of DWASA and propose measures for minimization of the water pollution risks based on identification of the hazards that the water supply is exposed to. Growths of population, economy and industry are challenging factors for DWASA (Dhaka Water Supply and Sewage Authority). For this study, Dhaka city which is divided among ten zones by DWASA was selected. Leakage values of zones were collected for seven years (2007-2013). From the data, monthly variations of leakage across the zones and average of leakage of each zone for different years were determined. A risk analysis matrix was created using the weighting value of leakage and number of connection for risk ranking. Finally, hazard zone was identified in city map showing spatial variations of major leakages in different water supply zones. The findings of the study suggest that DWASA- Zone 4 is at higher risky position than other zones. Findings can be used to develop operational plans and identify causes with key priorities for action.

Keywords: *Risk Assessment, Leakage, DWASA, Water Supply, Weighting value*

1 INTRODUCTION

Availability of potable, safe and affordable water is one of the most important development goals which ensures social and economic growth, promotes health and overall welling being of human being. The World Health Organization (WHO) estimates returns of $3-$34, depending on the region and technology, for each $1 invested in safe drinking water and basic sanitation (Hutton & Haller, 2004). It is thus important for the water experts and specialists to convey this important message to the politicians and decision makers. Policy-makers can be motivated to use these data to justify their actions, identify areas of deficiency and better prioritize actions (Wallace et al., 2008). Expanding safe drinking water and sanitation services would drastically cut the loss of life from water-related illness and free up scarce health resources in developing countries. According to the UN-Water Report (2008) five thousand children die each day from diarrhea alone or one every 17 seconds. The overall economic loss in Africa alone due to lack of access to safe water and basic sanitation is estimated at $28.4 billion a year, or around 5% of GDP. Upgrading water supply and sanitation services based on risk assessment can reduce vulnerability of people being affected by water borne diseases.

Water supply is provided to secure sufficient amounts of treated water of good quality at any time and location downstream from the treatment facilities (Persson, 2009). But water supply access in most developing countries is quite complex (Khadse et al., 2011). The rapidly increasing demand for water particularly in developing countries is an obvious obstacle to sustainability. Conversely the urgent necessity for its provision is similarly an obstacle with short term solutions often leading to serious long term problems (Gray, 2005). Thus, the problems are very acute in densely populated informal or slum areas of developing countries. The main drivers for increasing water demands are growing populations, increasing urbanization and economic growth (Meinzen-Dick & Ringler, 2006). Urbanization is occurring throughout the developing world at alarming rate and by 2025 over 50% of the world's population will be urban dwellers (UNCHS, 2001; WHO, 2007). Many households do not have piped water supply and have to rely on community based water sources. These mostly include public taps and water purchased from vendors (Whittington et al., 1991; Cairncross & Kinnear, 1992; Howard, 2001; Tatietse & Rodriguez, 2001). They also include a variety of small point water supplies such as boreholes with handpumps, protected springs and dug wells (Howard et al., 1999).

The traditional approach to water quality and safety management has relied on the testing of drinking water either at the point of its treatment works or at selected points within the distribution system. This approach does not take into consideration the water quality at its final phase or consumers point making the water vulnerable to possible contamination at collection point. Risk assessment, as defined by BS 7799:1999 Part 1 is "assessment of threats to, impacts on and vulnerabilities of information and information processing facilities and the likelihood of their occurrence". This rather unwieldy definition translates into risk being some function of threat, asset and vulnerability. This concept has been around for at least two decades. Risk assessment examines the severity or magnitude of risk to human health posed by contaminants (Wen et al., 2006).

A risk assessment report can be either quantitative or qualitative. In quantitative risk assessment, an attempt is made to numerically determine the probabilities of various adverse events and the likely extent of the losses if a particular event takes place. This includes the selection of assessment and measurement endpoints and the comparison of endpoint water quality measurements or distributions to a guideline value. Qualitative risk assessment involves the use of expert groups assessing water quality issues, either as contaminants, pollution sources or hazard events, and prioritizing these issues from this assessment. Methods vary over different components such as driving compliance frameworks, input information, base categorization (hazard or hazardous event based) and if they are qualitative or quantitative in assessment.

The objectives of risk assessment are to ensure the delivery of safe drinking water through identification of the hazards that the water supply is exposed to and the level of risk associated with each, minimization or reduction of each hazard, hazard monitoring and verification of the proposed measures for minimization of risks. Following this, the main purpose of the study is to show spatial variations of major leakages of distribution pipes in different water supply zones of Dhaka Water Supply and Sewerage Authority (DWASA) and propose measures for minimization of the water pollution risks—based on identification of the hazards that the water supply is exposed to.

2. STUDY AREA AND METHODOLOGY

Overall Study Area and Methodology involves selection of Study area and Data collection (Section 2.1), Hazard identification (Section 2.2) and Risk analysis (Section 2.3).

2.1 Study Area and Data Collection

Dhaka, the capital of Bangladesh, is the most densely populated cities which is situated in central Bangladesh at $23^0 42' 0'' N$ $90^0 22' 30'' E$, on the eastern banks of the Buriganga River. It covers a total area of 360 square kilometers (BBS, 1991, 2001 & 2011). Water Supply and Sewerage Authority (WASA) is a service oriented self-explanatory commercial organization in Bangladesh for providing water to the urban dwellers. It covers more than 360 sq. km service area with a production of nearly 2110 million liters per day (DWASA, 2011). Dhaka WASA (DWASA) is divided into 11 geographic zones where Dhaka city organized with 10 zones and 1 in Narayanganj city for improving their operation, maintenance, and customer care. DWASA distribution system has pipeline of nearly 3040 km. The total number of consumers for DWASA is residential 2,88,401 (92.71%), commercial 19,872 (6.39%). Piped water supplies are generally distributed according to three levels of services: house connections, yard connections and public standpipes. Assessing the distribution system possesses a more significant challenge than water treatment works due to unplanned expansion of pipe networks, an understanding of the hydraulics of the system, the materials, age and size of the pipes and the location of the water supply pipes in relation to areas where hazards exist. The system loss for Dhaka city is 28.8% (DWASA, 2012).

For this study, Leakage values of seven zones were collected for four years (2007-2010) and ten zones data were collected for three years (2011-13) from DWASA official website. From the data, monthly variations of leakage across the zones and average of leakage of each zone for different years were determined.

2.2 Hazard Identification

The cross contamination of groundwater leakaging into pipes is a major concern in the pipe network system of Dhaka city and causing various water borne diseases. This risk can be assessed by analyzing the condition of the pipe. Key indicators of pipe condition that could be considered are:

- ✓ Pipe age – the effects of pipe degradation becomes more apparent over time.
- ✓ Pipe diameter – small diameter pipes are more susceptible to beam failure.
- ✓ Pipe length and jointing - long water pipes are more susceptible to longitude breaks.
- ✓ Pipe material – assess vulnerability of pipe to failure based on combination of hydraulic pressure exerted on the pipe and corrosivity of soil in which pipe is laid.

Apart from the above causes, ingress of contaminated water during periods of low or no flow and prolonged storage in pipes are the main causes for deterioration of water quality.

2.3 Risk Analysis

In order to identify a hazard event in distribution systems, it is important to consider the source-pathway-receptor model of contamination (Fig. 1).

Figure 1: pathway-receptor model of contamination

In this model the source is the source of the hazards, the receptor is the water supply (in this case the pipes that form the distribution system) and pathways are the means by which the hazards can leave the ‘source’ and reach the ‘receptor’. The source-pathway-receptor model recognizes that the presence of a hazard in the environment is insufficient on its own to represent a risk; a feasible pathway must exist that allow hazards to travel from the source to the water supply. When this occurs, it is a ‘hazard event’.

The nature of the hazards will determine the likely health outcome. Pathogens and massive pollution by chemicals may lead to mortality, whereas lower levels of chemicals may only lead to morbidity. The location of the hazard event will influence the number of people affected for instance hazard events on major transmission mains or in service reservoirs will be likely to have an impact on many people, whereas a hazard event in a small tertiary pipe may only affect a very small number of people. Risks can be identified at various stages, and prioritized in terms of likelihood and seriousness (ADB, 2010). A risk-ranking matrix is developed to address both likelihood and severity. Most approaches use some form of semi-quantitative ranking system by allocating numbers to different levels of likelihood and different levels of severity. A risk score is then calculated by multiplying these two numbers together.

Risk = Likelihood * Severity (1)

The selection of the categories and the weighting allocated to different categories with guidelines to definitions are provided in Table 1 as there is no uniform 'industry standard'. The weightings were applied in South-East Water, Australia (Deere et al., 2001) and in Uganda (Godfrey et al., 2002). These are applied to each of the inspection points in order to define the severity of risk associated with individual hazard events in piped supply.

Table 1: Risk and severity; some guidance to definitions

Likelihood	**Definition**	**Weight**
Almost certain	Once a day	1
Likely	Once per week	0.8
Moderate	Once per month	0.6
Unlikely	Once per year	0.4
Rare	Once every 5 years	0.2
Impact	**Definition**	**Weight**
Catastrophic	Potentially lethal to large population	1
Major	Potentially lethal to small population	0.8
Moderate	Potentially harmful to large population	0.6
Minor	Potentially harmful to small population	0.4
Insignificant	No impact	0.2

3. ANALYSIS AND RESULTS

The results obtained following the outlined methodology are organized into five sub-sections. Section 3.1& 3.2 are for leakage data analysis, Section 3.3 is for overall data analysis comparison. Then city map has been shown in section 3.4 to identify hazard zone and finally risk reduction options are discussed to minimize hazard of zones (Section 3.5).

3.1 Leakage Data Analysis for 2007 to 2010

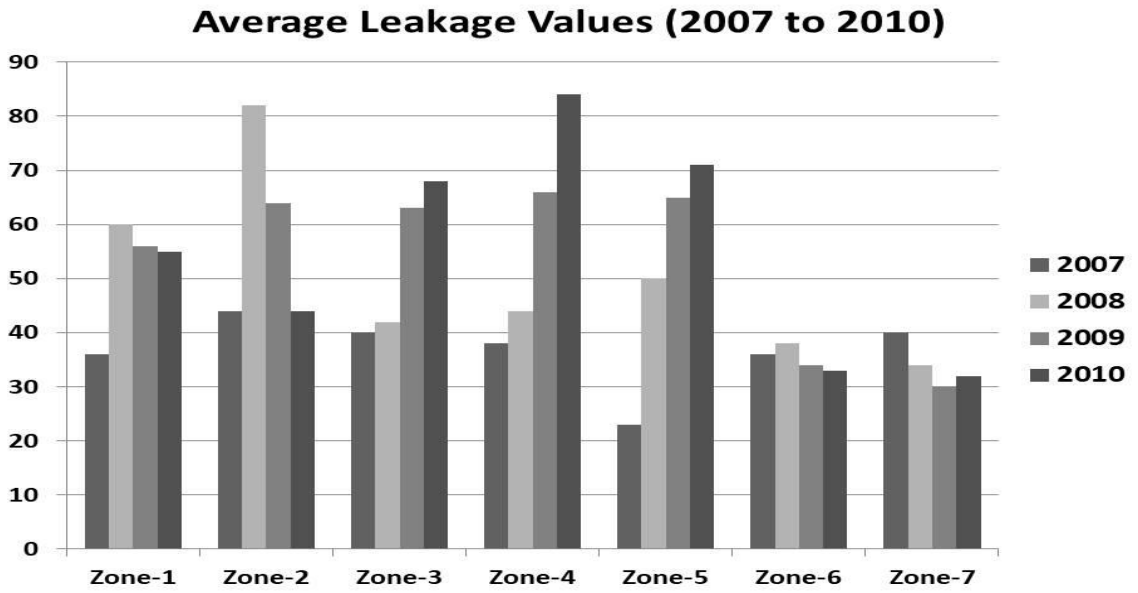

Figure 2: Average Leakage Values for Year 2007-2010

In the study, average leakage value of each year was estimated taking the monthly leakage values of the certain year. Subsequently, average leakage value of seven zones for year 2007 to 2010 has been showed in figure 2. From 2007 to 2008, Zone-2 has the peak average leakage values (44, 82). Zone-2 covers area involving B.D.R-3, Kalunagar Hazaribagh, Hazaribag Park. In 2009, average leakage values in zones waere very close to each other (56, 64, 63, 66, 65, 34, and 30) and thus no significant variation has been found. In year 2010, reduction in average value has been noticed in Zone-2. Besides, Zone-4 (Mirpur 6 /Ta, Rupnagar-1, Uttar Bissil) gained the highest average value (84). Furthermore, almost in each zone expect from Zone-2, average leakage values represent an increment in 2010.

Table 2: Average Leakage Values for Year 2007-2010

Zone	Weighting Value of Avg. Leakage Value (2007-08)	Weighting Value of Avg. Leakage Value (2008-09)	Weighting Value of Avg. Leakage Value (2009-10)
1	0.76	0.79	0.74
2	1.00	1.00	0.72
3	0.65	0.72	0.87
4	0.65	0.75	1.00
5	0.58	0.79	0.91
6	0.59	0.49	0.45
7	0.59	0.44	0.41

Using average leakage values of 2007 to 2010 (Figure 2), Table 2 has been generated exhibiting weighting value of average leakage for time period 2007-2008, 2008-2009, and 2009-2010. As average leakage values are larger in Zone-2 for 2007 and 2008, weighting values of the zone obtain the highest (2007-08, 2008-09). Following this concept and estimation, Zone-4 exhibited maximum weighting value for 2009-10. On that certain time period, Zone-2 achieved a weighing value between 0.7 and 0.8. In each time period, Zone-6 (Modhubag Madrasha, Moghbazar Wireless, Santibag) and Zone-7 (Sonakanda, Kadam Rasul, Paikpara) showed less weighing value than other zones.

3.2 Leakage Data Analysis for 2011 to 2013

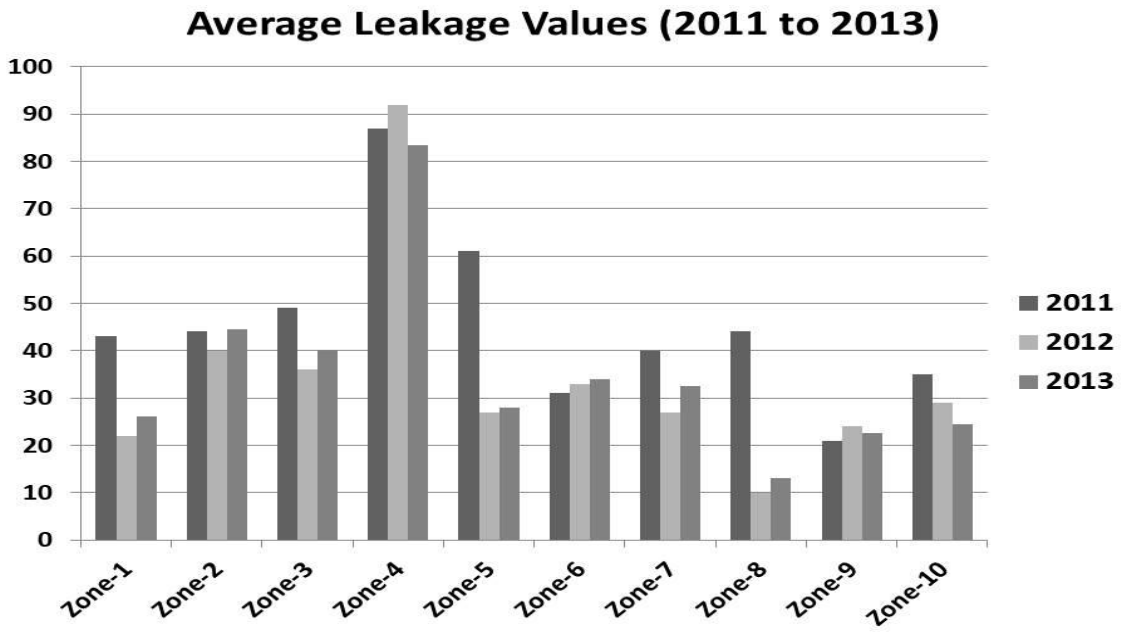

Figure 3: Average Leakage Values for 2011 to 2013

Ten zones average leakage values for 2011 to 2013 has been illustrated in figure 3. Average leakage values of Zone-4 were the highest in each year (87, 92 and 83.5) which is subsequent to 2010. Considerable changes has been noticed in Zone-5 (Banani-5, Shahin Bag) as 2012 and 2013 average values (27 and 28) were much lower than 2011 (61). Zone-6 to Zone-10 continued with their low average value compared to other zones.

Table 3: Weighting Value of Average Leakage Value 2011 to 2013

Zone	Weighting Value of Avg. Leakage Value (2011-12)	Weighting Value of Avg. Leakage Value (2012-13)
1	0.36	0.31
2	0.47	0.53
3	0.47	0.48
4	1.00	1.00
5	0.49	0.34
6	0.36	0.41
7	0.37	0.39
8	0.30	0.16
9	0.25	0.27
10	0.36	0.29

Weighing values of average leakage of two specific time period, 2011-12 and 2012-13, has been illustrated (Table 3) considering average leakage values for 2011 to 2013 (Figure 3). In both time periods, Zone-4 held the position of peak weighting value. Zone-2 had weighting values between 0.45 and 0.55. Low weighting values represent less average leakage values especially in Zone-6 to Zone-10.

Table 4: Monthly Leakage Values of 2012

Zone	Jan	Feb	Mar	April	July	August	Sep	Oct	Nov	Dec
1	38	19	17	18	17	13	17	12	15	29
2	49	32	29	25	38	22	29	40	85	48
3	52	60	42	43	32	20	21	26	37	26
4	117	86	69	179	107	61	100	85	93	86
5	22	27	33	36	22	15	14	28	20	29
6	22	39	36	27	29	32	22	30	50	59
7	30	19	35	28	20	20	44	24	33	35
8	12	10	5	10	14	13	7	4	12	9
9	22	18	22	25	20	22	28	30	35	25
10	29	33	27	31	38	24	35	17	20	13

Table 5: Monthly Leakage Values of 2013

Zone	Jan	Feb	Mar	April	May	June	July	Aug	Sep	Oct	Nov	Dec
1	35	37	22	22	19	30	45	29	31	33	27	22
2	96	22	22	22	41	51	59	42	53	53	66	59
3	60	60	50	50	40	50	50	25	30	40	37	36
4	83	101	52	52	84	72	58	77	59	74	95	86
5	31	26	20	20	21	25	25	23	12	34	47	57
6	61	36	29	29	25	15	39	35	23	63	39	46
7	46	40	43	43	35	27	45	29	34	36	37	31
8	7	5	10	10	16	15	21	31	14	26	19	15
9	22	15	20	20	20	18	20	22	26	25	22	20
10	17	20	20	20	21	20	25	20	25	20	15	10

Table 4 & 5 represent seasonal variations in leakage data for years 2012 and 2013. In 2012, the highest leakage was detected in the month of April (179). Total precipitation was 196.192 mm in April 2012 (Source: World Bank). Poor infrastructures like old aged pipes, lack of maintenance or illegal connections and high rainfall are responsible for high leakage. February month recorded the peak leakage in 2013 (Table 5). According to World Bank, average precipitation in February 2013 was 11.4669 mm. Consequently too dry period where cracks occur increases leakage value.

Table 6: Risk Analysis (2012-2013)

Zone	Weighting Value of Avg. Leakage Value	Number of Connections	Weighting Value from the Number of Connections	Risk
1	0.31	38458	1.00	0.31
2	0.53	30086	0.78	0.41
3	0.48	30266	0.79	0.38
4	1.00	35811	0.93	**0.93**
5	0.34	13659	0.36	0.12
6	0.41	33211	0.86	0.35
7	0.39	35688	0.93	0.36
8	0.16	26291	0.68	0.11
9	0.27	34935	0.91	0.25
10	0.29	29401	0.76	0.22

Risk analysis is the multiplication of weighting value of average leakage and weighting value from number of connections (Equation 1). As development of any society increases, number of connections also changes with time period. Table 6 illustrates estimation of risk analysis for ten zones in the time period 2012-13. As discussed earlier, Zone-4 presented the peak

weighting value for average leakage (2012-13). Weighting value from number of connection obtained the highest in Zone-1 (Bashaboo-3 (Middle), Boishakhi Housing, Forashgonj). Finally, Zone-4 is found to be the most risky zone (0.93) among the ten zones. Observing weighting values of Zone-2, the zone can also be considered as hazard zone having risk value 0.41.

3.3 Comparison of Overall Analysis (2007 to 2013)

In the Study, observation of average leakage value for different years (2007-2013) is essential to identify hazard zones of Dhaka City. Zone-1 average value is decreased from 2008 to 2013 (Figure 2 and Figure 3). Development in water supply management system, population change and zonal purpose contribute to the changes. Besides, Zone-1 possesses maximum number of connections in Dhaka City which indicates raising development and population of the zone. Zone-2 can be risky in some perspective (Risk-0.41). In 2007 and 2008, Zone-2 had the peak average leakage values. With time interval, average value variations have been noticed in the zone but any significant change is not found. Zone-3 had a consistency in peak average leakage in five years (2009-13). Consequently, this zone holds position of the most risky zone. Other zones stay in mostly uniform leakage values with changing time periods. Considerable reduction in leakage value has been exhibited throughout time period 2012-13.

3.4 Hazard Identification in City Map

One of the purposes of the paper is to identify most risky zone in Dhaka City map. According to the map (Figure 4), Zone-4 is included area Agargoan, West Agargoan, East Symoli, kallanpor, Paekpara, Pererbag, Taltola, West Sewreapara and West Kazipara.

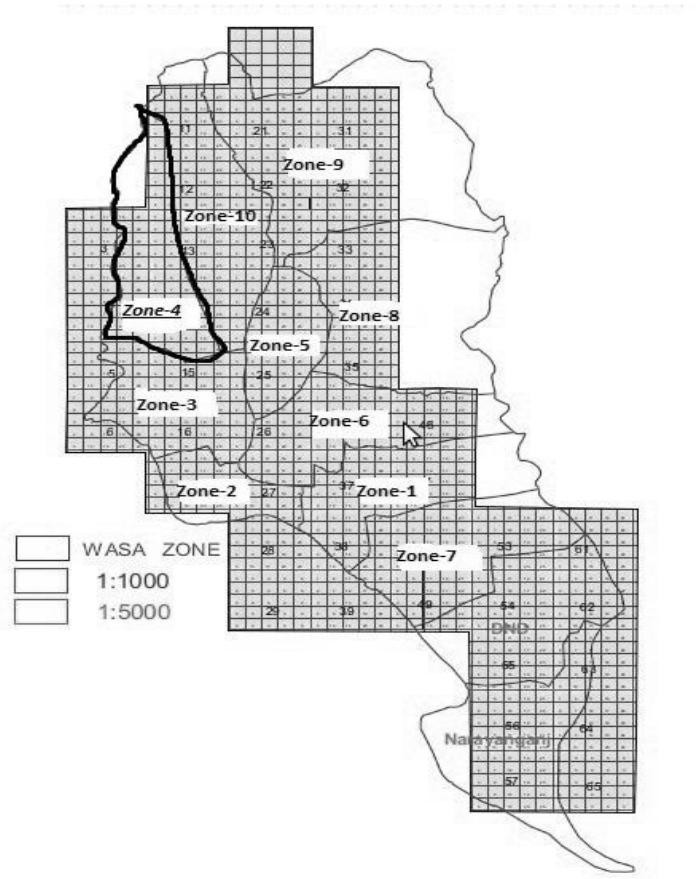

Map Source: www.dwasa.org.bd

Figure 4: Water Supply Zone in Dhaka City Highlighting Risky Zone

3.5 Risk Reduction Options

A number of different risk reduction measures can be taken to decrease the risks. For example, storage of water in open buckets, pitchers or dirty bottles or containers falls in red zone of risk matrix and this could be minimized through awareness program to store water in a hygienic way either by covering the pitchers, buckets or containers and getting water supply through network of pipes consisting of running water from the water supply authority. Ineffective mixing of chlorine leading to poor disinfection can be reduced by regular monitoring and water quality parameter tests with addition of optimum chlorine required. A stand by pump may be used to supplement the pump failure because of failure in continuous supply of electricity. The cross contamination of groundwater leaking into pipes can be reduced by replacing the aging pipe with new pipes but this involves a lot of cost.

4. CONCLUSION

Risk assessment with risk matrices and risk weighting and scoring method is a useful method and the data can be easily understood. However, the risk can be identified as the health and number of affected people who fall victims to a particular hazard. The major risks were found in the leakage and storage of water followed by the scarcity of water to ensure personal hygiene. Risk reduction options were found to reduce the risks significantly. By developing risk assessment, the system managers and operators will gain a thorough understanding of their system and the risks that must be managed. This knowledge can then be used to develop operational plans and identify key priorities for action. Effective policy and legal frameworks are necessary to develop, carry out and enforce the rules and regulations that govern water use and protect the resource. Water policy operates within a context of local, national, regional and global policy and legal frameworks that must all support sound water management goals. Corruption remains a poorly addressed governance issue in the water domain. This domain is a high-risk sector for corruption because water service provision is a near natural monopoly. The resource is becoming increasingly scarce in many countries, and the water domain involves large and often complex construction contracts. Furthermore, water has multifunctional characteristics and is used and managed by a mix of private and public stakeholders.

ACKNOWLEDGEMENTS

We are very grateful to Shahriar Shams, Assistant Professor, Department of Civil Engineering, Universiti Teknologi Brunei, Brunei Darussalam. Except his help it was not possible to complete the research.

REFERENCES

ADB (2010). Guidance note: Urban water supply sector risk assessment, Mandaluyong City, Philippines: Asian Development Bank. Accessed from 10 Dec. 2013.

BBS (1991, 2001 & 2011). Bangladesh Bureau of Statistics Bangladesh. Population Census, Dhaka, Government of Bangladesh.

Cairncross, S. & Kinnear, J. (1992). Elasticity of demand for water in Khartoum, Sudan. *Social Science and Medicine*, 34(2), 183-189.

Deere D, Stevens M, Davison A, Helm G, Dufour A. (2001) Management strategies. In: Fewtrell 1 L, Bartram J, editors. *Water 2 quality: guidelines, standards and health*, London: IWA Publishing, 257-288.

DWASA (2011). Dhaka water supply system and sewerage Authority. Annual Development Report; Water Supply and Sewerage Authority, Dhaka, Bangladesh.

DWASA (2012). Dhaka Water Supply and Sewerage Authority. Annual Development Report; Water Supply and Sewerage Authority, Dhaka, Bangladesh.

Godfrey, S., Howard, G., Niwagaba, C., Tibatemwa, S.M. & Vairavamoorthy, K. (2002). Improving risk assessment and management in urban water supplies. *Proceedings of the 28th WEDC Conference*, WEDC, Loughborough, UK.

Gray, N. (2005). Water Technology: An Introduction for Environmental Scientists and Engineers. Second ed. Butterworth, Heinemann.

Howard, G. (2001). Challenges in increasing access to safe water in urban Uganda: economic, social and technical issues*. In Microbial Pathogens and Disinfection By-products in Drinking Water: Health Effects and Management of Risks* (ed. G. F. Cruan, F. S. Hauchman & D. E. Robinson), ILSI Press, Washington, D.C., 483 – 499.

Howard, G., Bartram, J. K. & Luyima, P. G. (1999). Small water supplies in urban areas of developing countries. *In: Providing Safe Drinking Water in Small Systems: Technology, Operations and Economics* (Cotruvo, J. A., Craun, G. F. & Hearne, N.eds), Lewis Publishers, Washington, D.C., 83–93.

Hutton, G. & Haller, L. (2004). Evaluation of the Costs and Benefits of Water and Sanitation Improvements at the Global Level. *World Health Organization*, Geneva.

Khadse G.K., Kalita M.D., Pimpalkar S.N. & Labhasetwar P.K. (2011). Surveillance of drinking water quality for safe water supply-a case study from Shillong, India. *Water Resour Manag*, 25, 3321–3342.

Meinzen-Dick, R. & Ringler, C. (2006). Water Reallocations: Challenges, Threats and Solutions for the Poor. *Occasional Paper 2006/41*, UN Human Development Report Office.

Perrson, M. K. (2009) Tap, tank or bottle? – aspects of drinking water consumption in Eds. Jonas Forare. *Drinking water – sources, sanitation and safeguarding*, Formas, 113-133.

Tatietse, T. T. & Rodriguez, M. (2001). A method to improve population access to drinking water networks in cities of developing countries. *J. Wat. Suppl.: Res. & Technol.-AQUA*, 50(1), 47–60.

UNCHS (2001). Cities in a Globalizing World: Global Report on Human Settlements. *Earthscan Publications Ltd.*, London.

UN-Water (2008). Sanitation Is Vital for Health. *International Year for Sanitation*, New York.

Wallace, S., Corinne, J., Grover, V. I., Adeel, Z., Confalonieri, U. & Elliott, S. (2008). Safe Water as the Key to Global Health. *United Nations University International Network on Water, Environment and Health*, Hamilton, Canada.

Wen, T.H., Lin, N.H., Lin, C.H., King, C.C. & Su, M.D. (2006). Spatial mapping of temporal risk characteristics to improve environmental health risk identification: A case study of a dengue epidemic in Taiwan. *Science of the Total Environment*, 367 (2-3), 631-640.

Whittington, D., Lauria, D.T. & Mu, X. (1991). A study of water vending and willingness to pay for water in Onitsha, Nigeria. *World Development*, 19(2/3), 179-198.

World Health Organization (WHO) (2007). Maternal Mortality in 2005: Estimates Developed by WHO, UNICEF, UNFPA, and the World Bank, Geneva.

Proceedings of the 4th International Conference on Civil Engineering for Sustainable Development (ICCESD 2018), 9~11 February 2018, KUET, Khulna, Bangladesh (ISBN-978-984-34-3502-6)

MORPHOLOGICAL RESPONSES OF A TIDAL RIVER DUE TO CLIMATE CHANGE: A CASE STUDY FOR KARNAFULI RIVER, BANGLADESH

Sajal Kumar Roy[1] and Umme Kulsum Navera[2]

[1] Assistant Engineer, Bangladesh Water Development Board, Bangladesh,
e-mail: sajalkumar1a@gmail.com
[2] Professor, Department of Water Resources Engineering, BUET, Bangladesh,
e-mail: uknavera@gmail.com

ABSTRACT

Karnafuli River is an important river in Bangladesh and Chittagong seaport plays the biggest role in this country's economy. Navigability along the Seaport of Karnafuli River is dependent on the discharge and sediment transport with time. Sea Level Rise (SLR) and Temperature Rise (TMR) in the coast of Bay of Bengal are evident from different scientific reports. SLR is threatening the hydrodynamic and morphological behavior of coastal rivers including the navigability at the downstream of Karnafuli River. The backwater effects in terms of discharge and sediment transport have been carried out in this study. The future scenarios for rise in water level and temperature due to SLR and TMR have been projected for the next 25-30 years. Mathematical modeling has been carried out for 10cm, 25cm and 50cm SLR and 0.5°C, 1.5°C and 2.5°C TMR to assess the hydro-morphological responses. Morphological analysis has been carried out for three different conditions for mean sediment size d_{50}=100, 150 and 200 µm. Mathematical model study has been performed 3-Dimensionally by using Delft3D. The study reach includes from downstream of Kaptai Dam to Kafco in Karnafuli River. Results show that backwater discharge will increase 1.9% to 7.9% from the present discharge. Due to this the sediment transport will be decreased from 50 to 100 tons per second. Thus, the downstream of Karnafuli River and seaport will experience more sedimentation. The study has also focused on planform analysis, total sediment transport, settling velocity, sediment rating curves due to climate change effects on Karnafuli River.

Keywords: *Karnafuli River, Mathematical Modelling, Morphology, Climate Change, Sea Level Rise*

1. INTRODUCTION

The Karnafuli River is the principal river in Chittagong region of Bangladesh. The Karnafuli River has about a hundred numbers of tributaries and two-thirds of which lie in Bangladesh (IWM, 2013). The main rivers of that region are the river Karnaphuli, Rainkhiang, Kasalong, Halda, Ichamati, Feni, Sangu, Bakkhali, Naf and Matamuhari. Karnafuli River originates from Lusai Hills about two kilometers east of Sugarbasora in Mizoram state of India (CEGIS, 2014). It lies in the southern part of Bangladesh and finally meets the Bay of Bengal near the Chittagong seaport. The length of the river is almost one hundred and sixty kilometres (Karmakar, et al., 2011). The downstream of the River Karnafuli shows the typical estuarine features. The Karnafuli River is very important in the context of economy of Bangladesh and also for Kaptai Hydro-electric power plant.

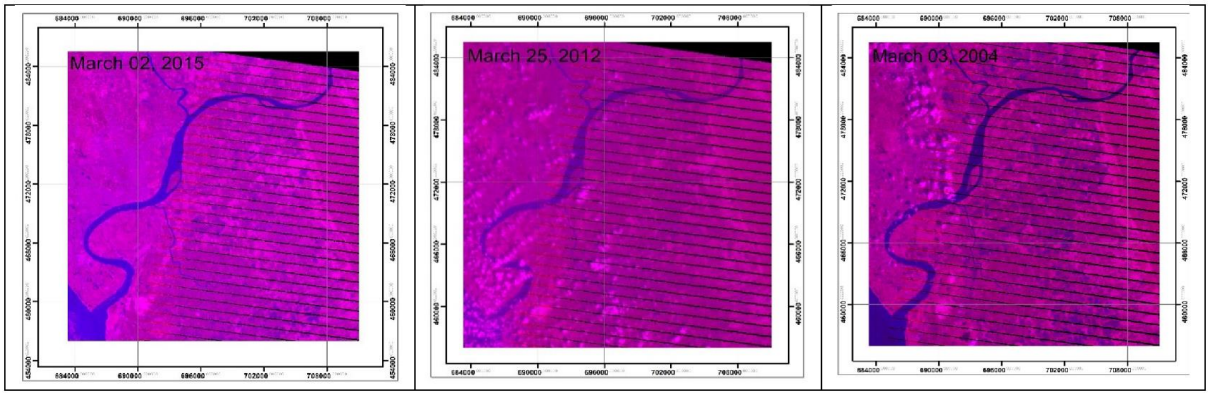

Figure 1: Satellite Images of Karnafuli River Reach

The sea port is in the south of Chittagong city, the second largest city in Bangladesh and is the nation's capital and administrative and economic center (ADB, 2011). It handles about 92% of the country's import-export trade (CPA, 2012). The most important seaport of Bangladesh is situated sixteen kilometers away from the sea mouth, Kafco (ADB, 2011). Another important part of the river is Kaptai dam which is located upstream of Karnafuli River. During monsoon period the high tidal flow and discharge is occurred in the Karnafuli River. The Chittagong Sea Port is experienced capital dredging for the succession of time. The past decade planform of the Karnafuli River shows stable bank lines (Figure 1). The river has shown same width along the reach with some bank erosion effect at certain location along the reach. The pattern of bend is observed almost same for the past decade as observed in the study.

Past literatures are the evidence of both global Sea Level Rise (SLR), Temperature Rise (TMR) warming and regional sea-level-rise including Bangladesh from the past coastal gauged water level data trends. The According to the third assessment report of the Intergovernmental Panel on Climate Change (IPCC) showed yearly Sea Level Rise (SLR) ranging 1.0 to 2.0 mm in the region1 (Unnikrishnan et al., 2015). The fourth and fifth IPCC reports show a yearly global mean SLR nearly 1.8 mm during 1961–2003 and 1.7 mm during 1901–2010 respectively (IPCC, 2007) (IPCC, 2013). The SLR is 2.15 mm per year has been found for past two decades at the location of Hiron Point gauged station (Brammer, 2013). The mean sea level is rising and sea level change was found from the gauged water level station to be 5.05 mm/year to 7.5 mm/year (CEGIS and DOE, 2011).

Due to SLR back water effect will generally take place thus will aggravate the retardation of a river outflow at the river mouth. The past studies have focused on the water level and salinity intrusion due to climate change. The author has carried out a set of mathematical model studies to show the hydro-morphological behavior due to backwater effect for SLR. The author has also found the siltation effect at d/s of Karnafuli River reach indicating threatening to the Chittagong Seaport. The Fourth Assessment Report of IPCC has depicted that the 100-year linear trend (1906-2005) of global average surface temperature is 0.74°C (Basak, et al., 2013). The change in temperature may affect the hydro-morphological behavior of the Karnafuli River for the future scenarios.

The present study will focus on the hydro-morphological analysis using mathematical modelling tool Delft3D for the future scenarios of Karnafuli River reach due to SLR and TMR as an impact on climate change. The study has included the development of 3D hydro-morphological and Heat flux models introducing 5 number of layers for the river Karnafuli River reach from downstream (d/s) of Kaptai Dam to estuary near Kafco. The mathematical model study has covered the hydro-morphological condition of base condition or 0 cm, 10 cm, 25 cm and 50 cm SLR conditions. Another set of Heatflux Models for base condition or

0.0°C, 0.50°C, 1.50°C and 2.50°C TMR conditions have conceded for the analysis of hydro-morphological assessment of Karnafuli River reach 3-Dimensionally. The morphological analysis has also been carried out by the author through another set of models for mean sediment size d_{50}=100, 150 and 200µm as river morphology largely depends on the sediment size. The outputs results obtained from the simulated conditions have focused on the total velocity distribution, sediment transport, suspended sediment transport, longitudinal or cross-sectional profile, erosion and deposition pattern of sediment sand.

2. METHODOLOGY

This study will be based on the effect of SLR and TMR due to climate change to Karnafuli River due to its' importance for having Chittagong Sea Port and Kaptai Dam and situated in the vulnerable area to SLR and TMR. The study will analyze the hydro-morphological assessment through selection of study area, data collection and data arrange, mathematical model setup, model calibration and validation, results analysis. The methodology of the study is presented in the following article.

2.1 Selection of Study Area

The Karnafuli River from d/s of Kaptai Dam to the the estuary at Kafco has been selected to assess the hydro-morphological change due to SLR and TMR. The main tributaries as Halda, Ichamati and Shikalbaha Canal (Khal) of almost 10 km from the confluence point of Karnafuli have also been considered in the study (Figure 2). Analysis of Karnafuli River has been made 3-Dimensionally including 5 number of vertical layers. The discharge from Kaptai Dam and the water level at Kafco have been the boundary condition of the simulated models. The location of calibration and validation location have been set to Kalurghat.

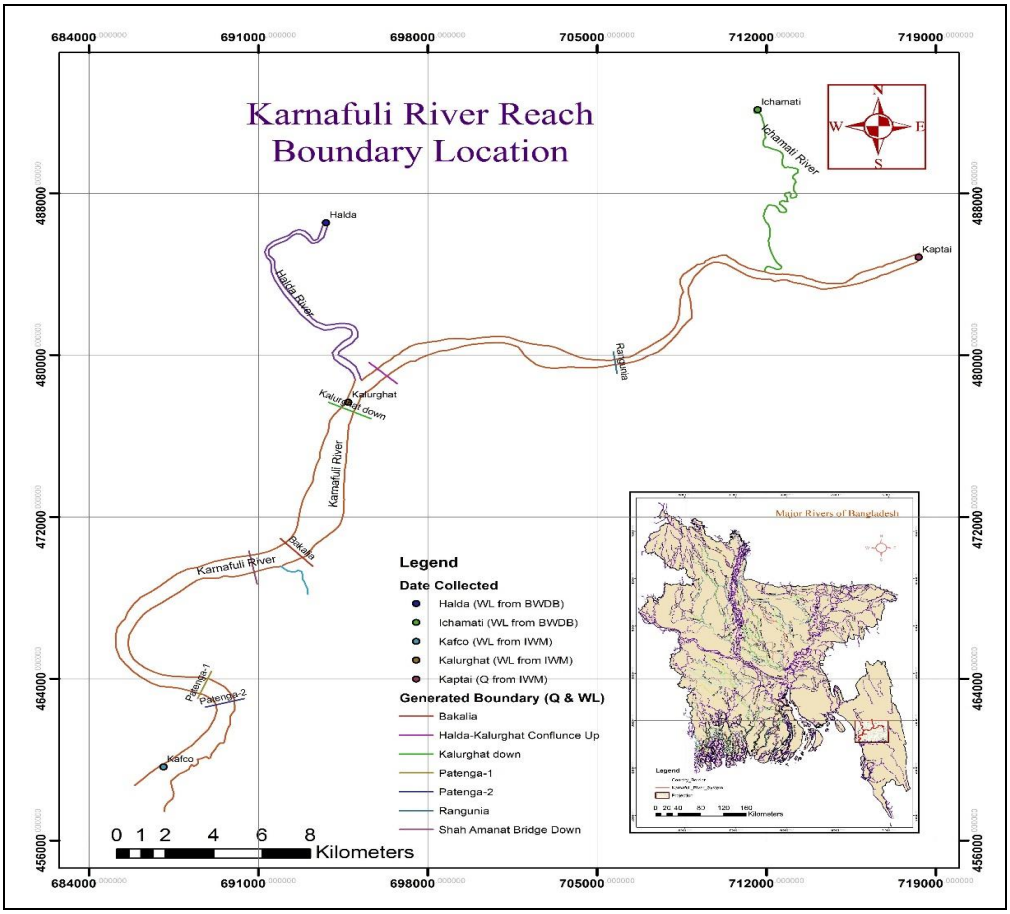

Figure 2: Study Reach with Boundary Locations

2.2 Data Collection and Data Arrange

The time series water level data at Kafco, Kalurghat and at Rangunia, Halda, Ichamati, the discharge data at d/s of Kaptai Dam, the cross sections data of the Karnafuli, Ichamati, Halda River and Shikalbaha Khal collected from both Bangladesh Water Development Board (BWDB) and Institute of Water Modelling (IWM) for the year of 2010 and 2011. Digital Elevation Model (DEM) of two major islands named Quapara and Bakalia Char has been collected from the electronic source as SRTM (30m×30m) from earth explorer. The size of the bed materials at Rangunia, Kalurghat and Kafco denoted as d_{50} and d_{75} and sediment concentration data for different locations have been collected from IWM. The satellite images of Karnafuli River reach from year 2004 to year 2015 has been collected.

2.3 Mathematical Model Setup

The mathematical model setup is a process that includes the selection of land boundary, generation of suitable grid spacing considering the river width, length and simulation time, making the bathymetry, preparing the roughness file for the river bed concerned, boundary condition file generation, to finally the simulation of the model including calibration and validation. The process of the model setup in this study is described in the following articles.

2.3.1 Background Governing Equations

The Delft3D-Flow-Morbasic equations of fluid flow, encode the familiar laws of mechanics as conservation of mass (the continuity equation) and conservation of momentum. The bed evolution is based on the sediment continuity where the first term expresses the changes in bed level in time and the second and third terms are the sediment fluxes (bed and suspended load) in the x and y directions, respectively. The Delft3D heat flux model includes the relative humidity, air temperature and the fraction of the sky covered by clouds is prescribed (in %). The Delft3D module is capable to compute the effective back radiation and the heat losses due to evaporation and convection.
The continuity equation in Cartesian coordinates is

$$\frac{\partial u}{\partial x}+\frac{\partial v}{\partial y}+\frac{\partial w}{\partial z}=0 \tag{1}$$

Where, *u*, *v* and *w* are the flow velocity components in the x, y and z direction.

The momentum equation used in Delft3D is

$$\rho\frac{D\mathbf{v}}{Dt}=\rho g-\nabla p+\mu\Delta\mathbf{v} \tag{2}$$

Where Δ is the Laplacian operator, ρ is the gravitational force and g is the gravitational acceleration.

The equation states that the bed level evolution in time is depended on the suspended and bed load gradients in the x and y directions.

$$\frac{\partial z_b}{\partial t}+\frac{\partial\left(S_{b,x}+S_{s,x}\right)}{\partial x}+\frac{\partial\left(S_{b,y}+S_{s,y}\right)}{\partial y}=0 \tag{3}$$

Where, $S_{b,x,y}$ = bed-load transport in x- and y-direction (kg m^{-1} s^{-1}), $S_{s,x,y}$ = sediment-load transport in x- and y-direction (kg m^{-1} s^{-1}), z_b = bed level (m).

The Van Rijn (1984) suspended and total sediment formula has been used for the morphological analysis with Delft3D (Delft3D-Flow, 2014).

.

2.3.2 3D Base Model Setup

Delft3D usually supports the use of a rectilinear, a curvilinear and a spherical grid system for setting up a model for flow of river or activities related to wave. In this study the rectangular curvilinear grid system has been used to prepare the hydro-dynamic and morpho-dynamic grid system of less than 2.0 aspect ratio. The grid generator program RGFGRID has been used in this thesis study to generate a rectangular grid system for model development. The rectangular grid system has used the land boundary and preferably the bathymetry for the preliminary set up the desired model. The land boundary is obtained from digitizing the satellite image map of resolution 30m×30m obtained from earthexplorer and the bathymetry is obtained upon using the tool QUICKIN with the help of cross section data provided by BWDB and IWM.

2.3.3 Base Model Calibration and Validation

The calibration is an iterative adjustment of the model parameters so that simulated data obtained from mathematical model represents the observed data of the river system to desired accuracy. The calibration of the model has been made for both hydrodynamic and morphological simulations. The base 3D model has been calibrated and validated against water level, discharge and erosion and deposition perspective. The hydrodynamic calibration and validation has been made at Kalurghat and at Patenga respectively for the year 2011 and 2010. The 3D validated model with the adjusted parameters as manning's roughness and morphological parameters has been used for the projected SLR and TMR scenarios. Calibration parameters has also included the model grid spacing, horizontal and vertical eddy diffusivity and the erosion factors of the Karnafuli River.

2.3.4 MOR-Model Setup for SLR Scenarios

The validated 3D base model has been used to estimate SLR scenarios for 0.0 cm (base condition), 10 cm, 25 cm and 50 cm due to climate change. The both hydrodynamic and morphological boundary conditions have been kept similar as the base condition (Table 1).

2.3.5 Heatflux-Model Setup for TMR Scenarios

The validated 3D base model has been used to estimate TMR scenarios for 0.0°C (base condition), 0.50°C, 1.50°C and 2.50°C due to climate change. The both hydrodynamic and morphological boundary conditions have been kept similar as the base condition (Table 1).

2.3.6 Mor-Model Setup for Different Sediment Size

The validated 3D base model has been used to estimate the scenarios for the different sediment size that constitute the sediment transport. The projected scenarios of morphological behaviour for d_{50}= 200µm,150µm and 100µm have been simulated in the study. This is because the sediment transport takes place with continuous sediment sorting or change to the flow direction. The both hydrodynamic and morphological boundary condition as sediment concentration have been kept similar for the four different sizes of sediments. The scenarios of the study are presented in Table 1.

Table 1: Scenarios developed in the study

Study Type	**Base condition**	**Climate Change/ different sediment size Scenarios**		
1. Hydro-morphological changes due to SLR	Post-monsoon, 2012	(+) 10 cm SLR	(+) 25 cm SLR	(+) 50 cm SLR
2. Hydro-morphological changes due to TMR	Post-monsoon, 2012	(+) 0.5°C TMR	(+) 1.5°C TMR	(+) 2.5°C TMR
3. Morphological changes with different sediment size	Post-monsoon, 2012	D_{50} =100 µm	D_{50} =150 µm	D_{50} =200 µm

3. RESULTS AND DISCUSSIONS

3.1 Hydrodynamic and Morphological Model Calibration and Validation

The hydrodynamic calibration of the model has been based on water level and discharge at Kalurghat (Figure 3 and 4). The calibration of morphological parameters has been adjusted based on simulated erosion and deposition presented in the parenthesis of Table 2 and illustrated in Figure 5. LB, MC and RB represent the Left Bank, Mid Channel and Right Bank respectively. The sediment boundary for the study of dredging has been set considering upstream and downstream at Rangunia and Kafco respectively. The 3D morphological model of 5 vertical layers has been set for the duration April, 2011 to March, 2012.

3.2 SLR Scenarios

The simulated hydro-morphological scenarios for 10cm, 25cm and 50cm SLR due to climate change has shown the increased backwater discharge ranges from 40 to 1291 m^3/hr/m near the d/s of Karnafuli River from sea mouth. Due to this backwater effect the sediment transport to the Bay of Bengal has also been decreased from for 650 kg/s/m for low tide and increased by 250 kg/s/m for high tide condition towards seaport. Thus, the siltation from mouth to seaport will experience more siltation. The backwater increased discharge from ocean and decreased sediment flow toward ocean are presented for month of August, 2012 (Figure 6). The changed in sediment rating curves for SLR scenarios are depicted in Figure 7. The mean total sediment transport along the dominating flow way (Figure 8) has shown the changed behaviour along the study reach for the backwater effect. The overall short term model analysed change in bathymetry of the Karnafuli River is presented in the Figure 9 for SLR. The backwater discharge from ocean to Karnafuli River due to SLR has been presented in Table 3. Negative sign represents the flow direction from ocean to Karnafuli River direction.

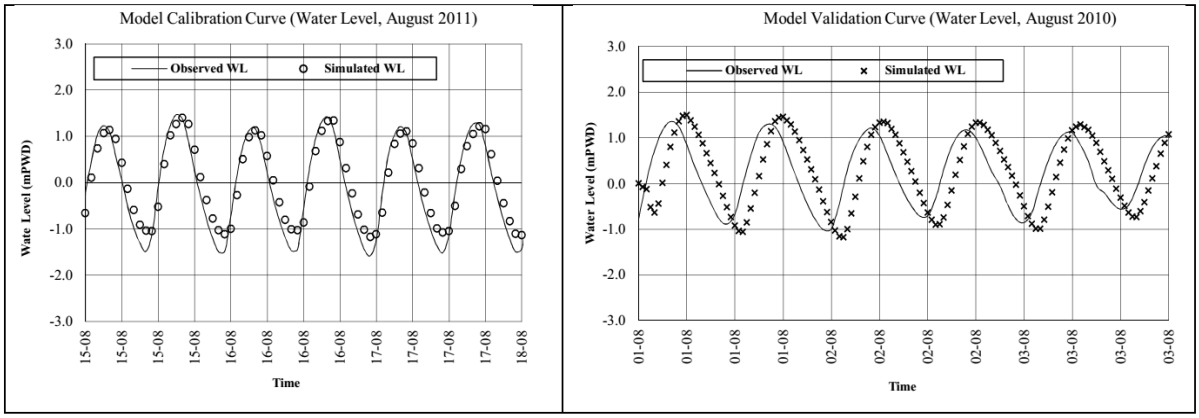

Figure 3: Model Calibration Curve with respect to Water Level at Kalurghat

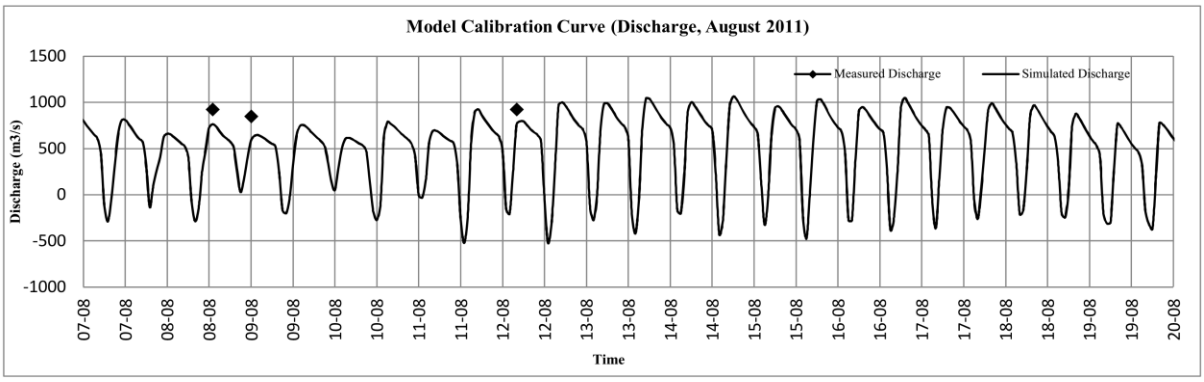

Figure 4: Model Calibration Curve with respect to Discharge at Rangunia

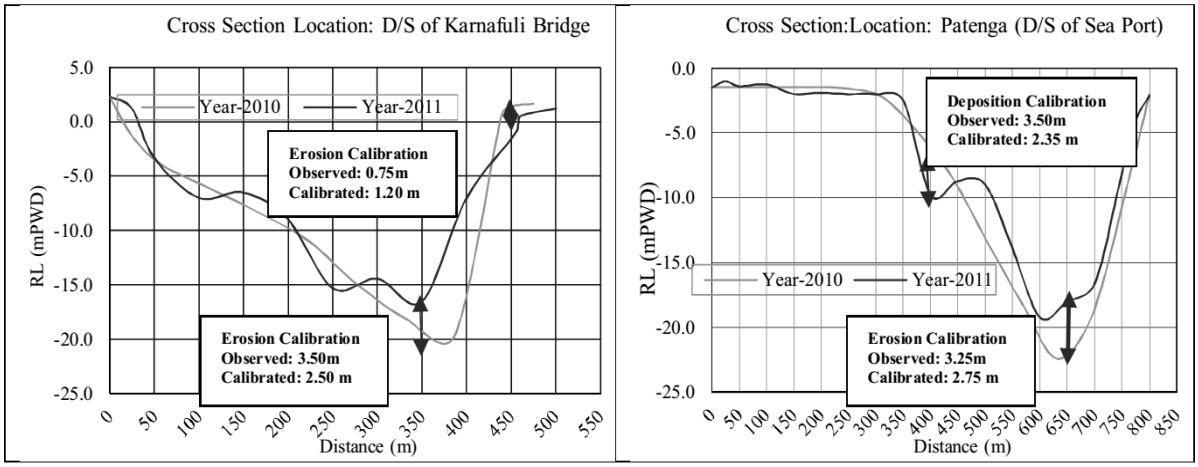

Figure 5: Morphological Model Calibration Curve with respect to Erosion/Deposition rate

Table 2: Morphological behavior (erosion/deposition) along Karnafuli River

Location	Erosion Rate (Bed) Unit: m/yr			Deposition Rate (Bed) Unit: m/yr		
	LB	MC	RB	LB	MC	RB
D/S of Karnafuli Bridge	1.05 (1.10)	3.50 (2.50)	0.75 (1.20)	1.10 (0.90)	4.20 (3.50)	0.95 (0.65)
D/S of Chittagong Sea Port	0.80 (1.10)	3.25 (2.75)	0.75 (0.85)	0.85 (0.55)	3.50 (2.35)	0.085 (0.30)

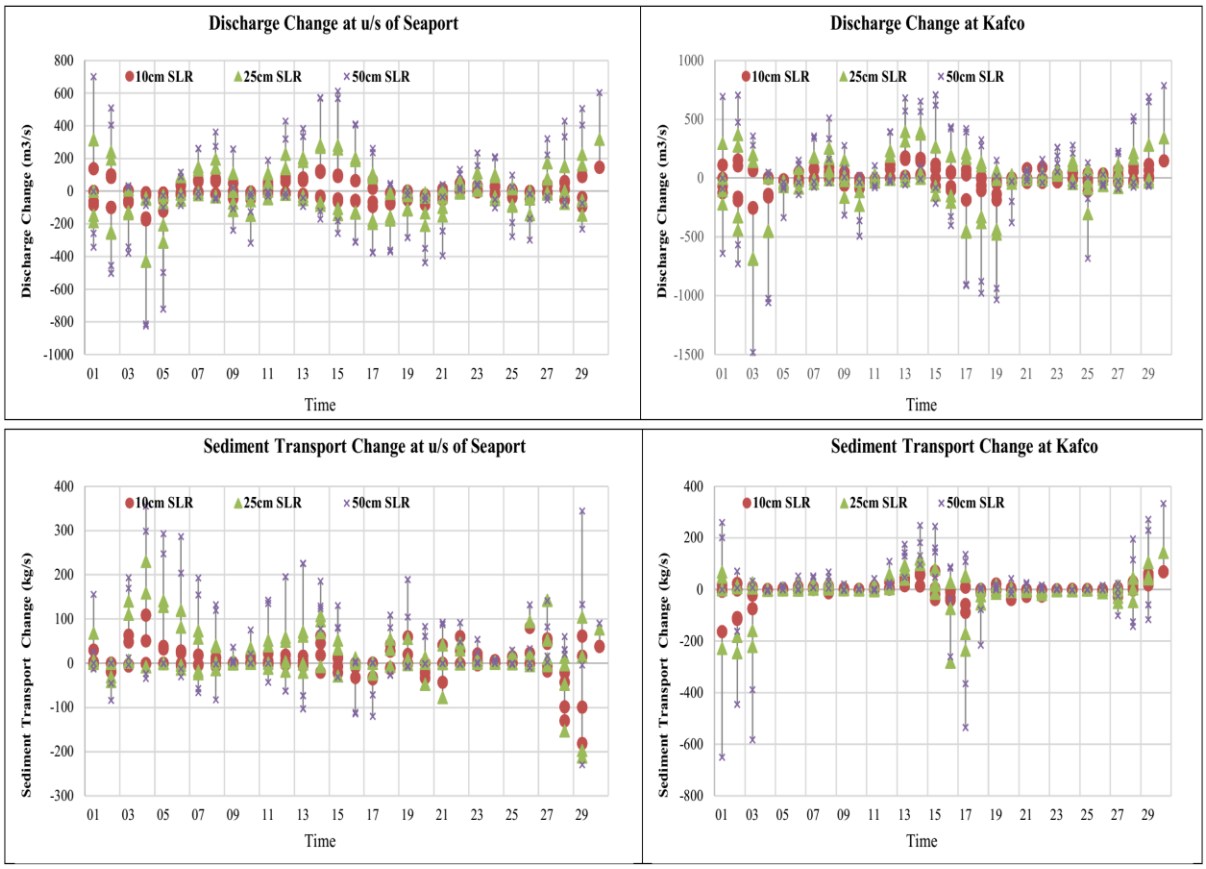

Figure 6: Change of Unit Discharge and Total Sediment Transport due to SLR scenarios

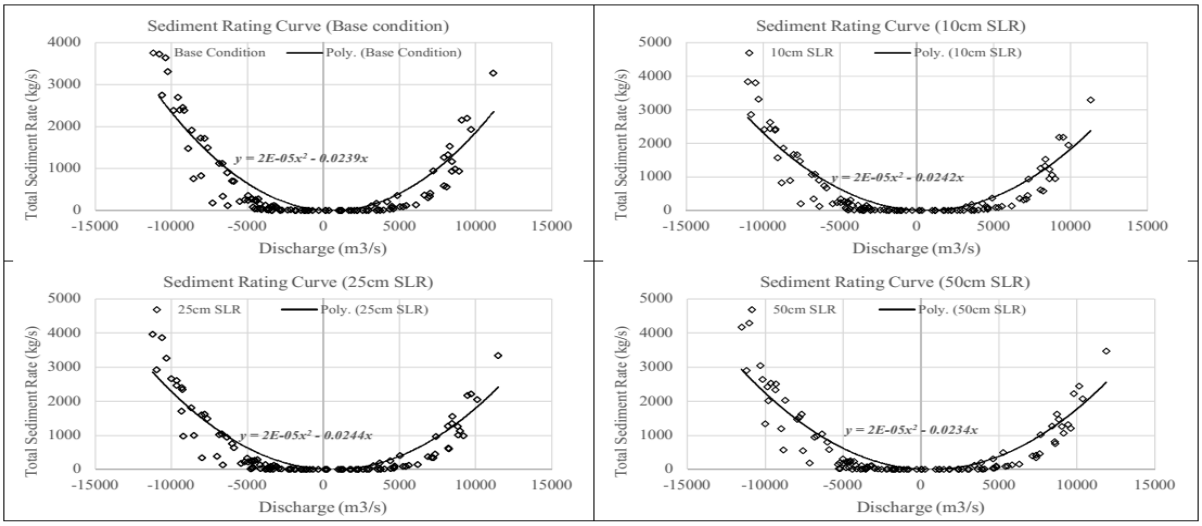

Figure 7: Sediment Rating Curve due to SLR scenarios

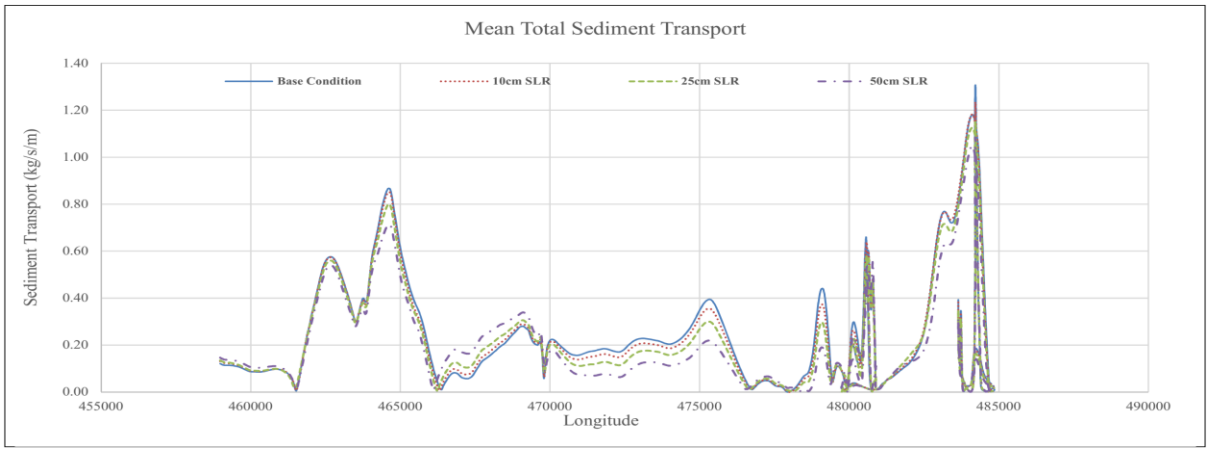

Figure 8: Change in Longitudinal Mean Total Sediment Transport due to SLR scenarios

Table 3: Backwater discharge ($m^3/s/m$) to Karnafuli River from Ocean due to SLR

Distance from Estuary (Km)	Backwater discharge from Ocean to u/s of Karnafuli River		
	10cm SLR	25cm SLR	50cm SLR
0	-202 (1.1%)	-207(1.2%)	-655(3.4%)
5	-310(1.5%)	-559(2.8%)	-1000(4.9%)
10	-192(1.0%)	-675(3.7%)	-1291(6.9%)
15	-234(1.1%)	-281(1.3%)	-565(2.6%)
20	-148(1.0%)	-311(2.0%)	-768(4.8%)
25	-40(1.0%)	-113(3.0%)	-317(8.2%)

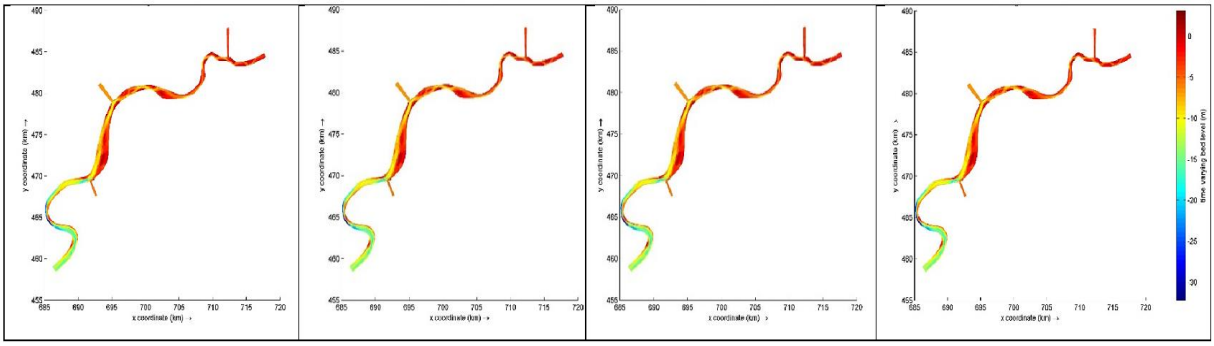

Figure 9: Simulated bathymetry for SLR scenarios

3.3 TMR Scenarios

The hydro-dynamical assessment has made for the 0.5°C, 1.5°C and 2.5°C temperature rise conditions. The hydrodynamical changes as discharge, velocity distribution, secondary has shown negligible results for the TMR as a result of climate change for the 0.5-2.5°C temperature change in the study area. The change in settling velocity is observed 1-1.5cm/s at Kafco and u/s of seaport area (Figure 10). The mathematical model simulated results have shown not significant results in morphological aspects from the average result. The noticeable results of change in sediment transport are presented during first week of August, 2012 (Figure 11).

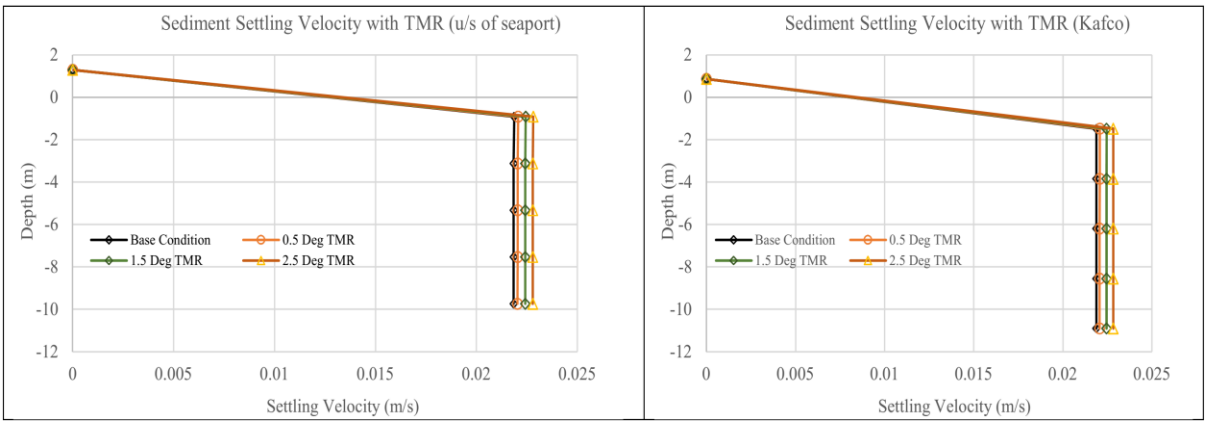

Figure 10: Change in Settling Velocity due to SLR scenarios

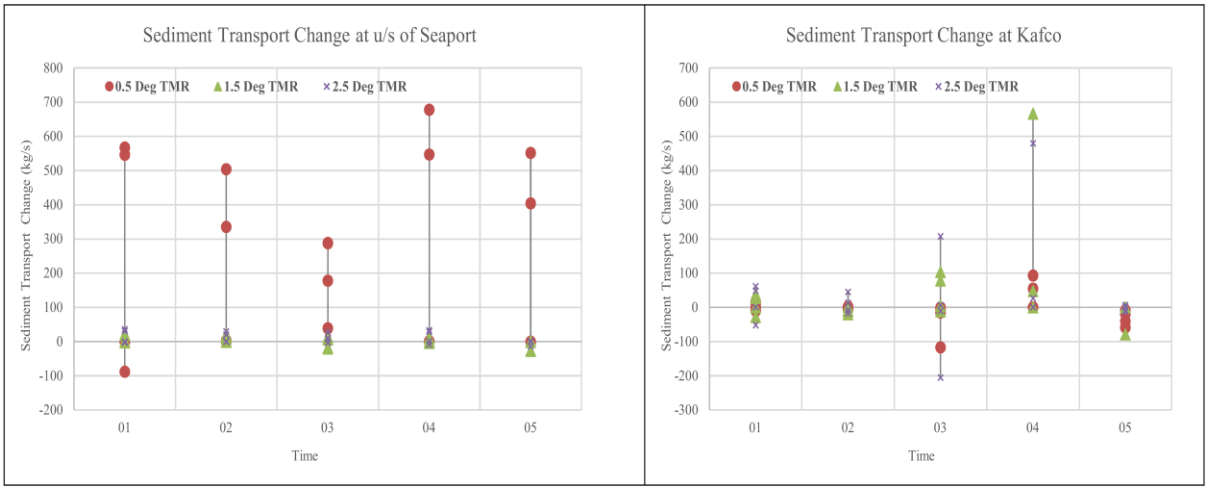

Figure 11: Change of Discharge and Total Sediment Transport due to TMR scenarios

3.4 Scenarios for different d_{50}

Sediment transport is one of the good representation of morphological characteristics of a river. The sediment transport mode largely depends the sediment characteristics as type of sediment, size of sediment etc. As the climate change is represented in terms of SLR and TMR for future scenario, the sediment size in the future condition may not be like present condition. As sediment flow changes with sediment particle size, the sediment transport rate is considered with different median size of sediment as d_{50}= 100, 150 and 200 µm. The base model of the study has considered d_{50}=180 µm based on bed material size distribution assessment of samples collected from d/s of Kaptai, Rangunia and Kalurghat. The mean total load transport along the longitudinal section of the thalweg line of Karnafuli River is depicted in the Figure 12.

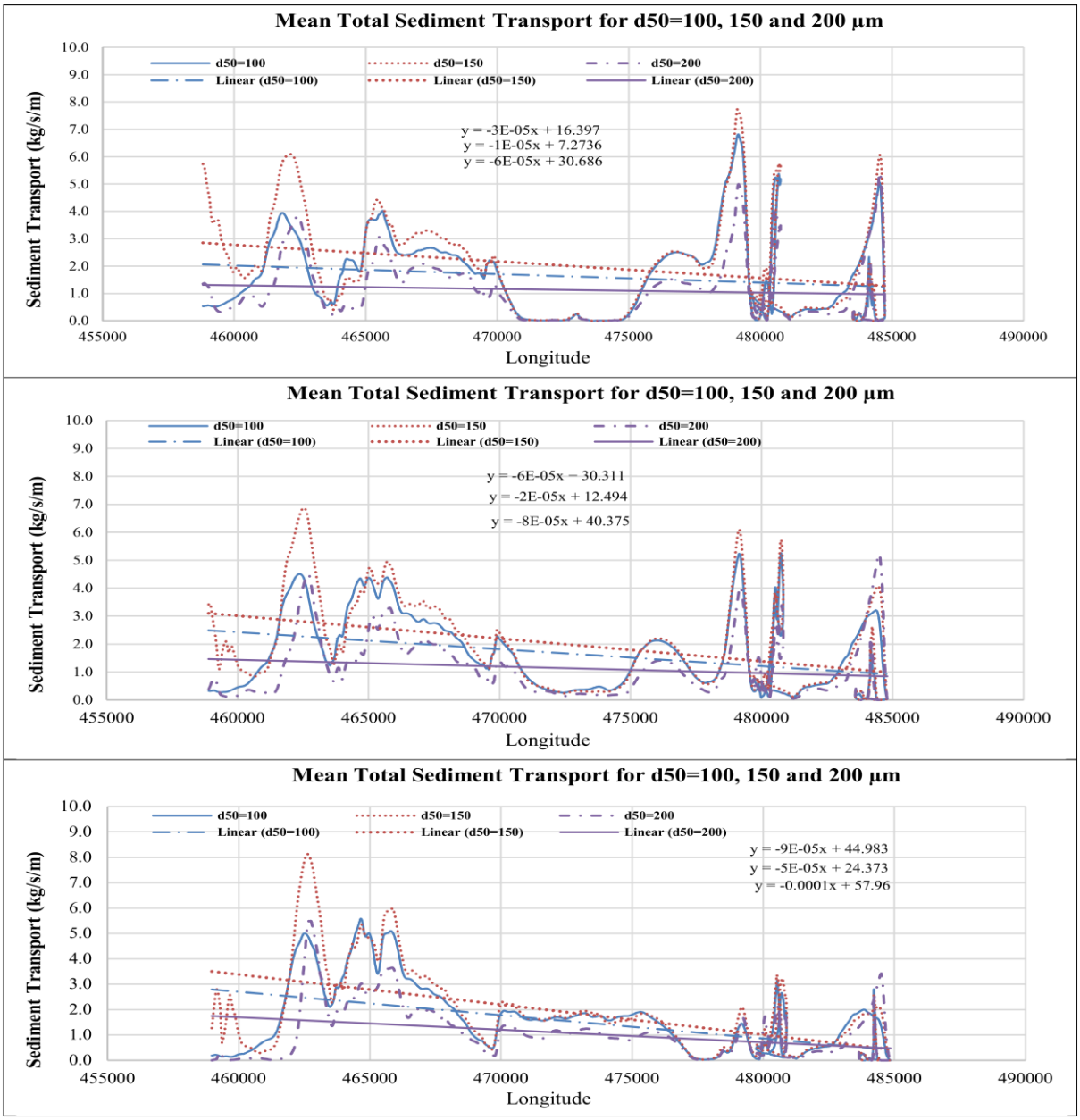

Figure 12: Longitudinal Sediment Transport with different sediment sizes along centre lines

4. CONCLUSIONS

The SLR and TMR due to climate change it is observed that the backwater effect and temperature rise may lead the hydro-morphological changes quite significantly. The very short time mathematical modelling study related to the Karnafuli River has shown that the backwater effect due to SLR has aggravated the siltation at the d/s of Karnafuli and reduced low tide flow towards Bay of Bengal. Please provide a brief conclusion on the basis of the results and discussions. On the other hand, the median sediment size variation has shown that the significant sediment transport rate along the Karnafuli River reach. The study has included the short term model analysed sediment transport analysis with median size d_{50} variation as the sediment transport is complex as it varies with time and types of sediment particles size. So, the d/s of Karnafuli River may be affected significantly in case of siltation. The more siltation will occur as a results of backwater effect about 1.9 to 7.9% of the main channel discharge at the d/s of Karnafuli river including Seaport for the long run against climate change effects.

ACKNOWLEDGEMENTS

The author is grateful to the Almighty for any work. The author is thankful to Kazi Tofail Hossain, Chief Engineer and Poly Das, Sub-Divisional Engineer, BWDB to assist me completing the study. The author is indebted a lot to the River Engineering Division, IWM and River Hydrology and Research Circle, BWDB, Dhaka for providing the necessary data.

REFERENCES

ADB, (2011). People's Republic of Bangladesh: Strategic Master Plan for Chittagong Port. Asian Development Bank. Submitted to GoB.

Basak, J. K., Titumir, R. A. M. and Dey, N. C., (2013). Climate Change in Bangladesh: A Historical Analysis of Temperature and Rainfall Data. Journal of Environment, Vol. 02, Issue 02, pp. 41-46.

Brammer, H., (2013). Bangladesh's Dynamic Coastal Regions and Sea Level Rise. Elsevier, Climate Risk Management, Vol. 01, pp. 51–62.

CEGIS and DoE, (2011). Programs Containing Measures to Facilitate Adaptation to Climate Change of the Second National Communication Project of Bangladesh. Dhaka, Final report, submitted to Department of Environment.

CEGIS, (2014). Geo-morphological and Planform Studies with Environmental and Social Impact Assessment on Study Capital Dredging and Sustainable River Management in Bangladesh (River Karnafuli). Dhaka. Submitted to BWDB.

CPA, (2012). Chittagong Port Authority Overview. Chittagong: Chittagong Port Authority.

Delft3D-Flow, (2014). User manual: Hydro-Morphodynamics, Deltares.

Gornitz, V. M., Daniels, R. C., White, T. W. and Birdwell, K. R., (1994). The development of a Coastal Risk Assessment Database: Vulnerability to Sea Level Rise in the US Southeast." Journal of Coastal Research, Vol. ??, pp. 327-338.

Gornitz, V., (1990). Mean Sea Level Changes in the Recent Past In Climate and Sea Level Change Observations Projections and Implications, Cambridge University Press, Cambridge.

Graves, A.L. and Gooch, R.S., (1986). Central Arizona Project Start Up. Proceedings of the Water Forum '86: World Water Issues in Evolution. ASCE, New York, N.Y., Vol. 1, 546-551.

IPCC, (2007a). Climate Change 2007: The Physical Science Basis. Contribution of Working Group I to the Fourth Assessment Report of the Intergovernmental Panel on Climate Change. Cambridge University Press, Cambridge, United Kingdom and New York, NY, USA.

IPCC, (2007b). Climate Change 2007: The Physical Science Basis, Summary for Policymakers. Contribution of Working Group I to the Fourth Assessment Report of the Intergovernmental Panel on Climate. Cambridge University Press, Cambridge, United Kingdom and New York, NY, USA.

IPCC, (2013). Climate Change 2013: The Physical Science Basis. Contribution of Working Group I to the Fifth Assessment Report of the Intergovernmental Panel on Climate Change. Cambridge University Press, Cambridge, United Kingdom and New York, NY, USA.

IWM, (2013). Prefeasibility Study to Restore the Environment of the Kaptai Lake the Rangamati Hill District, Volume I. Dhaka.

Karmakar, S., Haque, S. M., Hossain, M. M., and Shafiq, M., (2011). Water Quality of Kaptai Reservoir in Chittagong Hill Tracts of Bangladesh. Journal of Forestry Research, Vol. 22, Issue, 1, pp. 87−92. doi: 10.1007/s11676-011-0131-6.

Unnikrishnan, A. S., Nidheesh, A. G. and Lengaigne, M., (2015). Sea Level Rise Trends off the Indian Coasts During the Last Two Decades. Current Science, Vol. 108, Issue, 5, pp. 966-971.

Proceedings of the 4th International Conference on Civil Engineering for Sustainable Development (ICCESD 2018), 9~11 February 2018, KUET, Khulna, Bangladesh (ISBN-978-984-34-3502-6)

MORPHOLOGICAL RESPONSES OF A TIDAL RIVER DUE TO CLIMATE CHANGE: A CASE STUDY FOR KARNAFULI RIVER, BANGLADESH

Sajal Kumar Roy[1] and Umme Kulsum Navera[2]

[1] Assistant Engineer, Bangladesh Water Development Board, Bangladesh,
e-mail: sajalkumar1a@gmail.com
[2] Professor, Department of Water Resources Engineering, BUET, Bangladesh,
e-mail: uknavera@gmail.com

ABSTRACT

Karnafuli River is an important river in Bangladesh and Chittagong seaport plays the biggest role in this country's economy. Navigability along the Seaport of Karnafuli River is dependent on the discharge and sediment transport with time. Sea Level Rise (SLR) and Temperature Rise (TMR) in the coast of Bay of Bengal are evident from different scientific reports. SLR is threatening the hydrodynamic and morphological behavior of coastal rivers including the navigability at the downstream of Karnafuli River. The backwater effects in terms of discharge and sediment transport have been carried out in this study. The future scenarios for rise in water level and temperature due to SLR and TMR have been projected for the next 25-30 years. Mathematical modeling has been carried out for 10cm, 25cm and 50cm SLR and 0.5°C, 1.5°C and 2.5°C TMR to assess the hydro-morphological responses. Morphological analysis has been carried out for three different conditions for mean sediment size d_{50}=100, 150 and 200 µm. Mathematical model study has been performed 3-Dimensionally by using Delft3D. The study reach includes from downstream of Kaptai Dam to Kafco in Karnafuli River. Results show that backwater discharge will increase 1.9% to 7.9% from the present discharge. Due to this the sediment transport will be decreased from 50 to 100 tons per second. Thus, the downstream of Karnafuli River and seaport will experience more sedimentation. The study has also focused on planform analysis, total sediment transport, settling velocity, sediment rating curves due to climate change effects on Karnafuli River.

Keywords: *Karnafuli River, Mathematical Modelling, Morphology, Climate Change, Sea Level Rise*

1. INTRODUCTION

The Karnafuli River is the principal river in Chittagong region of Bangladesh. The Karnafuli River has about a hundred numbers of tributaries and two-thirds of which lie in Bangladesh (IWM, 2013). The main rivers of that region are the river Karnaphuli, Rainkhiang, Kasalong, Halda, Ichamati, Feni, Sangu, Bakkhali, Naf and Matamuhari. Karnafuli River originates from Lusai Hills about two kilometers east of Sugarbasora in Mizoram state of India (CEGIS, 2014). It lies in the southern part of Bangladesh and finally meets the Bay of Bengal near the Chittagong seaport. The length of the river is almost one hundred and sixty kilometres (Karmakar, et al., 2011). The downstream of the River Karnafuli shows the typical estuarine features. The Karnafuli River is very important in the context of economy of Bangladesh and also for Kaptai Hydro-electric power plant.

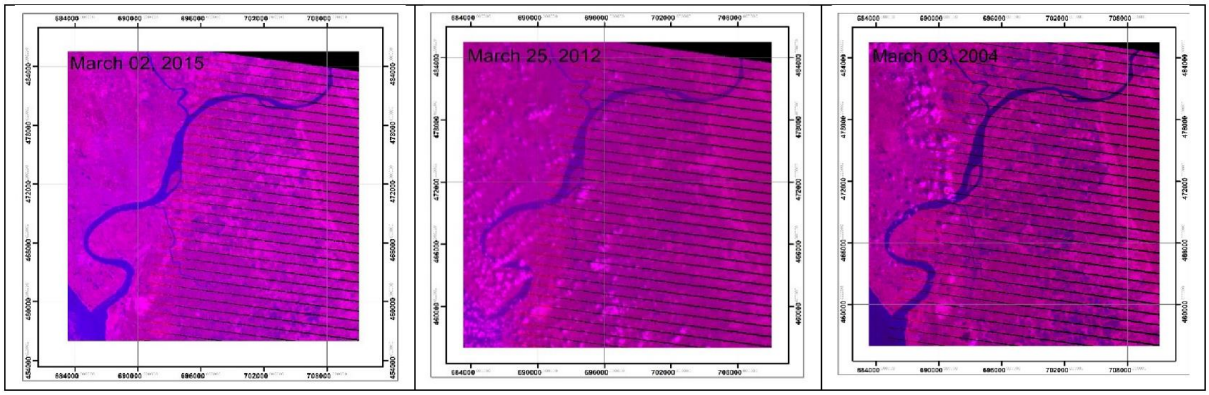

Figure 1: Satellite Images of Karnafuli River Reach

The sea port is in the south of Chittagong city, the second largest city in Bangladesh and is the nation's capital and administrative and economic center (ADB, 2011). It handles about 92% of the country's import-export trade (CPA, 2012). The most important seaport of Bangladesh is situated sixteen kilometers away from the sea mouth, Kafco (ADB, 2011). Another important part of the river is Kaptai dam which is located upstream of Karnafuli River. During monsoon period the high tidal flow and discharge is occurred in the Karnafuli River. The Chittagong Sea Port is experienced capital dredging for the succession of time. The past decade planform of the Karnafuli River shows stable bank lines (Figure 1). The river has shown same width along the reach with some bank erosion effect at certain location along the reach. The pattern of bend is observed almost same for the past decade as observed in the study.

Past literatures are the evidence of both global Sea Level Rise (SLR), Temperature Rise (TMR) warming and regional sea-level-rise including Bangladesh from the past coastal gauged water level data trends. The According to the third assessment report of the Intergovernmental Panel on Climate Change (IPCC) showed yearly Sea Level Rise (SLR) ranging 1.0 to 2.0 mm in the region1 (Unnikrishnan et al., 2015). The fourth and fifth IPCC reports show a yearly global mean SLR nearly 1.8 mm during 1961–2003 and 1.7 mm during 1901–2010 respectively (IPCC, 2007) (IPCC, 2013). The SLR is 2.15 mm per year has been found for past two decades at the location of Hiron Point gauged station (Brammer, 2013). The mean sea level is rising and sea level change was found from the gauged water level station to be 5.05 mm/year to 7.5 mm/year (CEGIS and DOE, 2011).

Due to SLR back water effect will generally take place thus will aggravate the retardation of a river outflow at the river mouth. The past studies have focused on the water level and salinity intrusion due to climate change. The author has carried out a set of mathematical model studies to show the hydro-morphological behavior due to backwater effect for SLR. The author has also found the siltation effect at d/s of Karnafuli River reach indicating threatening to the Chittagong Seaport. The Fourth Assessment Report of IPCC has depicted that the 100-year linear trend (1906-2005) of global average surface temperature is 0.74°C (Basak, et al., 2013). The change in temperature may affect the hydro-morphological behavior of the Karnafuli River for the future scenarios.

The present study will focus on the hydro-morphological analysis using mathematical modelling tool Delft3D for the future scenarios of Karnafuli River reach due to SLR and TMR as an impact on climate change. The study has included the development of 3D hydro-morphological and Heat flux models introducing 5 number of layers for the river Karnafuli River reach from downstream (d/s) of Kaptai Dam to estuary near Kafco. The mathematical model study has covered the hydro-morphological condition of base condition or 0 cm, 10 cm, 25 cm and 50 cm SLR conditions. Another set of Heatflux Models for base condition or

0.0°C, 0.50°C, 1.50°C and 2.50°C TMR conditions have conceded for the analysis of hydro-morphological assessment of Karnafuli River reach 3-Dimensionally. The morphological analysis has also been carried out by the author through another set of models for mean sediment size d_{50}=100, 150 and 200µm as river morphology largely depends on the sediment size. The outputs results obtained from the simulated conditions have focused on the total velocity distribution, sediment transport, suspended sediment transport, longitudinal or cross-sectional profile, erosion and deposition pattern of sediment sand.

2. METHODOLOGY

This study will be based on the effect of SLR and TMR due to climate change to Karnafuli River due to its' importance for having Chittagong Sea Port and Kaptai Dam and situated in the vulnerable area to SLR and TMR. The study will analyze the hydro-morphological assessment through selection of study area, data collection and data arrange, mathematical model setup, model calibration and validation, results analysis. The methodology of the study is presented in the following article.

2.1 Selection of Study Area

The Karnafuli River from d/s of Kaptai Dam to the the estuary at Kafco has been selected to assess the hydro-morphological change due to SLR and TMR. The main tributaries as Halda, Ichamati and Shikalbaha Canal (Khal) of almost 10 km from the confluence point of Karnafuli have also been considered in the study (Figure 2). Analysis of Karnafuli River has been made 3-Dimensionally including 5 number of vertical layers. The discharge from Kaptai Dam and the water level at Kafco have been the boundary condition of the simulated models. The location of calibration and validation location have been set to Kalurghat.

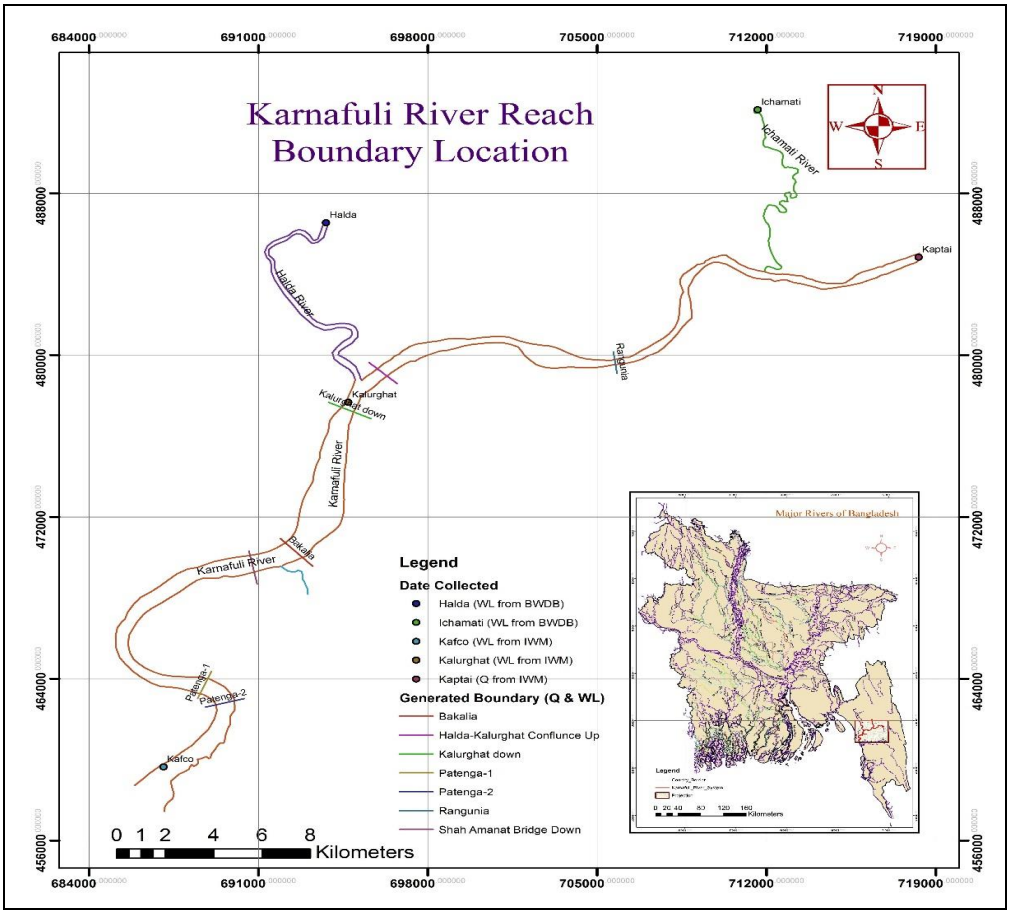

Figure 2: Study Reach with Boundary Locations

2.2 Data Collection and Data Arrange

The time series water level data at Kafco, Kalurghat and at Rangunia, Halda, Ichamati, the discharge data at d/s of Kaptai Dam, the cross sections data of the Karnafuli, Ichamati, Halda River and Shikalbaha Khal collected from both Bangladesh Water Development Board (BWDB) and Institute of Water Modelling (IWM) for the year of 2010 and 2011. Digital Elevation Model (DEM) of two major islands named Quapara and Bakalia Char has been collected from the electronic source as SRTM (30m×30m) from earth explorer. The size of the bed materials at Rangunia, Kalurghat and Kafco denoted as d_{50} and d_{75} and sediment concentration data for different locations have been collected from IWM. The satellite images of Karnafuli River reach from year 2004 to year 2015 has been collected.

2.3 Mathematical Model Setup

The mathematical model setup is a process that includes the selection of land boundary, generation of suitable grid spacing considering the river width, length and simulation time, making the bathymetry, preparing the roughness file for the river bed concerned, boundary condition file generation, to finally the simulation of the model including calibration and validation. The process of the model setup in this study is described in the following articles.

2.3.1 Background Governing Equations

The Delft3D-Flow-Morbasic equations of fluid flow, encode the familiar laws of mechanics as conservation of mass (the continuity equation) and conservation of momentum. The bed evolution is based on the sediment continuity where the first term expresses the changes in bed level in time and the second and third terms are the sediment fluxes (bed and suspended load) in the x and y directions, respectively. The Delft3D heat flux model includes the relative humidity, air temperature and the fraction of the sky covered by clouds is prescribed (in %). The Delft3D module is capable to compute the effective back radiation and the heat losses due to evaporation and convection.
The continuity equation in Cartesian coordinates is

$$\frac{\partial u}{\partial x}+\frac{\partial v}{\partial y}+\frac{\partial w}{\partial z}=0 \tag{1}$$

Where, *u*, *v* and *w* are the flow velocity components in the x, y and z direction.

The momentum equation used in Delft3D is

$$\rho\frac{D\mathbf{v}}{Dt}=\rho g-\nabla p+\mu\Delta\mathbf{v} \tag{2}$$

Where Δ is the Laplacian operator, ρ is the gravitational force and g is the gravitational acceleration.

The equation states that the bed level evolution in time is depended on the suspended and bed load gradients in the x and y directions.

$$\frac{\partial z_b}{\partial t}+\frac{\partial\left(S_{b,x}+S_{s,x}\right)}{\partial x}+\frac{\partial\left(S_{b,y}+S_{s,y}\right)}{\partial y}=0 \tag{3}$$

Where, $S_{b,x,y}$ = bed-load transport in x- and y-direction (kg m^{-1} s^{-1}), $S_{s,x,y}$ = sediment-load transport in x- and y-direction (kg m^{-1} s^{-1}), z_b = bed level (m).

The Van Rijn (1984) suspended and total sediment formula has been used for the morphological analysis with Delft3D (Delft3D-Flow, 2014).

.

2.3.2 3D Base Model Setup

Delft3D usually supports the use of a rectilinear, a curvilinear and a spherical grid system for setting up a model for flow of river or activities related to wave. In this study the rectangular curvilinear grid system has been used to prepare the hydro-dynamic and morpho-dynamic grid system of less than 2.0 aspect ratio. The grid generator program RGFGRID has been used in this thesis study to generate a rectangular grid system for model development. The rectangular grid system has used the land boundary and preferably the bathymetry for the preliminary set up the desired model. The land boundary is obtained from digitizing the satellite image map of resolution 30m×30m obtained from earthexplorer and the bathymetry is obtained upon using the tool QUICKIN with the help of cross section data provided by BWDB and IWM.

2.3.3 Base Model Calibration and Validation

The calibration is an iterative adjustment of the model parameters so that simulated data obtained from mathematical model represents the observed data of the river system to desired accuracy. The calibration of the model has been made for both hydrodynamic and morphological simulations. The base 3D model has been calibrated and validated against water level, discharge and erosion and deposition perspective. The hydrodynamic calibration and validation has been made at Kalurghat and at Patenga respectively for the year 2011 and 2010. The 3D validated model with the adjusted parameters as manning's roughness and morphological parameters has been used for the projected SLR and TMR scenarios. Calibration parameters has also included the model grid spacing, horizontal and vertical eddy diffusivity and the erosion factors of the Karnafuli River.

2.3.4 MOR-Model Setup for SLR Scenarios

The validated 3D base model has been used to estimate SLR scenarios for 0.0 cm (base condition), 10 cm, 25 cm and 50 cm due to climate change. The both hydrodynamic and morphological boundary conditions have been kept similar as the base condition (Table 1).

2.3.5 Heatflux-Model Setup for TMR Scenarios

The validated 3D base model has been used to estimate TMR scenarios for 0.0°C (base condition), 0.50°C, 1.50°C and 2.50°C due to climate change. The both hydrodynamic and morphological boundary conditions have been kept similar as the base condition (Table 1).

2.3.6 Mor-Model Setup for Different Sediment Size

The validated 3D base model has been used to estimate the scenarios for the different sediment size that constitute the sediment transport. The projected scenarios of morphological behaviour for d_{50}= 200µm,150µm and 100µm have been simulated in the study. This is because the sediment transport takes place with continuous sediment sorting or change to the flow direction. The both hydrodynamic and morphological boundary condition as sediment concentration have been kept similar for the four different sizes of sediments. The scenarios of the study are presented in Table 1.

Table 1: Scenarios developed in the study

Study Type	**Base condition**	**Climate Change/ different sediment size Scenarios**		
1. Hydro-morphological changes due to SLR	Post-monsoon, 2012	(+) 10 cm SLR	(+) 25 cm SLR	(+) 50 cm SLR
2. Hydro-morphological changes due to TMR	Post-monsoon, 2012	(+) 0.5°C TMR	(+) 1.5°C TMR	(+) 2.5°C TMR
3. Morphological changes with different sediment size	Post-monsoon, 2012	D_{50} =100 µm	D_{50} =150 µm	D_{50} =200 µm

3. RESULTS AND DISCUSSIONS

3.1 Hydrodynamic and Morphological Model Calibration and Validation

The hydrodynamic calibration of the model has been based on water level and discharge at Kalurghat (Figure 3 and 4). The calibration of morphological parameters has been adjusted based on simulated erosion and deposition presented in the parenthesis of Table 2 and illustrated in Figure 5. LB, MC and RB represent the Left Bank, Mid Channel and Right Bank respectively. The sediment boundary for the study of dredging has been set considering upstream and downstream at Rangunia and Kafco respectively. The 3D morphological model of 5 vertical layers has been set for the duration April, 2011 to March, 2012.

3.2 SLR Scenarios

The simulated hydro-morphological scenarios for 10cm, 25cm and 50cm SLR due to climate change has shown the increased backwater discharge ranges from 40 to 1291 m^3/hr/m near the d/s of Karnafuli River from sea mouth. Due to this backwater effect the sediment transport to the Bay of Bengal has also been decreased from for 650 kg/s/m for low tide and increased by 250 kg/s/m for high tide condition towards seaport. Thus, the siltation from mouth to seaport will experience more siltation. The backwater increased discharge from ocean and decreased sediment flow toward ocean are presented for month of August, 2012 (Figure 6). The changed in sediment rating curves for SLR scenarios are depicted in Figure 7. The mean total sediment transport along the dominating flow way (Figure 8) has shown the changed behaviour along the study reach for the backwater effect. The overall short term model analysed change in bathymetry of the Karnafuli River is presented in the Figure 9 for SLR. The backwater discharge from ocean to Karnafuli River due to SLR has been presented in Table 3. Negative sign represents the flow direction from ocean to Karnafuli River direction.

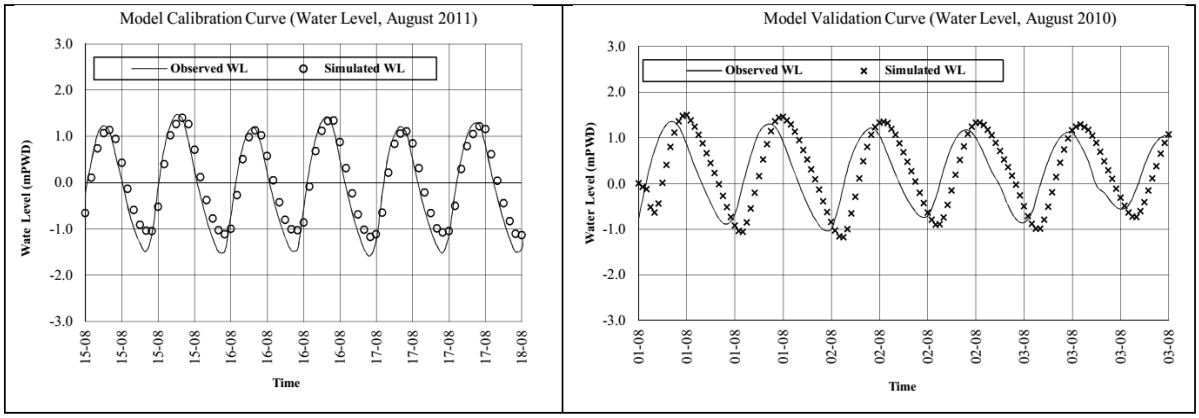

Figure 3: Model Calibration Curve with respect to Water Level at Kalurghat

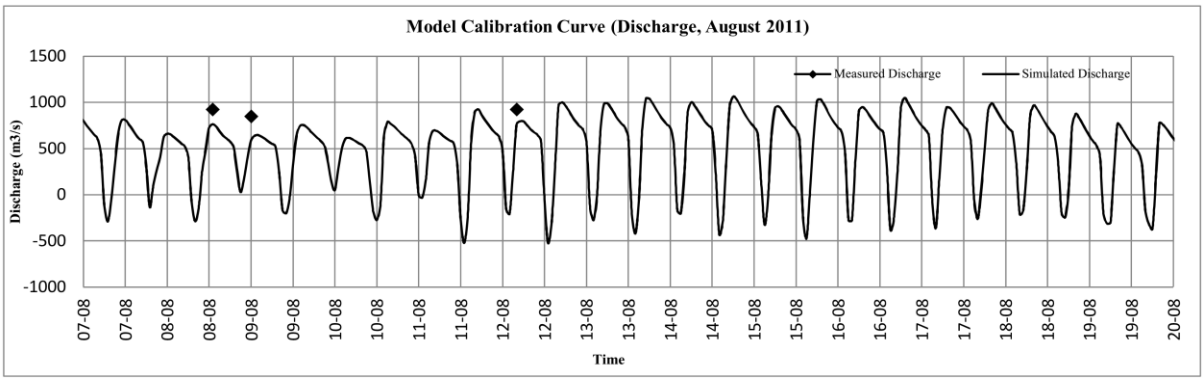

Figure 4: Model Calibration Curve with respect to Discharge at Rangunia

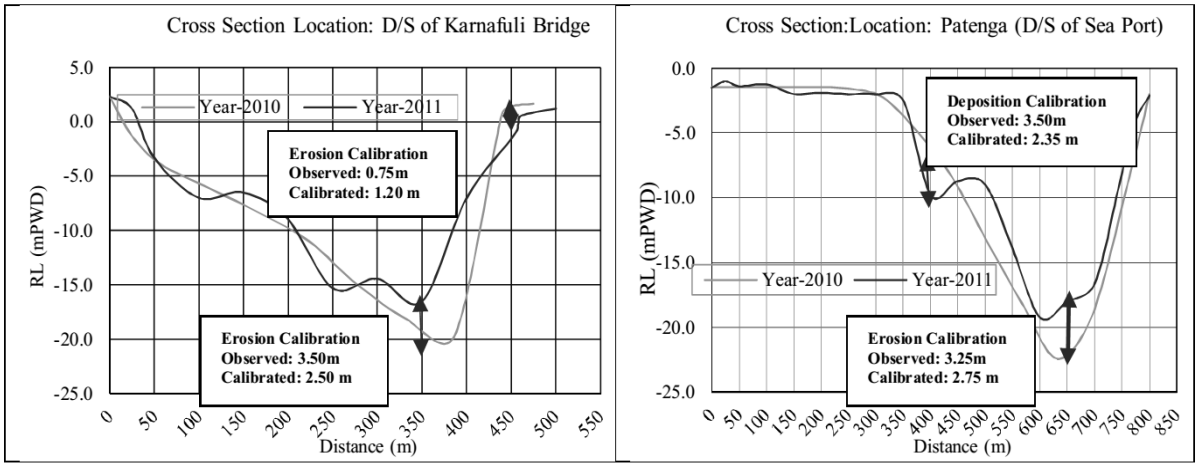

Figure 5: Morphological Model Calibration Curve with respect to Erosion/Deposition rate

Table 2: Morphological behavior (erosion/deposition) along Karnafuli River

Location	Erosion Rate (Bed) Unit: m/yr			Deposition Rate (Bed) Unit: m/yr		
	LB	MC	RB	LB	MC	RB
D/S of Karnafuli Bridge	1.05 (1.10)	3.50 (2.50)	0.75 (1.20)	1.10 (0.90)	4.20 (3.50)	0.95 (0.65)
D/S of Chittagong Sea Port	0.80 (1.10)	3.25 (2.75)	0.75 (0.85)	0.85 (0.55)	3.50 (2.35)	0.085 (0.30)

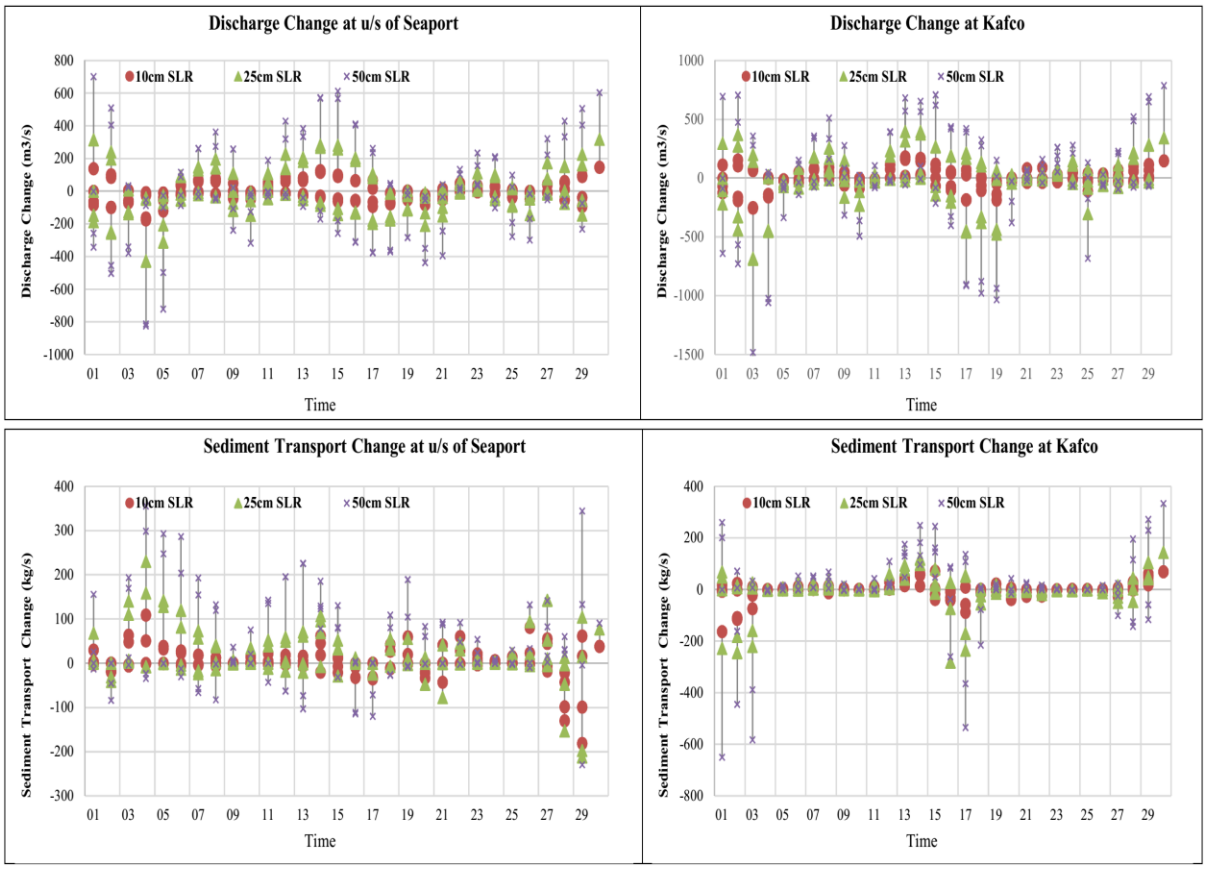

Figure 6: Change of Unit Discharge and Total Sediment Transport due to SLR scenarios

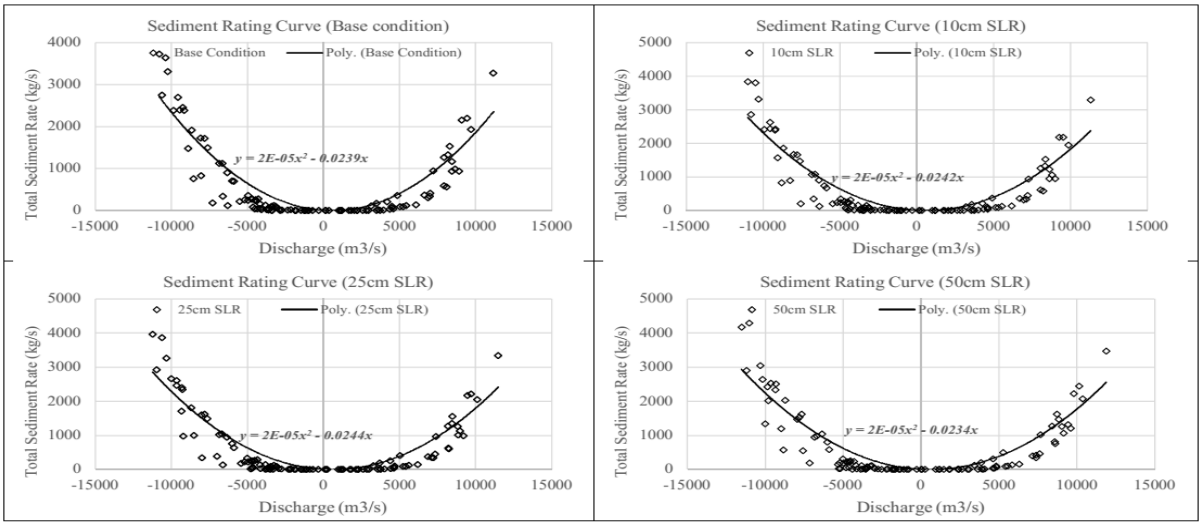

Figure 7: Sediment Rating Curve due to SLR scenarios

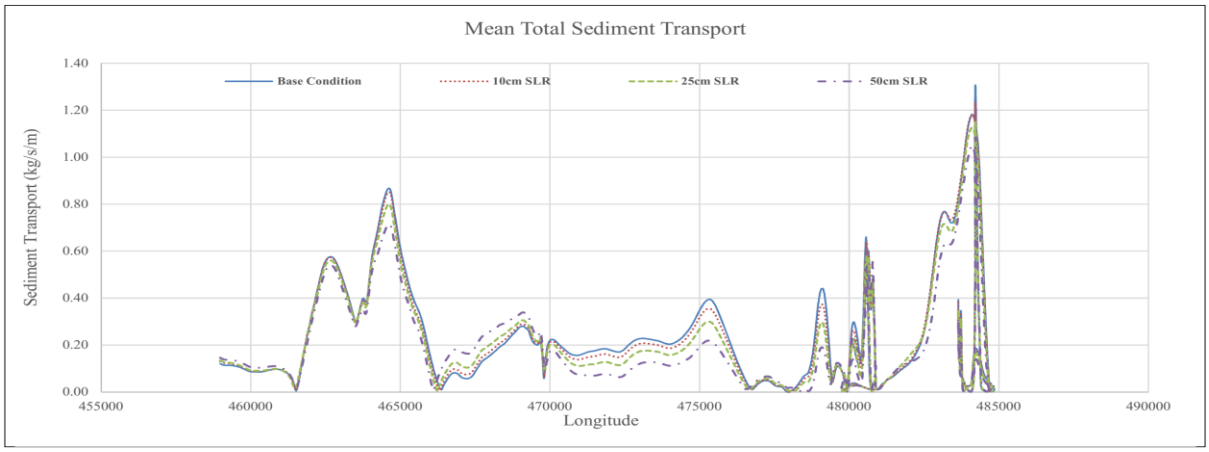

Figure 8: Change in Longitudinal Mean Total Sediment Transport due to SLR scenarios

Table 3: Backwater discharge ($m^3/s/m$) to Karnafuli River from Ocean due to SLR

Distance from Estuary (Km)	Backwater discharge from Ocean to u/s of Karnafuli River		
	10cm SLR	25cm SLR	50cm SLR
0	-202 (1.1%)	-207(1.2%)	-655(3.4%)
5	-310(1.5%)	-559(2.8%)	-1000(4.9%)
10	-192(1.0%)	-675(3.7%)	-1291(6.9%)
15	-234(1.1%)	-281(1.3%)	-565(2.6%)
20	-148(1.0%)	-311(2.0%)	-768(4.8%)
25	-40(1.0%)	-113(3.0%)	-317(8.2%)

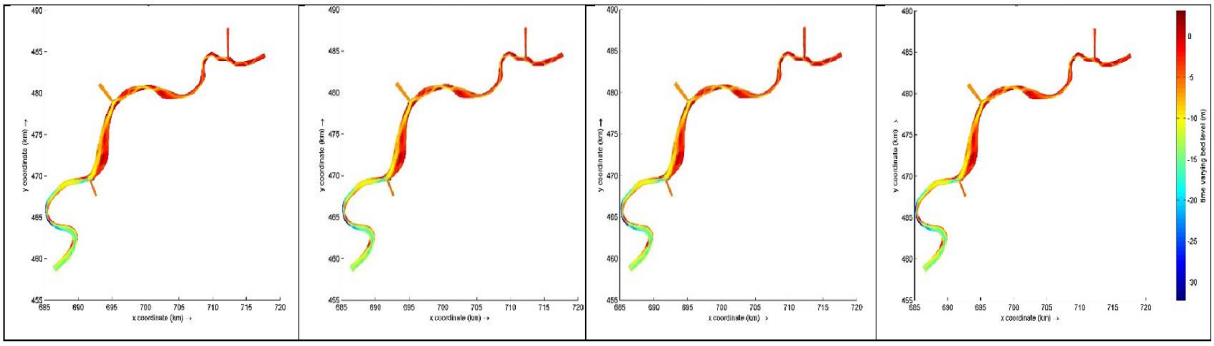

Figure 9: Simulated bathymetry for SLR scenarios

3.3 TMR Scenarios

The hydro-dynamical assessment has made for the 0.5°C, 1.5°C and 2.5°C temperature rise conditions. The hydrodynamical changes as discharge, velocity distribution, secondary has shown negligible results for the TMR as a result of climate change for the 0.5-2.5°C temperature change in the study area. The change in settling velocity is observed 1-1.5cm/s at Kafco and u/s of seaport area (Figure 10). The mathematical model simulated results have shown not significant results in morphological aspects from the average result. The noticeable results of change in sediment transport are presented during first week of August, 2012 (Figure 11).

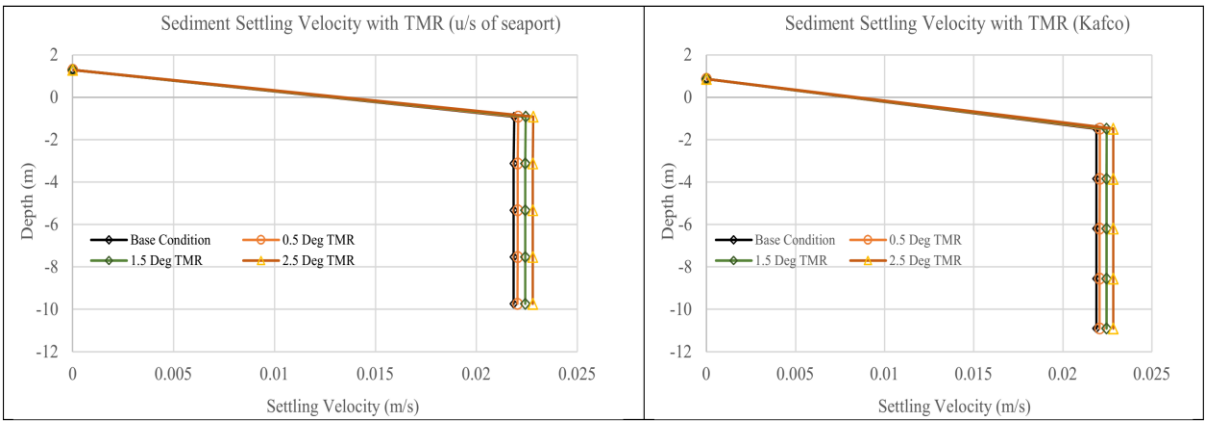

Figure 10: Change in Settling Velocity due to SLR scenarios

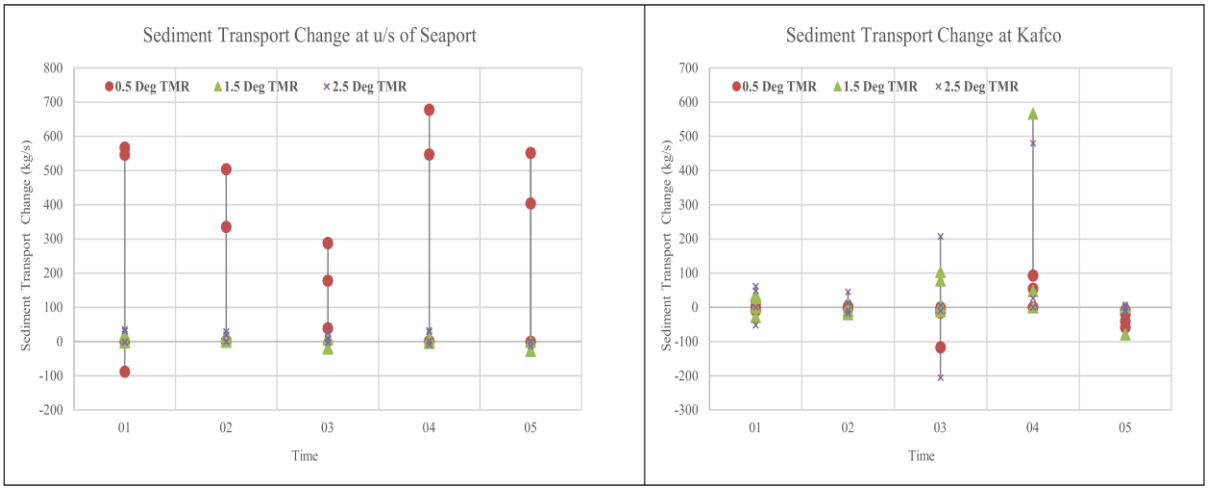

Figure 11: Change of Discharge and Total Sediment Transport due to TMR scenarios

3.4 Scenarios for different d_{50}

Sediment transport is one of the good representation of morphological characteristics of a river. The sediment transport mode largely depends the sediment characteristics as type of sediment, size of sediment etc. As the climate change is represented in terms of SLR and TMR for future scenario, the sediment size in the future condition may not be like present condition. As sediment flow changes with sediment particle size, the sediment transport rate is considered with different median size of sediment as d_{50}= 100, 150 and 200 µm. The base model of the study has considered d_{50}=180 µm based on bed material size distribution assessment of samples collected from d/s of Kaptai, Rangunia and Kalurghat. The mean total load transport along the longitudinal section of the thalweg line of Karnafuli River is depicted in the Figure 12.

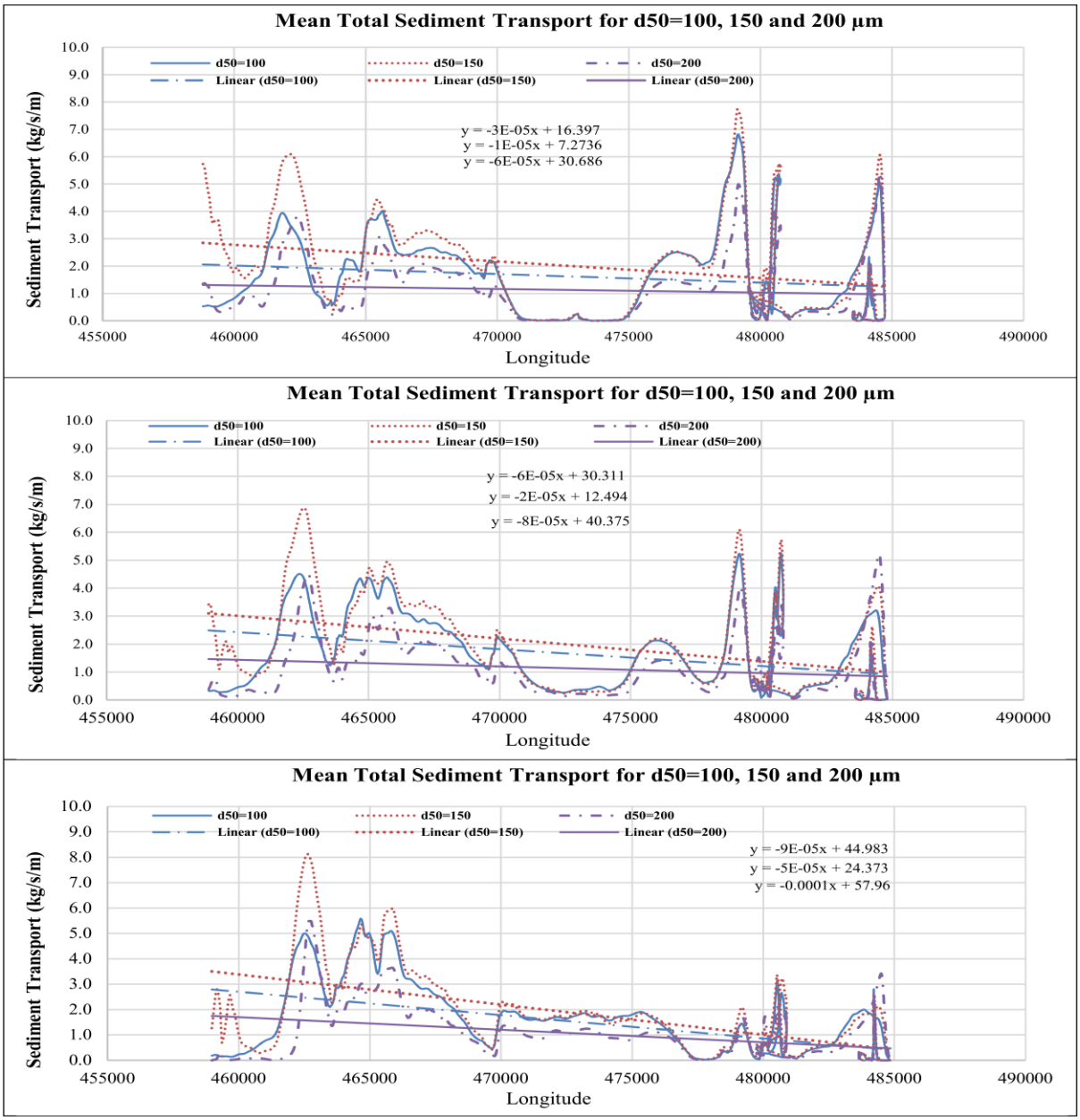

Figure 12: Longitudinal Sediment Transport with different sediment sizes along centre lines

4. CONCLUSIONS

The SLR and TMR due to climate change it is observed that the backwater effect and temperature rise may lead the hydro-morphological changes quite significantly. The very short time mathematical modelling study related to the Karnafuli River has shown that the backwater effect due to SLR has aggravated the siltation at the d/s of Karnafuli and reduced low tide flow towards Bay of Bengal. Please provide a brief conclusion on the basis of the results and discussions. On the other hand, the median sediment size variation has shown that the significant sediment transport rate along the Karnafuli River reach. The study has included the short term model analysed sediment transport analysis with median size d_{50} variation as the sediment transport is complex as it varies with time and types of sediment particles size. So, the d/s of Karnafuli River may be affected significantly in case of siltation. The more siltation will occur as a results of backwater effect about 1.9 to 7.9% of the main channel discharge at the d/s of Karnafuli river including Seaport for the long run against climate change effects.

ACKNOWLEDGEMENTS

The author is grateful to the Almighty for any work. The author is thankful to Kazi Tofail Hossain, Chief Engineer and Poly Das, Sub-Divisional Engineer, BWDB to assist me completing the study. The author is indebted a lot to the River Engineering Division, IWM and River Hydrology and Research Circle, BWDB, Dhaka for providing the necessary data.

REFERENCES

ADB, (2011). People's Republic of Bangladesh: Strategic Master Plan for Chittagong Port. Asian Development Bank. Submitted to GoB.

Basak, J. K., Titumir, R. A. M. and Dey, N. C., (2013). Climate Change in Bangladesh: A Historical Analysis of Temperature and Rainfall Data. Journal of Environment, Vol. 02, Issue 02, pp. 41-46.

Brammer, H., (2013). Bangladesh's Dynamic Coastal Regions and Sea Level Rise. Elsevier, Climate Risk Management, Vol. 01, pp. 51–62.

CEGIS and DoE, (2011). Programs Containing Measures to Facilitate Adaptation to Climate Change of the Second National Communication Project of Bangladesh. Dhaka, Final report, submitted to Department of Environment.

CEGIS, (2014). Geo-morphological and Planform Studies with Environmental and Social Impact Assessment on Study Capital Dredging and Sustainable River Management in Bangladesh (River Karnafuli). Dhaka. Submitted to BWDB.

CPA, (2012). Chittagong Port Authority Overview. Chittagong: Chittagong Port Authority.

Delft3D-Flow, (2014). User manual: Hydro-Morphodynamics, Deltares.

Gornitz, V. M., Daniels, R. C., White, T. W. and Birdwell, K. R., (1994). The development of a Coastal Risk Assessment Database: Vulnerability to Sea Level Rise in the US Southeast." Journal of Coastal Research, Vol. ??, pp. 327-338.

Gornitz, V., (1990). Mean Sea Level Changes in the Recent Past In Climate and Sea Level Change Observations Projections and Implications, Cambridge University Press, Cambridge.

Graves, A.L. and Gooch, R.S., (1986). Central Arizona Project Start Up. Proceedings of the Water Forum '86: World Water Issues in Evolution. ASCE, New York, N.Y., Vol. 1, 546-551.

IPCC, (2007a). Climate Change 2007: The Physical Science Basis. Contribution of Working Group I to the Fourth Assessment Report of the Intergovernmental Panel on Climate Change. Cambridge University Press, Cambridge, United Kingdom and New York, NY, USA.

IPCC, (2007b). Climate Change 2007: The Physical Science Basis, Summary for Policymakers. Contribution of Working Group I to the Fourth Assessment Report of the Intergovernmental Panel on Climate. Cambridge University Press, Cambridge, United Kingdom and New York, NY, USA.

IPCC, (2013). Climate Change 2013: The Physical Science Basis. Contribution of Working Group I to the Fifth Assessment Report of the Intergovernmental Panel on Climate Change. Cambridge University Press, Cambridge, United Kingdom and New York, NY, USA.

IWM, (2013). Prefeasibility Study to Restore the Environment of the Kaptai Lake the Rangamati Hill District, Volume I. Dhaka.

Karmakar, S., Haque, S. M., Hossain, M. M., and Shafiq, M., (2011). Water Quality of Kaptai Reservoir in Chittagong Hill Tracts of Bangladesh. Journal of Forestry Research, Vol. 22, Issue, 1, pp. 87−92. doi: 10.1007/s11676-011-0131-6.

Unnikrishnan, A. S., Nidheesh, A. G. and Lengaigne, M., (2015). Sea Level Rise Trends off the Indian Coasts During the Last Two Decades. Current Science, Vol. 108, Issue, 5, pp. 966-971.

Proceedings of the 4th International Conference on Civil Engineering for Sustainable Development (ICCESD 2018), 9~11 February 2018, KUET, Khulna, Bangladesh (ISBN-978-984-34-3502-6)

APPLICATION OF LANDSAT IMAGERY AND VEGETATION INDEX PROPERTY TO ASSESS THE SHORELINE CHANGES ALONG COX'S BAZAR–TEKNAF COAST

Umme Kulsum Navera[1] and Md. Safin Ahmed[2]

[1] Professor, Department of Water Resources Engineering, BUET, Bangladesh,
e-mail: uknavera@gmail.com
[2] Graduate Student, Department of Water Resources Engineering, BUET, Bangladesh,
e-mail: safinporag23@gmail.com

ABSTRACT

Bangladesh is located at the head of the Bay of Bengal. The coast of Bangladesh is known as a zone of vulnerabilities as well as opportunities which involves coast and island boundaries. Nearly 33% of the total population of Bangladesh lives near the coast. There are three distinct coastal zones (western, central and eastern) in Bangladesh. The eastern coastal zone consists of sandy beaches and hilly areas and is morphologically very dynamic. Soil characteristics of the eastern coastal zone are dominated by submerged sands and mudflats which forms a long sandy beach of 145 km from Cox's Bazar towards Teknaf. This shoreline is an important zone which facilitates tourism opportunity, fishing industry, natural resources and regional highway. For tourism, uninterrupted and stable sandy beach is of prime importance. Cox's Bazar-Teknaf shoreline has been experiencing severe erosion at a number of places due to wave action. Wave and wind induced motion results in sediment distribution and shaping of nearshore morphology. The study has been performed by using Remote Sensing and GIS techniques. The shoreline shifting analysis has been performed by the process of open source Landsat images from 1980 to 2017. Satellite derived band algebra; Normalized Difference Vegetation Index (NDVI) has been utilized to identify the vegetation cover. The satellite images of an object carry a unique index property. In this study the index property of vegetation cover has been used to delineate more stable shorelines. At different locations, the average change in shoreline goes up to 120 m in erosion and 100m in deposition. Based on the coastline shifting the erosion behaviour and the vulnerable areas are identified.

Keywords: *Remote Sensing, Geographic Information System, NDVI, Shoreline*

1. INTRODUCTION

Coastal zones are interfaces of land and ocean balancing geosphere, atmosphere and biosphere (Enmark, 2007) and it is a dynamic area comprising the natural boundary between land and ocean (Lazin, 2016). The coastal zone is composed of the coastal plain, the continental shelf and the water that covers the shelf. It also includes other major features such as large bays, estuaries lagoons, coastal dune fields, river estuaries and deltas (Inman el at.1973, Crossland el at., 2005, Fedra, el at., 1988).

The coastal Zone of Bangladesh covers an area of 47,201 Km^2 (WARPO, 2006). This coastal area has abundance of resources and has been developed for a wide variety of purposes such as settlement, agriculture, fisheries, tourism and communication (Alam et. al., 1999). Approximately 46 million people lives here with 2.85 million hectares of cultivable land in this area (Bala and Hossain, 2010). This coastal zone provides 20% of the rice production of Bangladesh (Begum and Fleming, 1997). The coastal zone of Bangladesh is different from the rest of the country due to its unique geo-physical characteristics and vulnerability due to several natural disasters like erosion, deposition, cyclone, storm surges, sea level rise, settlement and also various forms of pollution (Akter, 2015).

The impact of growing population and development along the shoreline have been greatly discussed in the literature such as in Cendrero,1989; Turner et al., 1996; Nicholls & Small, 2002; UNISDR, 2003. Understanding coastal processes and beach morpho-dynamics to evaluate the shoreline changes is not only a scientific goal but also a requirement to support coastal management plans (Galgano & Leatherman, 1991; Honeycutt et al., 2001; Pajak & Leatherman, 2002). The importance of understanding shoreline changes in different time scales (short and long) is needed to identify the priority areas (such as erosion prone areas) for coastal management (Esteves, 2004).

1.1 Study Area

The study area consists 85 km of sandy beach line from Cox's Bazar to Teknaf (Figure1). The image analysis has been carried out by using Landsat images and the erosion or deposition has been detected in every 500 m interval throughout this 85 km Shoreline.

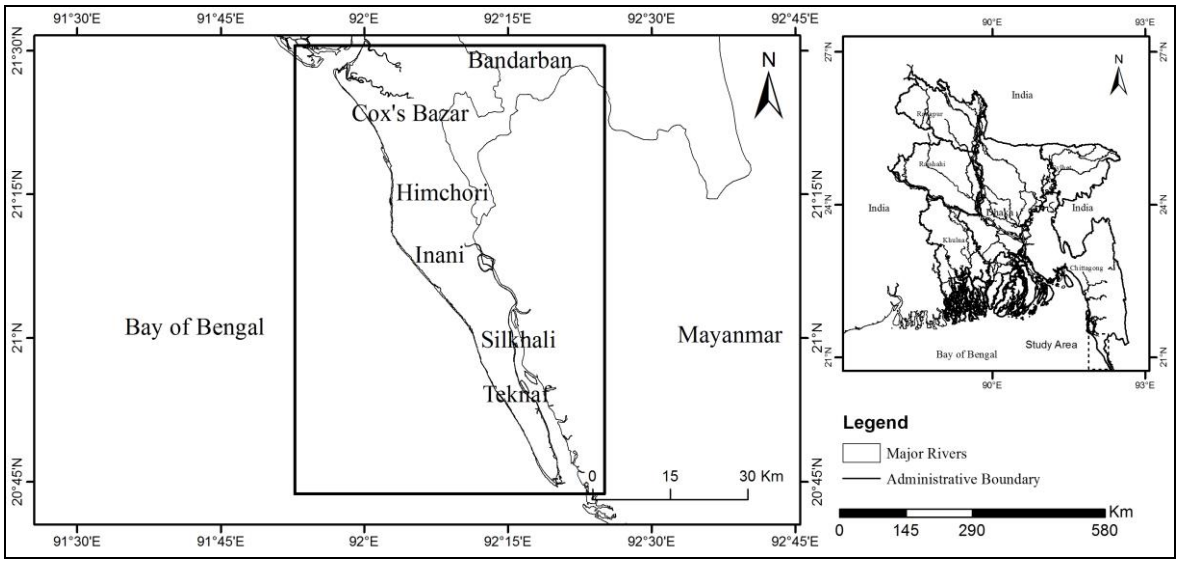

Figure 1: Location map of the study area

2. METHODOLOGY

The spatial and temporal changes in shoreline of coastal areas can be evaluated qualitatively and quantitatively by using historic maps, aerial photographs, remote sensing and GIS technique, beach profiles, topographic and bathymetric surveys. These datasets might provide a variety of means to analyse the rate of changes of shoreline position. It is well documented that Remote Sensing together with Geographic Information System (GIS) can quantify the coastal processes, erosion and accretion especially in the last decades (Durduran 2010, Sener et al. 2010). Different methods for coastline extraction from optical imagery have been developed (Bosworth et al. 2003, Di et al. 2003, Foody et al. 2005, Dewidar and Frihy 2008). It has become critical to assess the amount of erosion and accretion for the management of coastal zone and socio-economic developments in the coastal areas. Shoreline delineation is a complex and time-consuming task and the shoreline variability and trend analysis largely depends on the accuracy of the shoreline delineation. However, temporal and spatial dimensionality must be taken care for shoreline demarcation during investigation (Islam et al., 2014).

The objective of the present study is to measure the spatial and temporal shifting of shoreline by using multi temporal satellite data. This study will also find the dynamic nature of the Cox's Bazar-Teknaf shoreline and will identify the vulnerable zones along the

shoreline. In this context, geospatial techniques i.e., the Remote Sensing and Geographic Information System (GIS) have been used.

2.1 Landsat Data

The Landsat Program is a series of Earth-observing satellites. Landsat missions 1 through 5 carried the Landsat Multispectral Scanner (MSS), while missions 4 and 5 used the Landsat Thematic Mapper (TM) scanner. Landsat 8 has two sensors with its payload, the Operational Land Imager (OLI) and the Thermal Infra-Red Sensor (TIRS).). Landsat sensors record reflected and emitted energy from Earth in various wavelengths of the electromagnetic spectrum. The electromagnetic spectrum includes all forms of radiated energy from tiny gamma rays and x-rays all the way to huge radio waves. Landsat records this information digitally and it is downlinked to ground stations, processed, and stored in a data archive. It is this digital information that makes remotely sensed data invaluable. (USGS)

2.2 Data Set

Multi-temporal Landsat satellite images of the study area have been acquired by optical sensors during the dry season (February-April) from 1980 to 2017 (Table 1) were downloaded from Earth Explorer. Satellite images acquired during the dry season were selected because during the dry season, vegetation cover and other ground conditions, particularly the water level, are relatively consistent from year to year which is essential for assessing the inter-year change of erosion and accretion (Hossain et al., 2013).

Table 1: Satellite images used for this study

Satellite	Sensor	Band Composite	Spatial Resolution of Band Composite(m)	Year
Landsat	MSS	2, 3, 4	60	19 February 1980
	TM	3, 4, 5	30	22 February 1989 25 February 1993 18 February 1996 29 February 2000 8 February 2004 13 February 2006 8 February 2010
	OLI	4, 5, 6	30	21 April 2013 11 February 2017

2.3 Satellite Images Analysis

The remotely sensed satellite images have been analysed by using Geographic Information System (GIS). All satellite images were projected onto the Bangladesh Transverse Mercator (BTM) projection system, whose specifications are: (1) Ellipsoid = Everest 1830, (2) Projection = Transverse Mercator, (3) Central meridian = 90° E, (4) False easting = 500,000 m and (5) False northing = 2,000,000 m (ISPAN, 1992). The analysis of the images started with the digitization of the shorelines from all satellite images. All selected satellite images have been carefully analysed for shorelines and vegetation covers using the ArcView GIS software. Figure 2 describes the Schematic diagram of shoreline movement from 1980-2017 and similar method was used by Hossain et al., 2013. To quantify the changes in shoreline at different locations a total of 166 transects at 500 m intervals along the 85 km study reach have been digitized and coordinate points between the shoreline and transects have been determined.

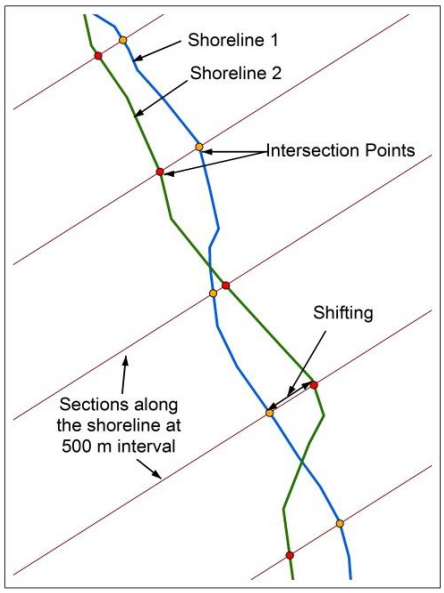

Figure 2: Schematic diagram of shoreline movement

2.4 Shoreline Shifting

Shoreline is the interface between the land and the sea. It is dynamic and its spatial position changes over many time scales (Moore, 2000). Shoreline changes describe the way in which the position of the shoreline moves with time, the direction of movement and the rate. The shoreline may move landwards through the process of erosion; or seawards by sediment accretion (Boak and Turner, 2005). Shoreline changes can be measured over different time scales ranging from geological to diurnal (WIOMSA, 2015). It is a highly challenging task to identify the cause of shoreline changes without field measurement, but Remote Sensing and GIS technique provides an opportunity to quantify the shoreline changes by image analysis.

2.5 NDVI calculation

The Normalized Difference Vegetation Index (NDVI) is a numerical indicator that uses the visible and near-infrared bands of the electromagnetic spectrum to observe green vegetation. NDVI was first used in 1973 by Rouse et al. from the Remote Sensing Centre of Texas A&M University. Generally, healthy vegetation will absorb most of the visible light that falls on it, and reflects a large portion of the near-infrared light. Unhealthy or sparse vegetation reflects more visible light and less near-infrared light. Bare soils on the other hand reflect moderately in both the red and infrared portion of the electromagnetic spectrum (Holme et al., 1987). The NDVI algorithm subtracts the red reflectance values from the near-infrared and divides it by the sum of near-infrared and red bands.

$$NDVI = \frac{(NIR - RED)}{(NIR - RED)} \qquad (1)$$

Theoretically, calculations of NDVI for a given pixel always result in a number that ranges from minus one (-1) to plus one (+1); in practice extreme negative values represent water, values around zero represent bare soil and close to +1 (0.8 - 0.9) indicates the highest possible density of green leaves (Weier and David, 2000).

3. RESULTS AND DISCUSSIONS

The shifting of the Cox's Bazar-Teknaf shoreline with respect to transects has been calculated. Table 2 and Table 3 shows the average value within the specified time and the maximum values indicate the highest value within the same time period for the total study reach. The positive value indicates deposition and negative value denotes the amount of erosion.

Table 2: Short term shoreline shifting due to deposition and erosion

	Deposition (m)		Erosion (m)	
Year	Average	Maximum	Average	Maximum
1980-1989	60.69	174.93	-102.13	-380.56
1989-1993	72.29	405.10	-20.92	-57.75
1993-1996	35.03	141.43	-55.64	-219.50
1996-2000	82.92	309.10	-36.85	-110.43
2000-2004	50.08	218.87	-81.32	-352.82
2004-2006	23.72	121.45	-32.57	-149.80
2006-2010	111.92	322.71	-50.82	-141.01
2010-2013	37.35	277.94	-59.68	-245.74
2013-2017	28.65	89.72	-57.41	-380.40

Table 3: Long term shoreline shifting due to deposition and erosion

	Deposition (m)		Erosion (m)	
Year	Average	Maximum	Average	Maximum
1980-1989	60.69	174.93	-102.13	-380.56
1980-1993	68.37	269.39	-64.21	-174.76
1980-1996	88.04	250.79	-97.96	-276.75
1980-2000	57.59	363.20	-94.80	-253.12
1980-2004	80.26	184.95	-100.64	-411.95
1980-2006	87.54	378.11	-114.79	-311.71
1980-2010	72.71	529.64	-79.55	-344.32
1980-2013	56.55	263.99	-73.47	-431.88
1980-2017	97.20	420.45	-96.77	-326.62

Figure 3 and Figure 4 describes the short and long term average deposition and erosion amount through the 85 km long shoreline. From the first graph it has been found that there is dramatic change in the amount of erosion and deposition. And after the year 2010 the value of erosion has increased whereas the amount of deposition has decreased. This indicates a net increasing in erosion for last 7 years.

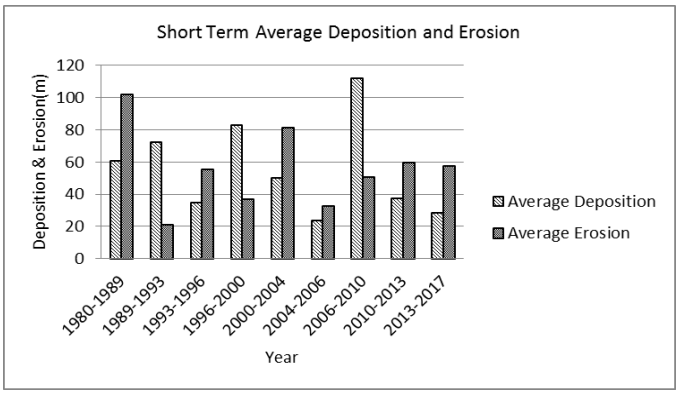

Figure 3: Changes in short time deposition and erosion

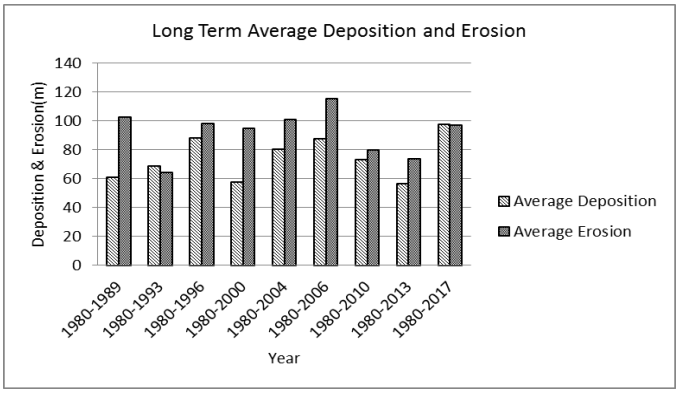

Figure 4: Changes in long time deposition and erosion

Figure 5 (a) and 5 (b) illustrates the changes in deposition and erosion along the shoreline between Cox's bazar and Teknaf. It has been found that Himchari area which is about 12 km from Cox's Bazar is the most vulnerable area based on erosion.

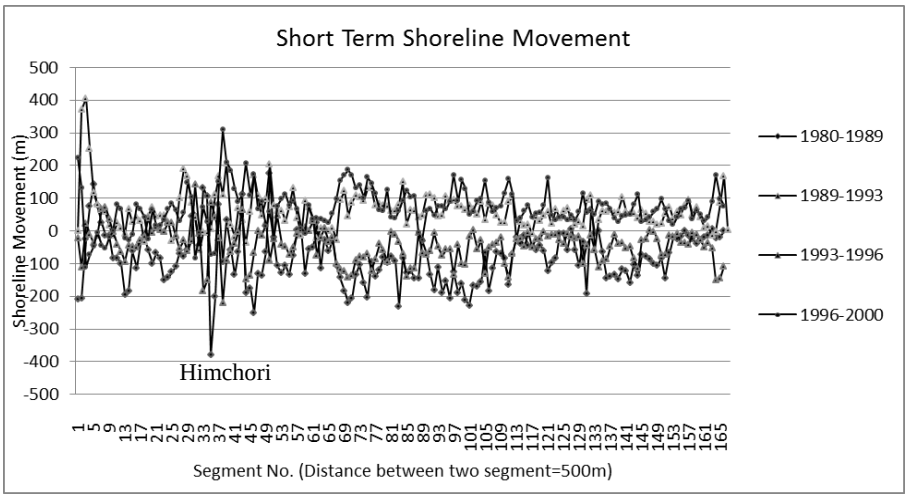

Figure 5 (a): Changes in shoreline between Cox's bazar and Teknaf

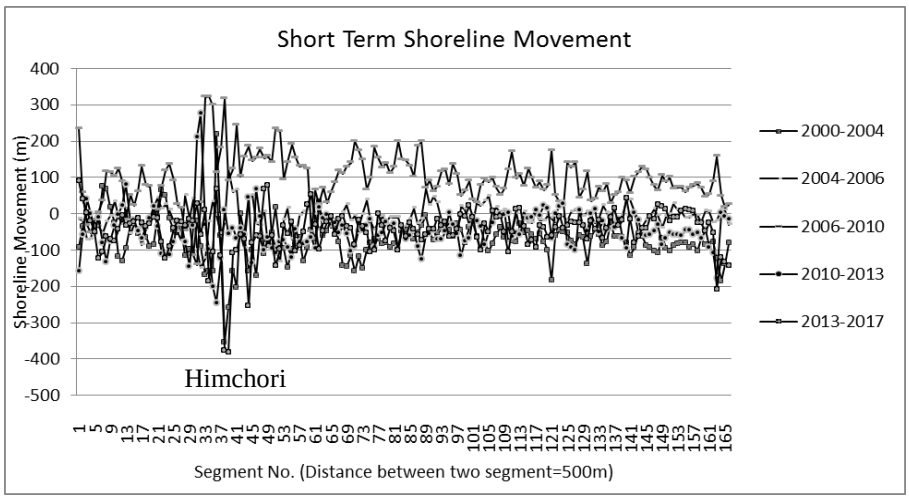

Figure 5 (b): Changes in shoreline between Cox's bazar and Teknaf

The total length of the study area has been divided into three sub-sections to identify the shoreline changes clearly which are shown in Figure 6 and this figure also presents the shoreline changes for last 37 years. Figure 7 to Figure 9 depicts the short time shoreline changes in different years and it has been found that the highest erosion occurred in between section A-A and B-B. The shoreline during the year 2004-2006 shows minimum average deposition (23m) and the maximum deposition occurs during the year 2006-2010 which is around 112m. The maximum erosion 102m occurred during the period 1982-1989 and the minimum erosion 20m occurred during 1989-1993.

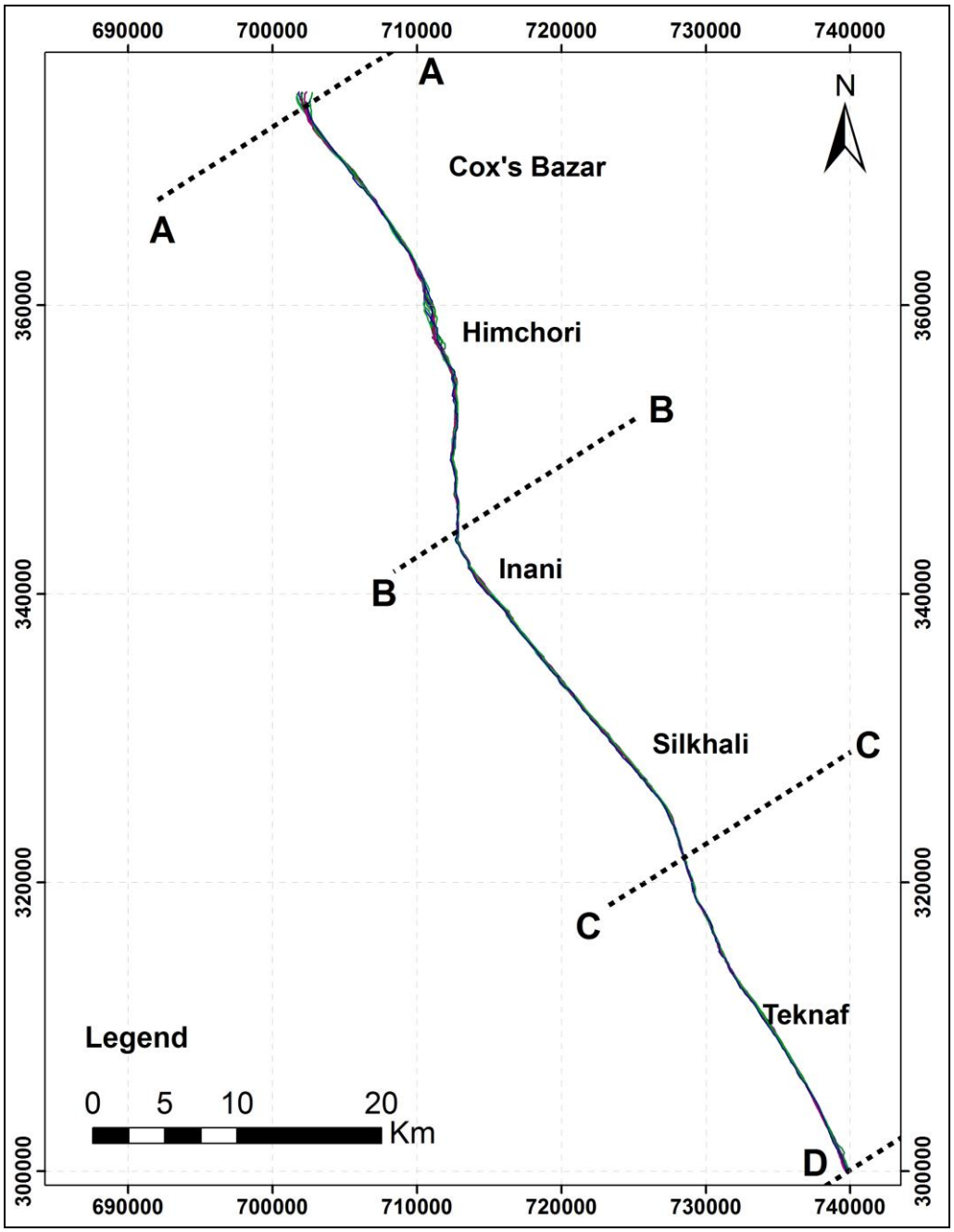

Figure 6: Shorelines of different years between cox's bazar and Teknaf

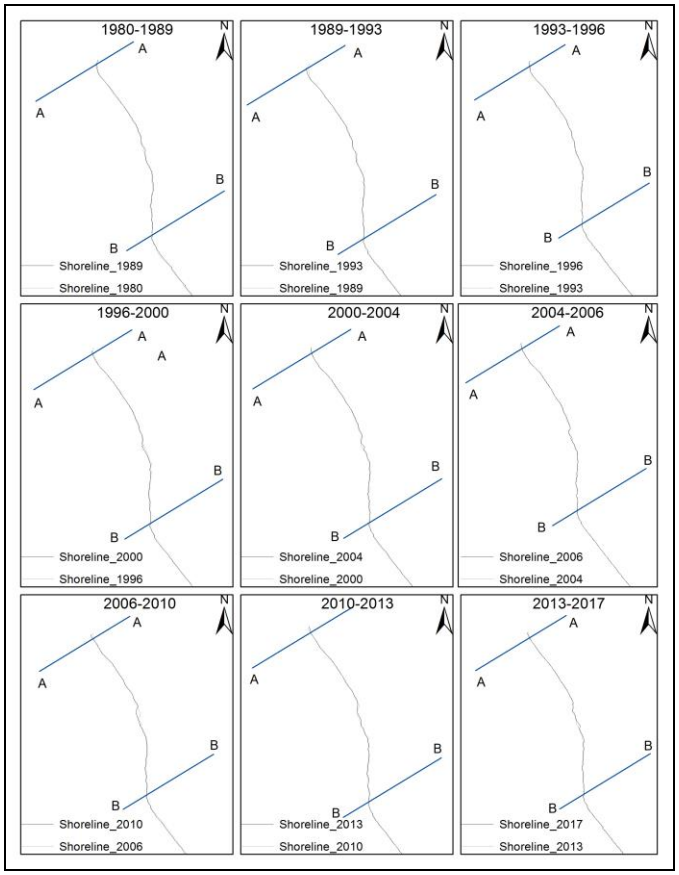

Figure 7: Short term shoreline shifting within section A-A and B-B

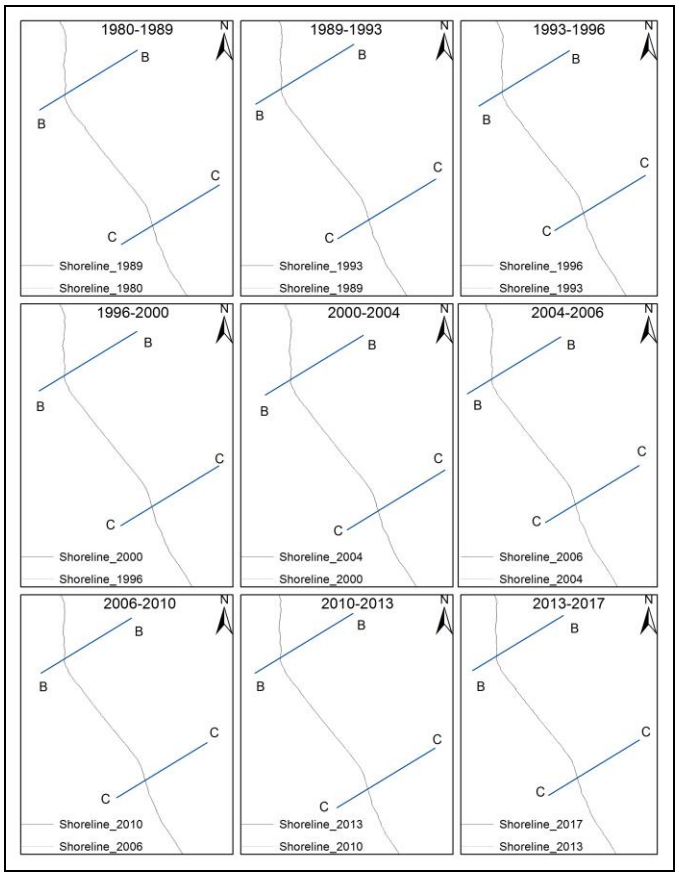

Figure 8: Short term shoreline shifting within section B-B and C-C

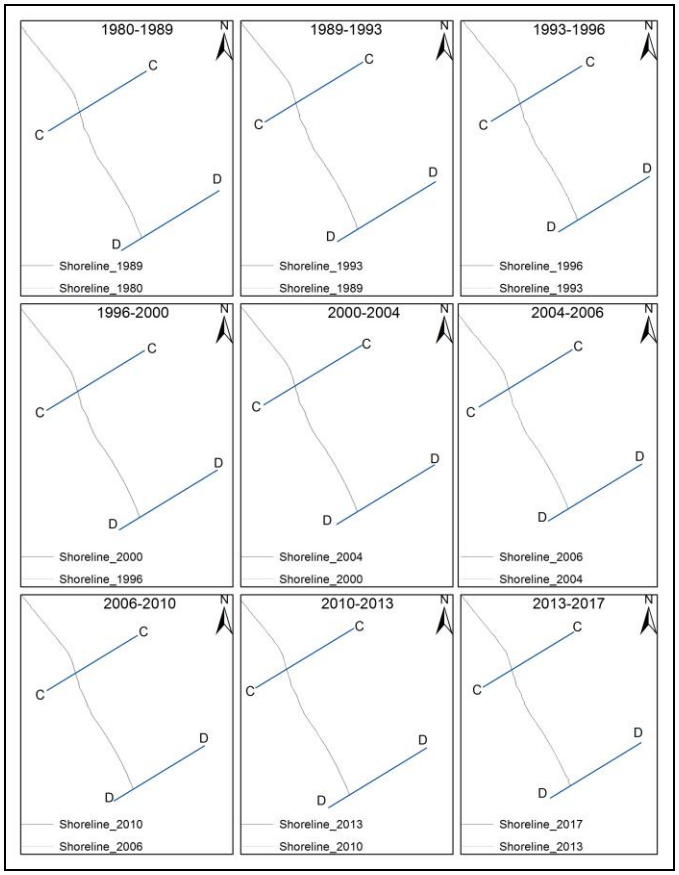

Figure 9: Short term shoreline shifting within section C-C and D-D

Figure 10 illustrates the NDVI values for the respective years considered and it can be clearly visible from the figures that areas having lower NDVI values (less vegetation) are more susceptible to shoreline changes, which indicates that the areas are more dynamic in nature. The areas with high NDVI values (high vegetation coverage) are more stable in the study area.

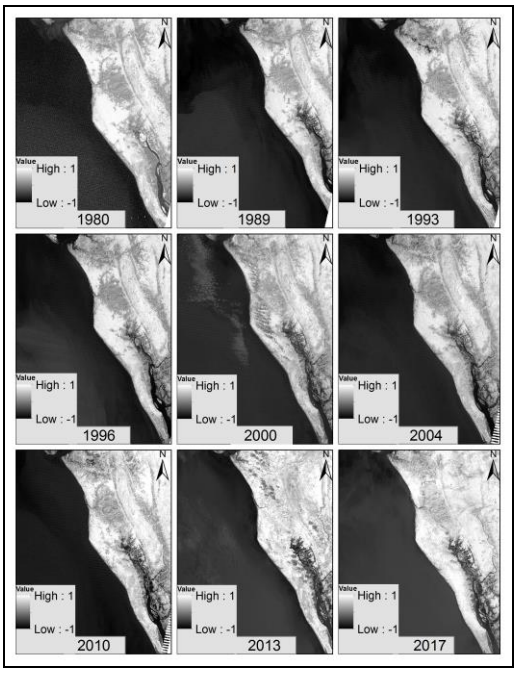

Figure 10: NDVI values within the study reach

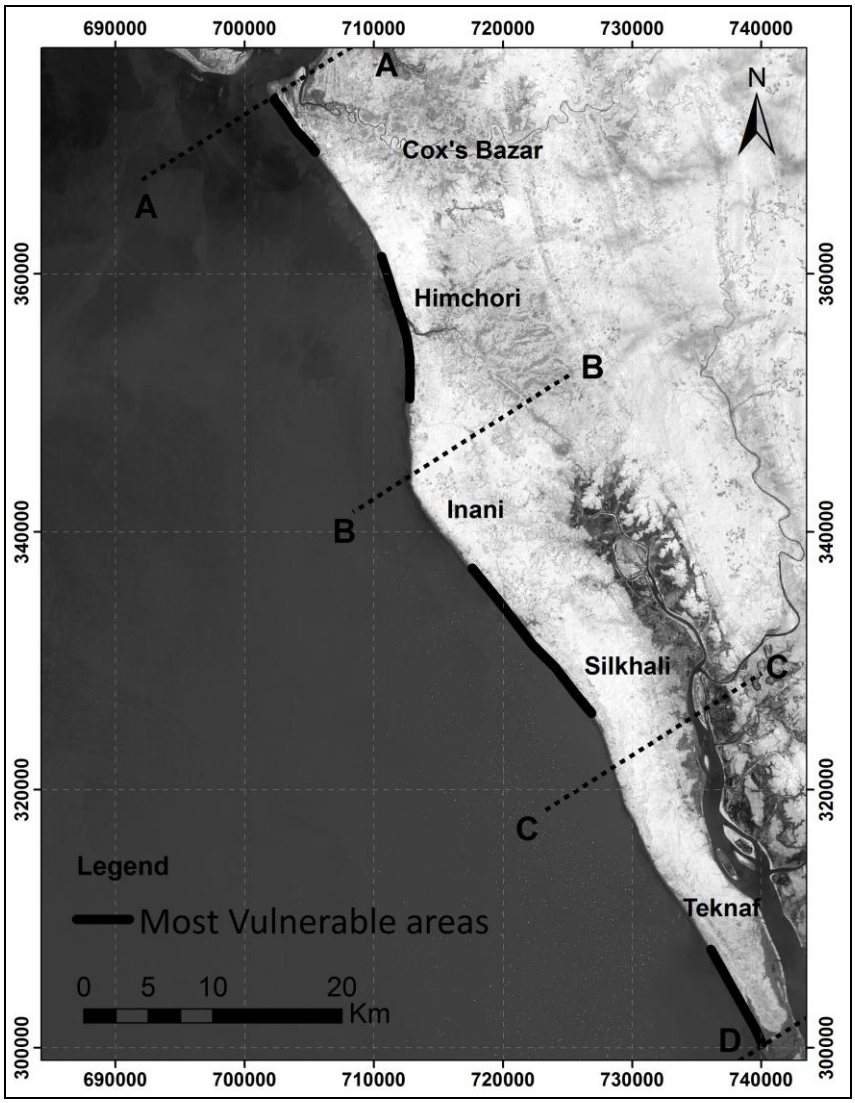

Figure 11: Most Vulnerable areas within the study reach

Figure 11 highlights the most dynamic and vulnerable locations along the Cox's Bazar-Teknaf shoreline. From this figure it can be said that there is considerable shifting almost in every sections. Maximum erosion and deposition has been found near Himchori area. The Inani region is also very dynamic in nature.

4. CONCLUSIONS

The Cox's Bazar-Teknaf shoreline is found to be very dynamic in nature. From the time series analysis of Landsat imagery from 1980 to 2017, it has been found that the shoreline shifting occurs with respect to every transect lines. For the different 3 segments, the shoreline shifting rate is found to be higher in the section A-A and B-B during last 37 years. Based on the results of this study it can be said that special shore protection measures need to be taken for the current and future planning and management of Cox's Bazar-Teknaf shoreline. All the concerning protection works or defensive mechanism for any development project should be taken without disturbing the natural coastal processes that has been going on from time immoral.

REFERENCES

Akter S., 2015. Assessment of Nearshore Hydrodynamic Process along the Coasts of Cox's Bazar, M. Sc. Thesis, Bangladesh University of Engineering and Technology

Alam M.D., Huq, N.E., and Rashid, M.S. 1999. Morphology and Sediments of the Cox's Bazar Coastal Plain South-East Bangladesh, Journal of Coastal Research, 15(4), 902- 908, Royal Palm Beach (Florida), ISSN 0749-0208

Bala B., Hossain M. 2010. Modelling of Food Security and Ecological Footprint of Coastal Zone of Bangladesh, Environ Dev Sustain 12: 511-529

Begum S., Fleming g. 1997. Climate Change and Sea Level Rise in Bangladesh, part II, Effects. Mar Geod 20: 55-68

Boak. E., Turner, I. 2005. Shoreline Definition and Detection: A Review. Journal of Coastal Research 21: 688-703

Bosworth, J., T. Koshimizu. and S.T. Acton. 2003. Multi-resolution Segmentation of Soil Moisture Imagery by Watershed Pyramids with Region Growing Merging. International Journal of Remote Sensing 24(4): 741-760.

Cendrero, A., 1989. Land-Use Problems, Planning and Management in the Coastal Zone; An Introduction, Ocean and Shoreline Management, 12(5-6): 367-381.

Crossland, C.J., Baird, D., Ducrotoy, J.P., Lindeboom, H., Buddemeier, R. W., Dennison, W.C., Maxwell, B. A., Smith, S. V., and Swaney, D. P., 2005, "The Coastal Zone – a Domain of Global Interactions", Coastal Fluxes in the Anthropocene Global Change – The IGBP Series, Chapter 1, pp. 1-37.

Dewidar, K.,and Frihy, O. E. 2008. Pre and Post-Beach Response to Engineering Hard Structures Using Landsat Time-Series at the Northwestern Part of the Nile delta, Egypt. J. Coastal Conservation 11(2):133-142.

Di, K., J. Wang., R. Ma. and R. Li. 2003. Automated Shoreline Extraction from High Resolution IKONOS Satellite Imagery. Proceedings of the ASPRS 2003 Annual Conference, Anchorage, May 2003

Durduran, S. S. 2010. Coastline change assessment on water reservoirs located in the konya basin area, Turky, using multitemporal Landsat imagery. Environ. Monitoring Assessment 164: 453-461

Enemark, S., 2007, "Coastal Areas and Land Administration – Building the Capacity", Strategic Integration of Surveying Services, 6th FIG Regional Conference 2007, San Jose, Costa Rica, 12-15 November, 2007.

Esteves, L. S. 2004. Shoreline Changes and Coastal Evolution as Parameters to Identify Priority Areas for Management in Rio Grande do Sul, Brazil. Revista Pesquisas em Geociências, 31 (2): 15-30, Instituto de Geociências, UFRGS.ISSN 1518-2398 Porto Alegre, RS – Brasil.

Fedra, K. and Feoli, I. M., 1988, "GIS Technology and Spatial Analysis in Coastal Zone Management", EEZ Technology, Ed. 3, pp. 171-179.

Foody, G. M., Muslim, A. M., and Atkinson, P. M., 2005, Super-resolution Mapping of the Waterline from Remotely Sensed Data. International Journal of Remote Sensing 26(24): 5381-5392.

Galgano, F.A. and Leatherman, S.P. 1991. Shoreline change analysis: a case study. Coastal Sediments '91 (1): 1043-1053.

Holme, A.McR., Burnside, D.G. and Mitchell, A.A. 1987. The Development of a System for Monitoring Trend in Range Condition in the Arid Shrublands of Western Australia, Australian Rangeland Journal 9:14-20.

Honeycutt, M. G., Crowell, M. & Douglas, B. C., 2001. Shoreline Position Forecasting: Impact of Storms, Rate-Calculation Methodologies, and Temporal Scales. Journal of Coastal Research, 17(3): 721-730.

Hossain, M. A., Gan, T. Y., Baki, A. B. M., 2013, Assessing Morphological Changes of the Ganges River Using Satellite Images, doi: 10.1016/j.quaint.2013.03.028

Inman, D. L. and Brush, B. M., 1973, "The Coastal Challenge", Science, New Series, Vol.181, No. 4094 (Jul. 6, 1973), pp. 20.32.

Islam, M. A., Hossain, M. S., Hasan, T. and Murshed, S. 2014, Shoreline Changes along the Kutubdia Island, South East Bangladesh Using Digital Shoreline Analysis System. Bangladesh J. Sci. Res. 27(1): 99-108, 2014 (June)

ISPAN 1992, Technical Notes Series 1. ISPAN/USAID, Flood Plan Coordination Organization, Dhaka, Bangladesh

Lazin, R., 2016. Assessment of Nearshore Sediment Transport along Cox's Bazar Coast Using DELFT3D Model, B. Sc. Thesis, Bangladesh University of Engineering and Technology

Moore, L., 2000. Shoreline Mapping Techniques, Journal of Coastal Research 16: 111-124

Pajak, M. J. & Leatherman, S. 2002. The high water line as shoreline indicator, Journal of Coastal Research, 18(2): 329-337.

Roderick, M., R. C. G. Smith, and G. Ludwick., 1996, Calibrating long term AVHRR Derived NDVI imagery. Remote Sensing of Environment 58: 1-12.

Rouse, J. W., R. H. Haas, J. A. Schell, and D. W. Deering 1973. Monitoring Vegetation Systems in the Great Plains with ERTS, Third ERTS Symposium, NASA SP-351 I, 309-317.

Sener, E., A. Davraz, and S. Sener, 2010, Investigation of Ak- sehir and Eber Lakes (SW Turky) Coastline Change with Multi Temporal Satellite Images. Water Resources Management 24(4): 727-745.

Turner, R. K.; Subak, S. & Adger, W. N. 1996, Pressures, Trends and Impacts in Coastal Zones: Interactions between Socioeconomic and Natural Systems. Journal of Environmental Management, 20(2): 159-173.

UNISDR 2003, United Nations International Strategy for Disaster Reduction, Natural Disasters and Sustainable Development: Understanding the Links between Development, Environment and Natural Disasters. 30p. Available at: http://www.unisdr.org/eng/risk-reduction/wssd/Dr-and-SD-English.pdf Accessed in: 01 May 2004.

USGS, United States Geological Survey, Landsat Missions, (https://landsat.usgs.gov/)

WARPO 2006, Coastal Development Strategy, Water Resources Planning Organization (WARPO), Ministry of Water Resources, Government of the Peoples Republic of Bangladesh, Dhaka, Bangladesh

Weier, J. and Herring, D., 2000, Measuring Vegetation NDVI & EVI, (www.earthobservatory.nasa.gov) August 30, 2000

WIOMSA 2015, Shoreline Change in Tanzania and Kenya, Manual for Assessment and Design of Mitigation Strategies, A Manual prepared under the MASMA (Marine Science for Management) Program of the WIOMSA (Western Indian Ocean Marine Science Association)

Proceedings of the 4th International Conference on Civil Engineering for Sustainable Development (ICCESD 2018), 9~11 February 2018, KUET, Khulna, Bangladesh (ISBN-978-984-34-3502-6)

VERIFICATION OF APHRODITE PRECIPITATION DATA SETS OVER BANGLADESH

Md. Atiqul Islam[1], Asif Ahmed[2], Md. Munirujjaman Munir[2] and Zarif Zaman Khandakar[2]

[1] Assistant Professor, Department of Civil Engineering, Khulna University of Engineering & Technology, Bangladesh, e-mail: atiqul@ce.kuet.ac.bd
[2] Undergraduate Student, Department of Civil Engineering, Khulna University of Engineering & Technology, Bangladesh

ABSTRACT

We investigate the preformance of Asian Precipitation-Highly-Resolved Observational Data Integration Towards Evaluation (APHRODITE) of water resources precipitation products over Bangladesh taking rain gauge data as reference for a 3 years period (January 2003-December 2005). Various statistical and categorical indices such as coefficient of correlation, bias, relative bias, mean absolute error, root mean square error, probability of detection, and false alarm ratio, are applied to measure the performance of the product. With the coefficient of correlation value of 0.82, $Bias$ of 0.91, $RBias$ of –9.5%, MAE of 8.4 mm, and $RMSE$ of 16.0 mm the product tends to underestimate rainfall values during the study period. Although, the POD score of 0.99 demonstrates very good skill in detecting the occurrence of rainfall events, FAR values of 0.26 indicates a considerable amount of false alarms. Moreover, as the precipitation threshold increases, the underestimation becomes more prominent over the study region. Analysis on the basis of location of the rain gauges also shows that APHRODITE consistently underestimates rainfall values with the increase of extreme rainfall thresholds.

Keywords: *Gauge-based Rainfall Observation, Precipitation, Bangladesh, APHRODITE, Extreme, Threshold*

1. INTRODUCTION

Precipitation is one of the most important components of hydrologic cycle and precise estimation of this component is very crucial as it affects human life directly and indirectly. Rain gauge and ground-based radar are the most popular conventional tools to measure rainfall at point and regional scales, respectively. However, rain gauge data suffers from spatial representativeness error whereas ground-based radar has different types of error such as inappropriate Z-R relationship, beam blockages, bright band effects, and so on. Furthermore, ground-based rainfall measurement facilities (i.e. rain gauges and radars) are very sparse in most parts of the world except few developed countries due to their high costs to establish and maintaining infrastructures. Therefore, many projects and organizations are involved to generate gauge-based precipitation data sets at finer spatial and temporal resolutions for ungauged and sparsely gauged basins around the globe such as Asian Precipitation-Highly-Resolved Observational Data Integration Towards Evaluation (APHRODITE) of water resources (Yatagai et al., 2009; Yatagai et al., 2012), the Global Precipitation Climatology Centre (GPCC; Schneider, Fuchs, Meyer-Christoffer & Rudolf, 2008), the University of Delaware (UDEL; Willmott & Matsuura, 1995), the University of East Anglia's Climate Research Unit (CRU; Mitchell & Jones, 2005), and Precipitation Reconstruction over Land (PREC/L; Chen, Xie, Janowiak & Arkin, 2002) datasets.

The Asian Precipitation-Highly-Resolved Observational Data Integration Towards Evaluation (APHRODITE) of water resources project aims to produce state-of-the-art precipitation data sets with high spatial and temporal resolution for Asia. This product is produced using the rain gauge data obtained from a dense rain gauge network consisting of 5000~12000 rain

gauge stations across Asia. This is the only continental-scale long term (1951-2007) precipitation products for Asia based on rain gauge data. The product can be used for climate change analysis, water resources management, improved statistical downscaling, warnings and forecasting's related purposes, evaluation of satellite precipitation products, and validation of regional climate models. Moreover, APHRODITE algorithm improves the estimation of orographic rainfall by integrating rain gauge measurements, remotely sensed data, and geographic information (Yatagai et al., 2012). It also applies a superior quality control method (Hamada, Arakawa & Yatagai, 2012) which reduces the errors automatically and objectively. Current APHRODITE data covers Monsoon Asia, Russia, Middle East, and Japan. Figure 1 shows the mean annual precipitation over Monsoon Asia derived from APHRODITE data during 2003-2005.

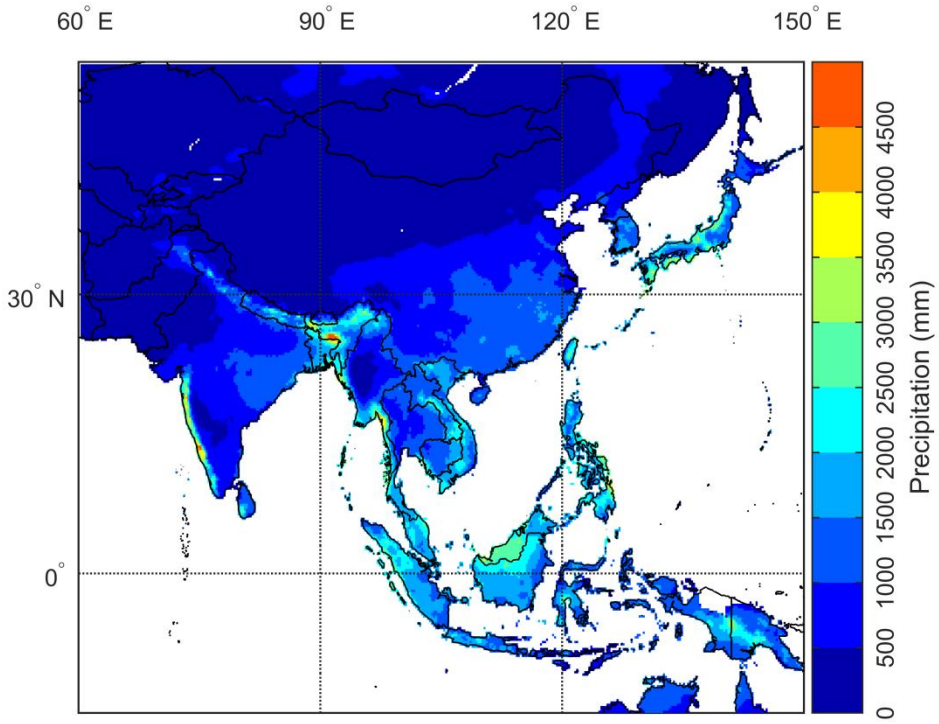

Figure 1: Mean annual rainfall (mm/year) during 2003-2005 over Monsoon Asia derived from APHRODITE precipitation products.

Currently, APHRODITE data is being used to validate satellite rainfall products (Duncan & Biggs, 2012; Jamli, 2015; Jamandre & Narisma, 2013) and to analyse climate change (Gillies, Wang & Huang 2012; Wang & Gillies, 2013). Gillies, Wang and Huang (2012) investigated the changes in winter precipitation over China using APHRODITE precipitation data as reference. Duncan & Biggs (2012) evaluated TMPA 3B42-V6 satellite rainfall estimates relative to ground-based APHRODITE precipitation data over Nepal. Jamli (2015) validated PERSIANN satellite precipitation products through comparison with APHRODITE data set over Iran.

This effort intends to verify APHRODITE data sets over Bangladesh using ground-based rain gauge records to exploit its performance to be used as reference observations. Rain gauge observations can be applied for the validation of satellite-retrieved rainfall estimates. However, gauge data provide point estimate whereas satellite pixels represent an averaged value within an area of 11 km × 11 km (for 0.10° grid box) or 27 km × 27 km (for 0.25° grid box). Therefore, comparison of a pixel with a point estimate may affect the validation results significantly. For the precise estimation of errors and uncertainties of satellite data sets, it is necessary to compare satellite pixel with a reference pixel. However, most of the developing countries of the world such as Bangladesh does not have any gridded reference precipitation

data. Nevertheless, the rain gauge network of Bangladesh is very sparse throughout the country. For this reason, APHRODITE precipitation products have the potentiality to be used as a key decisive source of rainfall information for the evaluation of satellite rainfall estimates over Bangladesh.

After introduction section 2 describes study area and data sets. Methodology is presented in section 3. Section 4 offers results and discussions and section 5 draws some conclusions based on the findings of the present study.

2. STUDY AREA AND DATA SETS

2.1 Study area

Bangladesh is located in South Asia between 20°-27° latitude and 88°-93° longitude (see Figure 2). It is bordered by India in West, East, and North and Bay of Bengal in South (see Figure 1). Bangladesh has a tropical monsoon climate and receives heavy rainfall during monsoon period from June to September. Rainfall also vary substantially in space and time over Bangladesh. Natural calamities that come from extreme rainfall such as floods and landslides are very common in the study area.

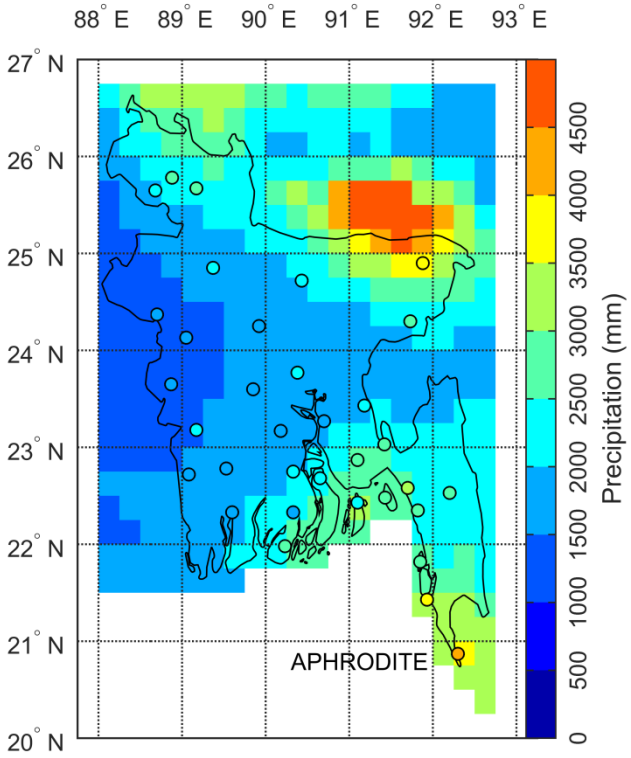

Figure 2: Mean annual rainfall (mm/year) during 2003-2005 over Bangladesh derived from APHRODITE precipitation data. Circles denote the rain gauge locations and the face colour of each circle represents mean annual rainfall (mm/year) during 2003-2005 at that location.

2.2 Rain gauge data

Rain gauge data are collected from Bangladesh Meteorological Department (BMD). Quality controlled 3 h rainfall accumulations of 34 rain gauges are used in the present study (see Figure 2). Rain gauges are operated in Coordinated Universal Time (UTC) time scale. Rainfall accumulation at 18 UTC represents accumulated rainfall between 15 UTC and 18 UTC. Daily accumulations are computed from the 3 h data to synchronize with the daily accumulations of APHRODITE data.

2.3 APHRODITE data

In this research, APHRODITE V1101 precipitation products with daily temporal and 0.25° × 0.25° (latitude and longitude) spatial resolution are evaluated over Bangladesh. Geographical coverage of the data set extends between -15° S-55° N latitude and 60° E-150° E longitude. The gauge data for APHRODITE precipitation products were collected from three sources: i) Global Telecommunication System (GTS)-based data, ii) precompiled data from other projects or organizations, and iii) APHRODITE's own collection. For the V1101 product, an updated automatic quality control scheme was applied to remove erroneous gauge observations throughout the whole domain and the entire study period. However, few issues were handled manually such as i) to check invalid dates and shifted columns, ii) to check each station whether there is location information or not, and iii) to prepare a list of stations with erroneous data for exclusion.

To produce daily climatology the following steps were applied: i) quality controlled daily (except GTS data) data are accumulated to produce monthly accumulations, ii) monthly accumulations, including those obtained in step 1, are collected and the average value is obtained if the station has more than 5 years data, iii) the world climatology is produced at 0.05° resolution, iv) the ratios of the monthly accumulations (computed in step 2) to the world climatology values (computed in step 3) are found out for each month, v) the ratios obtained in step 4 are interpolated using Sheremap (Willmott, Rowe & Philpot, 1985) at 0.05° resolution, vi) the interpolated scores of step 5 are multiplied with the world climatology computed in step 3, vii) the first six components of the fast Fourier transform of the values obtained in step 6 are accepted as the daily climatology.

APHRODITE algorithm interpolates the ratios of the daily precipitation to the daily climatology using angular distance weighting scheme as follows: i) a small weight is provided to a cell on the leeward side of a high ridge if the ridge is situated between the target cell and the nearest rain gauge, ii) a large weight is assigned to a target cell on a slope that inclines to a rain gauge, iii) a lookup table is prepared for each month to define the correlation distance, which is obtained from the global 20-km mesh model developed by Meteorological Research Institute (MRI) of the Japan Meteorological Agency (JMA) and used to define the weighting function.

3. METHODOLOGY

To verify the detection capability of APHRODITE satellite precipitation products the following statistics are used:

$$CC = \frac{\sum_{i=1}^{N}\left(P_{A_i}-\overline{P_A}\right)\left(P_{O_i}-\overline{P_O}\right)}{\sqrt{\sum_{i=1}^{N}\left(P_{A_i}-\overline{P_A}\right)^2}\sqrt{\sum_{i=1}^{N}\left(P_{O_i}-\overline{P_O}\right)^2}} \quad (1)$$

$$Bias = \frac{\sum_{i=1}^{N} P_{A_i}}{\sum_{i=1}^{N} P_{O_i}} \quad (2)$$

$$RBias = \frac{\sum_{i=1}^{N}\left(P_{A_i}-P_{O_i}\right)}{\sum_{i=1}^{N} P_{O_i}} \times 100 \quad (3)$$

$$MAE = \frac{\sum_{i=1}^{N}\left|P_{A_i}-P_{O_i}\right|}{N} \quad (4)$$

$$RMSE = \left[\frac{\sum_{i=1}^{N}\left(P_{A_i}-P_{O_i}\right)^2}{N}\right]^{1/2} \quad (5)$$

where P_{A_i} and P_{O_i} are the ith data of APHRODITE and rain gauge observations respectively. N is the total number of APHRODITE and rain gauge data pair. $\overline{P_A}$ and $\overline{P_O}$ are the mean APHRODITE and rain gauge estimates respectively. Coefficient of correlation (CC) is used to measure the conformity between APHRODITE and rain gauge observations. The value of CC lies between -1 and +1. -1 denotes a perfect negative correlation whereas +1 represents a perfect positive correlation. The value of 0 indicates no correlation between the two data sets. $Bias$ is defined as the ratio of the sum of APHRODITE data to the sum of the rain gauge data. Bias greater than 1 indicates overestimation of rainfall while less than 1 indicates underestimation. $Bias$ value of 1 shows no bias in the estimated precipitation products. Relative bias ($RBias$) represents systematic bias of APHRODITE rainfall data. Mean absolute error (MAE) is employed to show the mean error of the precipitation product. Root mean square error ($RMSE$) presents the magnitude of mean error alike MAE, however, $RMSE$ provides larger weight to greater error.

In addition, two categorical indices i.e. probability of detection (POD) and false alarm ratio (FAR) are computed to assess the skill of APHRODITE rainfall estimates. POD is defined as the ratio of the correct identification of rainfall occurrences to the total number of reference rainfall occurrences whereas FAR reveals the ratio of the false identification of precipitation to the total number of APHRODITE precipitation occurrences (Mehran & AghaKouchak, 2014; Wilks, 2006).

$$POD = \frac{N_H}{N_H + N_M} \tag{6}$$

$$FAR = \frac{N_F}{N_H + N_F} \tag{7}$$

where

$$N_H = \sum_{i=1}^{N} \left(\left(P_{A_i} > 0 \;\&\; P_{O_i} > 0 \right) \;\&\; \left(P_{A_i} \geq 1 \mid P_{O_i} \geq 1 \right) \right) \tag{8}$$

$$N_M = \sum_{i=1}^{N} \left(\left(P_{A_i} = 0 \;\&\; P_{O_i} > 0 \right) \;\&\; \left(P_{A_i} \geq 1 \mid P_{O_i} \geq 1 \right) \right) \tag{9}$$

$$N_F = \sum_{i=1}^{N} \left(\left(P_{A_i} > 0 \;\&\; P_{O_i} = 0 \right) \;\&\; \left(P_{A_i} \geq 1 \mid P_{O_i} \geq 1 \right) \right) \tag{10}$$

4. RESULTS AND DISCUSSION

Figure 3 shows the scatterplot of daily APHRODITE data and rain gauge observations greater than or equal to 1 mm/day for the entire study period (2003-2005) over Bangladesh. It is worth mentioning here that a rainfall threshold 1.0 mm/day is considered to differentiate between rain and no rain. APHRODITE product demonstrates reasonable agreement with the reference rain gauge data at lower rainfall accumulations (below 50 mm/day). About 90% of the rainfall observed by the rain gauges is below 50 mm/day. From Figure 3 one can see that APHRODITE underestimates rainfall values substantially particularly above 100 mm/day. Overall, the accuracy of the product decreases consistently with the increase of the amount of rainfall accumulated by the gauges.

Third column of Table 1 summarizes the statistics of Figure 3. In this column, the values of $Bias$ (0.91) and $RBias$ (–9.5%) confirm that APHRODITE underestimated the rainfall accumulations over the study area. However, the coefficient of correlation CC (0.82) shows good correspondence of APHRODITE data with reference observations. The scores of 8.4

mm and 16.0 mm for MAE and $RMSE$, respectively, reveal a considerable difference between APHRODITE and gauge data. The value of 0.99 for POD denotes excellent rainfall

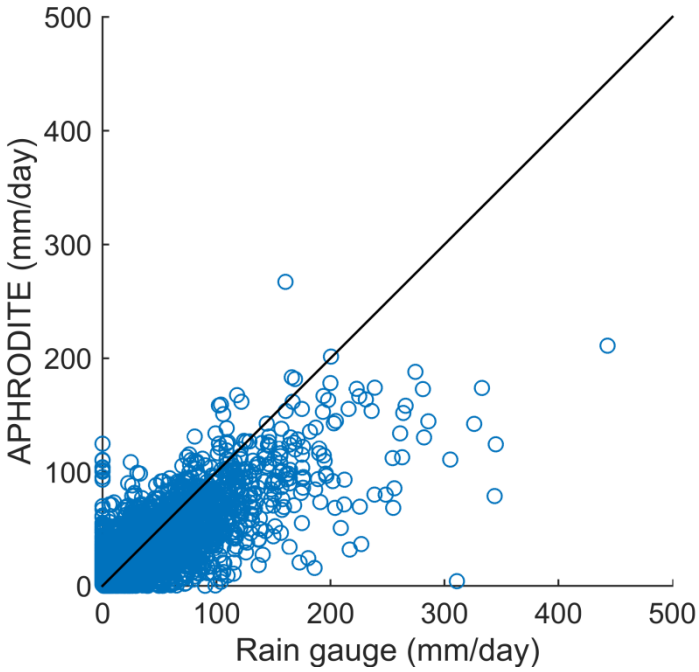

Figure 3: Comparison of APHRODITE precipitation data with rain gauge observations for daily temporal accumulation during 2003-2005.

detection capability of the product, while FAR represents that the product gives a considerable number of false alarms during the study period. As the rainfall threshold increases from 1 mm to 50 mm, the skill of the product decreases significantly (compare fourth column with third column of Table 1). CC and $Bias$ decrease from 0.82 to 0.53 and from 0.91 to 0.70, respectively. Moreover, the product show 217%, 308%, and 184% increase in $RBias$, MAE, and $RMSE$, respectively. In fact, Table 1 shows increasingly worse error statistics as the rainfall threshold increases (from left to right). For rainfall accumulations greater than or equal to 100 mm, APHRODITE exhibits very limited rainfall detection skill. However, FAR scores decrease remarkably with the rainfall threshold whereas POD remains almost constant.

Table 1: Comparison of error statistics for different rainfall thresholds (P denotes rainfall accumulations in mm)

	Unit	**Rainfall thresholds**		
		$\boldsymbol{P \geq 1}$	$\boldsymbol{P \geq 50}$	$\boldsymbol{P \geq 100}$
N	--	15941	1453	319
CC	--	0.82	0.53	0.32
$Bias$	--	0.91	0.70	0.65
$RBias$	%	-9.5	-30.1	-35.4
MAE	mm	8.4	34.3	60.7
$RMSE$	mm	16.0	45.4	76.0
POD	--	0.99	1.00	1.00
FAR	--	0.26	0.01	0.02

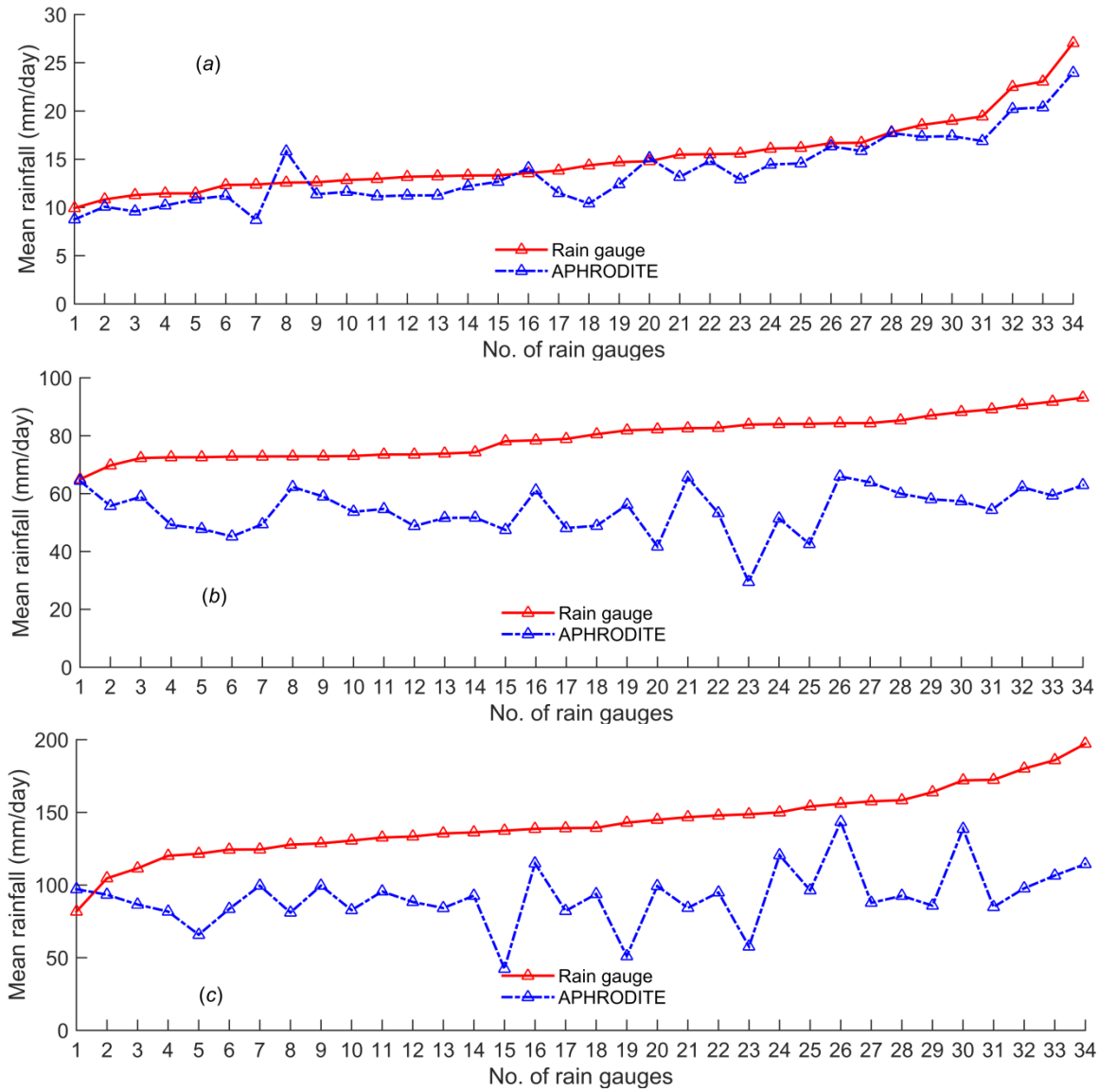

Figure 4: Mean daily rainfall accumulation at each gauge location as measured by APHRODITE product and rain gauges for (a) ≥ 1 , (b) $P \geq 50$, and (c) $P \geq 100$ during 2003-2005 (P indicates rainfall accumulation in mm).

Figure 4 represents mean daily rainfall values at the 34 rain gauge locations for the various rainfall thresholds. Figures 4(a), 4(b), and 4(c) are computed according to the ascending order of the mean daily collections of the rain gauges. When entire data are included in the analysis, the difference between APHRODITE and rain gauge accumulations are very small at most of the rain gauge locations (see Figure 4(a)). The difference increases substantially as the rainfall thresholds increase (see Figures 4(b) and 4(c)). It is worth pointing out here that the maximum limit of y axis of Figures 4(a), 4(b), and 4(c) are not the same. Figures 4(b) and 4(c) highlight that the underestimation of APHRODITE becomes more significant with the increase of the thresholds. Furthermore, Figure 4 confirms the findings of Table 1. Jamandre and Narisma (2013) compared APHRODITE precipitation products with station observations over Philippines. They found that APHRODITE performed well within 20-50 mm/day precipitation range and underestimated extreme rainfall accumulations (above 50 mm/day). In the present study, relatively better performance of APHRODITE rainfall data sets when entire data are considered in the analysis may be ascribed to the fact that the overestimation at lower rainfall amounts compensating the underestimation at higher rainfall

values (see Figure 3). Moreover, higher rainfall values are also underestimated during the study period over Bangladesh (above 50 mm/day).

5. CONCLUSIONS

Accurate estimation of precipitation is very important for hydrological modelling, extreme weather forecasting and monitoring, and climate analysis. Unfortunately, ground-based rainfall measurement facilities are very sparse or non-existent in most parts of the world, especially in the developing countries such as Bangladesh. There are several freely available (ground-based and space-borne) precipitation products which can be used in the ungauged basins. However, it is necessary to evaluate the rainfall products against available reference observations before incorporating the data into practical applications.

Accordingly, this study aims to verify the Asian Precipitation-Highly-resolved Observational Data Integration Towards Evaluation (APHRODITE) of water resources project with respect to available rain gauge measurements over Bangladesh. This ground-based product is produced using very dense rain gauge network over Monsoon Asia. In this approach, APHRODITE is evaluated using various statistical and categorical skill matrices for daily temporal accumulation and different rainfall thresholds.

The computed $\boldsymbol{CC}$, $\boldsymbol{Bias}$, $\boldsymbol{RBias}$, $\boldsymbol{MAE}$, and $\boldsymbol{RMSE}$ scores indicate that APHRODITE tends to underestimate the rainfall during the study period. As the extreme rainfall threshold increases, the error statistics show very serious underestimation. However, false alarm ratios decrease considerably with the thresholds. Location wise analysis of the product also reveals that APHRODITE underestimates the rainfall values and this underestimation increases with the increase of extreme precipitation thresholds. Therefore, it is suggested that appropriate correction method should be applied before incorporating this product into any kind of practical applications over Bangladesh.

ACKNOWLEDGEMENTS

Rain gauge data were collected from Bangladesh Meteorological Department (BMD). APHRODTIE data were obtained from the respective mission website and are thankfully acknowledged.

REFERENCES

Chen, M., Xie, P., Janowiak, J. E., & Arkin, P. A. (2002). Global land precipitation: A 50-yr monthly analysis based on gauge observations. *Journal of Hydrometeorology*, 3, 249-266. https://doi.org/10.1175/1525-7541(2002)003<0249:GLPAYM>2.0.CO;2

Gillies, R. R., Wang, S., & Huang, W. (2012). Observational and supportive modelling analyses of winter precipitation change in China over the last half century. *International Journal of Climatology*, 32(5), 747-758. doi: 10.1002/joc.2303

Hamada, A., Arakawa, O., & Yatagai, A. (2011). An automated quality control method for daily raingauge data. *Global Environmental Research*, 15(2), 183-192.

Jamandre, C. A., & Narisma, G. T. (2013). spatio-temporal validation of satellite-based rainfall estimates in the Philippines. *Atmospheric Research*, 122, 599-608.

Jamli, J. B. (2015). Validation of satellite-based PERSIANN rainfall estimates using surface-based APHRODITE data over Iran. *Earth Sciences*, 4(5), 150-160. doi:10.11648/j.earth.20150405.11

Mehran, A., & AghaKouchak, A. (2014). Capabilities of satellite precipitation data sets to estimate heavy precipitation rates at different temporal accumulations. *Hydrological Processes*, 28(4), 2262-2270. doi:10.1002/hyp.9779

Mitchell, T. D., & Jones, P. D. (2005). An improved method of constructing a database of monthly climate observations and associated high-resolution grids. *International Journal of Climatology*, 25, 693-712. doi: 10.1002/joc.1181

Schneider, U., Fuchs, T., Meyer-Christoffer, A., & Rudolf, B. (2008). *Global precipitation analysis products of the GPCC*. Retrieved from ftp://ftp.dwd.de/pub/data/gpcc/PDF/GPCC_intro_products_2008.pdf.

Wang, S., & Gillies, R. R. (2013). Influence of the Pacific quasi-decadal oscillation on the monsoon precipitation in Nepal, *Climate Dynamics*, 40(1-2), 95-107. http://dx.doi.org/10.1007/s00382-012-1428-7

Wilks, D. S. (2006). *Statistical methods in the atmospheric science* (2nd ed.). Burlington, MA, USA: Academic Press.

Willmott, C. J., & Matsuura, K. (1995). Smart interpolation of annually averaged air temperature in the United States. *Journal of Applied Meteorology*, 34, 2577-2586. https://doi.org/10.1175/1520-0450(1995)034<2577:SIOAAA>2.0.CO;2

Willmott, C J., Rowe, C. M., & Philpot, W. D. (1985). Small scale climate maps: A sensitivity analysis of some common assumptions associated with grid-point interpolation and contouring. *The American Cartographer*, 12, 5-16.

Yatagai, A., Arakawa, O., Kamiguchi, K., Kawamoto, H., Nodzu, M. I., & Hamada, A. (2009). A 44-year daily gridded precipitation dataset for Asia based on a dense network of rain gauges, *SOLA*, 5, 137-140, doi:10.2151/sola.2009-035

Yatagai, A., Kamiguchi, K., Arakawa, O., Hamada, A., Yasutomi, N., & Kitoh, A. (2012). APHRODITE: Constructing a long-term daily gridded precipitation dataset for Asia based on a dense network of rain gauges. *Bulletin of American Meteorological Society*, 93, 1401-1415. doi:10.1175/BAMS-D-11-00122.1

Proceedings of the 4th International Conference on Civil Engineering for Sustainable Development (ICCESD 2018), 9~11 February 2018, KUET, Khulna, Bangladesh (ISBN-978-984-34-3502-6)

DETERMINATION OF GROUND WATER LEVEL IN CHITTAGONG CITY

Sayma Akter[1] and M. N. Anwar[2]

[1] Lecturer, Southern University Bangladesh, Bangladesh, e-mail: saymaaktercuet42@yahoo.com
[2] Student, Southern University Bangladesh, Bangladesh, e-mail: saymaaktercuet42@yahoo.com

ABSTRACT

Southern part of Bangladesh is now facing water scarcity problems in both agriculture and secured livelihood. Ground water forms the major portion of earth's fresh water source and it is almost safe to drink. Depletion of ground water table due to continuous pumping causing scarcity of water in the city area of Bangladesh. So information about ground water table is required for future recommendation of ground water supply to general people. For the investigation purpose, depth of water table has been determined in one seasons with respect to mean sea level. 41 wards of Chittagong City Corporation have been selected for this purpose where depth of water table is measured from the shallow and Deep tube well. The present investigation includes field investigation for locating of tube well in Chittagong City Corporation area with the aim of measuring water level from ground surface. From the investigation, it has been established that, water table with respect to mean sea level is different at different wards. During field investigation, 88 shallow tubes well and 89 deep tube well in 41 wards were found. The overall view shows that, in almost every ward, to find fresh water deep tube well is must as shallow tube well can't frequently pump water. From the investigation, it is clear that ground water table is lowering day by day. At the beginning of rainy season when it started to rain the water table comes up. Ground water through shallow tube well is not sufficient to fulfill the required demand for the general people as it is becoming out of reach through shallow well day by day. Depth of water table with respect to mean sea level is quite lower in ward 5 & depth of water table with respect to mean sea level is quite higher in ward 14. Average Depth of water table with respect to mean sea level is quite lower in ward no 5 & quite higher in ward no 15. The study was also carried out to assess groundwater table of Chittagong city. From this analysis, it is found that the GW level is lowering in almost all the region of the study. The present study can be concluded with the following decisions: The study shows the groundwater level in the study area is lowering day by day. This scarcity of GW is caused due to excessive extraction and dependence on GW for irrigation and other purposes. The ground water level is decreasing day by day due to intensive use of ground water. So, alternative water source should be ensured to mitigate the problem. Steps must be taken for using rain water, after preserving in tanks in the rainy season as alternate source of groundwater.

Keywords: *Ground water, scarcity, depletion, Sea Level, investigation, measure, variation*

1. INTRODUCTION

Ground water forms the major portion of earth's fresh water supply. About 97% of the earth's fresh water supply is stored in the underground. Ground water can be used as a reliable earth's fresh water supply is stored in the underground formation with the increase in population, the design for water system is essential to meet the increasing demand for water is also increasing throughout the world. Effective management of ground water system in essential source of water supply irrespective of the climate. In the monsoon areas of south-east Asia, ground water way becomes an important source of supply especially for irrigation purposes in the dry months. 94% of all the water-works use ground water and they supply 77% for the ground water (Aziz, 1975). The depth at which soil pore spaces or fractures and voids in rock become completely saturated with water is called the water table. Groundwater is recharged from and eventually flows to the surface

naturally, natural discharge often occurs at springs and seeps, a can form oases or wetlands. Ground water is also often withdrawn for drinking, agricultural, municipal & industrial use by constructing & operating extraction wells. The study of the distribution and movement of ground water is hydrogeology, also called ground water hydrology.

Southern part of Bangladesh is now facing water scarcity problems in both agriculture and secured livelihood. Ground water is a vital source of water supply for Bangladesh. Bangladesh is almost entirely underlain by water-bearing formations at depths varying from zero to 20 m below ground surface (Md. A. H. Mirdad et. al, 2010).

Ground water in Bangladesh, except in some places, is available at a shallow depth. Ground water levels are at or near ground level during the period January-may. Ground water rises as a result of recharge during January-may. There are several areas of Bangladesh where ground water withdrawals are causing a large deceive in ground water level during dry seasons. The ground water withdrawal and recharge characteristics suggest that the actual recharge can be increased approaching the potential limits by creating addition storage through increased abstraction during the dry season. According to MPO (1991) estimates, out of 42543 mm^3 total useable recharge, 40% is available through shallow tube wells (Md. A. H. Mirdad et. al, 2010).. In this study, therefore the main focus will be found out the variation of the groundwater table of Chittagong city corporation area (Ahmed et. al, 2000)

2. METHODOLOGY

Chittagong city is the second largest city of Bangladesh, considered the heart of all commercial and business activity. Chittagong water supply and sewerage authority (cwasa) which is the authority for water supply and sewerage only supply water to one-third of city dwellers. Rest of people depends on the shallow tube well and deep tube well. Location of ground water table in Chittagong city corporation area has been shown in study area map of figure- 1. For the investigation purpose specific problem has been identified and through which important information can be found .

2.1 Investigation Of Shallow and Deep Tube well In Chittagong City Corporation Area

At the beginning of the work first task is to find out the shallow and Deep tube well in the 41 ward's City Corporation. Shallow tube well is not available in Chittagong city corporation area. Are Deep tube well has been found available in Chittagong city corporation. Tube well has found in-41 wards that was shown by the figure-1.

2.2 Determination Of Ground Water Level

At the beginning of the work first task is to find out the shallow and Deep tube well in the 41 ward's City Corporation. Shallow tube well is not available in Chittagong city corporation area. Are Deep tube well has been found available in Chittagong city corporation. Tube well has found in-41 wards that was shown by the figure-2.

2.2.1 Reduced Level of Ground Surface in Well Location by Mobile GPS

Reduced level of ground surface in well location can be easily found by mobile GPS. Mobile GPS is a space based global navigation satellite system that provides reliable location and time information in all weather & all times anywhere. On the well location, switch on the mobile GPS by using internet. Then wait for five minutes to set its location properly. Then it will give value of longitude latitude & elevation of that specific location with respect to mean sea level.Mobile GPS device gives almost accurate elevation in the location. Mobile GPS device works accurately in the open area.

2.2.2 Depth of Water Table in Different Seasons by Thick Wear -

Depth of water table has been measured from the ground level at well location by opening the head of well. After opening the head of the well, wait for 10-15 minutes to drop the water in the well pipe. Then using a thick wear with a small steal at its bottom, entering into the well pipe until the wear is in a state of less weight. Then by using tape, find the depth from the wire. In this process, the depth is measured Dry season. Once at the ending of Dry season (In April) after some rainfall when water table is recharged and comes up.

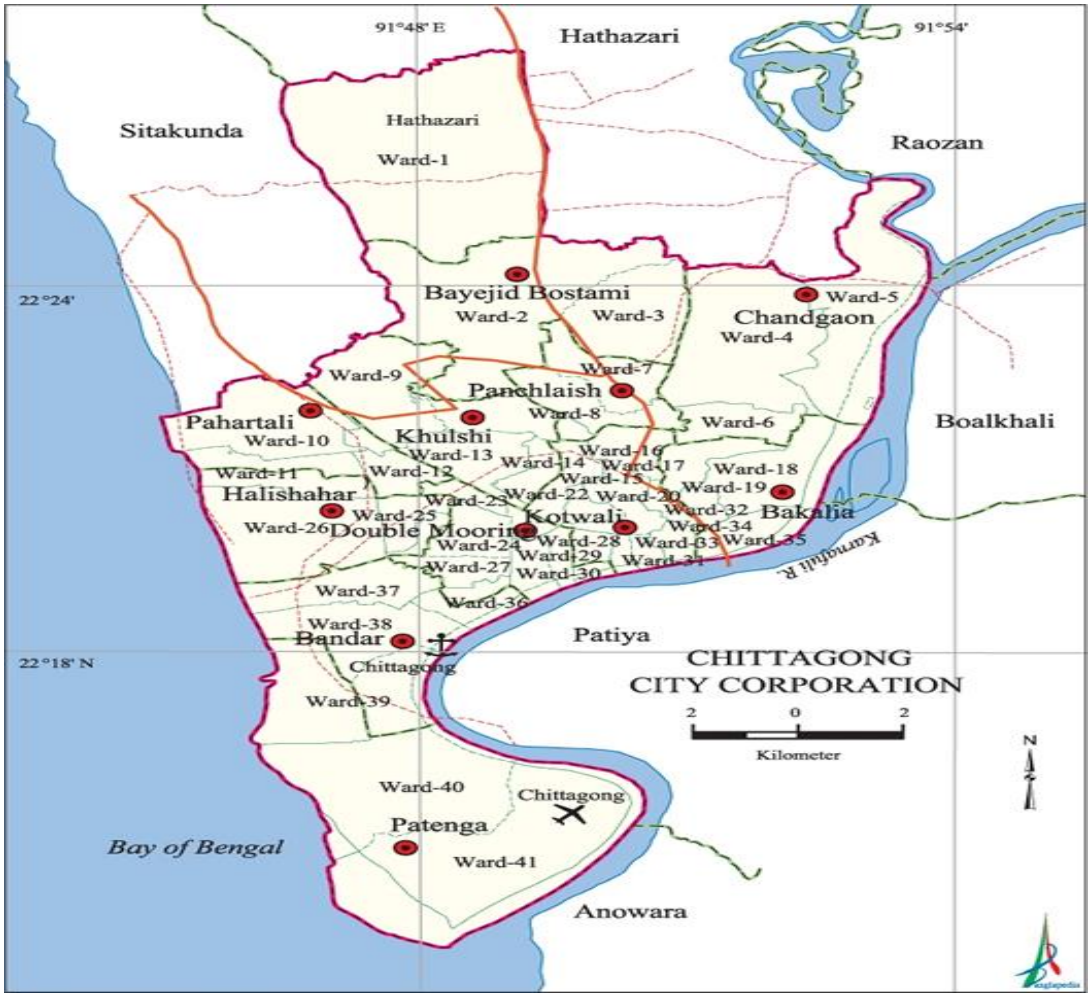

Figure 1: Location map of shallow and deep tube wells in Chittagong City

Figure-2: Determination of ground water level by thick wear in shallow tube well

3. ILLUSTRATIONS

3.1. Figures and Graphs

From Figure-3 it shows the depth of water table with respect to mean sea level is quite lower in ward no 5 (hazi razak monjil, gafur road, one kilometer) and depth of water table with respect to mean sea level is quite higher in ward no 14 (kazi orcid, high level road, lalkhan bazar).

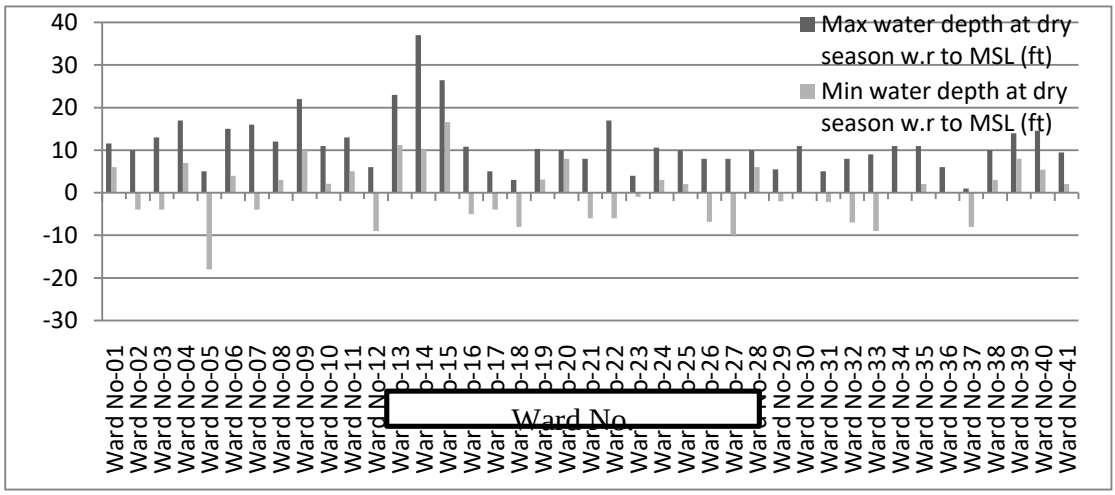

Figure: 3 Graphical representation of water table in dry season.Equations

From figure-4 it shows the average Depth of water table with respect to mean sea level is quite lower in ward no 5 & quite higher in ward no 15.

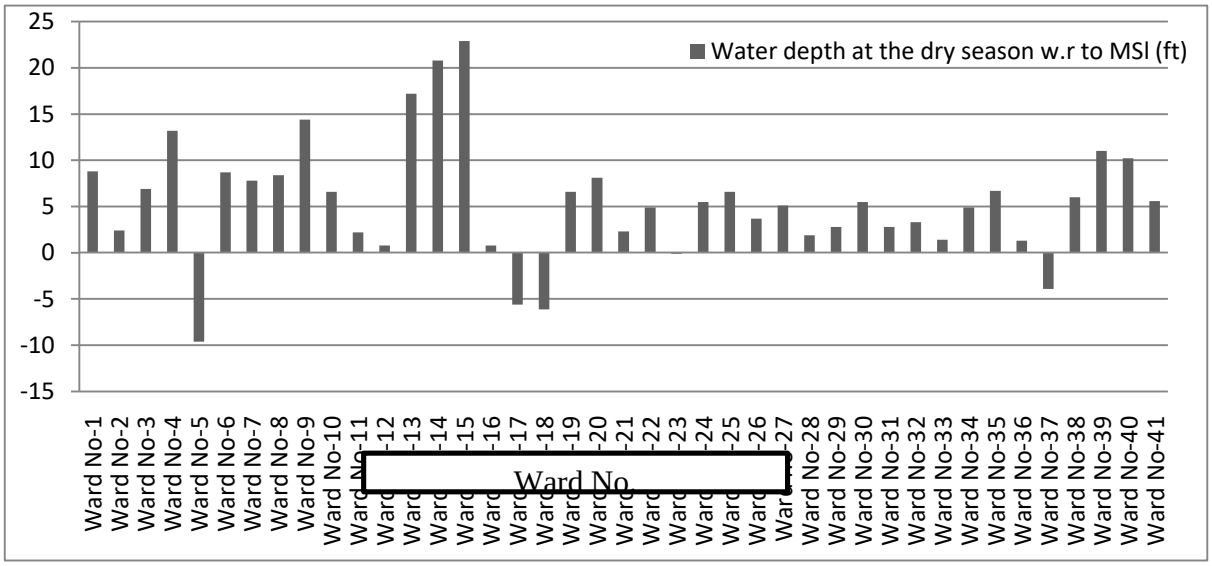

Figure:4 Graphical representation of Avg. water table in dry season.

3.2. Results of Ground Water Table of Shallow and Deep Tube Wells –

(i) Depth of Water Table in Dry Seasons from MSL -

Depth of water table measured in dry seasons from ground level & adjustment of depth from mean sea level has been shown in Table 1.

Ward No.	Ward Name	Well location	Elevation (RL of ground surface w.r. to MSL)	At the beginning of dry season
01	South Pahartali	1) Mona Meya Shorkar Bari, House No#11, Road No#03, Aman Bazar.	25'	25'-16'=9'
		2) Katar Para, Aman Bazar.	23'	23'-17'=6'
		3) Kathal Bagan, House No#10, Baluchora	23'	23'-16'=7'
		4) Romjan Ailr Bari, House No#06, Khilla Para,	24'	24'-13'=11'
		5) Shanti Colony	28'	28'-11'=11'
02	Jalalabad	1) Etiquette Ali Lodeg, H/N#03,Nasirabad	29'	29'-37'=-8'
		2) Sarja Kanon, House No#09, Sersha, Oxyzen.	31'	31'-35'=-4'
		3) Rohim Member Bari, RohomanNagor,	28'	28'-18'4"=9'8"
		4) Kader Ali House, Lane No# 05, Nasirabad	33'	33'-23'=10'
		5) Burma Colony, Bayazid Bostami	25'	25'-21'=4'
03	Panchlaish	1) Rof Rof Tower, House No# 02, Lane No#01, Katalgong.	25"	25'-29'=-4'
		2) Noor Garden, House No# 19, Lane No# 02, Katalgong.	28'	28'-35'=7'
		3) Mushi Colony, Abdul Hamid Road, Shulakbahar.	29'	29'-16'=13'
		4) Habibullah Road, Noyarhat,	36'	

			Bayejid		36'-25'7"=10'5"
04	Chandgaon	1)	Etiquette IBBL Officer Tower, Khaza Road.	24'	24'-13'=11'
		2)	Jafor Company House, House No#08, Khaza Road.	20'	20'-13'=7'
		3)	Pathainnagoda, Bohoder Hat, Chandgaon	30'	30'-16'=14'
		4)	Khadija Tower, Road No#03, Hous No#04.	27' 31'	27'-10'=17' 31'-14'=17'
		5)	Jalal Khan Chowdhury Bari Road		
05	Mohara	1)	S.Rose. House, South Mohora, Kalurghat.	20'	20'-35'=-15'
		2)	Nikti Bobon, CNB, Kalurghat.	16'	16'-34'=-18'
		3)	KhalekVali, Road No#03, House No#15,	20'	20'-30'=-10'
		4)	Hazi Razak Monjil, Lane No#02, Gafur Road, One Kilometer.	33'	33'-28'=5'
06	East Sholashahar	1)	Railway Colony, Sholashahar	31'	31'-16'=15'
		2)	Rahmania High School, Sholashahar	23'	23'-17'=6'
		3)	Khaja Hotel, Rohoman Nogor	26'	26'-14'=12'
		4)	Shohel Place, House No#7,Road No#3,Kapashgola	23'	23'-19'=4'
		5)	Phanto Neer, Hamidulla Meya Road	27'	27'-21'=6'
07	West Sholashahar	1)	Hamzarbag Colony,	36'	36'-22'6"=13'6"
		2)	Chowdhury Complex, Mohammadpur	32'	32'-27'=5'
		3)	Hossain Ahmed Chowdhury City Corporation School	37' 27'	37'-21'=16'
		4)	Khan Bari, House No#14, Road No#1, Mohammadpur		27'-31'=-4'
08	Sulakbahar	1)	Shah Habibullah Road, Noyarhat.	29'	29'-17'=12'
		2)	Munshi Colony, Vaktapur	26'	26'-15'8"=11'4"
		3)	Daraga Bari, Chaillatali Bazaar.	32'	32'-25'=7'
		4)	Kholla Meya Sodhagor Bari, Lane no#2, Sulakbahar	30'	30'-27'=3'
09	North Pahartali	1)	Pahartali Rail Way Colony,	39'	39'-29'=10'
		2)	Ambagan Rail Way Colony,Pahartali	42'	42'-26'10"=14'2"
		3)	Nobi Bobon, Mosque Lane,Bachamia Road	45'	45'-34'=11'
		4)	Jalala Menson, Nesariya Housing Society,	65'	65'-43'=22"
10	North Kattali	1)	Jiku Shorkar House, Post Office Road,Kattali	39'	39'-28'=11"
		2)	Madrasa Road, North Kattali	26'	26'-19'=7'
		3)	Reque Menson, House No#07,Road No#7, Proshanti Society.	29'	29'-26'2"=2'10"
		4)	Laky Monjil, House No#03, Road No#2, Proshanti Society.	30'	30'-24'9"=5'3"

11	South Kattali	1)	Ma Monjil, House No#6, Monsurabad, Colonel Hat.	25'	25'-32'=-7'
		2)	Rowson Tower, House No#10, Road No#7, Proshanti R/A.	23'	23'-34'6"=-11'6"
		3)	Firoz Shah Colony, Colonel Hat.	24'	24'-19'=5'
		4)	Kazir Bari, Lane No#2, Post Office Road, Colonel Hat.	26'	26'-15'=11'
		5)	Poros, Lane No#1, Office Road	30'	30'-17'=13'
12	Saraipara	1)	Soronika,House No#11,Shanti Bag R/A,	22'	22'-31'=-9'
		2)	Noju Meyar Lane, Saraipara	25'	25'-19'=6'
		3)	M.Kholil Company Bari, Sobujbag, Saraipara	23'	23'-21'=2'
		4)	Raja Baburci House, Saraipara	21'	21'-17'5"=3'7"
13	Pahartali	1)	Etiquette Khulshi Complex, South Khulshi, Block-B, Lane No#3, Road No#1.	68'	68'-45'=23'
		2)	Mishon South Point, Road No#1, Khulshi	57'	57'-41'=16'
		3)	Jawotola Railway Colony, Road No#2,	51'	51'-39'10"=11'2"
		4)	New Jawtala Primary School	78'	78'-51'=27'
		5)	Nondon, House No#11, Sagun Bagan	60'	60'-39'=21'
14	Lalkhan Bazar	1)	Etiquette Aurora, Road No#1. Hill Side R/A, Near Momota Hospital,	102'	102'-67'7"=34'4"
		2)	Selicon Kazi Orcid, House No#3 Hilevel Road, Lalkhan Bazar.	98'	98'-61'=37'
		3)	Monju House, Buttaia Colony, Lalkhan Bazar.	48'	48'-37'2"=10'10"
		4)	Samsi Colony, Lalkhan Bazar.	46	46'-33'9"= 12'3"
		5)	Tigerpass Railway Colony	50'	50'-41'=9'
15	Bagmoniram	1)	Sky Lack, Lane No#1, Kazirdewri.	112'	112'-85'8"=26'4"
		2)	Hazir Bari, Lane No#3, Kazi Para, Kazirdewri.	87'	87'-64'=23'
		3)	Gov.Empoloy Colony Mosque, Golphar Circel, Mehedibag.	66'	66'-41'=25'
		4)	Khorshed House, Lane No#1, Dampara.	59'	59'-42'6"=16'6"
16	Chawkbazar	1)	Hosen Tower, Near D.T Road, Chawkbazar .	26'	26'-39'=-13'
		2)	Chaianeed, House No#3,Parchiaheel, Chawkbazar.	38'	38'-43'=-5'
		3)	Kalam Colony, D.T. Road, Chawkbazar.	27'	27'-17'=10'
		4)	Rohoman Bari, Lane No#2,Gasheya Para, Chawkbazar .	29'	29'-18'4"=10'8"
17	West Bakalia	1)	Aleya House,Lane #02, W.Bakalia	25'	25'-29'=-4'

		2)	Shajam Compamyr Bari, Bakalia	28'	28'-23'=5'
		3)	Karim Tower, House No#5/D, Lane#4.	22'	22'-36'=-14'
		4)	Active Alom Tower, Lane#01		
		5)	Hazi Alauddin Road,	20'	20'-38'=-18'
				24'	24'-21'=3'
18	East Bakalia	1)	Cast View, House No#11, Road No#3, E.Bakalia	23'	23'-31'=-8'
		2)	Shopno need, House No#08, Road No#01	20'	20'-35'3"=-14'9"
		3)	Kheleda Colony, Bakalia	24'	24'-21'=3'
		4)	Kazi Kanon, House No#14, Bakalia	20'	20'-28'=-8'
19	South Bakalia	1)	Jaitun Cotej, Noya Mosque Area,	28"	28'-24'2"=3'10"
		2)	EkraTowar, Road No# 4, S.Bakalia	26'	26'-31'=5'
		3)	Khadizanebas, H/N#8, Bakalia	30'	30'-23'=7'
		4)	Bakalia Khal Para,	29'	29'-18'9"=10'3"
20	Dewan Bazar	1)	Shadat Tower, House No#16, Road No#1, Dewan bazar.	30'	30'-21'5"=8'7"
		2)	Sale Nur Tower, House No#9, Road No#4,	34'	34'-25'=9'
		3)	BogerbilLabour Colony, Dewan Bazar.	27'	27'-19'=8'
		4)	Shohid Cont. Bari, Dawan Bazar.	31'	31'-21'=10'
21	Jamal Khan	1)	Rokeya Cotez, House No#05,Hamsen Lane	42'	42'-38'=4'
		2)	Oli Bobon, House No# 10, Emdad Colony	39'	39'-45'=-6'
		3)	Kanu Das House, Dopa Para	45'	45'-37'=8'
		4)	Meyar Bari, Gunacor Lane.	40'	40'-37'2"=2'10"
22	Enahet Bazar	1)	Harun Sodagorer Bari, H/N#12, Lane No#2, Gowal Para,	52'	52'-46'=6'
		2)	Romjan Monjil, House No#08, Lane No#3.	51'	51'-57'=-6'
		3)	Hasena Vila, H/N#03, Batali Road, Mosque Lane,	49'	49'-47'=2'
		4)	Baki Sodagor Bari,College Road,	56'	56'-39'=17'
23	North Pahartooly	1)	Raj Monjil, House No#12, Doniwala Para, Dewan Hat.	29'	29'-37'=-8'
		2)	Hoque Tower, House No#01, Road No#5, Oposit Site of Passpot Office. Monsurabad.	35'	35'-34'=-1'
		3)	Sultan Colony, Lane No#1, Dewan Hat.	31'	31'-27'=4'
		4)	Supariwala Para, House No#4, Dewan Hat.	27'	27'-28'=-1'
		5)	Manan Bobon, Chanmeyar Bill,	30'	30'-24'6"=5'6"
24	North Agrabad	1)	Etiquette Mowlana Tower, Port Connacting Road, Boro pool,	20'	20'-17'=3'
		2)	Newaj Monjil, House No# 08, N.Agrabad.	22'	22'-19'=3'
		3)	Raja Mear Bari, Road No#02, Muhuri Para,	20'	20'-14'=6'
		4)	Mosque Colony, Moinna Para,	25'	25'-14'6"=10'6"
		5)	Jahan Monjil, Askara Bad,	21'	21'-16'=5'
25	Rampur	1)	Tara Nebas,Rampur Post	23'	23'-21'=2'

			Office Road		
		2)	Bow Bazar Mosque Lane	21'	21'-32'=10'
		3)	Pukur Par Mosjid	28'	28'-21'=7'
		4)	Rose Bally, Panir Kol, Lane No#2,	26'	26'-19'=7'
26	North Halishahar	1)	Kazi Orcid, House No#19, K-Block, Karnofuli R/A, Halishahar.	27'	27'-17'=10'
		2)	Alom Tower, House No#09, No 08 Gate. Halishahar	25'	25'-31'4"=-6'8"
		3)	Askara bad Colony, N.Halishahar	23'	23'-27'=4"
		4)	Rahat Ara Lane, Nowa Bazar	26'	26'-19'=7'
27	South Agrabad	1)	CGS Colony,SouthAgrabad	25'	25'-18'=7'
		2)	Al Nahian Primary School,	27'	27'-19'=8'
		3)	Woab Tower, House No#5, Road No#03, CDA R/A.	23'	23'-17'9"=5'3"
		4)	CDA R/A, Mosque Lane.	21'	21'-21'=0'
28	Patantooly	1)	Patantooly City Corporation Girl's High School.	27'	27'-37'=-10'
		2)	Baitul Hamad Mosque,Patantooly	23'	23'-20'=3'
		3)	Sultan Colony, Patantooly	32'	32'-24'=8'
		4)	Gaibi Mosque Lane	25'	25'-19'=6'
29	West Madarbari	1)	Nikthi Bobon, Majir Gat, Madarbari	26'	26'-21'=5'
		2)	Rabeya Workshop, Madarbari	29'	29'-23'6"=5'5"
		3)	Ma Monjil, House No#5/D, West Madarbari	27'	27'-29'=-2'
		4)	Dalower House, House No#7, W. Madarbari	24'	24'-26'=2'
30	East Maderbari	1)	Monu Meya Mosque Lane,	25'	25'-14'=11'
		2)	Archaid, House No#4/B,Lane No#2	26'	26'-26'=0'
		3)	Kabir Monjil, Nala Para, East Maderbari	22'	22'-18'=4'
		4)	Primary Techer's Institute, Ice Factori Road.	20'	20'-13'6"=6'6"
31	Alonkar	1)	Sagorika Colony, Sagorika.	23'	23'-18'=5'
		2)	Alonkar Kacha Bazar, Alonkar,	27'	27'-25'9"=1'3"
		3)	Baitul Jannat Mosque, Alonkar	24'	24'-26'10"=-2'2"
		4)	Naj Tower, Sagorika	29'	29'-27'=2'
32	Anderkilla	1)	Kholipa Potti, Anderkilla	28'	28'-21'6"=6'6"
		2)	Jemjson Hall, Anderkilla	36'	36'-28'=8
		3)	MAK Sajid Tower, House No# 18/A, Anderkilla	29'	29'-36'=-7'
		4)	Sultan Monjil, House No#7, Lane No#01,	28'	28'-25'4"=2'8"
		5)	Arc, House No#5, Chairman Goli	33'	33'-27'=6'
33	Firingi Bazar	1)	Behari Colony, Firingi Bazar	20'	20'-17'=3'
		2)	Al-Alam Tower, Monosha Gate.	19'	19'-19'=0'
		3)	Meya Sodhagor House, House No#9, Sultan Meya Lane	20'	20'-29'=-9'
		4)	Behari Colony, 3 No Lane, Firingi Bazar		
		5)	Shadarghat Port Colony,	23'	23'-19'=4'

				25'	25'-16'=9''
34	Patharghata	1)	ShakMonjil, Lane No#2, Iqbal Road	33'	33'-29'=4'
		2)	Bank Colony Road	42'	42'-31'=11'
		3)	NazuSodhagorBari,Lane No#1,Brick Field Road	32'	32'-28'=4'
		4)	Amir Ail Road	29'	29'-29'=0'
35	Boxir Hat	1)	Meyaji Colony, LaneNo#03, Boxir Hat,	39'	39'-28'=11'
		2)	Manik Sodagor House, Boxir Hat	30'	30'-35'=-5
		3)	Hendhu Para, Boxir Hat	33’	33-24'9''=8'3''
		4)	Komol Kanon,House No#7,Lane No#5	29'	29'-31'=2'
36	Goshaildanga	1)	K.K. Tower, Hanif Sowdagor Lane	32'	32'-27'=5'
		2)	Goshaildanga Kali Bari Lane No#1	24'	24'-24'=0'
		3)	Becha Shah Mosjid Colony	27'	27'-21'=6'
		4)	Multi Sitred Colony	25'	25'-27'=-2'
		5)	Billa Pada	25'	25'-28'=-3'
37	North Middle Halishahar	1)	Moshjid Quarter, 13#No. Road, Bandar Port Colony.	20'	20'-28'=-8'
		2)	Road No#7, House No#10, Bandar Port Colony	18'	18'-26'=-8'
		3)	SerajMenson, Road No#5/D, Uttara R/A.	25'	25'-24'=1'
		4)	Aleya Tower, Road No#2/A, Uttara R/A.	25'	25'-25'=0'
38	South Middle Halishahar	1)	Sarja Bobon, House No#3/A, Road No#4,	33'	33'-28'=5'
		2)	Baitul Asa Moshjid Quarter, Boro Pool,	27'	27'-24'=3'
		3)	Kalam Colony, Pukur Par, Boro Pool.	29'	29'-19'=10'
		4)	Iseabally Tower, House No#12, Lane No#2	35'	35'-29'=6'
39	South Halishahar	1)	Rokaya Nebas, House No#08, Akmal Ali Road.	30'	30'-21'=9'
		2)	Lane No#2,Halishahar A Block. Foliatali Bazar	29'	29'-15'=14'
		3)	Behari Colony, Halishahar	24'	24'-11'=13'
		4)	Gass Tower, House No#04, Halishahar B Block	27'	27'-19'=8'
40	North Potenga	1)	Omol Kanon, Hindhu Para, Lane No#01, Kathgar	33'	33'-21'3''=11'9''
		2)	Potenga City Corporation Girl’s High School.	39'	39'-24'6''=14'6''
		3)	Jala Manson, Lane No#05,Kathgar	32'	32'-26'8''=5'4''
		4)	Mohima House, Road No#02,	34'	34'-25'=9'
41	South Potenga	1)	South Para, Road No#2, BondhorTila,	28'	28'-19'7''=8'5''
		2)	Golden Beach Road, Patenga	26'	26'-16'7''=9'5''
		3)	R&R Tower, Road No#01, South Potenga.	23'	23'-21'=2'
		4)	See Place, South Potenga.	25'	25'-23'=2'

CONCLUSIONS

Ground water table in Chittagong City Corporation area is in a position where day by day the water table is lowering. In this research, the result derived from the investigation has been presented below:

i. Water tables are different in different wards.
ii. During field investigation, 88 shallow tubes well and 89 deep tube well in 41 wards were found.
iii. Ground water through shallow tube well is not sufficient to fulfill the required demand for the general people as it is becoming out of reach through shallow well day by day.
iv. Depth of water table with respect to mean sea level is quite lower in ward no 5 (Hazi Razak Monjil, Gafur Road, One Kilometer).
v. Depth of water table with respect to mean sea level is quite higher in ward no 14 (Kazi Orcid, High Level Road, Lalkhan Bazar).
vi. Average Depth of water table with respect to mean sea level is quite lower in ward no 5 & quite higher in ward no 15.

The study shows the groundwater level in the study area is lowering day by day.This scarcity of GW is caused due to excessive extraction and dependence on GW for irrigation and other purposes.

ACKNOWLEDGEMENTS

We would like to express our sincere gratitude to our supervisor “Prof.(Engr.) M.Ali Ashraf” Head of Civil Engineering Department, Southern University Bangladesh” and for the continuous support of our research, for his patience, motivation, and immense knowledge. His guidance helped me in all time of research and writing of this thesis. Finally, we take this opportunity to express gratitude to all of the Department faculty members for their help and support.

REFERENCES

Ahmed, M. F. &Rahman, M. M. (2000).Water Supply and Sanitation.ITN – Bangladesh, Dhaka-1000.pp: 331 – 338.

Ahmed, A. (1990). Safe water supply in Rural Himalayas: Environmental Problems and Strategies. In the proceedings of the 18th National Health Conference on Health Problems of the Nineties, Lahore, Pakistan, 2-5 December 1990. pp: 123-138.

Groundwater Resources Development in Bangladesh: (Contribution to Irrigation for Food and Constraints to Sustainability). Anwar Zahid and Syed Reaz Uddin Ahmed, Ground Water Hydrology Division, Bangladesh Water Development Board, Dhaka, Bangladesh.

H.M. Raghunath, Groundwater New Age International (P) Limited, Publishers, New Delhi, 1996.

Md. A. H. Mirdad, S. K. Palit; Determination of Ground Water Level in the South-East (Chittagong) Part of Bangladesh. American Journal of Civil Engineering. Vol. 2, No. 2, 2014, pp. 53-59. doi: 10.11648/j.ajce.20140202.17

S.K. Garg. Water Supply Engineering, Khanna Publishers, 2-B Nath Market, Nai Sarak, Delhi-1100.

Proceedings of the 4th International Conference on Civil Engineering for Sustainable Development (ICCESD 2018), 9~11 February 2018, KUET, Khulna, Bangladesh (ISBN-978-984-34-3502-6)

APPLICATION OF DELFT3D MATHEMATICAL MODEL IN THE JAMUNA RIVER FOR TWO-DIMENSIONAL SIMULATION

Orpita Urmi Laz[1] and Umme Kulsum Navera[2]

[1] *Postgraduate student, Department of Water Resources Engineering, Bangladesh University of Engineering and Technology, Bangladesh, e-mail: orpita12@yahoo.com*
[2] *Professor, Department of Water Resources Engineering, Bangladesh University of Engineering and Technology, Bangladesh, e-mail: uknavera@gmail.com*

ABSTRACT

The Jamuna River, one of the most important rivers in Bangladesh which has been playing a vital role in our social economic structure, experiences severe erosion almost every year. Severe erosion poses a constant threat to the people and have long-term negative impact on socio-economic status. Apart from this natural hazards, some man-made interventions i.e. construction of the Bangabandhu Bridge, groynes etc. interrupt the natural flow of the river and therefore changes the hydraulic environment. In order to study the possible changes in river bed morphology due to manmade interventions application of 2D model in the Jamuna River is unavoidable. This study focus principally the different hydrodynamic characteristics of the selected reach of the river by applying a 2D model Delft 3D. The study reaches covers from 30 ksm upstream of Bangabandhu Bridge to 20 kms downstream of this bridge. Boundary conditions for upstream and downstream are defined by discharge and water level data respectively. The model has been developed with the bathymetry data collected from Bangladesh Water Development Board (BWDB). The model has been calibrated with the available observed data for the period of April to July 2010 and validated onto the period of April to August, 2011. The hydrodynamics of the selected area have been simulated by solving two-dimensional depth integrated momentum and continuity equations numerically with finite difference method. The knowledge developed herein may be useful in providing an opportunity in assessing improvement in future prediction and also to suggest the effect of possible development work to be implemented on this river.

Keywords: *Jamuna River, Calibration, Validation.*

1. INTRODUCTION

The Jamuna River usually faces high dynamics and is usually surrounded by network of interlacing channels with numerous sandbars or chars (Marra, Kleinhans & Addink, 2014). These chars are formed as the sediment-carrying capacity of the flow exceeds the incoming sediment load, which is also known as aggradation of the channel (Baki & Gan, 2012). The Jamuna River also experiences severe erosion, operates in several spatial and temporal scales and strongly related to the magnitude of monsoonal peak discharge, leads bank retreat from hundreds of meters annually and causes possible damage to public infrastructure living along its course and on chars (Mount, Tate, Sarker & Thorne, 2013), (Mosselman, 2006). Therefore, understanding of the river's dynamic behaviour is required to control erosion as well as reduce the damage to public infrastructure.

On the other side, the construction of Bangabandhu Bridge has a significant impact on the dynamics of bar morphology and channel shifting. River training structures along with the bridge creates a water slope between the upstream and downstream level near the bridge section which results in bank erosion (Bhuiyan, Rakib, Takashi, Rahman & Suzuki, 2010). Construction of the bridge has provided the first road and rail link between the northwest and eastern part of the country (Bayes, 2007). Apart from movement of cargo and passenger

streams, it promotes conveyance of electricity and natural gas, and telecommunication links to the western region. Thus contributing economic development and eliminating the disparities between the eastern and western districts. Hence, hydraulic conditions in the vicinity of the bridge as well as hydro-morphological forecasts of the river at the critical locations within the bridge area are essential to know and predict the navigability and erosion patterns. Previously extensive studies have been conducted at different duration to assess the behavior of Jamuna River (Jagers, 2003), (Uddin, Rahman, 2012). This study gives an idea of the hydrodynamic characteristics of Jamuna River which will further support the future application of 2D mathematical model under several scenarios. The Study area covers about 50 km reaches of Jamuna River between Kazipur at the upstream end and Chauhali at the downstream end, covers Balkuchi, Sirajganj on the right bank and Gopalpur, Bhuapur on the left bank which are important places to be considered along the study reach. The location of the study area is shown in Figure 1.

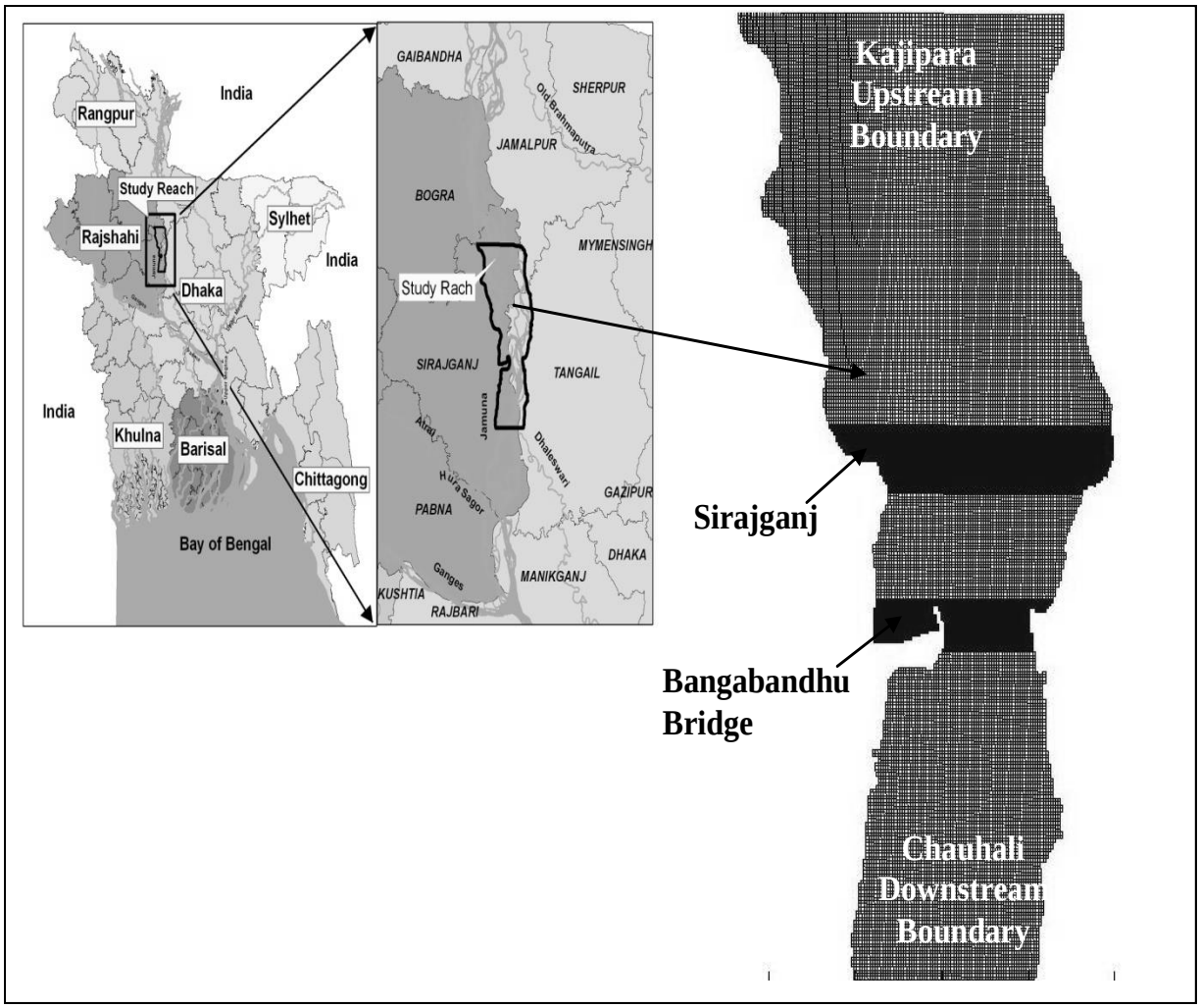

Figure 1: Study Area on the Jamuna River

2. METHODOLOGY

In order to simulate the hydrodynamics of Jamuna River, a 2D hydrodynamics model Delft3D has been applied. Flow, MOR, Wave, WAQ are different modules of Delft3D. Delft3D-FLOW module has been implemented in this study, which is a multidimensional (2D

or 3D) hydrodynamic and transport simulation program. The non steady flow and transport phenomenon is being calculated by this module, resulting from tidal and meteorological forcing on a rectilinear or a curvilinear boundary fitted grid.

3. GRID GENERATION AND BATHYMETRY

In order to carry out continuous simulation curvilinear grid was used, which was generated, modified and visualized by Delft3D-RGFGRID module. This module generates grid in Cartesian coordinate system. The grid was extended over the upstream near Kazipur to downstream close to Chowhali.

The model consists of a total of 299 and 146 cells in M-N directions respectively with dimensions of (124×171) m^2. Surveyed bathymetric data was collected from IWM and interpolated into mesh nodes using the Delft3D-QUICKIN module. Bathymetry file was generated for Delft3D after a series of processes such as grid cell averaging, triangular interpolation and internal diffusion. The hydrodynamic simulation time has been set to 122 days with time step of 1 minute.

4. BOUNDARY CONDITIONS

Time series discharge data was used at the upstream inflow boundary near Kazipur and water level data in the downstream direction near Chowhali collected from Shirajganj station.

In the year 2010, the water level rises abruptly during April to July as well as the discharge also increased abruptly. Again in 2011, it can be observed from the hydrograph that the water level raised abruptly during April to June, fluctuated slightly during the next three months then slightly falls from the end of August almost to the mid of September then again slightly raises in the end of September. In case of discharge similarly abruptly discharge raised from April to July then slightly fluctuated downward for the next three months, and falls rapidly during the end of August to September.

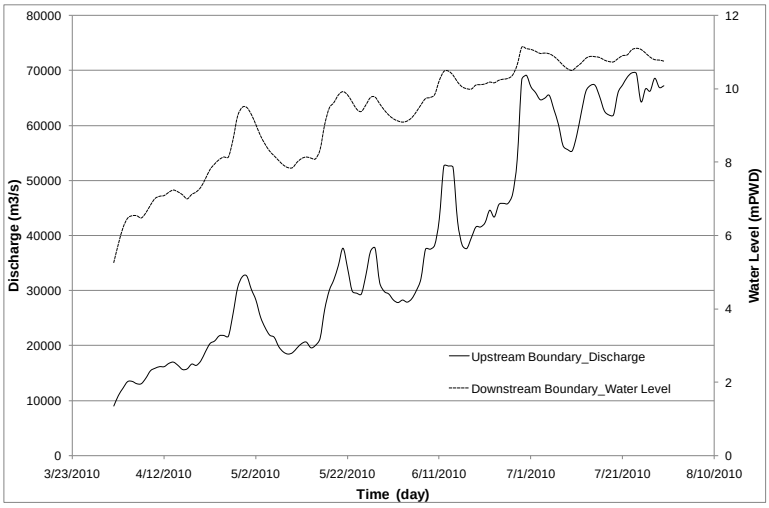

Figure 2: Time series hydrographs from April to July 2010 used in the model as Boundary Conditions for Calibration Period

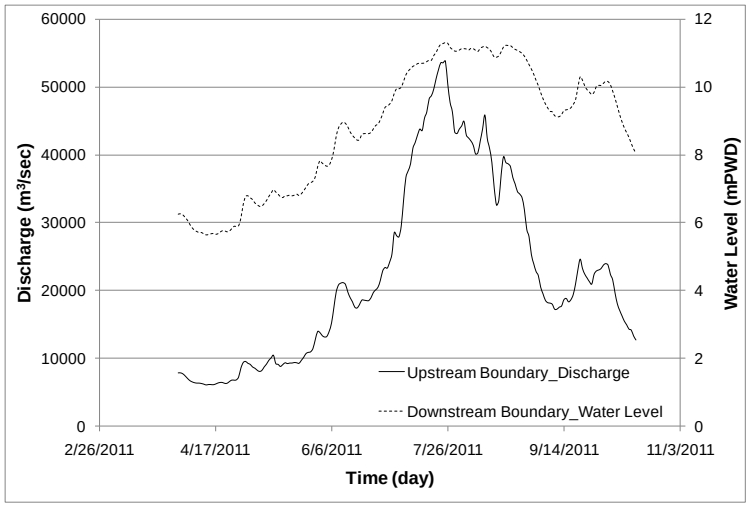

Figure 3: Time series hydrographs from April to October 2011 used in the model as Boundary Conditions for Validation Period

5. CALIBRATION AND VALIDATION

Initially the sensitivity of the model has been analysed to concentrate on the influential parameters that impact the calibration in order to determine the models performance.

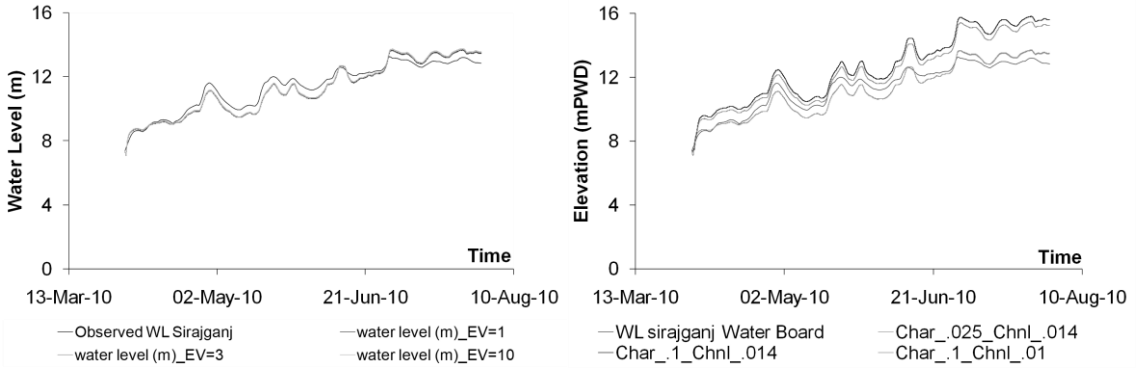

Figure 4: Influence of Manning parameter and Eddy viscosity on amplitudes of water level

The developed Delft3D model was calibrated using water level as the parameter for calibration. Data has been collected from IWM. The model was calibrated by using the observed water level elevation data at Shirajganj station. The calibrated model, performed fairly well with the measured water level.

In order to examine the range of validity of the calibrated model, the simulated results have been compared with the observed data without adjusting the values of calibration parameters. The simulated and observed water level showed quite good agreement with slight variation.

Roughness and eddy viscosity were the parameters that have been used as a trial to obtain suitable match with the observed field condition. Manning's roughness co-efficient was adjusted with the varying water depth i.e. n=.014, when water depth was lower than 6m and n=.025, when water depth was higher than 6m. The value of eddy viscosity was considered 1.

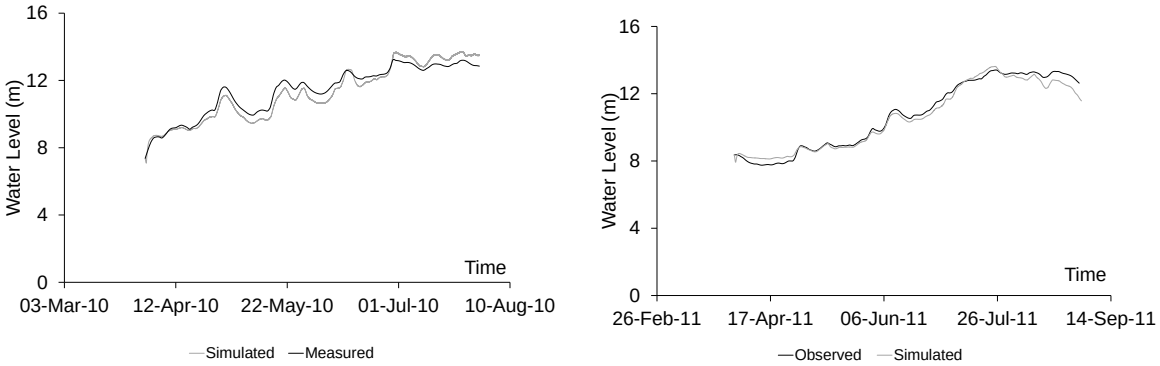

Figure 5: Simulated and measured water levels of Jamuna River for calibration and validation at Shirajganj

6. RESULTS AND DISCUSSIONS

The next step involved was running the model successfully for the whole year and to compare it with observed bed level data of December 2010. Bathymetry of April 2010 has been taken as base for simulation.

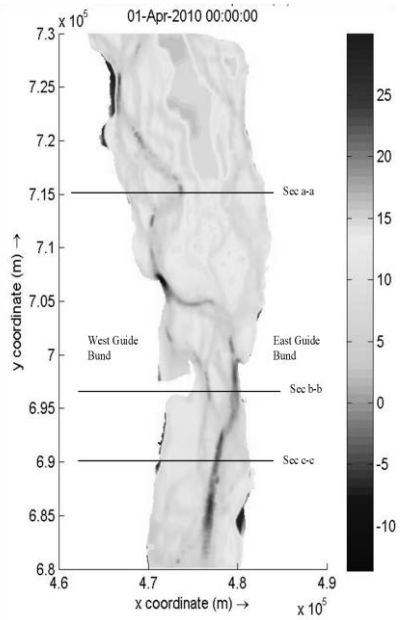

Figure 6: Cross Sections shown in Bathymetry of selected reach of the Jamuna River for comparison

The simulated bed level data presented in this study have not been quantitatively verified due to the scarcity of observed data. However, the ranges of simulated results seem to be reasonable and consistent with the observed one. Comparisons of the simulated bed level against the observed one at various sections of December 2010 are shown in Figure 7.

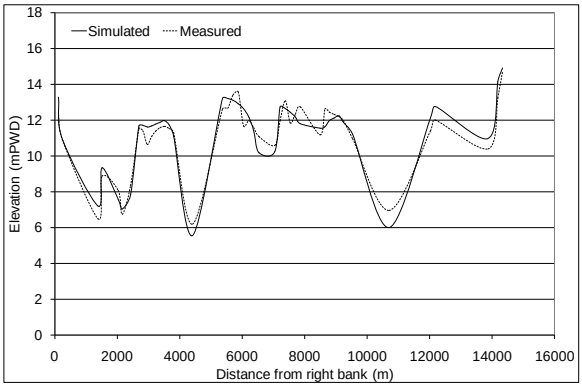

(a) Sec a-a

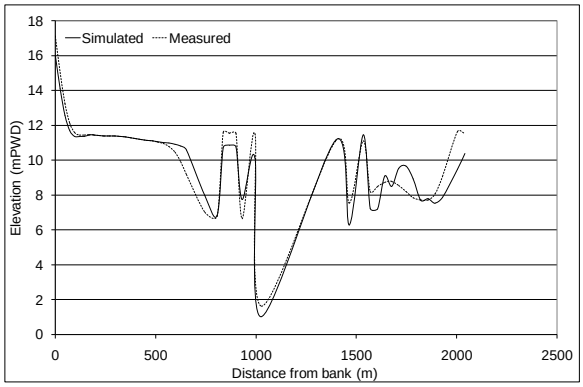

(b) Sec b-b

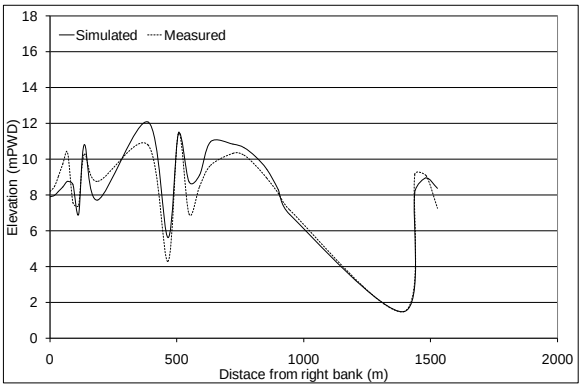

(c) Sec c-c

Figure 7: Comparison of Cross-Sections

Overall, this study was mainly focused on the calibration and validation processes, which showed quite satisfactory results and the morphological assessment has been done successfully. Thus, this model can be applied for further development and/or future interventions in the Jamuna River.

7. CONCLUSIONS

Two-dimensional (2D) depth averaged model has been developed for the Jamuna River. Calibration and validation of the model shows significant compliance with the observed data against water surface elevations at Sirajganj. Only the high flow data has been considered as most of the morphological activities occur during this period. Model results are generated for bed level and water level at various locations. Further use of this model is to assess the morphological changes such as erosion or sedimentation of the river, relation between the sediment transport and depth average velocity as well as shifting process of river course. Through the application of this model, the change in river behaviour under different scenarios can also be assessed for proper planning of any development project on Jamuna River.

ACKNOWLEDGEMENTS

Authors are gratefully acknowledging the cooperation rendered by Bangladesh Water Development Board (BWDB) (IWM) for providing the necessary data for this study. Also special thanks to Deltares for making Delft open source which has been applied on this study.

REFERENCES

Bayes, A. (2007). Impact assessment of Jamuna Multipurpose Bridge Project (JMBP) on poverty reduction. *Department of Economics, Jahangirnagar University. Savar, Bangladesh*.

Bhuiyan, M. A., Rakib, M. A., Takashi, K., Rahman, M. J. J., & Suzuki, S. (2010). Regulation of Brahmaputra-Jamuna River around Jamuna Bridge Site, Bangladesh: Geoenvironmental Impacts. *Journal of Water Resource and Protection*, *2*(02), 123.

Baki, A. B. M., & Gan, T. Y. (2012). Riverbank migration and island dynamics of the braided Jamuna River of the Ganges–Brahmaputra basin using multi-temporal Landsat images. *Quaternary International*, *263*, 148-161.

Jagers, H. R. A. (2003). *Modelling planform changes of braided rivers*. University of Twente.

Mosselman, E. (2009). Bank protection and river training along the braided Brahmaputra-Jamuna River, Bangladesh. *Braided Rivers: Process, Deposition, Ecology and Management, edited by: Smith, GHS, Best, JL, Bristow, CS, and Petts, GE, Blackwell, Oxford, UK*, 277-287.

Mount, N. J., Tate, N. J., Sarker, M. H., & Thorne, C. R. (2013). Evolutionary, multi-scale analysis of river bank line retreat using continuous wavelet transforms: Jamuna River, Bangladesh. *Geomorphology*, *183*, 82-95.

Marra, W. A., Kleinhans, M. G., & Addink, E. A. (2014). Network concepts to describe channel importance and change in multichannel systems: test results for the Jamuna River, Bangladesh. *Earth Surface Processes and Landforms*, *39*(6), 766-778.

Uddin, M. N., & Rahman, M. M. (2012). Flow and erosion at a bend in the braided Jamuna River. *International Journal of Sediment Research*, *27*(4), 498-509.

CHANGING PATTERN OF THE SHORELINE GEOMETRY AS OBSERVED IN CHITTAGONG DISTRICT

Reaz A Mullick*[1] and Ashraful Islam[2]

[1] Professor, Chittagong University of Engineering and Technology (CUET), Bangladesh, e-mail: reazmullick@cuet.ac.bd
[2] Research Assistant, Chittagong University of Engineering and Technology (CUET), Bangladesh, e-mail: ashraful.cuetbd@gmail.com

ABSTRACT

In this research, the dynamicity of the shoreline geometry of Chittagong district of Bangladesh is unveiled in terms of temporal and spatial change. The shoreline is divided into three segments according to their three different spatial distributions. Multi temporal LANDSAT images were used to monitor shoreline positional change from the year 1977 to 2017. LANDSAT images were radiometrically corrected and McFeeters' normalized difference water index (NDWI) was calculated to effectively differentiate water and land features. A histogram based thresholding method along with scene based visual interpretation was used to extract the shorelines. Linear Regression Rate (LRR) was calculated for determining shoreline rate-of-change . Analysis based on the images of last 40 years shows that, the shoreline is shifting towards landward in the entire study area with different rates. In the northern segment, the average rate is 2.56 m/yr. More than 3.36 km^2 land area was withdrawn and 1.76 km^2 land area was gained. In the middle segment, the rate of shoreline shifting is 6.01 m/yr and more than 2.9 km^2 area was lost. No significant land area is gained. In the southern segment, the average shifting rate of 4.37 m/yr is seen landwards and more than 6.4 km^2 area was lost. Little over 0.17 km^2 land area was gained. Overall, for the last 40 years, a 12.66 km^2 land area withdrawn and 1.93 km^2 land area loss are observed along the shoreline of Chittagong district.

Keywords: *Shoreline Change Rate, Chittagong, Remote Sensing, Weighted Linear Regression*

1. INTRODUCTION

Shoreline is a line that coincides with the physical interface of land and sea or other water feature (Dolan et al., 1980). While conducting any analysis on the shoreline or its geometry, it must be considered in a temporal sense, and the time scale chosen will depend on the context of the investigation (Boak and Turner, 2005). In their paper, Boak and Turner also commented that Remote Sensing (RS) is becoming popular now-a-days to detect shoreline using multispectral and hyper-spectral satellite imaging and being widely used globally by many scientists and researchers which is evident in the works of Li and Damen, 2010, Alesheikh, Ghorbanali and Nouri, 2007, Bouchahma and Yan, 2012, Kuleli, et al., 2011, Siripong, 2010 etc. RS along with Geographic Information System (GIS) technologies are used to determine the dynamic nature of shore as well as to detect and monitor temporal and spatial change of an existing water feature (Erener and Yakar, 2012). RS and GIS were also used by Mukhopadhyay et al., 2012 to detect and analyze shoreline where they used multi temporal LANDSAT images from United States Geological Survey (USGS) agency. In this study, remotely sensed satellite LANDSAT images were used to detect shoreline position of Chittagong coastal zone of Bangladesh in different years. These orthorectified and radiometrically corrected images are used in this study furthermore to determine the shoreline geometry and their change rate in a temporal basis. It is noted that a shoreline of a coastal zone has a dynamic environment where shoreline can change due to various factors such as coastal erosion and deposition, tides, storms, biological activities and man-made causes (Kostiuk, 2002).

The shoreline of Bangladesh is of dynamic in nature. As there is a lack of steadiness, the conception that a rising sea-level with global warming will submerge Bangladesh's coastal area is somewhat an exaggerated statement (Brammer, 2013). A systematic assessment of rates of shoreline change of Bangladesh over a 20-year period from 1989 to 2009, using LANDSAT satellite images were performed by Sarwar and Woodroffe, 2013. They concluded that, the seaward margin of the Sundarbans in western Bangladesh has retreat rates of up to 20 m/yr. In the Noakhali-Feni coastal zone, rates of erosion were balanced by rapid accretion of the main promontory by more than 600 m/yr. Meghna estuary was especially dynamic with land deposition trend. Rates of change were more subdued in the Chittagong and Cox's Bazaar coastal zones of southeast Bangladesh. The overall area changed relatively little across the entire coastline over the 20-year period with land gain of up to 315 km^2, countered by land loss of about 307 km^2. So there is net overall land gain observed all over in Bangladesh.

However the methods used for shoreline change detection for Bangladesh were based on End Point Rate (EPR) statistics which only considers two shoreline locations: the oldest and the newest. But keeping in mind the dynamicity of the coastal Bangladesh, several temporal images should be used to detect short term changes. Regression techniques were used in the works of Dolan, Fenster and Holme, 1991 and Genz et al., 2007 to determine shoreline change rate where they considered several shorelines of the same area of interest but different years. In this study the shoreline change is determined using both EPR and Linear Regression Rate (LRR) methods. These methods are utilized vitally in shoreline change statistics calculation in the works of Bouchahma and Yan, 2012, Oyedotun, 2014, Kuleli et al., 2011 etc. In this study, Linear Regression Rate has been considered to detect the change statistics of the shoreline geometry of coastal Chittagong and based on the rate a crude prediction for the year 2050 has been made.

2. METHODOLOGY

In order to conduct the study, it was necessary to detect shoreline boundary. First of all, subset of the raw satellite imagery was taken so that it falls within the area of interest (Bouchahma and Yan, 2012). Then the radiometric correction of the image was done to convert the raw Digital Number (DN) to Top of Atmospheric (ToA) Reflectance (Chander, Markham and Helder, 2009) and Mcfeeters Normalized Difference Water Index (NDWI) was calculated from it (Mcfeeters, 1996). After that, Otsu's Binary Thresholding Method was applied to form a binary image which facilitated to segregate water feature from non-water feature (Otsu, 1979). As a result, the coinciding line with the physical interface of water and non-water feature was extracted as shoreline (Boak and Turner, 2005). All of the temporal images were processed using the above method to extract shoreline. After that, cell to cell comparison was made to detect the extent of spatial land area withdrawal and gain (Bouchahma and Yan, 2012). Digital Shoreline Analysis System (DSAS) (an ArcGIS extension) was used to measure change statistics of the shorelines linear regression method (Thieler et al., 2017).

2.1 Study area and data

Chittagong district of Bangladesh is selected as study area to see the shoreline geometry in terms of temporal and spatial change. The shoreline is divided into three segments according to their three different spatial distributions based on the confluence of the Karnafuli and the Shangoo River with the Bay of Bengal, namely, northern segment, in the north part of Karnafuli, middle segment, in the middle of Karnafuli and Shangoo and southern segment situated in the south of Shangoo. They are designated as A, B and C in figure 1. These segments represent 3 sites of Chittagong district namely Chittagong Town, Anowara and Banshkhali respectively.

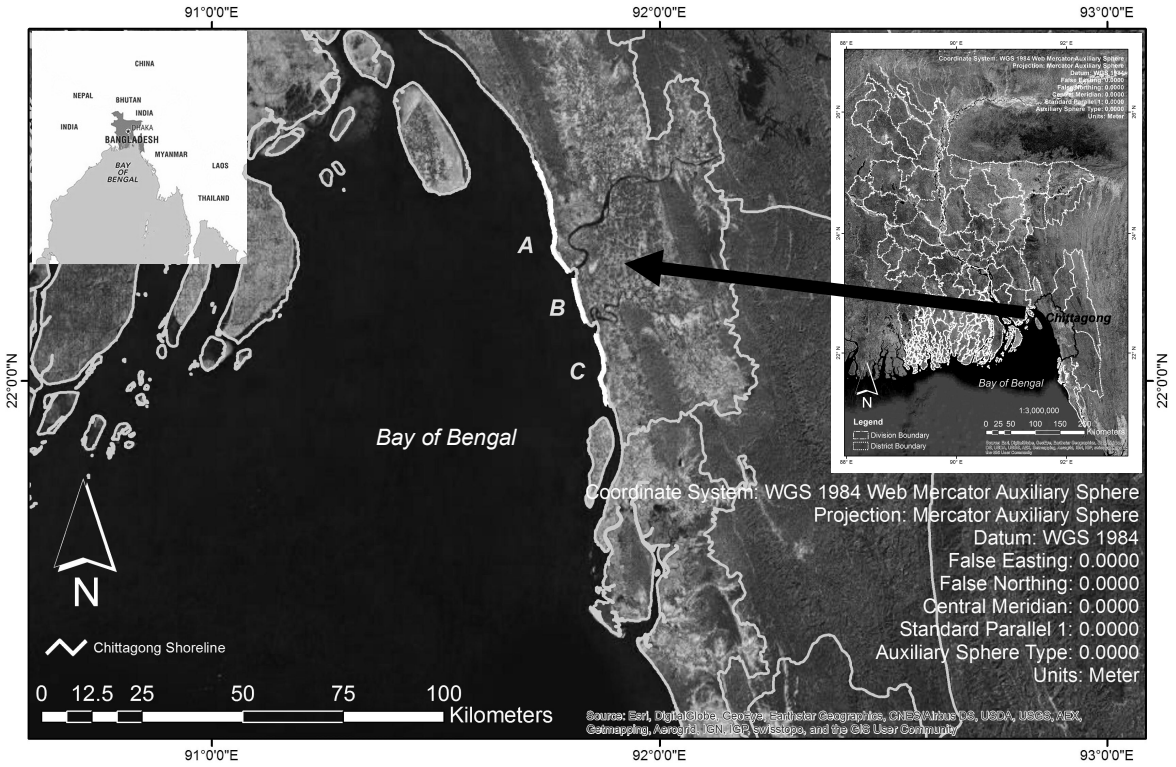

Figure 1: Location of the study area

Multi temporal LANDSAT images were used to monitor shoreline positional change from the year 1977 to 2017. LANDSAT satellite images are generated from the MSS, TM, ETM and OLI sensor platforms which collect different reflected spectral bands of lights from the earth objects (Chander, Markham and Helder, 2009). These LANDSAT images were acquired from the USGS (United States Geological Survey) website (https://earthexplorer.usgs.gov/) which provides NASA (National Aeronautics and Space Administration) archived LANDSAT images (USGS, 2017). The images were selected considering the acquisition date of the data. The dry season of Bangladesh, typically late winter season most likely has less cloud cover (table 1) and for analyzing images sits in a quite favorable condition (Queensland Government, 2007). The properties of the satellite images are given in table 1.

Table 1: Properties of LANDSAT satellite images used in the study

Respective year	Date Acquired (M/D/Y)	Sensor	Path/Row	Land Cloud Cover	Spatial Resolution	Projected Co-ordinate system
1977	01/02/1977	LANDSAT_2 MSS	146/45	0.00	60m	WGS_1984 _46N
1980	01/14/1980	LANDSAT_3 MSS	146/45	0.00	60m	WGS_1984 _46N
1988	02/12/1988	LANDSAT_5 TM	136/45	1.00	30m	WGS_1984 _46N
1993	01/24/1993	LANDSAT_5 TM	136/45	0.00	30m	WGS_1984 _46N
1997	01/19/1997	LANDSAT_5 TM	136/45	0.00	30m	WGS_1984 _46N
2002	02/26/2002	LANDSAT_7 ETM	136/45	0.00	30m	WGS_1984 _46N
2007	02/24/2007	LANDSAT_7 ETM	136/45	0.00	30m	WGS_1984 _46N

Respective year	Date Acquired (M/D/Y)	Sensor	Path/Row	Land Cloud Cover	Spatial Resolution	Projected Co-ordinate system
	01/23/2007*	LANDSAT_7 ETM	136/45	1.00	30m	WGS_1984 _46N
2014	01/02/2014	LANDSAT_8 OLI	136/45	0.07	30m	WGS_1984 _46N
2017	01/02/2017	LANDSAT_8 OLI	136/45	0.01	30m	WGS_1984 _46N

*The Landsat 7 images of the year 2007 have data gaps due to problem with scan line corrector. The data gap was masked using another image of the same acquisition year (Yin et al., 2017). The image denoted by the asterisk is used to fill gaps of the other one.

2.2 Image pre-processing and radiometric correction procedure

The LANDSAT satellite images were provided with pixel values representing digital numbers (DN) which were required radiometric correction for better accuracy and scientific analysis as mentioned by Chander et al., 2009 (figure 2a). Moreover, in order to calculate NDWI, DN has to be converted to ToA reflectance for better performance and is proven in the works of (Alesheikh et al., 2007), (Zhai et al., 2015), (Haque and Basak, 2017), (Gao, 1996) etc. For LANDSAT MSS, TM and ETM sensor derived images, Chander, 2009 suggested to convert DN to Radiance using the following formula:

$$L_\lambda = \left(\frac{LMAX_\lambda - LMIN_\lambda}{Q_{calmax} - Q_{calmin}}\right)(Q_{cal} - Q_{calmin}) + LMIN_\lambda$$

Or,

$$L_\lambda - G_{rescale} \times Q_{cal} + B_{rescale}$$

And Radiance is converted to ToA reflectance using the following formula:

$$\rho_\lambda = \frac{\pi \cdot L_\lambda \cdot d^2}{ESUN_\lambda \cdot \cos\theta_s}$$

For LANDSAT OLI images ToA reflectance can be converted from DN using the following formula directly (U.S. Geological Survey, 2016):

$$\rho_\lambda = \frac{M_p \times Q_{cal} + A_p}{\sin\theta_E}$$

The values of Q_{cal} Q_{calmin} Q_{calmax} $LMIN_\lambda$ $LMAX_\lambda$ θ_E M_p A_p are provided with the LANDSAT image in a metadata file. d, $ESUN_\lambda$ both are calculated using the earth sun distance chart and mean exoatmospheric solar irradiance chart provided by Chander, 2009. All the images used were level 1 data product, so they were already orthorectified, geometrically corrected and co-registered. The formula incorporates sun angle correction too. Figure 2b shows the resulting change of pixel values from conversion of DN to ToA reflectance.

Here,

$$G_{rescale} = \frac{LMAX_\lambda - LMIN_\lambda}{Q_{calmax} - Q_{calmin}}$$

$$B_{rescale} = LMIN_\lambda - \left(\frac{LMAX_\lambda - LMIN_\lambda}{Q_{calmax} - Q_{calmin}}\right) Q_{calmin}$$

Where,

L_λ = Spectral radiance at the sensor's aperture [W / (m^2 sr μm)]

Q_{cal} = Quantized calibrated pixel value [DN]

Q_{calmin} = Minimum quantized calibrated pixel value corresponding to $LMIN_\lambda$ [DN]

Q_{calmax} = Maximum quantized calibrated pixel value corresponding to $LMAX_\lambda$ [DN]

$LMIN_\lambda$ = Spectral at-sensor radiance that is scaled to Q_{calmin} [W / (m^2 sr μm)]

$LMAX_\lambda$ = Spectral at-sensor radiance that is scaled to Q_{calmax} [W / (m^2 sr μm)]

$G_{rescale}$ = Band-specific rescaling gain factor [W / (m^2 sr μm) / DN]

$B_{rescale}$ = Band-specific rescaling bias factor [W / (m^2 sr μm)]

ρ_λ = Planetary ToA reflectance [unitless]

π = Mathematical constant equal to ~3.14159 [unitless]

d = Earth–Sun distance [astronomical units]

$ESUN_\lambda$ = Mean exoatmospheric solar irradiance [W / (m^2 μm)]

θ_s = Solar zenith angle [degrees] *sin will be used for using elevation angle (θ_E)

θ_E = Solar elevation angle [degrees]

M_p = Reflectance multiplicative scaling factor for the band [unitless]

A_p = Reflectance additive scaling factor for the band [unitless]

2.3 Spectral index:

There are many Remote Sensing Based Water Feature Indices to delineate water and non water features such as Normalized Difference Water Index (NDWI) (Mcfeeters, 1996), (Gao, 1996), Normalized Difference Moisture Index (NDMI) (Wilson and Sader, 2002), Modified Normalized Difference Water Index (MNDWI) (Xu and Xulin, 2014), Water Ratio Index (WRI) (Shen and Li, 2010), Normalized Difference Vegetation Index (NDVI) (Rouse et al., 1973), Automated Water Extraction Index (AWEI) (Feyisaa et al., 2014) etc. Because multi-temporal sattelite LANDSAT images were used in this study a suitable index had to be chosen that uses the band common in all historical and current sensors (MSS, TM, ETM, OLI). Though both the Mcfeeters, 1996 NDWI and NDVI index is calculated using Green and Near Infrared band of the sattelite image which are common bands attainable by all LANDSAT sensors (Khorram et al., 2012), the NDWI proposed by (Mcfeeters, 1996) is best for delineating water features with great accuracy (Mcfeeters, 2013) and also the result of Comparison of NDWI Results between Theoretical and Manually Adjusted Threshold proves to be most accurate than other mentioned indices (Das and Pal, 2016). The ToA reflectance of Green and Near Infrared band of the sattelite images were used for calculating Mcfeeters NDWI (Mcfeeters, 1996). It is calculated using the following formula:

$$\mathrm{NDWI} = \frac{\mathrm{Green}_{\mathrm{ToA}} - \mathrm{NIR}_{\mathrm{ToA}}}{\mathrm{Green}_{\mathrm{ToA}} + \mathrm{NIR}_{\mathrm{ToA}}}$$

Here,

$\mathrm{Green}_{\mathrm{ToA}}$ = Top of atmospheric (ToA) reflectance of green band

$\mathrm{NIR}_{\mathrm{ToA}}$ = Top of atmospheric (ToA) reflectance of near infrared band

The NDWI image gives a value ranges from +1 to -1 where typically the positive value represents water and the negative value represents non-water feature as described by Mcfeeters in 1996 (figure 2c).

2.4 Segregation of water and non-water feature:

The NDWI image typically gives positive result for water feature and negative for non-water feature (Mcfeeters, 1996). But it is scene specific and a histogram based thresholding is necessary to create a binary image (0 and 1) depicting water and non water feature (Ji, Zhang, and Wylie, 2009). Binary threshold segmentation method of (Otsu, 1979) was applied on the NDWI images to separate the land from the sea (figure 2d). The threshold calculated automatically to divide the image into two main segment water and land. This segmentation gave improved accuracy for shoreline extraction as the value of the threshold presented by Otsu is set according to the local characteristics (Bouchahma and Yan, 2012). The MSS images had a spatial resolution of 60m (table 1) which were re-sampled to 30m to match with other sensor provided images.

2.5 Post processing of binary raster image

Some isolated pixels that differ from surrounding pixels were generalized by filtering. A 3 × 3 mode filter has been applied for this post-processing operation that replaced the isolated pixels to the most common neighboring class (either water class or non water class) (Ahmed and Ahmed, 2012) (Bartuś, 2014). The jagged boundaries of the water and non water classes were smoothened by using boundary clean tool that eliminates less significant groups of pixels creating small-surfaces (Bartuś, 2014). Raster binary image was then converted to vector and the abutting line of water and non water class was traced to extract final shoreline (figure 2e). Some of the line features were manually manipulated so that it coincides with the actual real time shoreline and this was performed using visual interpretation of RGB raster imagery.

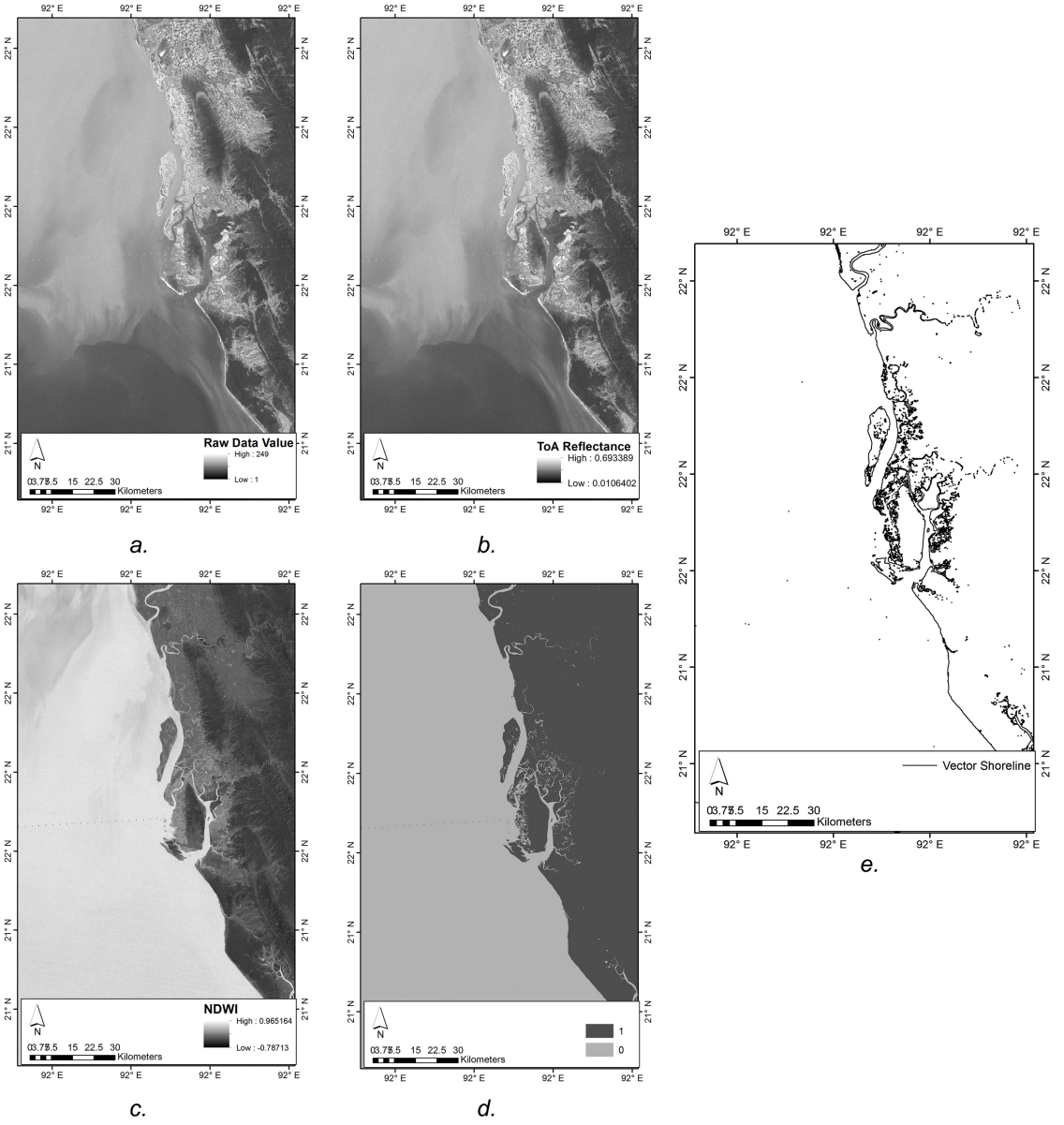

Figure 2: The resulting output from applying the methodological workflow. [a.] The raw LANDSAT satellite image derived from USGS containing DN values; [b.] The corrected image from converting DN to ToA reflectance; [c.] NDWI image derived by applying the Mcfeeteres formula; [d.] Obtained binary image by applying Otsu's Binary Thresholding formula (1=Land and 0=water); [e.] Vector line data representing shoreline

2.6 Statistical parameters used:

Digital Shoreline Analysis System (DSAS) were used to perform change statistics calculation (Thieler et al., 2017) which is capable of calculating Shoreline Change Envelope (SCE) considering 9 points, Net Shoreline Movement (NSM), End Point Rate (EPR) and Linear Regression Rate (LLR). These parameters are widely used in shoreline statistics (Dolan, Fenster and Holme, 1991), (Genz et al., 2007) and DSAS is capable of calculate them automatically. 9 shoreline of the same area for different years were considered. 50m spaced and 1km long transect lines were casted from offshore to landward from a baseline situated 200m Off Coast. +/- 5m uncertainty and 95% confidence interval was set as default parameter to calculate change statistics. DSAS generates transects that are cast

perpendicular to the baseline at a user-specified spacing along-shore (figure 3). The transect shoreline intersections along this baseline are then used to calculate the rate-of-change statistics (Bouchahma and Yan, 2012).

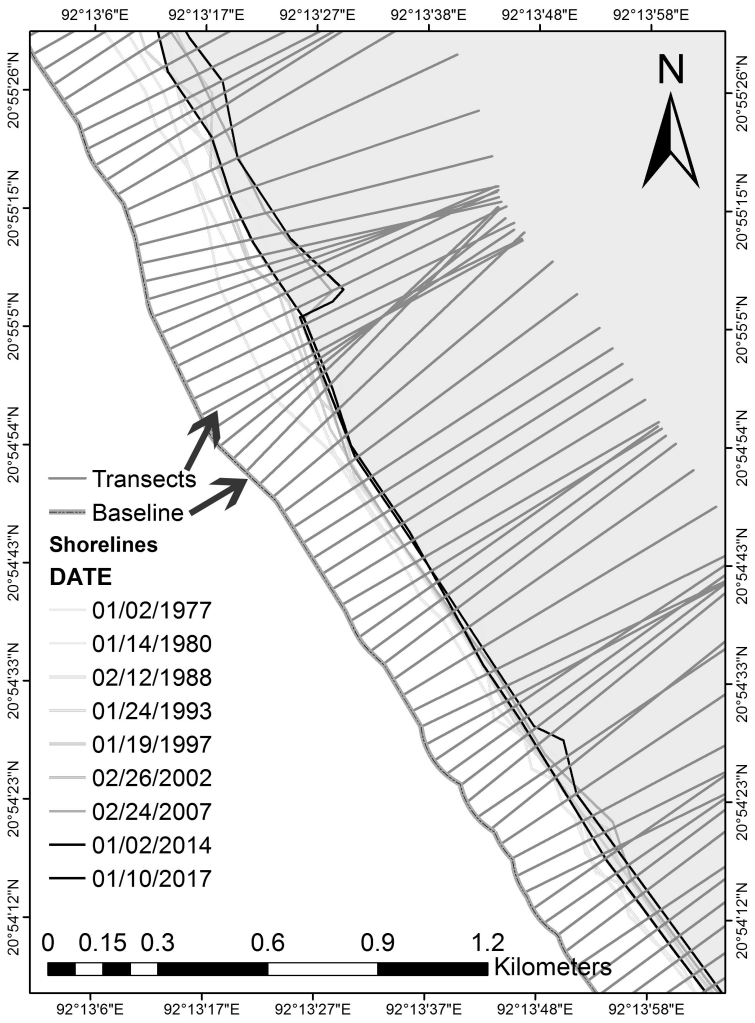

Figure 3: The distances from the baseline to each intersection point along a transect are used to compute EPR and LRR statistics

2.7 Land loss and gain calculation:

The differences of the values of the two binary thresholded images were made using Raster Calculator in ArcGIS to determine the land loss and gain value within the two designated years. It is a simple yet effective change detection method used by (Bouchahma and Yan, 2012) and (Kuleli et al., 2011). For both the images, Water class was reclassified to value 2 and non-water class was reclassified to value 1. The resulting image difference gives values 0, -1 and +1 result. The image differenciation were done using ArcGIS software. From the attribute table, the pixel counts were converted to square kilometers and land withdrawal and land deposition for two different years were computed.

3. RESULTS AND DISCUSSION

The SCE is the distance between the Coastline farthest from and closest to the baseline at each transect between the study time period. It doesn't represent rate. The result shows that in segment A the shoreline has moved farthest in the Beribadh Area near Patenga which is

more than 700 meters (figure 4). Shoeline movement is less significant in segment B and C, although the northern most part of segment C shows some significant movement throughout the study time period.

NSM Reports the distance between the oldest and youngest Coastlines for each transect. It indicates the shifting towards either land or sea. In segment A, Beribadh Area near Patenga has almost 400m landward shifting whereas the same area near norththern Zeley Para shows 600m seaward shifting. Other parts of the B and C segments shows less significant shifting of shoreline (figure 4).

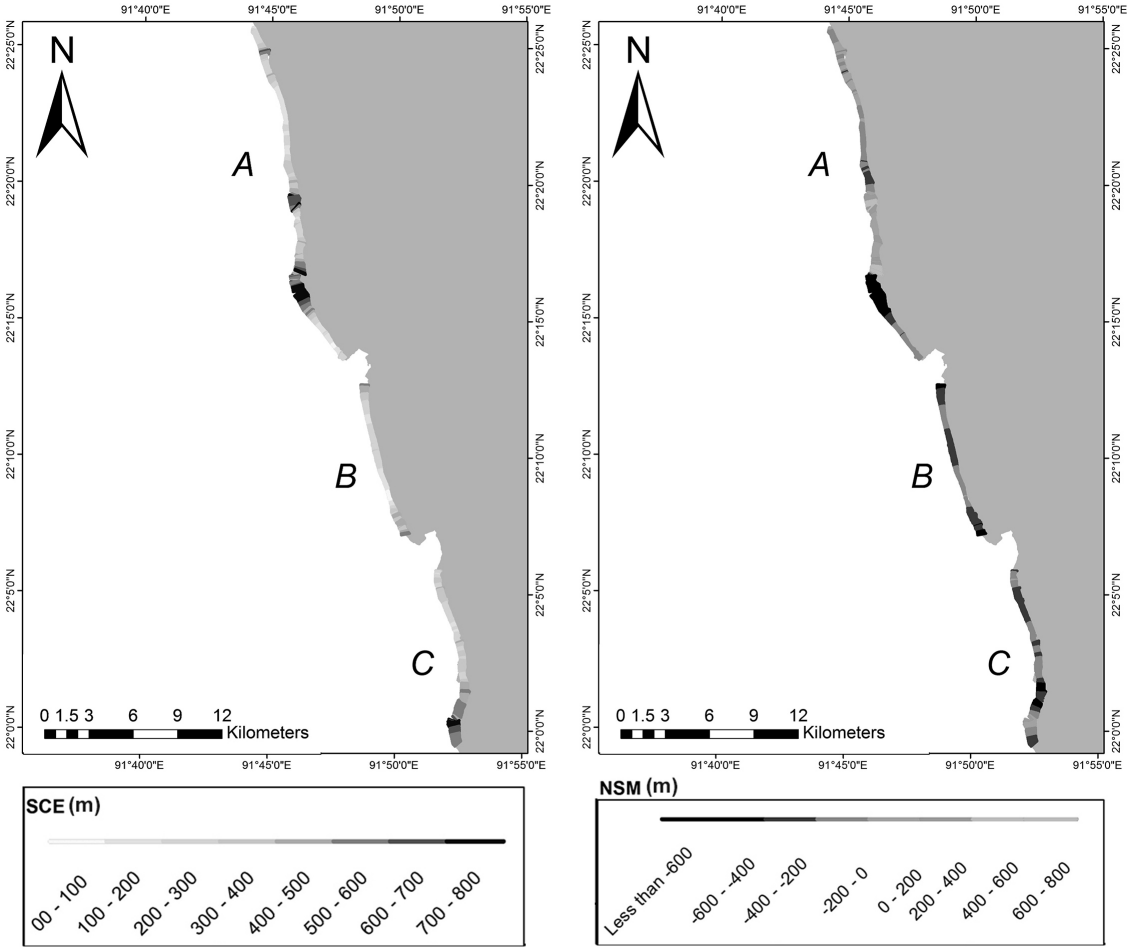

Figure 4: Shoreline Change Envelope (SCE) and Net Shoreline Movement (NSM) (values are in meter)

In this study the rate of change statistics was calculated using LRR method. Additionally EPR was calculated to compare the results. LRR considers all the 9 year's shoreline position whereas EPR considers only the youngest and the oldest (Thieler et al., 2017). As a result, in terms of accuracy, the performance of LRR is superior to EPR. Still, both has been calculated and plotted in graph. Graphically, the results seem quite similar. In segment A, both seaward and landward shifting trend of the shoreline is observed. Seaward shifting rate is high in the Zeley Para Beribadh Area (>16 m/yr) and landward shifting rate is high near Patenga Beach area (>18 m/yr). Segment B shows somewhat low landward shifting rate in Anowara area. Segment C also follows somewhat similar trend in Banshkhali area although in the southern part, some seaward shifting is seen near Maheshkhali. EPR and LRR shows

an average difference of 0.3m (figure 5). Overall in Chittagong, landward shifting of shoreline is significant in all the segments.

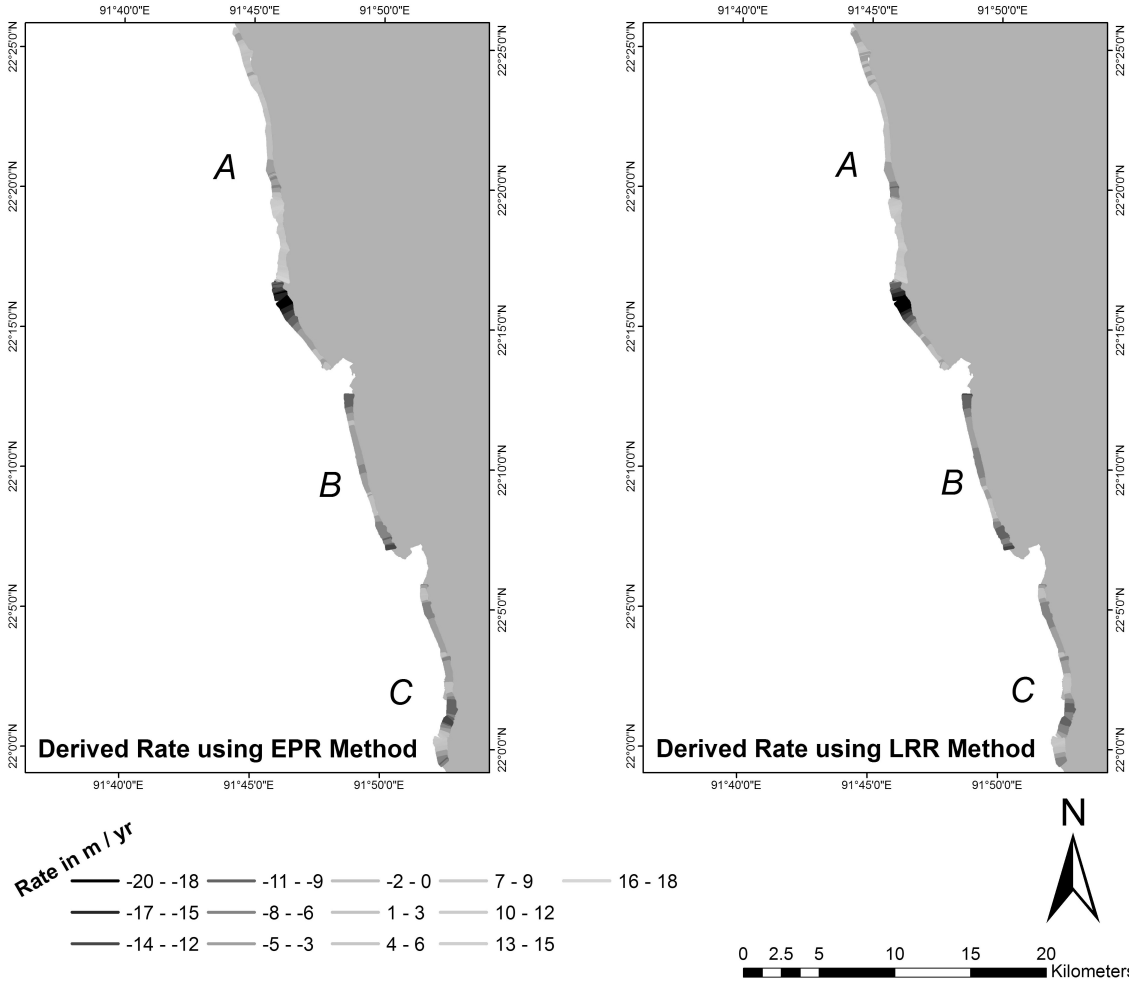

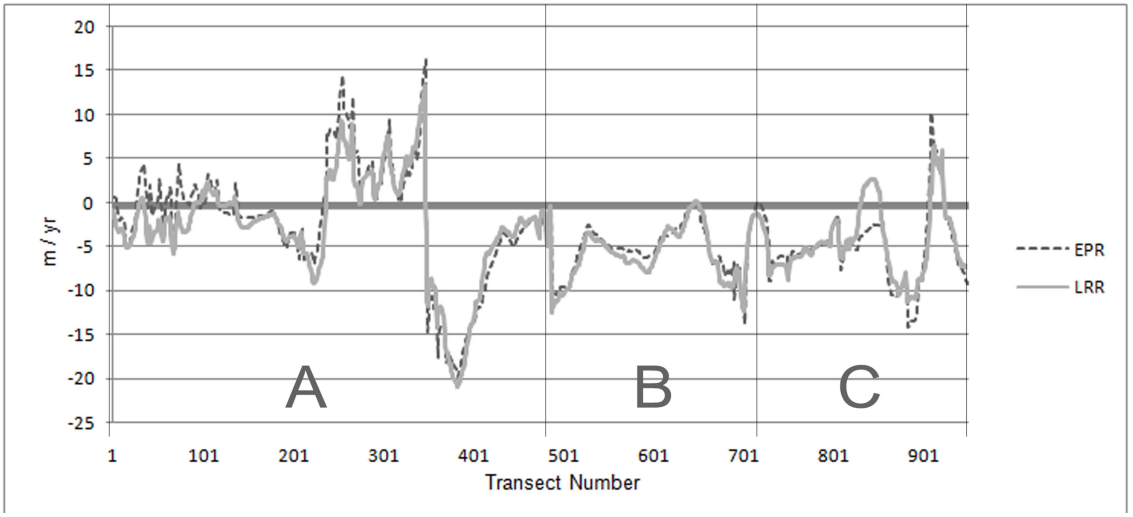

Figure 5: The resulted rates of shoreline changes (land withdrawal or deposition) estimated at each transect are plotted alongshore of the study area

Analysis based on the calculation of land area geometry shows that, the shoreline is shifting towards landward in the entire study area with different rates. In the northern segment, the

average rate is 2.56 m/yr. More than 3.36 km^2 land area was withdrawn and 1.76 km^2 land area was gained. In the middle segment, the rate of shoreline shifting is 6.01 m/yr and more than 2.9 km^2 area was lost. No significant land area is gained. In the southern segment, the average shifting rate of 4.37 m/yr is seen landwards and more than 6.4 km^2 area was lost. Little over 0.17 km^2 land area was gained. Overall, for the last 40 years, a 12.66 km^2 land area withdrawn and 1.93 km^2 land area loss are observed along the shoreline of Chittagong district. The results are summarized in table 2.

Table 2: Change Statistics and Loss-gain results

Segment	EPR Method Average Rate (m / yr)	LRR Method Average Rate (m / yr)	Net Land Area (sq km) loss (1977-2017)	Net Land Area (sq km) gain (1977-2017)	Total
A	-1.7995	-2.557	3.356	1.768	-1.588
B	-5.430	-6.012	2.902	0	-2.902
C	-4.825	-4.371	6.418	0.175	-6.243
Grand Total					**-10.733**

Using the LRR method, the rate derived was also used to depict a crude picture of the shoreline position in the year 2050. The distance from the current shoreline and future shoreline position was used to calculate the predicted land area loss and gain. In segment A, 1.01 km^2 of land area will be gained and 2.43 km^2 of land area will be withdrawn. So, overall, 2.43 km^2 of land area will be lost. No land area will be gained in segment B and 2.5 km^2 of land area will be lost. In segment C, 1.22 km^2 of land area will be deposited and a massive 7.85 km^2 of land area will be extincted (figure 6).

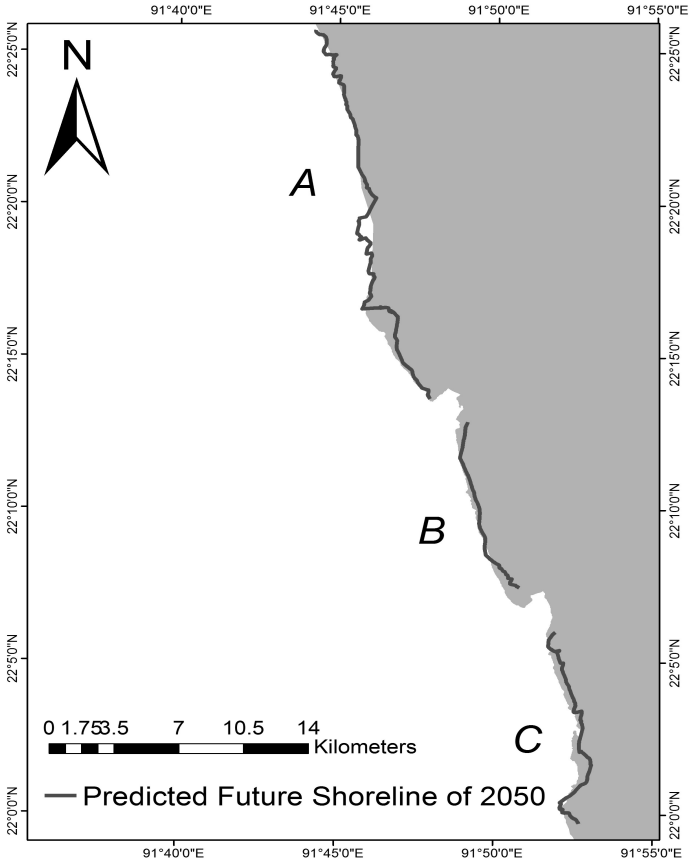

Figure 6: Predicted shoreline for the year 2050

4. CONCLUSION

The historical evolution and temporal morphodynamics of shoreline position and geometry are of significant importance in evaluating the spatial dynamics of the coastal system behaviour (Oyedotun, 2014). The study is aimed towards the development of a method for automatic measurement of shoreline changes of Chittagong coastal region using LANDSAT data and hence indicating the dynamics and trend in change in shoreline geometry. Overall, landloss is more prominent in Chittagong and the trend of landward movement of the coastline in different segments indicates sea level rise is at motion. However, land gain has been remarkable around the area of Beribadh, Zeley Para and also in the south part of Banshkhali area. It is noteworthy that the statement of the extent of sea level rise will submerge Bangladesh's coastal area (Brammer, 2013) is somewhat an exaggerated statement which is proved by the prediction of shoreline for Chittagong. This study points out the areas that need special consideration while making zoning plan or other structure plan. It is also important to keep monitor the changes around the potential land loss prone areas and take in consideration these changes on the future urban and tourism planning.

ACKNOWLEDGEMENTS

This research work was funded by *Directorate of Research and Extension, Chittagong University of Engineering and Technology, Chittagong-4349, Bangladesh*. We express our gratitude to our colleagues from *Chittagong University of Engineering and Technology* who provided intuition and adroitness that tremendously supplemented the research.

REFERENCES

Ahmed, B., and Ahmed, R. (2012). Modeling Urban Land Cover Growth Dynamics Using Multi-Temporal Satellite Images: A Case Study of Dhaka, Bangladesh. *International Journal of Geo-Information , 1*, 3-31.

Alesheikh, A. A., Ghorbanali, A., and Nouri, N. (2007). Coastline change detection using remote sensing. *International Journal of Environmental Science and Technology , 4* (1), 61-66.

Bartuś, T. (2014). Raster images generalization in the context of research on the structure of landscape and geodiversity. *Geology, Geophysics and Environment , 40* (3), 271–284.

Boak, E. H., and Turner, I. L. (2005). Shoreline Definition and Detection: A Review. *Journal of Coastal Research , 21* (4), 688–703.

Bouchahma, M., and Yan, W. (2012). Automatic Measurement of Shoreline Change on Djerba Island of Tunisia. *Computer and Information Science , 5* (5), 17-24.

Brammer, H. (2013). Bangladesh's dynamic coastal regions and sea-level rise. *Climate Risk Management , 1*, 51-62.

Chander, G., Markham, B. L., and Helder, D. L. (2009). Summary of current radiometric calibration coefficients for Landsat MSS, TM, ETM+, and EO-1 ALI sensors. *Remote Sensing of Environment, 113*, 893–903.

Das, R. T., and Pal, S. (2016). IDENTIFICATION OF WATER BODIES FROM MULTISPECTRAL LANDSAT IMAGERIES OF BARIND TRACT OF WEST BENGAL. *International Journal of Innovative Research and Review , 4* (1), 26-37.

Dolan, R., Fenster, M. S., and Holme, S. J. (1991). Temporal analysis of shoreline recession and accretion. *Journal of Coastal Research , 7*, 723-744.

Dolan, R., Hayden, B. P., May, P., and May, S. K. (1980). The reliability of shoreline change measurements from aerial photographs. *Shore and Beach , 48* (4), 22–29.

Erener, A., and Yakar, M. (2012). Monitoring Coastline Change Using Remote Sensing and GIS Technologies. *International Conference on Earth Science and Remote Sensing. 30*, pp. 310-315. Hong Kong: Lecture Notes in Information Technology.

Feyisaa, G. L., Meilbya, H., Fensholtb, R., and Proudb, S. R. (2014). Automated Water Extraction Index: A new technique for surface water mapping using Landsat imagery. *Remote Sensing Environment , 140*, 25-35.

Gao, B. (1996). NDWI A Normalized Difference Water Index for Remote Sensing of Vegetation Liquid Water From Space. *Remote Sensing Environment , 58*, 257-266.

Genz, A. S., Fletcher, C. H., Dunn, R. A., and Frazer, L. (2007). The predictive accuracy of shoreline change rate methods and alongshore beach variation on Maui, Hawaii. *Journal of Coastal Research , 23* (1), 87-105.

Haque, M. I., and Basak, R. (2017). Land cover change detection using GIS and remote sensing techniques: A spatio-temporal study on Tanguar Haor, Sunamganj, Bangladesh. *The Egyptian Journal of Remote Sensing and Space Sciences* , in press.

Ji, L., Zhang, L., and Wylie, B. (2009). Analysis of Dynamic Thresholds for the Normalized Difference Water Index. *Photogrammetric Engineering and Remote Sensing , 75* (11), 1307–1317.

Khorram, S., Koch, F. H., van der Wiele, C. F., and Nelson, S. A. (2012). *Remote Sensing.* New York: Springer.

Kostiuk, M. (2002). USING REMOTE SENSINGDATA TO DETECT SEA LEVEL CHANGE. *Land Satellite Information.*

Kuleli, T., Guneroglu, A., Karsli, F., and Dihkan, M. (2011). Automatic detection of shoreline change on coastal Ramsar wetlands of Turkey. *Ocean Engineering , 38*, 1141–1149.

Li, X., and Damen, M. C. (2010). Coastline change detection with satellite remote sensing for environmenta lmanagement of the Pearl River Estuary, China. *Journal of Marine Systems , 82*, S54–S61.

Mcfeeters, S. K. (1996). The use of normalized difference water index (NDWI) in the delineation of open water features. *International Journal of Remote Sensing , 17* (7), 1425–1432.

Mcfeeters, S. K. (2013). Using the Normalized Difference Water Index (NDWI) within a Geographic Information System to Detect Swimming Pools for Mosquito Abatement: A Practical Approach. *Remote Sensing , 5*, 3544-3561.

Mukhopadhyay, A., Mukherjee, S., Mukherjee, S., Ghosh, S., Hazra, S., and Mitra, D. (2012). Automatic shoreline detection and future prediction: A case study on Puri Coast, Bay of Bengal, India. *European Journal of Remote Sensing , 45*, 201-213.

Otsu, N. (1979). A threshold selection method from gray level histograms. *IEEE Transactions on Systems, Man and Cybernetics , 9* (1), 62-66.

Oyedotun, T. D. (2014). *Geomorphological Techniques.* London: British Society for Geomorphology.

Queensland Government. (2007). *Wetland Mapping and Classification Methodology.* Queensland: Department of Environment and Heritage Protection.

Rouse, J. W., Haas, R. H., Schell, J. A., and Deering, D. W. (1973). Monitoring Vegetation Systems in the Great Plains with ERTS (Earth Resources Technology Satellite). *Third Earth Resources Technology Satellite Symposium* (pp. 309-317). Greenbelt: NASA.

Sarwar, M., and Woodroffe, C. D. (2013). Rates of shoreline change along the coast of Bangladesh. *Journal of Coastal Conservation , 17* (3), 515-526.

Shen, L., and Li, C. (2010). Water Body Extraction from Landsat ETM+ Imagery Using Adaboost. *Proceedings of 18th International Conference on Geoinformatics* (pp. 1-4). Beijing: Geographical Society of China.

Siripong, A. (2010). DETECT THE COASTLINE CHANGES IN THAILAND BY REMOTE SENSING. *International Archives of the Photogrammetry, Remote Sensing and Spatial Information Science , XXXVIII* (8), 992-996.

Thieler, E. R., Himmelstoss, E. A., Zichichi, J. L., and Ergul, A. (2017). *Digital Shoreline Analysis System (DSAS) version 4.0—An ArcGIS extension for calculating shoreline change (ver. 4.4, July 2017).* U.S. Geological Survey Open-File Report 2008-1278.

U.S. Geological Survey. (2016). *LANDSAT 8 (L8) DATA USERS HANDBOOK.* Sioux Falls: EROS.

USGS. (2017, October 25). *About USGS*. Retrieved May 2, 2017, from USGS: https://earthexplorer.usgs.gov

Wilson, E. H., and Sader, S. A. (2002). Detection of forest harvest type using multiple dates of Landsat TM imagery. *Remote Sensing of Environment , 80*, 385–396.

Xu, D., and Xulin, G. (2014). Compare NDVI extracted from Landsat 8 imagery with that from Landsat 7 imagery. *American Journal of Remote Sensing , 2* (2), 10-14.

Yin, G., Mariethoz, G., Sun, Y., and McCabe, M. F. (2017). A comparison of gap-filling approaches for Landsat-7 satellite data. *The International Journal of Remote Sensing , 38* (23), 6653-6679.

Zhai, K., Wu, X., Qin, Y., and Du, P. (2015). Comparison of surface water extraction performances of different classic water indices using OLI and TM imageries in different situations. *Geo-spatial Information Science , 18* (1), 32-42.

Proceedings of the 4th International Conference on Civil Engineering for Sustainable Development (ICCESD 2018), 9~11 February 2018, KUET, Khulna, Bangladesh (ISBN-978-984-34-3502-6)

FLUVIAL STAGE AND SEDIMENT DISHCHARGE RATING WITH POSSIBLE MAXIMUM SCOUR DEPTH PREDICTION OF A SELECTED REACH OF THE JAMUNA RIVER

Makduma Zahan Badhan[1] and Md. Abdul Matin[2]

[1] Department of Water Resources Engineering, BUET, , Bangladesh. Email: makduma.badhan10@gmail
[2] Professor, Department of Water Resources Engineering, BUET, Bangladesh.

ABSTRACT

A study has been undertaken to develop a fluvial stage-discharge rating curve for Jamuna River. Past Cross-sectional survey of Jamuna River reach within Sirajgonj and Tangail has been analyzed. The analysis includes the estimation of discharge carrying capacity, possible maximum scour depth and sediment transport capacity of the selected reaches. To predict the discharge and sediment carrying capacity, stream flow data which include cross-sectional area, top width, water surface slope and median diameter of the bed material of selected stations have been collected and some are calculated from reduced level data. A well-known resistance equation has been adopted and modified to a simple form in order to be used in the present analysis. The modified resistance equation has been used to calculate the mean velocity through the channel sections. In addition, a sediment transport equation has been applied for the prediction of transport capacity of the various sections. Results show that the existing drainage sections of Jamuna channel reach under study have adequate carrying capacity under existing bank-full conditions, but these reaches are subject to bed erosion even in low flow situations. Regarding sediment transport rate, it can be estimated that the channel flow has a relatively high range of bed material concentration. Finally, stage- discharge curves for various sections have been developed. Based on stage-discharge rating data of various sections, water surface profile and sediment-rating curve of Jamuna River have been developed and also the flooding conditions have been analyzed from predicted water surface profile.

Keywords: *Fluvial; Stage-discharge rating curve; Sediment rating curve; Water surface profile; Scour depth.*

1. INTRODUCTION

In Bangladesh, most of the river courses are of alluvial in nature. Due to their great tendency to change course, large rivers have been subject to investigation and studies. Stage, discharge and sediment transport change daily and seasonally. Changes in stage continuously influence scour and fill patterns along the channel bed as well as the magnitude of hydraulic resistance. In dealing with natural rivers with movable beds, the engineer is confronted with the problem of unavailability of stream flow data. Unless adequate discharge and sediment transport capacity data are available for performing practical engineering works, evaluation of frictional effects can be based almost upon the modified equations and developed rating relationships. Also, it is not feasible to measure the discharge everyday due to economic consideration. Thus stream flow data is not recorded regularly, instead water levels are recorded and the stream flow is deduced by means of rating curves. A rating curve is used to convert records of water level into flow rate. The flow boundary of an alluvial river is not fixed, but undergoes changes in characteristic geometry and dimensions through mutual interaction between the flow and the bed. When the discharge in an alluvial channel is low, the velocities as well as the shear stresses are small, the sediment particles remain at rest and the flow is similar to that over a rigid boundary. If the discharge is gradually increased, the velocity and shear stress also increase and a critical stage (threshold condition) is reached when the particles on bed begins move. At still higher values

of shear stress, the particles comprising the channel bed are set in motion and the bed deforms from its initial plane condition. The use of rating curve of a river channel has long been of interest to hydraulic engineers and modelers. A numerical model requires a logical scheme, where stage and velocity can be predicted for a given channel characteristics including bed material, bed slope and discharge. Engineers are often faced with problems of designing a channel to accommodate a given discharge with a given bed slope and an unknown sediment discharge.

In the light of the above, this study attempts to explore the possible application of flow resistance equation in order to develop a stage-discharge and sediment discharge rating curve. Prior to the application of a flow resistance equation, a well-known predictor developed by Garde and Ranga Raju has been adopted and modified to a relatively simple form for easy application in alluvial channels. Finally, water surface profile for the study section is developed from the prepared rating curves. Also the possible maximum scour depth is calculated by using regime equation.

Here, the study reach is selected within the district of Sirajganj and Tangail from E894018.91 to E894912.29 and N240310.89 to N242415.08 (BTM coordinate) and covers about 40 km reach of the Jamuna River. We choose eight cross-section stations in the downstream of Jamuna bridge for our analysis purposes. The average longitudinal slopes of the study reach ranges between 0.000055m/m to 0.00025 m/m. The reach length is selected for its nearly straight topography in maximum cross sections for the simplicity in analysis.

2. METHODOLOGY

Stage-discharge predictors can be proposed by using some techniques. There are different methods for predicting fluvial discharge. Here we are considering the bed materials size in establishing a mean velocity equation thus the study is related to the fluvial process. In this study, the Grade and Ranga Raju equation has been adopted to calculate the mean velocity through the channel sections and total sediment transport capacity prediction is done by applying Ackers-White equation. Here, we have also used Sheilds diagram to predict erosion and deposition characteristics of selected river reach of Jamuna and Lacey's Regime equation is also used for clear water scour depth calculation for our analysis purposes.

2.1 Stage-Discharge Predictor

Based on the analysis of large number of data from canals, rivers and laboratory flume, Garde and Ranga Raju (1993) obtained a relationship and later Ranga Raju graphically presented a function of the form

$$K_1 \frac{U}{\sqrt{g(\Delta\rho_s/\rho)R}} = f\left[K_2\left(\frac{R}{d}\right)^{1/3}\left(\frac{S}{\Delta\rho_s/\rho}\right)\right] \quad (1)$$

Were U is the mean velocity, R is the hydraulic radius, S is the channel longitudinal slope, d is the sediment size and $\Delta\rho_s/\rho$ is the relative sediment density. The empirical coefficients K_1 and K_2 are functions of sediment size.The data used for development of Eq. (1) cover a wide range of sediment sizes and flow conditions. Comparing their procedure with observed data, Garde and Ranga Raju stated that the mean velocity can be predicted within ± 30 percent accuracy. However, the functional form was only presented graphically, but if the relationship is to be adapted to other computer applications, it is worth to fit a function to this relationship.

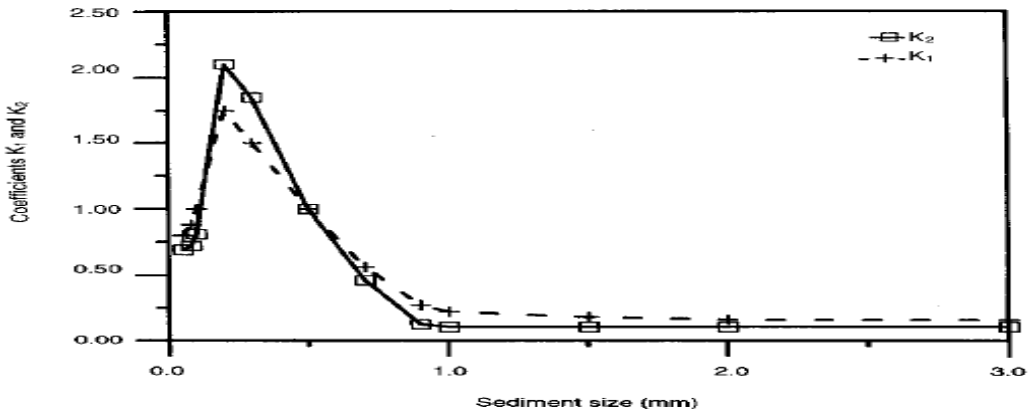

Figure 1: Coefficients K_1 and K_2 versus sediment size (**Abdulaziz A. A. and Matin M.A., "**Fluvial Stage-discharge Rating of Wadi Hanifa Main Channel", Journal of King Saud University, Engineering Sciences: 12(1); 45-63.)

The graphical relation derived from the functional form Eq. (1) can be very closely approximated, after rearranging, by the following expression:

$$\frac{U}{U_*} = \lambda(K_2^x / K_1)\left(\frac{\Delta\rho_s}{\rho}\right)^{(1/2-x)}\left(\frac{R}{d}\right)^{x/3} S^{(x-1/2)} \qquad (2)$$

Where U_* is the shear velocity [= $\sqrt{(gRS)}$], is the empirical coefficient and x is an exponent and need to be evaluated using the observed data. In this study, the values of λ and x for three different regimes have been evaluated further by fitting observed data from Ranga Raju for median condition.

Expressing the entire coefficient term $\boldsymbol{\lambda}(K_2^*/K_1)$ of Eq. (22) by an inverse of a single resistance F_f, Eq. (2) can be rewritten as:

$$\frac{U}{U_*} = \frac{1}{F_f}\left(\frac{S}{\Delta\rho_s/\rho}\right)^{(x-1/2)}\left(\frac{R}{d}\right)^{x/3} \qquad (3)$$

In which the values of F_f are function of sediment size and can be obtained from Figure 2. Values F_f of have been calculated using coefficients K_1, K_2 (Figure 1). Venoni reported a similar form of Eq. (3), which was another version of Garde and Ranga Raju equation. Also, Eq. (2.3) has a similar form of the dimensionless Manning-Strider type equation for exponent x =1/2. However, for movable bed alluvial channels the value of x varies for three different regimes due to variation of resistance occur from various bed formations.

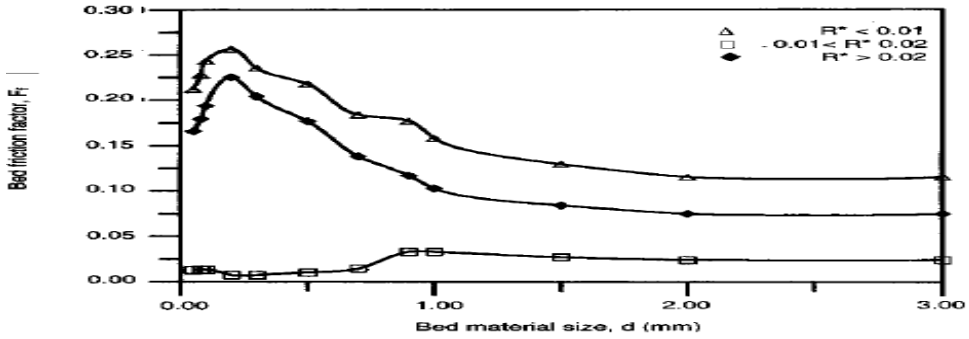

Figure 2: Alluvial resistance factor as a function of sediment size. (Abdulaziz A. A. and Matin M.A., "Fluvial Stage-discharge Rating of Wadi Hanifa Main Channel", Journal of King Saud University, Engineering Sciences: 12(1); 45-63.)

Bathymetric survey data (2013) of eight sections in Jamuna river reach have been collected from Bangladesh Water Development Board (BWDB) and used in the present analysis. Location of the present study and cross-sections details is shown in previous chapters. The actual cross sections are analyzed for different flow depths, increasing from the bed level to the bank-full level. The procedure includes the computation of hydraulic mean depth (D) at different water levels. For each cross cross-sections the hydraulic mean depth at each water level is computed conventionally using the following relation:

$$D_i = \frac{1}{T_i}\left(\sum A_{i-1} + \frac{1}{2}(T_{i+1} + T_i)(h_{i+1} - h_i)\right) \quad (4)$$

where A is the flow area, T is the top width and h is the water level at level i ,i=1,2,3…up to number of division, from lowest bed level to bank full level. However, sections associated with floodplain are analyzed by using flow division procedure. In this procedure, the main channel and side channel velocities are calculated separately with the assumption that small amount of exchange of shear stress at the interface of water between main and side channel is accounted. Therefore, in calculating the hydraulic mean depths of two channel portions, wetted perimeter of entire main channel including this interface is considered, while for the side channels only the wetted perimeter for bed and banks are considered. For Jamuna river reach, sediment characteristics do not vary significantly. Typical grain size distribution curve of bed materials of Jamuna is shown in Fig. 2.3. It can be seen from the shape of grain-size distribution curve of Jamuna, the median sediment size is close to.22mm. This sediment size can be considered as representative size of the selected river reach of Jamuna.

Thus for bed material size d_{50}=0.22 mm, relative density, $\Delta\rho_s/\rho$ =1.65, the parameter R* found to be within 0.01 to 0.02 for transition flow regime. Therefore, using the F_f value as obtained from lower regime curve of Figure 2, and with R = D, Eq. (3) becomes;

$$\frac{U}{U_*} = 75.4275(S)^{0.692}\left(\frac{D}{d_{50}}\right)^{0.3973} \quad (5)$$

For given bed slope, S and median sediment size, d_{50} Eq. (4) and Eq. (5) have been used to calculate the mean velocity for any given stage. Accordingly, discharge may be computed by multiplying the mean velocity with the corresponding flow area.

2.2 Shear stress calculation using Sheild's Diagram

The average shear stress on the bed of an open channel at which the sediment particles just begin to move is called the critical shear stress. Shield was the first to give a semi-theoretical analysis for determination of critical shear stress and his analysis is commonly used. He expressed a graphical relation between dimensionless critical shear stress $\tau_*=\tau_c/(\Delta\rho_s g d_{50})$ and boundary Reynolds number, $R_e=U_* d/\upsilon$), for incipient motion of bed particles. Here τ_c is the critical shear stress, υ is the kinematic viscosity of water and g is the acceleration due to gravity. In the turbulent region, it was shown in Shields diagram (after Chang) that range between 0.047 and 0.06 for Reynolds number 100< R_e* <500. Thus, for known values of flow depth, slope and sediment size, the shear stress difference can be computed. We can then calculate the difference between computed shear stress and critical shear stress. Positive sign of shear stress difference means beds and banks are subject to erosion while negative sign means they are subject to deposition.

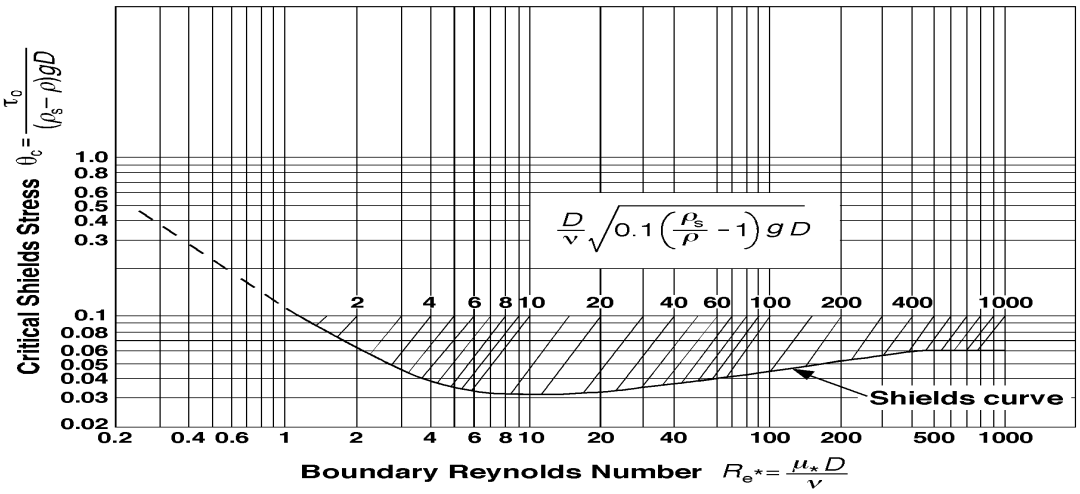

Figure 3: Sheild's diagram for shear stress calculation (Shields, A.,1936. "Application of similitude mechanics and the research on turbulence to bedload movement." Mitteilungen der Preussischer Versuchsanstalt f¨ur Wasserbau und Schiffbau 26. In German (Anwendung der A¨ hnlichkeitsmechanik und der Turbulenzforschung auf di Geschiebebewegung**)."**

2.3 Estimation of scour depth

During floods, the channel bed may undergo scour due to flowing of water. This general scour of the river bed may cause several problems such as bank instability. Although the bed levels may be restored by deposition as the floods recedes, it is necessary for the hydraulic engineers to estimate maximum bed scour depth adjacent to the banks. This is particularly important when a hydraulic structure like culvert or bridge abutments need to be constructed in the channel bed.

Predicting a general scour can be dealt with as a problem of determining equilibrium boundary shear stress responsible for resistance of grains to motion. The grain at the surface of a stationary bed must be subject to $\tau \leq \tau_c$. Hence a depth can be estimated to satisfy this threshold requirement. No suitable theoretical method has yet been available in literature for proper estimation of general scour depth in natural channels. However, many empirical equations are proposed. Here for our analysis purposes, we use Lacey's regime formula. This is widely used in this sub-continent to find out scour depth in unconsolidated alluvial rivers. This empirical regime formula is:

$R = 0.47\ (Q/f)^{1/3}$ (6)

With, $D_s = XR - h$ (7)

Where, D_s (m) Scour depth at design discharge
Q (m^3/s) Design discharge
h (m) Depth of flow, may be calculated as (HFL-LWL)
f (-) Lacey's silt factor = $1.76\ (d_{50})^{1/2}$
d_{50} (mm) Median diameter of sediment particle
X (-) Multiplying factor for design scour depth

2.4 Total sediment transport capacity

The total sediment transport rate is an integral part of any problem involving alluvial channels, because these channels do not just carry water, but water and sediment. The sediment flow in a channel is partly responsible for its instability, such as erosion and deposition, silting of reservoirs etc. Therefore, the sediment transport rate must be known to the hydraulic engineers for designing a new channel on the same plain.

The total sediment load in nature is the sum of bed load, suspended load and wash load. However, excluding wash load, sum of bed and suspended load is often called total load. Bed material load also sometimes referred as total load. Several total load prediction formulas are available in related literatures. For instance,the Colby equation, Engelund-Hansen formula, Yang equation and Ackers and White equation which are well known and widely used as sediment discharge predictors. White *et al.* compared eight different formulae using 1000 flume and 260 field measurements.

It was shown that Ackers-White equation predicts 68% of data within discrepancy ratio range 0.5 to 2 compared to 63% by Enge!und-Hansen equation. The laboratory data include 0.04 to 4.494 mm and field data from 0.095 to 68 mm. Lau and Krishnappan (1994) tested eight different formulae using their laboratory sediment discharge data. They found that the prediction by Ackers-White equation agrees reasonably well with observed data. Using sediment data of Sacramento river, Nakata also tested eleven sediment discharge formula. He showed that the overall prediction by Ackers-White equation looks excellent. Based on the evidences from these literatures, Ackers-White equation has been selected for prediction of sediment transport rate through the selected river reach of Jamuna. Moreover, this equation can be applicable to wide range of sediment sizes.

3.4.1 Ackers-White formula

Based on Bagnold's stream power concept, Ackers and White (1973) related the concentration of bed-material load as a function of the mobility number F_{gr}:

$$C_s = cs\frac{d}{R}\left(\frac{U}{U_*}\right)^n\left(\frac{F_{gr}}{A}-1\right)^m \quad (8)$$

Where n, c, A, and m are coefficients. The mobility number F_{gr} is given by

$$F_{gr} = \frac{{U_*}^n}{[gd(s-1)]^{1/2}}\left[\frac{U}{(32)^{1/2}log\left(\frac{10R}{d}\right)}\right]^{1-n} \quad (9)$$

They also expressed the sediment size by a dimensionless grain diameter d_g:

$$d_g = d\left[\frac{g(s-1)}{v^2}\right]^{1/3} \quad (10)$$

Where, υ is the kinematic viscosity of water.
In deriving the mobility factor for sediment transport, they distinguished bed load and suspended load. The transport of coarse sediments in the form of bed load is attributed to the stream power that generates the grain shear stress which is reflected in the second part of F_{gr} in Eq. (9). For fine sediments, which travel mainly in suspension, the turbulent intensity that sustains the suspension is assumed to be a function of the total bed shear; thus the stream power is $\tau_o U$. The first part of F_g reflects the power expenditure associated with turbulent intensity of the flow. The coefficient n is the transition exponent, which depends on the sediment size; it is used when both modes of transport are present and it is zero for coarse sediments with bed load only. The coefficient A may be interpreted as the critical value for F_{gr}
For application in the Jamuna river reach, the Ackers-White equation can be expressed as:

$$C_s = 0.0295\left(\frac{d_{50}}{D}\right)\left(\frac{U}{U_*}\right)^{0.583}\left(\frac{F_{gr}}{0.2375}-1\right)^{3.076} \quad (11)$$

in which, the particle mobility number F_{gr} is given by

$$F_{gr} = 16.758(U_*)^{0.583}\left[\frac{U}{5.657log\left(\frac{10R}{d_{50}}\right)}\right]^{0.417} \quad (12)$$

Here, calculated values of coefficients for Jamuna river are as follows:
c = 0.0111256
n = 0.583
A = 0.238
m = 3.076
In Eq. (11), C_s is the total load concentration by weight and it is expressed in ppm by multiplying the calculated value with 10^6. For known sediment size, channel slope, flow depth and mean velocity, Eq. (12) is used for the computation of F_{gr}.

3. ILLUSTRATIONS

3.1 Figures and Graphs

Predicted mean velocity equation has been applied to generate stage discharge data for each cross-section. A typical stage-discharge curve has been generated for each of the eight cross-sections. Stage-discharge curves for upstream station RMJ 6.1 and downstream station RMJ 3.0 are shown in Figure 4 ad Figure 5. These can be used as discharge predictor by knowing water level of the flow. This water level can be measured in the field by installing water level recorder at suitable location of the channel reach. The two curves have very good correlation coefficient values.

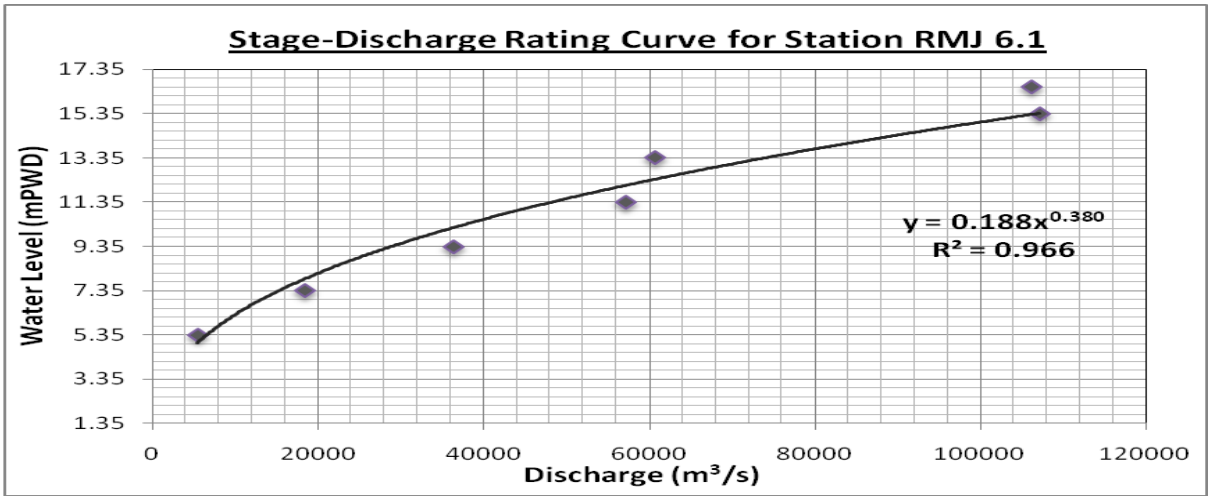

Figure 4: Typical stage-discharge rating curve for station RMJ 6.1.

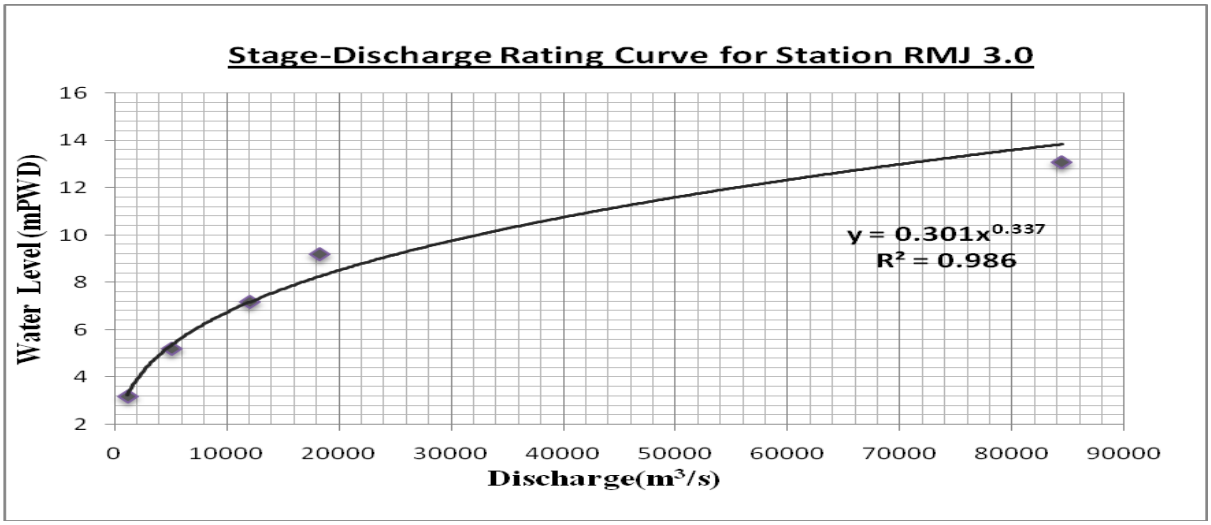

Figure 5: Typical stage-discharge rating curve for station RMJ 3.0

Based on stage-discharge data, water surface profiles of the entire reach have been drawn for different discharges. Here, water surface profiles for two discharges such as Q = 10000 m^3/s and Q = 30000 m^3/s are shown in Figure 6 and Figure 7. Bank full ad bed levels of the reach are also shown in the figures. From these profiles, it is seen that the selected Jamuna river reach can carry discharge up to about 10000 m^3/s without flooding the banks. The reach can carry discharge up to about 30000 m^3/s but flooding occurs at stations RMJ 4.0 and RMJ 3.0.Their combined water surface profiles is shown in Figure 3.3.

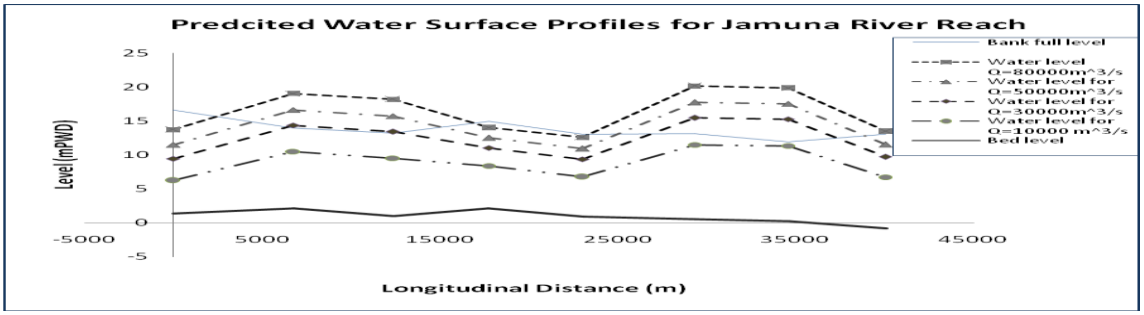

Figure 6: Predicted water surface profiles for Jamuna River reach for different discharges

Using estimated values from Acker's-White equation, a set of sediment rating curve is prepared for different flow depth conditions. For highest flow depth at bank-full condition, the sediment rating curve is drawn. Also, rating cures have been generated here for three different longitudinal slopes in order to observe the variations with slopes. A mean sediment curve in terms of total sediment concentration versus discharge intensity (discharge per unit width) has been constructed as shown in Figure 3.4. This figure can be used to predict the total load concentration for given longitudinal slope and discharge intensity.

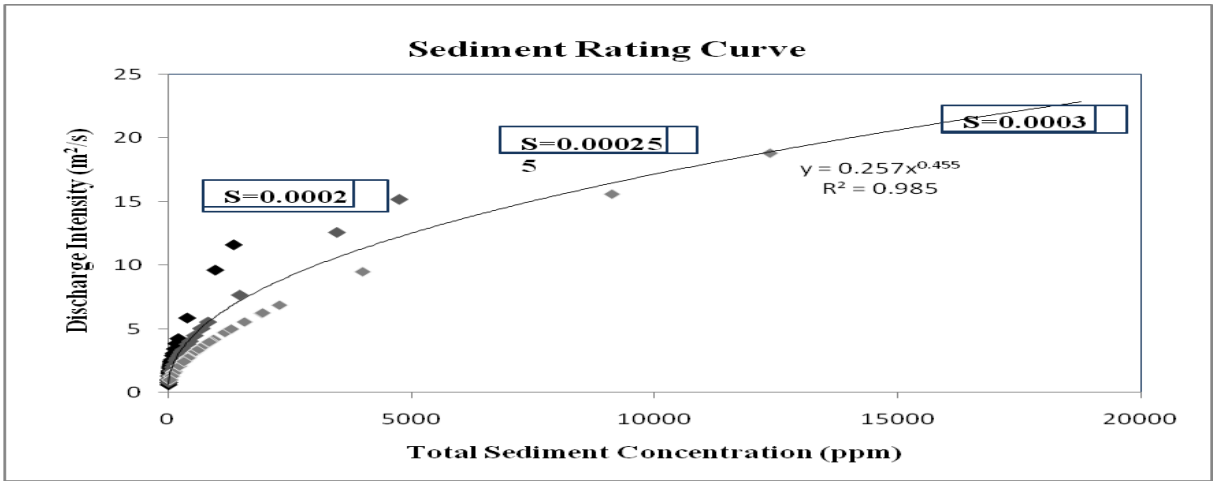

Figure 7: Sediment rating curves in terms of discharge intensities for different bed slopes versus total load concentration.

3.2 Tables

Eight cross-sections over 40 km length of Jamuna river reach have been used to determine flow and sediment transporting capacity. The geometric dimensions of these sections are shown in Table 3.1. It can be seen that the selected reach are becoming flared towards the downstream side.

Table 3.1: Geometric dimensions of selected cross-sections along study reach at bank-full condition

Station No.	Distance (d/s) (m)	Max. depth (m)	Bank-full width (m)	Flow Area (m^2)	Hydraulic Mean depth (m)	Average bed slope*10^{-4}
RMJ 6.1	0	15.23	11187	64391.56	5.76	2.51
RMJ 6.0	6755.96	11.82	16400	65584.69	4.00	1.14
RMJ 5.1	5607	12.22	14300	41830.49	2.93	2.00
RMJ 5.0	5378.46	12.80	16615	89610.01	5.39	2.14
RMJ 4.1	5274	12.18	21100	86405.72	4.10	2.37
RMJ 4.0	6269.95	12.57	13000	71649.20	5.51	5.58
RMJ 3.1	5288.3	11.65	12100	56334.30	4.66	5.86
RMJ 3.0	5466.28	13.07	15160	78432.04	5.17	1.90

Estimated discharge capacity, shear stresses, maximum erosion depth and sediment concentration have been estimated for various existing cross-sections under bank full conditions and under constant flow depth of 6 m. Results are shown in Table 1 and Table 2.

Table 1: Discharge capacity, shear stress differences and depth of scour through the eight cross-sections of Jamuna river reach for bank-full condition

Cross Section Station No.	Depth at Bank-Full Level (m)	Shear Stress Difference (τ-τ_c) (N/m^2)	Discharge Capacity (m^3/s)	Depth of Scour (m)
RMJ 6.1	15.23	+14.01	106216.35	23.73
RMJ 6.0	11.82	+4.30	30420.73	15.64
RMJ 5.1	12.22	+5.56	28607.26	15.32
RMJ 5.0	12.8	+11.14	115074.29	24.37
RMJ 4.1	12.18	+9.35	97987.07	23.10
RMJ 4.0	12.57	+2.84	18926.10	13.35
RMJ 3.1	11.65	+2.50	13557.77	11.95
RMJ 3.0	13.07	+9.48	84425.93	21.98

***(τ-τ_c)=ρgDS- τ_*($\Delta\rho$gd)**

*(+) ve sign means bed and banks are subjected to erosion

Table 2: Discharge capacity, shear stress differences and max. depth of scour through the eight cross-sections of Jamuna river reach for 6m flow depth**.**

Cross Section Station No.	Shear Stress Difference (τ-τ_C) (N/m^2)	Discharge Capacity (m^3/s)	Depth of Scour R (m)
RMJ 6.1	+12.50	18511.34	13.25
RMJ 6.0	+4.16	4883.47	8.50
RMJ 5.1	+6.79	4457.36	8.25
RMJ 5.0	+6.01	9450.02	10.59
RMJ 4.1	+6.97	12351.12	11.58
RMJ 4.0	+1.09	1052.60	5.10
RMJ 3.1	+1.50	1108.61	5.19
RMJ 3.0	+4.79	5145.74	8.65

As computed and shown in Table 1, the discharge capacity of cross-section RMJ 6.1 is found to be 106216.35 m^3/s when the flow depth is 15.23 m. Maximum discharge capacity of cross-sections RMJ 6.0, RMJ 5.1, RMJ 4 and RMJ 3.1 are found less compared to other cross sections in the reach. Reason is that, these four cross sections are relatively shallower or narrower under bank-full condition and have less flow area as well as less bank full width listed in Table 3.1.Consequently, higher carrying capacity is envisaged for station RMJ 5.0 which is 115074.29 m^3/s for a flow depth of 12.8 m. Obviously, may other branch channels are linked to the reach along the sides of station RMJ 5.0, providing higher flow capacity of the main river channel itself. Otherwise, the downstream banks of RMJ 5.0 are subjected to heavy flooding as downstream station after RMJ 5.0 have lower discharge carrying capacity. However, for constant flow depth of 6 m, the corresponding discharge through the sections RMJ 6.1 and RMJ 4.1 are estimated as 18511.34 m^3/s and 12351.12 m^3/s respectively which are the higher as shown in Table 5.2. For sections, RMJ 4.0 and RMJ 3.1, the estimated discharges are found to be 1052.60 m^3/s and 1108.61 m^3/s respectively, which are obviously very low compared to those discharges at bank-full levels. This is due to the fact that, these sections have a narrow deep cut at a depth close to 6 m, which provides less flow area in discharge computation. It is worth mentioning here that, the discharge close to bank-full stages increases at a higher magnitude when compared with that of low stages.

The higher rate of discharge increment is due to wider water conveying area associated with flood plain. Foregoing results are obtained based on constant sediment size. However, it can be estimated that for a constant longitudinal slope, the maximum discharge through the reach in bank-full condition will give upto 22% change in values and for ±20% change in longitudinal slope will give a ±50% change in discharge. On the other hand, for a specific bed slope, 10% decrease of sediment size will give only 5% increase in predicted discharge.

Table 3: Discharge intensity and erosion depth from bed level for RMJ 6.1

Cross Section Station No.	Various Flow Depths (m)	Discharge Intensity (m2/s)	Depth of Scour from WL. (m)	Erosion Depth from Bed Level (m)
RMJ 6.1	4m	2.5	8.84	4.84
	6m	7.67	13.25	7.25
	8m	12.59	16.6	8.6
	10m	15.2	19.31	9.31
	Bank full	9.49	23.73	8.5

Maximum possible erosion depths for various sections have also been computed. It is observed that for discharge intensity 15.2 m^2/s and d_{50} = 0.22 mm, erosion depth can reaches up to 9.31 m from the lowest bed level for the case of cross-section RMJ 6.1. For station RMJ 4.0 and RMJ 3.1 erosion depth from lowest bed levels are negligible. In these cases, depositions are suspected along the irregular cross-sections.

Table 4: Estimated sediment concentration for bank-full condition.

For Bank Full condition		
Cross Section Station No.	**Discharge Intensity (m^2/s)**	**Total Sediment Conc.(ppm)**
RMJ 6.1	9.49	2147.86
RMJ 6.0	4.76	615.44
RMJ 5.1	2.63	185.94
RMJ 5.0	8.39	1731.73
RMJ 4.1	4.98	670.21
RMJ 4.0	8.74	1861.10
RMJ 3.1	6.35	1051.97
RMJ 3.0	7.76	1506.67

The total sediment transporting capacity of the channel reach is calculated from Ackers-White's equation in which the mean velocity is computed using predicted mean velocity equation. Total sediment concentration is computed using constant sediment size and constant longitudinal slope. Thus, using different longitudinal slopes, variations are illustrated in the last portion of this chapter. Here, estimated sediment concentrations along with discharge intensities for selected stations under bank-full condition are shown in Table 3.5. For all the cross-sections under bank-full condition, predicted sediment concentration is found to range between 185.94 ppm to 2147.86 ppm. However, these concentrations are very close to clear water flow except RMJ 6.1 and RMJ 4.1 and don not produced any significant impact on the overall flow regime of the river reach. For increasing discharge intensity, total sediment concentration is also increasing.

4. CONCLUSIONS

Fluvial stage-discharge rating has been done by using modified resistance equation for various cross-sections of the Jamuna river reach. Computed water surface profile shows that the channel reach can carry discharge up to 30000m^3/s, without causing over bank spills for

a considerable portion of the reach. Further computation shows that serious flooding is occurs under bank-full discharge 50000 m^3/s and 80000 m^3/s respectively. From computed shear stress differences, it is observed that severe bed and bank erosion occur at bank-full condition. From computed erosion depth, it can be predicted that erosion from bed level increases with increasing flow depth for selected stations. Combined with proposed mean velocity equation, sediment transport rate is also predicted using modified Ackers-White equation for selected Jamuna river reach. It is seen that for constant bed material size and longitudinal slope, total sediment concentration is increasing with increasing discharge intensity. For higher slopes, the predicted total sediment concentration is also increasing.The river reach has high range of bed material concentration (within the range 7 ppm to 4766 ppm) for different flow depth condition. Higher the flow depth, higher the total sediment concentration.It is concluded from our analysis that the predicted equations may not be valid for other reach along the Jamuna river. But is shows a satisfactory performance for the river reach under study. Verification of our proposed equations using observed water level, water discharge and total sediment concentration data of Bahadurabad station doesn't fully satisfy our prediction. Dissimilarity in bed slope, bed and bank materials sizes, long distance from selected river reach, location upstream of Bharmaputra-Jamuna basin system may be the reasons behind those anomalies.

ACKNOWLEDGEMENTS

The authors would like to acknowledge the cooperation of Bangladesh Water Development Board for providing the bathymetry data of Jamuna River.

REFERENCES

Abdulaziz A. A. and Matin M.A., "Fluvial Stage-discharge Rating of Wadi Hanifa Main Channel", Journal of King Saud University, Engineering Sciences: 12(1); 45-63.

Ackers, P. and White, W.R. "Sediment Transport: A New Approach and Analysis". Journal of Hydraulic Division, ASCE, 99 No. HYl l, (September, 1973). 2041-2060.

Ranga Raju, K.G. Flow Through Open Channels. 2nd ed. New Delhi: Tata McGraw Hill Pub. Co., 1993.

Shields, A.,1936. "Application of similitude mechanics and the research on turbulence to bedload movement." Mitteilungen der Preussischer Versuchsanstalt f˙ur Wasserbau und Schiffbau 26. In German (Anwendung der A¨ hnlichkeitsmechanik und der Turbulenzforschung auf di Geschiebebewegung)."

Van Rijn, L.C. "Equivalent Roughness of Alluvial Bed". Journal of Hydraulic Division, ASCE, 108, No. HYIO (October, 1982), 1215-1218.

White, W.R., Milli, H. and Crabbe, A.D. "Sediment Transport: An Appraisal of Available Methods". *Hydraulic Research Station,* UK: Wallingford, Report No. INT-119, Vol. 1&2, 1973.

White, W.R., Paris, E. and Bettess, R. "The Frictional Characteristics of Alluvial Streams: A New Approach". Proc. ICE, 69, No.I (September, 1980),737-750.

Yang, C.T. "Unit Stream Power and Sediment Transport". Journal of Hydraulic Division, ASCE, 98, No. HYlO (October, 1972), 1805-1826.

Proceedings of the 4th International Conference on Civil Engineering for Sustainable Development (ICCESD 2018), 9~11 February 2018, KUET, Khulna, Bangladesh (ISBN-978-984-34-3502-6)

ASSESSMENT OF DRAINAGE CAPACITY OF CHAKTAI AND RAJAKHALI KHAL IN CHITTAGONG CITY AND INUNDATION ADJACENT OF URBAN AREAS

Faisal Mahmood[1] and Md. Abdul Matin[2]

[1] Department of Water Resources Engineering, BUET, Bangladesh. Email: faisal.shovon.007@gmail.com
[2] Professor, Department of Water Resources Engineering, BUET, Bangladesh.

ABSTRACT

Chittagong city is known as the business port city of Bangladesh. Water logging due to intense rainfall makes the life of Chittagong city dwellers miserable every year as the roads and lowlying areas become inundated. Proper estimation of runoff volume generated from intense rainfall is thus important. The study focuses on estimating the capacity of the existing drainage channel network of the Chittagong urban area, mainly Chaktai and Rajakhali khal and their branches which carry water from the south eastern parts of Chittagong city. This case study deals with a systematic approach for the estimation of urban runoff from the catchment area of this khals. The catchment area of Chaktai and Rajakhali khal is delineated into 10 watersheds by using ArcGIS. The existing situation of the channel drainage capacity for rainfall runoff is estimated using HEC-HMS hydrologic model for 2 different considerations -2 hour 5 year return period rainfall and 2 hour 10 year return period rainfall. Lag time and time and time of concentration variations in different watersheds are estimated from the runoff hydrographs. Afterwards, the maximum water level at different sections of the khals for the rainfall runoff are generated using HEC- RAS 1D model and urban inundation maps are produced for different scenarios. The study reveals that the geometry of major drainage channels are not adequate enough to drain out the excess rainfall runoff to the Karnaphuli river. Surplus rainfall storage spills over the channels and inundates the adjacent locality. Dredging of channel sections is an important requirement for the improvement of the scenario. The study also identifies possible solutions as an essential input towards arriving at appropriate planning decisions for the improvement of city drainage system.

Keywords: *Rainfall runoff; Drainage Capacity; Hydrologic; Inundation; Dredging.*

1. INTRODUCTION

Urban drainage congestion during monsoon due to heavy rainfall causes much inconvenience and economic losses for the Chittagong urban area residents. The reasons behind this urban flooding can be attributed to heavy rainfall, inadequate drainage system, high tide twice a day in Karnaphuli river, unplanned urban development, encroachment and congestion of channels and urban development of local water retention bodies. The various drainage channels passing throughout the city play an important role in carrying out the runoff to the Karnaphuli river (Ashraf, M.A. & Chowdhury, S.A, December 2009).The major khals passing through Chittagong urban area are Chaktai Khal, Rajakhali Khal, Moheshkhal, Jamalkhan khal and Nasir khal. All of these khals are connected to each other through interconnecting branches and finally drain out to Karnaphuli river to the south.

Both Chaktai and Rajakhali Khals, two main drainage channels of Chittagong, terminate in the river Karnaphuli traversing through this area**.** Part of the area is densely populated. Remaining part of the area is expected to be developed in the immediate future as the area falls within Bakalia earmarked as a thrust area for development in the Structure Plan for Chittagong, 1995.

14 municipality wards lie within the catchment area of Chaktai and Rajakhali and their branch khals shown in Figure 1. They are Enayetbazar, Lalkhanbazar, Alkaran, Firingeebazar, Anderkilla, Patherghata, Dewanbazar, Jamalkhan, Chawkbazar, South Bakalia, West Bakalia, Boxirhat, East bakalia & East Sholahshahar. Almost all of these areas are industrially well developing and construction of paved surfaces and residential and commercial facilities are increasing the area of impervious surfaces. Increase of imperviousness results in producing high volume of discharge, as well as short duration flood-peaks (Hassan, M.M. & Nazem, M.M, June 2016).

Water logging can be mitigated by properly designing drainage networks and facilities. The initial steps of the prospect are numerical modeling of the rainfall runoff analysis of the study area. Further, the problem can be analyzed by assessing the flood routing and highest water level to these drainage congestion flooding (Papry, I. & Ahmed, January 2015). Inundation maps of the area suggests the areas that we need to focus to plan the proper drainage and development works like retention ponds and pumping stations required for the study area. The study also determines the minimum depth and areas the channels needs to be dredged in to drain the highest magnitude of storm water safely towards the Karnaphuli river outlet.

2. METHODOLOGY

2.1 Data Collection:

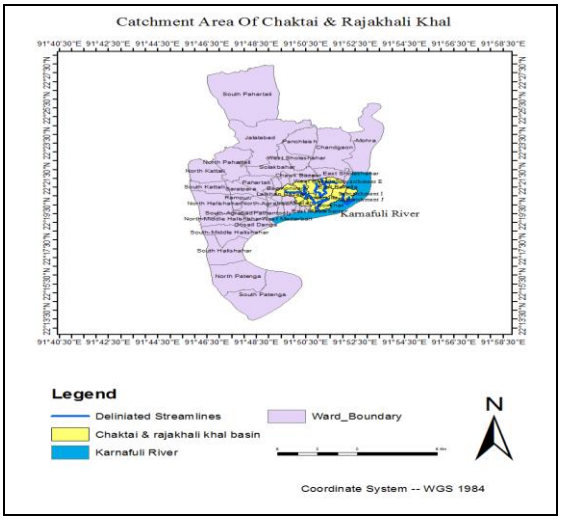

Figure 1: Ward Map of Chittagong urban area locating the Study Area

Both primary and secondary data were needed to fulfill the study. Primary data includes photographs of salient features to determine the flow paths, of the study area. Secondary data includes design rainfall data, Google earth satellite image data, cross-sectional features of channels, maps and GIS shape files.

2.2 Design Rainfall data:

The design rainfall data was generated from IDF curves of Chittagong City for the interval 1984-2016. (Rimi, S,S & Matin, A, M, 21-23 December 2016)

2.3 Watershed Delineation :.

30m x30m Landsat satellite DEM was used for watershed delineation of the study area. Arc hydro tools were used in the process. GeoSWMM was used to delineate the streams of the watershed using the Agree Dem raster of the Catchment Area – and the digitized polylines of the urban area channel network. The watershed polygon Raster was produced and – 18

watersheds were found for the digitized channels, among which- 10 watersheds lie within the study area. The 10 sub catchments were then imported as GIS shape files for the HEC HMS basin analysis The area is delineated into 10 sub catchments from where rain and storm water runs off to the river. The sub catchments are named respectively as Sub catchment A, Sub catchment B, Sub catchment C, Sub catchment D, Sub catchment E, Sub catchment F, Sub catchment G, Sub catchment H, Sub catchment I & Sub catchment J.

2.4 Calculation of Lag time And Time of Concentration for All the Sub catchments

NRCS developed the following equation (NRCS lag formula.) for watersheds with areas of less than about 8 km^2 (2000 ac) and Curve Number CN between 50 and 95 (Haan, C.T., Barfield, B.J. and Hays, J.C, 1994).

$$tL = \frac{l^{0.8(1000-9CN)^{0.7}}}{1900CN^{0.7}\,y^{0.5}} \quad (1)$$

$$tL = \frac{l^{0.8}(2540-22.86CN)^{0.7}}{1410CN^{0.7}Y0.5} \quad (2)$$

The lag t_L is in hours. The hydraulic length l from the outlet to the most hydraulically remote point in the watershed is in feet (Eq. 1) or meters (Eq 2). CN is a dimensionless parameter between zero and hundred, CN = 0 represents an infinitely abstracting catchment with maximum potential retention, S= ∞, and a CN value of 100 represents a condition of zero potential retention (i.e. impervious catchment). Y is the average land slope of the watershed in percent.

The hydraulic length, l is obtained from ArcGIS 10.4.1, by taking the lengths of the flow paths in the different sub catchments. The corresponding land use types were obtained from ARCGIS supervised image classification on Google earth satellite images. The average basin slope, Y (%), was determined from the equation (Chow, 1964).

$$Y = \frac{100(C\,I)}{A} \quad (3)$$

Where, Y= average land slope, %
C= summation of the length of the contour lines that pass through the watershed drainage area on the quad sheet, ft
I= contour interval used, ft
A= drainage area, ft^2 (1 acre = 43,560 ft^2)

2.5 Design Rainfall Depths:

The equation of IDF curves of Chittagong City for the interval 1984-2016 (Figure 2) was obtained as--

$$I = \frac{1122T_r^{0.213}}{T_d^{0.673}} \quad (4)$$

Here, I= intensity in mm/hr
Tr = Return Period, in Years
Td= Duration, in minutes

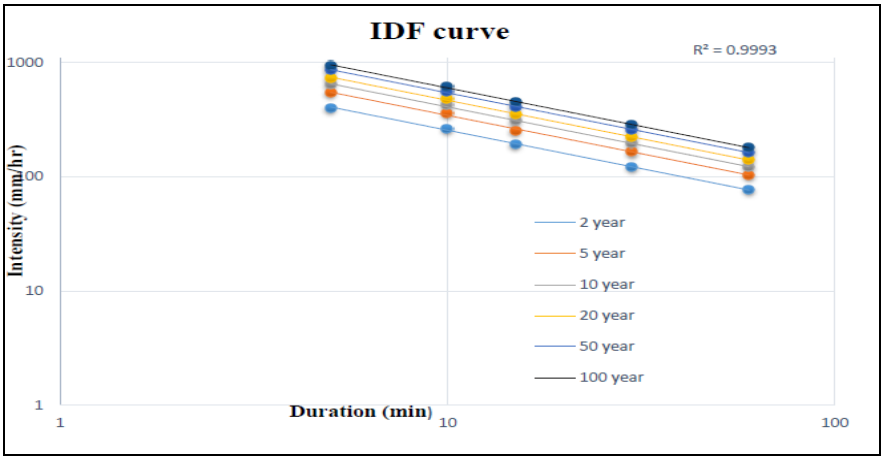

Figure 2: IDF Curve obtained from Gumbel Distribution method for Chittagong city (1984-Recent)

The model was simulated with the following rainfall events:

- ✓2h 5-Year Return Period
- ✓ 2h 10-Year Return Period

The design rainfall hyetographs are shown in Figure 3.

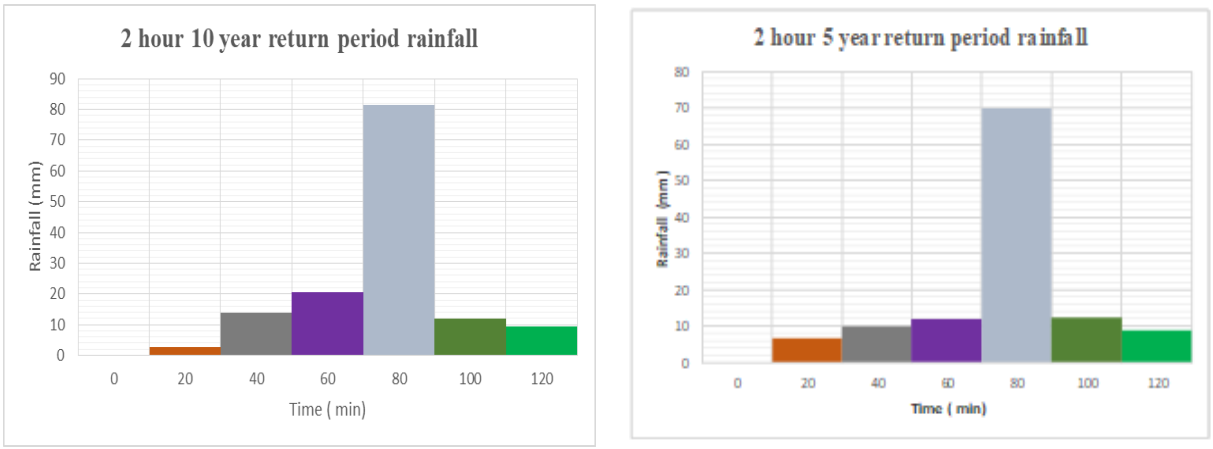

Figure 3: Precipitation hyetographs obtained from IDF curve of Chittagong City

2.6 HEC HMS runoff model

The SCS Unit Hydrograph was used as Transform Method. SCS Curve Number was chosen in Loss Method. Surface Method and Canopy Method were chose as “none”. Also it was assumed that there was no base flow infiltrated through the ground. A meteorological model manager was created. A precipitation gauge was added under time-series data manager. Finally, a control specification was set up.

Model Specific data: In the rainfall-runoff model of HEC-HMS, area, initial abstraction, curve number, imperviousness (%), lag time were given as inputs of catchment parameter. In time-series data manager, rainfall values were input in precipitation gauge as input hyetographs of 20 minute interval, as shown in Figures.

Model Simulation: A fixed time stem of 20 minute has been used as simulation period. 2 different return period rainfalls were used as design rainfall and control specifications time was selected as 12 hours. So the 12 hour runoff model was computed for the catchment area.

2.7- HEC-RAS 1D Flood Routing Model

2.7.1 Processing of Geometric Data

Cross Section Geometry: Width and elevations at the mouth of Chaktai and Rajakhali khals were observed from previous studies. The other location cross sectional width was calculated from the latest google earth satellite image of the study area. The cross section data of all the reaches were then interpolated at 20 m interval. The 1D model layout is illustrated in Figure 2.

Downstream reach length: The downstream cross section reach lengths describe the distance between the current cross section and the next cross section downstream are calculated from Google Earth.

Manning's n value: Initially roughness coefficient is assumed to be 0.025.

2.7.2 Unsteady Flow Data

At the beginning of the simulation, initial flow and boundary conditions at all of the external boundaries of the river reach is provided.

Boundary Conditions: For unsteady flow model, the boundary conditions are as follows:
HEC-HMS model output inflow hydrographs for Chaktai channel outlet was provided as Chaktai khal upstream boundary.
HEC-HMS model output inflow hydrograph for Rajakhali channel outlet was provided as Rajakhali khal upstream boundary.

At downstream boundary—stage hydrograph of Karnaphuli upstream at Sadarghat station and khal 18 station was provided.

2.7.3 Bed slope calculation:

Let the average cross sectional dimension of the channel is respectively 50m top width & 7m depth (Google earth image observation)
So, the trapezoidal area

$$A = (b + zh)h \quad (5)$$

Where b = bottom width of channel (assume 20 m)
z= side slope of channel = 7/15 =0.47 (assume 0.5)
h= channel depth = 7m

The wetted perimeter of the channel section

$$P = b + 2h\sqrt{1 + z^2} \quad (6)$$

From above calculation A=374.5 m^2
P=65.65 m
Hydraulic radius $R = \frac{A}{P}$ (7)
So, R= 5.70 m

Manning's equation for discharge calculation-

$$Q = \frac{1}{n} * AR^{\frac{2}{3}} * Sf^{0.5} \quad (8)$$

Where n= Manning's roughness coefficient considered 0.025
S_f = bed slope of channel

From above calculation, S_f = 0.0000026.

2.7.4 Performing Unsteady Flow Computations

After the geometry and unsteady flow data have been entered, unsteady flow analysis is performed from 7 December 2016 12.00 P.M to 8 December 2016 12.00 A.M. From the 12 hour model simulation, various water levels measurements at different cross sections were observed.

2.7.5 Calibration of Model:

Calibration is the adjustment of a model's parameters, such as roughness and hydraulic structure coefficients, so that it reproduces observed data to an acceptable accuracy. Calibration of model was done by checking the model water level value at the boundary cross section of Chaktai and Rajakhali channels with the observer tidal stage hydrograph of Karnaphuli river upstream measured by CDA.

2.8. Inundation Map from ARCGIS

The flood inundation map for the selected catchment was prepared using Arcgis 10.4.1 The DEM of the study area was reclassified using the highest water level observed in the channel reaches from WGS 1984 datum. The DEM initially had class value ranges from -3 to 52. That indicates the low and high land topographies respectively. By using a break point at the highest water elevation found for simulation of 2 year return period rainfall and 5 year return period rainfall the raster was reclassified into two segments.

Inundated Area (Raster grids having value below highest flood level) Uninundated Area (Raster grids having value above highest flood level) The reclassified raster was then exported as GIS maps using layout view of ARCMAP.

3. RESULT AND DISCUSSION

The final delineated catchment area and the streams are shown in the Figure 4. 10 intersecting watersheds were found to lie within the region of the study area channels. That indicated that, Storm water or rainwater from this catchment pass through this drainage networks and streams and discharges to the outlet. Table 1 and 2 represents the geometric and hydraulic characteristics of the catchments.

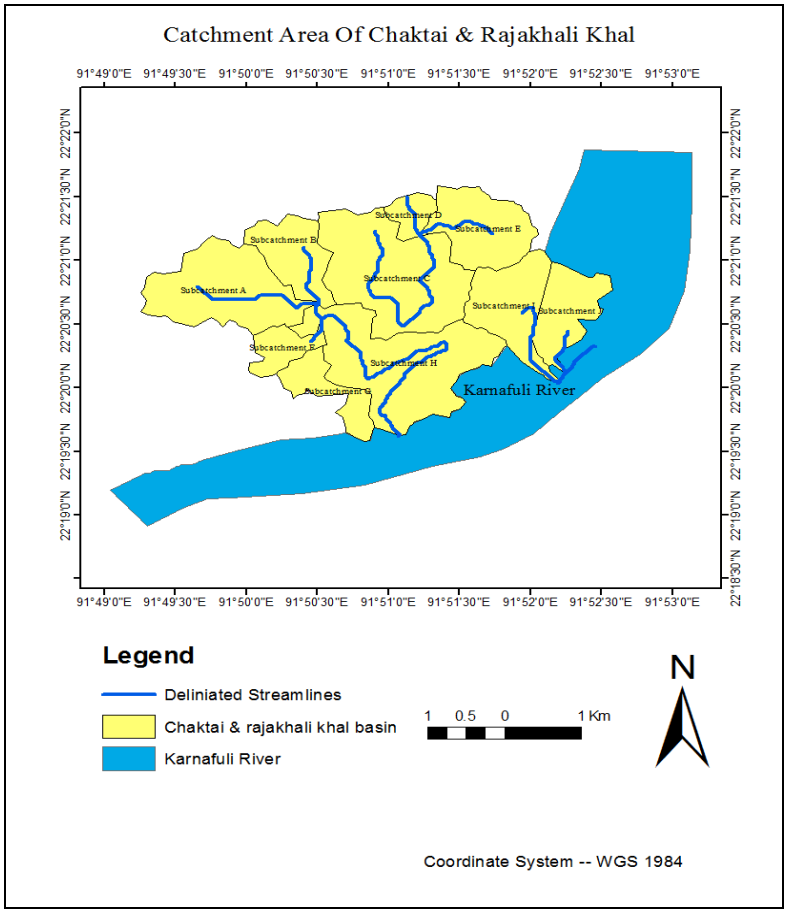

Figure 4: Watershed delineation of Catchment area

Table 1: Area of Delineated watersheds

Sub catchment Name	Area (km^2)
A	0.99
B	1.327
C	2.81
D	0.335
E	1.326
F	0.472
G	0.667
H	2.886
I	1.289

Table 2: Calculation of Lag Time and Time of Concentration

Catchment	Summation Of Length Of Contours (ft)	Area Of basin (ft^2)	Contour interval I (m)	Contour Interval (ft)	Average Land Slope Y (%)	Weighted Curve Number	Initial Abstraction (mm)	Hydraulic Length (L)	Lag Time TL (hr)	Lag time TL (min)	Time Of Concentration (Tc)
Sub basin A	1456744.22	22286880.94	0.30	0.98	6.43	77.25	14.96	1812.34	0.57	34.04	56.73
Sub basin B	543250.47	10661402.56	0.30	0.98	5.01	71.78	19.97	1063.46	0.49	29.42	49.04
Sub basin C	954257.57	30248904.20	0.30	0.98	3.10	75.20	16.75	3768.50	1.56	93.44	155.74
Sub basin D	123631.50	3606246.40	0.30	0.98	3.37	77.18	15.02	668.45	0.35	21.21	35.34
Sub basin E	554502.08	14279803.35	0.30	0.98	3.82	76.97	15.20	1174.44	0.52	31.47	52.45
Sub basin F	261241.86	5082462.14	0.30	0.98	5.06	85.02	8.95	429.93	0.16	9.46	15.77
Sub basin G	228339.23	7172317.60	0.30	0.98	3.13	75.01	16.92	886.99	0.49	29.40	49.00
Sub basin H	893504.98	31065742.41	0.30	0.98	2.83	77.65	14.62	4707.84	1.81	108.82	181.37
Sub basin I	383468.12	13874210.62	0.30	0.98	2.72	50.89	49.02	1573.82	1.56	93.71	156.18
Sub basin J	59318.40	10489005.13	0.30	0.98	0.56	0.00	---	779.44	---	---	----

After inputting the precipitation data observed from the IDF curve of Chittagong city, the rainfall runoff model was simulated for 12 hours. The runoff hydrographs showing the peaks for different catchments obtained from the model are detailed in Figure 5-8.

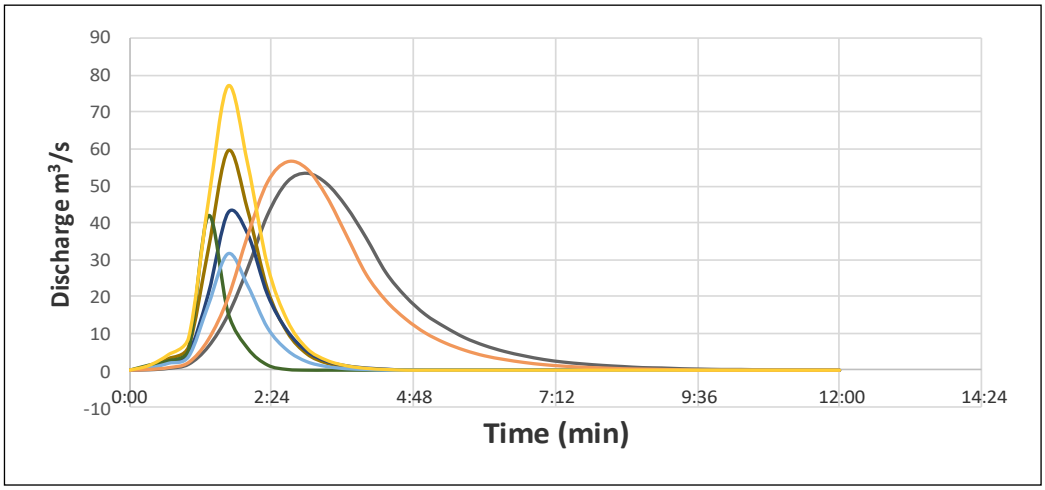

Figure 5: Runoff Hydrographs for 2h 10 year return period rainfall

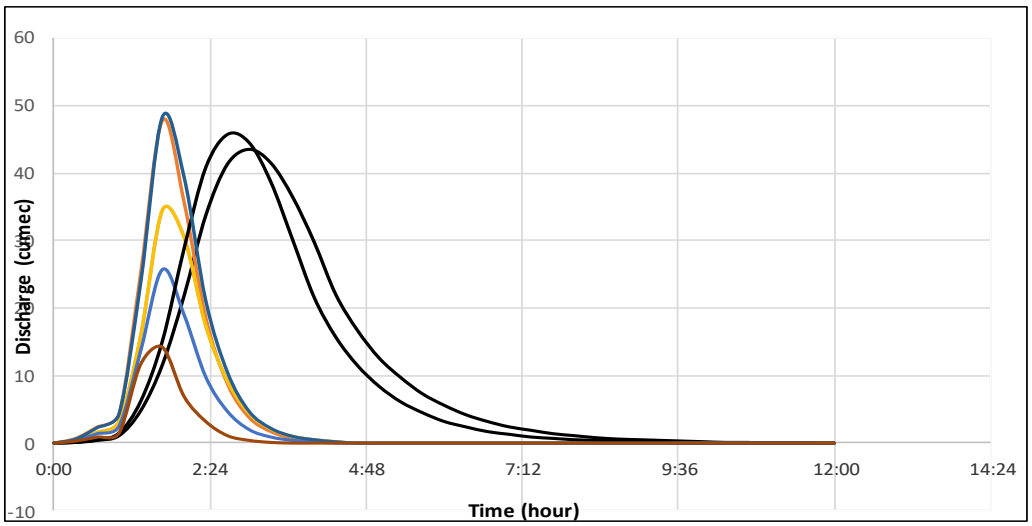

Figure 6: Runoff Hydrographs for 2h 5 year return period rainfall

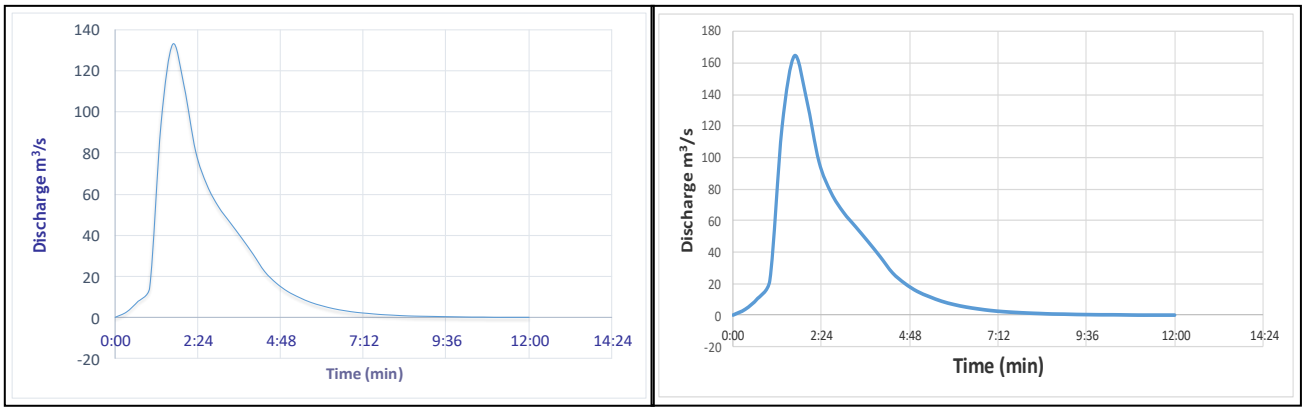

Figure 7: Inflow hydrographs at Chaktai outlet for 2h 5year and 2h 10 year return period rainfall

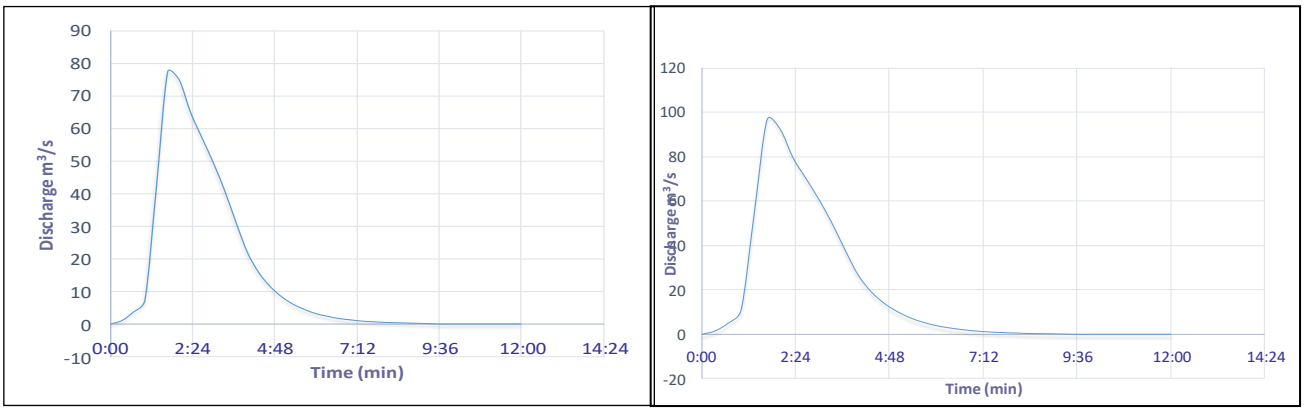

Figure 8: Inflow hydrographs at Rajakhali outlet for 2h 5year and 2h 10 year return period rainfall.

From Hec Ras 1D flow routing for 5 years and 10 years return period of rainfall- the comparison in maximum water level at different sections for both the model runs are given in Table 3. It is observed that the maximum spilling water level at different sections of khals increase 0.3-0.5 m due to tidal surge effect at downstream of khals.

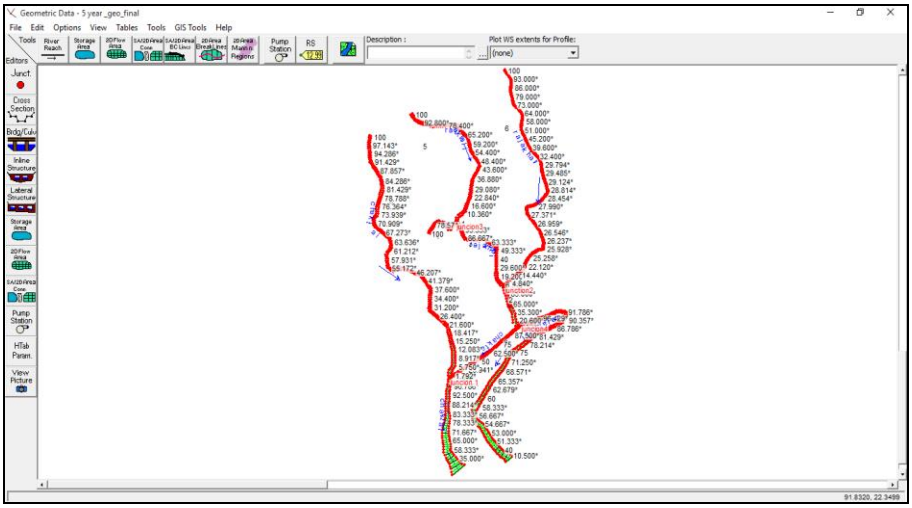

Figure 9: Geometric Data window of Hec Ras 1D (Major Drainage Channels of Chittagong)

Table 3: Maximum Water level observed from model

Channel Name	Reach	5 years return period WL (m)	10 years return period WL (m)
Chaktai	1	4.94	5.39
Chaktai	2	5.04	5.70
Chaktai	3	6.30	6.30
Rajakhali	1	4.94	5.70
Rajakhali	2	5.24	6.11
Rajakhali	3	5.73	6.59
Rajakhali	4	6.17	6.77
Rajakhali	5	6.32	6.94
Rajakhali	6	6.07	6.65

For determining the peak discharge of subcatchments theoretically, the rational formula (Eq 9) for peak discharge is used. The comparison is shown in Table 4.

$$Qp = \frac{CIA}{3.6} = 0.2778CIA \quad (9)$$

Where, I= rainfall intensity in mm/hr

A= drainage area in km^2

Q_p= Theoretical peak discharge in m^3/s

C= Run off Coefficient

Table 4: Comparison of Model Discharge and Rational Discharge (Q= CIA)

	Subcatchment Name	Model peak discharge	Rainfall Intensity mm/hr	Area (km^2)	Theoretical peak discharge
5 year return period	A	34.5	126	0.99081	34.68112427
	B	47.8	126	1.327	46.4487156
	D	14.2	126	0.335	11.725938
	E	48.3	126	1.326	46.4137128
	F	34.8	126	0.472	16.5213216
	G	25.7	126	0.667	23.3468676
10 year return period	A	42.7	146	0.99081	40.18606463
	B	59.5	146	1.327	53.8215276
	D	17.3	146	0.335	13.587198
	E	59.8	146	1.326	53.7809688
	F	41.9	146	0.472	19.1437536
	G	31.6	146	0.667	27.0527196

As the Khal 18 station records the extreme water levels of Karnaphuli river upstream, the model was calibrated –for sadarghat station observed tidal water level for 5 year return period rainfall & Khal 18 data for 10 year return rainfall. The calibration graphs are shown in Figure 10.

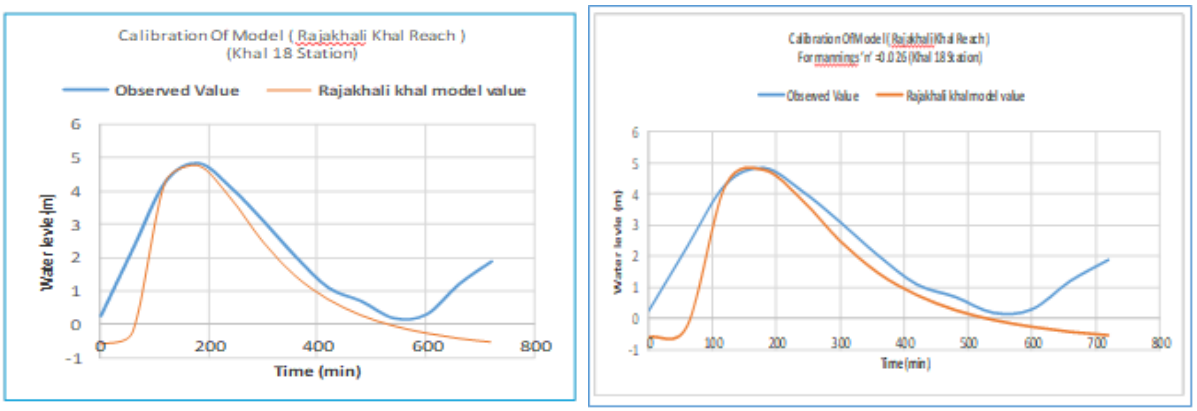

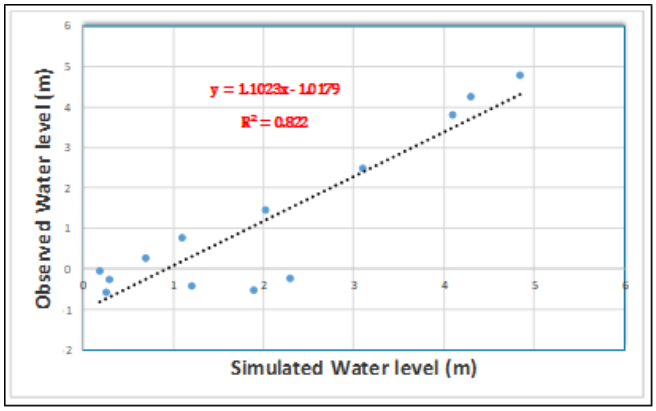

Figure 10: Model Calibration with observed water level of khal 18 station

From the simulated peak water level value, the catchment area was inundated over the Digital elevation model of the area. The low-lying areas in the DEM are flooded due to the spilling and inadequacy of the canal to pass away the drainage water to Karnaphuli. The Inundation maps for different conditions prepared from Arcmap 10.4.1 is illustrated in Figure 11.

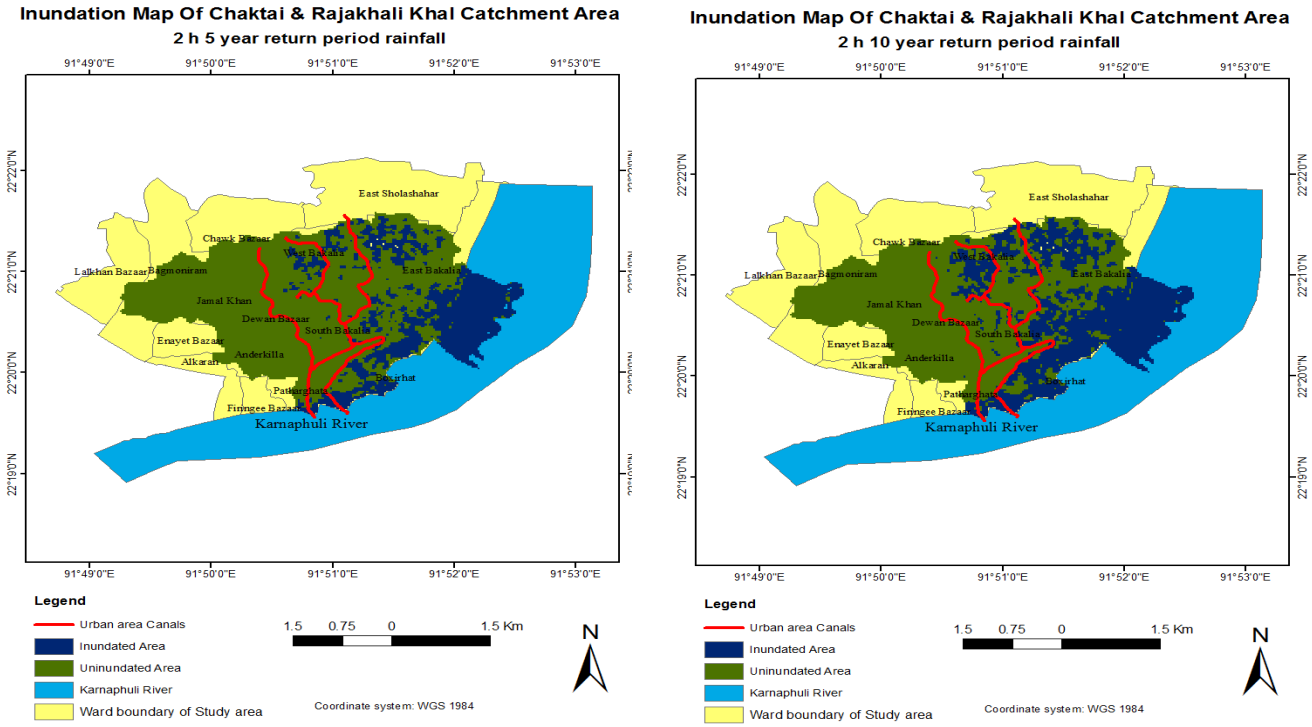

Figure 11: Inundation maps for 2h 5 year and 2h 10 year return period rainfall

4. CONCLUSIONS

The larger sub catchments drain out water from both the channel branches and so the outflow divides into two drainage channels. The dominant channels are Chaktai and Rajakhali khal. This channels and their branches drain storm runoff from 10 sub catchments of area about 14 km^2. Chaktai khal discharges more water to the Karnaphuli river than Rajakhali khal. Hydrodynamic model calibration was done by using Manning's roughness values ranging between 0.025 and 0.033.

The total peak runoff to Chaktai khal for 5 year return period rainfall is found to be 132.7 m^3/s and for Rajakhali khal is 77.5 m^3/s. The total peak runoff to Chaktai khal for 10 year return period is 164.4 m^3/s and for Rajakhali khal is 64.7 m^3/s.
The maximum water level for 5 year return period rainfall in the khals was found to be 6.32 m. The maximum water level for 10 year return period rainfall in the khals was found 6.94m.

The HEC-HMS model output yields slightly higher values of peak discharge, and in undeveloped sub catchments, the rational method produces higher values of peak discharge.

The inundation maps have been generated for peak rainfall runoff and highest high water (spring tide) level near Sadarghat station. It was found that almost 2.15 km^2 of the low lying areas get inundated for 2h 5 years return period rainfall and about 3.5 km^2 area gets inundated for 2h 10 year return period rainfall.

To some extent, it is hoped that the results obtained from the study will be useful for the planners and engineers for the proper design of drainage infrastructure in Chittagong urban area.

ACKNOWLEDGEMENTS

The authors would like to acknowledge the cooperation of Chittagong City Corporation (ChCC), Chittagong Port Authority (CPA) and Chittagong Development Authority (CDA), for providing necessary information and master plans of the city.

REFERENCES

Ashraf, M.A. & Chowdhury, S.A. (December 2009). Drainage Planning in the Cities of Bangladesh: Case Study. *Journal of Bangladesh Institute of Planners Vol. 2*, 49-60.

Chow, V. (1964). Handbook of applied hydrology—A compendium of waterresources technology. In V. Chow, *Handbook of applied hydrology—A compendium of waterresources technology* (pp. 14.1–14.54). New York: McGraw-Hill Book Co.

Haan, C.T., Barfield, B.J. and Hays, J.C. (1994). *Design hydrology and sedimentology for small catchments.* New York: Academic.

Hassan, M.M. & Nazem, M.M. (June 2016). Examination of land use/land cover changes, urban growth dynamics, and environmental sustainability in Chittagong city, Bangladesh. *Environment, Development and Sustainability*, Volume 18, Issue 3, pp 697–716.

Papry, I. & Ahmed. (January 2015). Drainage Condition in Water Logged Areas of Central Part in Chittagong City Corporation. *International Journal of Engineering Science Invention ISSN (Online): 2319*, Volume 4 Issue 1 PP 24-29.

Rimi, S,S & Matin, A, M. (21-23 December 2016). Analysis of Rainfall Runoff Data for Generation of Intensity Duration Frequency Relationships for Selected Urban Cities of Bangladesh. *Proceedings of 3rd International Conference on Advances in Civil Engineering, CUET, Chittagong, Bangladesh.* Chittagong.

Proceedings of the 4th International Conference on Civil Engineering for Sustainable Development (ICCESD 2018), 9~11 February 2018, KUET, Khulna, Bangladesh (ISBN-978-984-34-3502-6)

IDENTIFYING THE IMPACTS ON RURAL LIVELIHOOD DUE TO SEASONAL VARIATION OF DAHUK RIVER DISCHARGE IN BANGLADESH

Muhammad M Rahaman[1], Shah A Moyeen[2] and M K Shehab[3]

[1] *Professor, Department of Civil Engineering, University of Asia Pacific, Bangladesh, e-mail: rahamanmm@gmail.com*
[2] *Graduated Student, Department of Civil Engineering, University of Asia Pacific, Bangladesh, e-mail: shahuapbd@gmail.com*
[3] *Research Assistant, Department of Civil Engineering, University of Asia Pacific, Bangladesh, e-mail: k.shehabce@gmail.com*

ABSTRACT

This article explores the impacts of seasonal discharge fluctuation of Dahuk river on the livelihoods of the residents of 'Tetulia' Upazila under 'Panchagarh' district in Bangladesh. 75% of the respondents in the study area depend on Dahuk river for their livelihoods and sustenance where water scarcity in the non-monsoon period is a challenging issue. In the monsoon period, the discharge of Dahuk river was 48.6 m^3 per second while it was only 0.08 m^3 per second in the non-monsoon period. The study reflects on the significant impacts of this discharge variation on the natural, physical and financial resources. Moreover, a large number of farmers, fishermen and stone miners had to change their professions due to the adverse impacts of seasonal water scarcity. In the study, livelihoods diversification index is used for identifying the diversification of stakeholder's income in the monsoon and non-monsoon periods. Well-structured questionnaire survey, focus group discussion (FGD), participatory rural appraisal (PRA), and crosscheck interviews are performed for primary data collection. Finally, the study attempts to develop a sustainable rural livelihood framework to overcome the vulnerabilities of the stakeholder's livelihood in the study area approach in line with the United Nations Sustainable Development Goals. The implementation of sustainable livelihood framework in Dahuk River basin could reduce the repugnant consequences due to seasonal variation of Dahuk river's flow in the study area.

Keywords: *Dahuk river, livelihood, sustainable rural livelihood framework, sustainable development goals.*

1. INTRODUCTION

The availability of freshwater has major consequences over life and all social and economic processes. The system of fresh water is, therefore, a service of the ecosystem which, when interrupted, effects both the vitality of ecological systems as well as human well-being (Reid et al., 2005). The catastrophic changes of climate influence the Earth's ecosystem as well as people's livelihoods (Gain et al., 2012). As a major source of water, rivers are the crucial part of the ecosystem and play the vital role to the survival of civilization. Dahuk is a transboundary river, which originates from the marshlands Southwest of 'Jugibhita' within the 'Rajganj' block in the 'Jalpaiguri' district in India. It traverses the international border and crosses the 'Trinoihat' union at 'Tetulia' Upazila in 'Panchagarh' district of Bangladesh (BWDB, 2011; IUCN, 2014; Figure 1). Traveling to the South, Dahuk river flows through the western part of 'Tetulia' Upazila and, finally, it enters India (BWDB, 2011; IUCN, 2014). The main Dahuk stream is a major right-bank tributary of the 'Mahananda' (IUCN, 2014), but it has no branch river in Bangladesh (BWDB, 2011). Seasonal discharge variation of Dahuk river has caused severe impacts on natural, physical and financial resources, as well as on stakeholders' professions which is a serious challenge to achieve sustainable development goals (SDGs, 2017).

The total length of Dahuk river inside in Bangladesh is 14 km (BWDB, 2011). In Bangladesh, the river width varies in different locations, the lowest, highest and average width of the river is 20m, 139m, and 80m respectively. According to BWDB (2011), the river discharge was 1.43 m^3 per second in December 2010. Theoretically the river is perennial, however, the discharge is only 0.08 m^3 per second during the non-monsoon season more specifically in February – April (BWDB, 2011).

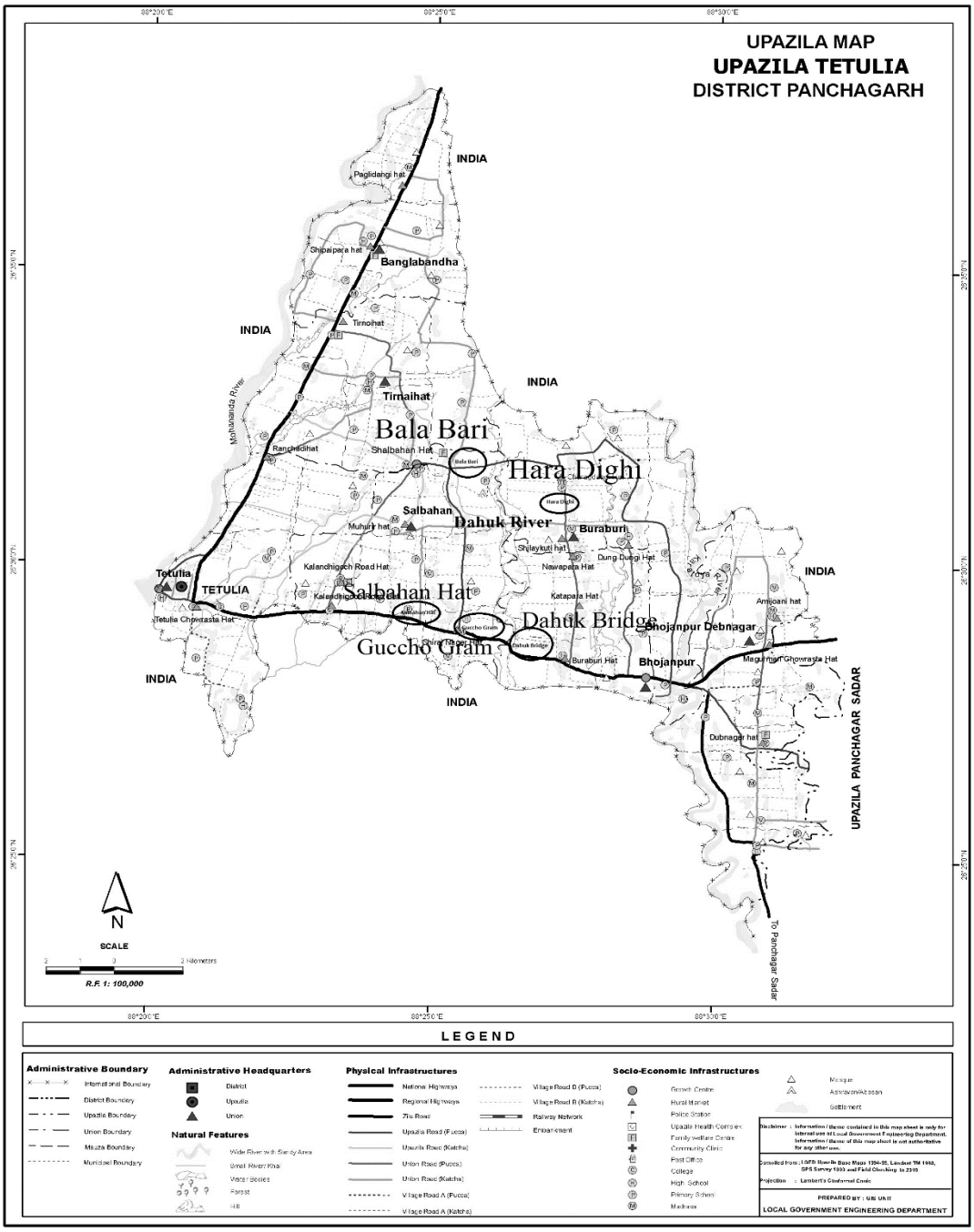

Figure 1: Tetulia Upazila of Panchagarh district.
Source: LGED (2016)

In the monsoon season, particularly during July to September, the discharge is about 48.6 m^3 per second (BWDB, 2011; IUCN, 2014). For years, the crucial roles of the Dahuk river basin wetland ecosystem inside Bangladesh include groundwater recharge, irrigation, sediment trapping, soil fertilization, food chains maintenance, crop production, livestock

grazing, fisheries production, source of stone and sand, essential minerals and other nutrients provision, wildlife habitat provision and aesthetic beautification.

Bangladesh is the downstream country of the Dahuk river basin. The freshwater availability depends on water diverted from upstream India (cf. BWDB, 2011). Also, the transboundary water sharing between India and Bangladesh, especially in the dry season, is long-term unsolved problem (Bhaduri & Barbier, 2008; Rahaman, 2009; Rahaman & Varis, 2009; Rahman & Rahaman, 2017). Besides, constructing dams and other developing projects in the upstream is an obstacle of free flow of sediment that is adversely affecting the flora and fauna in the study area. For ensuring the vitality of ecosystem and livelihood of the local people along the Dahuk river basin, transboundary water resources management is vital (cf. Jagerskog & Zeitoun, 2009).

Nations, like India and Bangladesh, that share water bodies should be cooperating to explore the opportunity for effective development of transboundary river basin (Jagerskog & Zeitoun, 2009). In many rivers basins around the world, transboundary water sharing mechanisms exist (for details see: Rahaman, 2015). Integrated Water Resources Management approach could be the best way to reach the sustainable development goals along the international rivers basins (SDGs, 2017) because it springs a negotiation among different water users, permits for a more comprehensive, fair and sustainable utilization of water resources (Peña, 2011; Rahaman and Varis, 2005).

The seasonal variation of discharge in the Dahuk river inside Bangladesh has a major impact on natural, physical and economic resources, as well as on stakeholders' profession, which poses a serious challenge to achieve the sustainable development goals (SDGs, 2017).. Many farmers, fishers, and stone miners have changed their walks of life with the variety of Dahuk's discharge. Furthermore, 75% respondents in the study area depend on Dahuk River for their livelihoods. Besides, with the growth of inhabitant and increasing the need for water, maintaining water resources in Dahuk basin is a prominent challenge.

Overall, the study provides the foundation for understanding the impacts of seasonal variation of Dahuk River discharge on the rural livelihood of villagers in “Tetulia Upazila” of Panchagarh district in Bangladesh. Additionally, it stresses the need to develop a sustainable rural livelihood framework approach intended to overcome the vulnerability of stakeholder's living. Finally, the study attempts to develop a sustainable rural livelihood framework approach to overcome the vulnerability of stakeholder's livelihood in the study area in line with United Nations Sustainable Development Goals (SDGs, 2017). Implementation of the proposed sustainable livelihood framework in Dahuk River basin could diminish the negative impacts on the rural livelihood in the study area due to seasonal variation of Dahuk river discharge.

2. METHODOLOGY

The research was carried in Dahuk river basin inside Bangladesh. In this study, a questionnaire survey is used to collect primary data. The survey is conducted in four villages namely 'Guccha Gram', 'Haradhighi', 'Balabari' and 'Shalbahan Bazar' in 'Tetulia' Upazila of 'Panchagarh' district of Bangladesh. In the questionnaire survey, a total of 100 people are interviewed. All respondents were chosen randomly from different villages located in Dahuk River basin area of Bangladesh. The focus of the survey is to ascertain how the seasonal variation of the Dahuk river discharge influences the livelihoods of the stakeholders, crop production, fisheries, and emigration. Besides, the crosscheck interviews (Afroze, 2014) were also done to justify the primary data by Upazila Nirbahi Officer (UNO) and Upazila Agricultural Officer (UAO) of Tetulia Upazila. Additionally, Focus Group Discussion (FGD) is performed in the study area. The Participatory Rural Appraisal (PRA) tool is also used in

FGD that represents the information about the living status, recent changes in lifestyles, and stakeholder's interest level to be involved in the addressing land and water resources management (cf. Allan & Curtis, 2002).

3. DATA ANALYSIS AND RESULTS

3.1 Overview of the stakeholder's livelihoods of Dahuk river

47% of respondents of the study area are women. Most of them enthusiastically participated in the interviews as well as in the group discussions. However, the respondents are classified into three groups based on their age. 31% of respondents are middle-aged (34±3 years) and more active. Stakeholders, who are 41-50 years old, make more capital. Additionally,

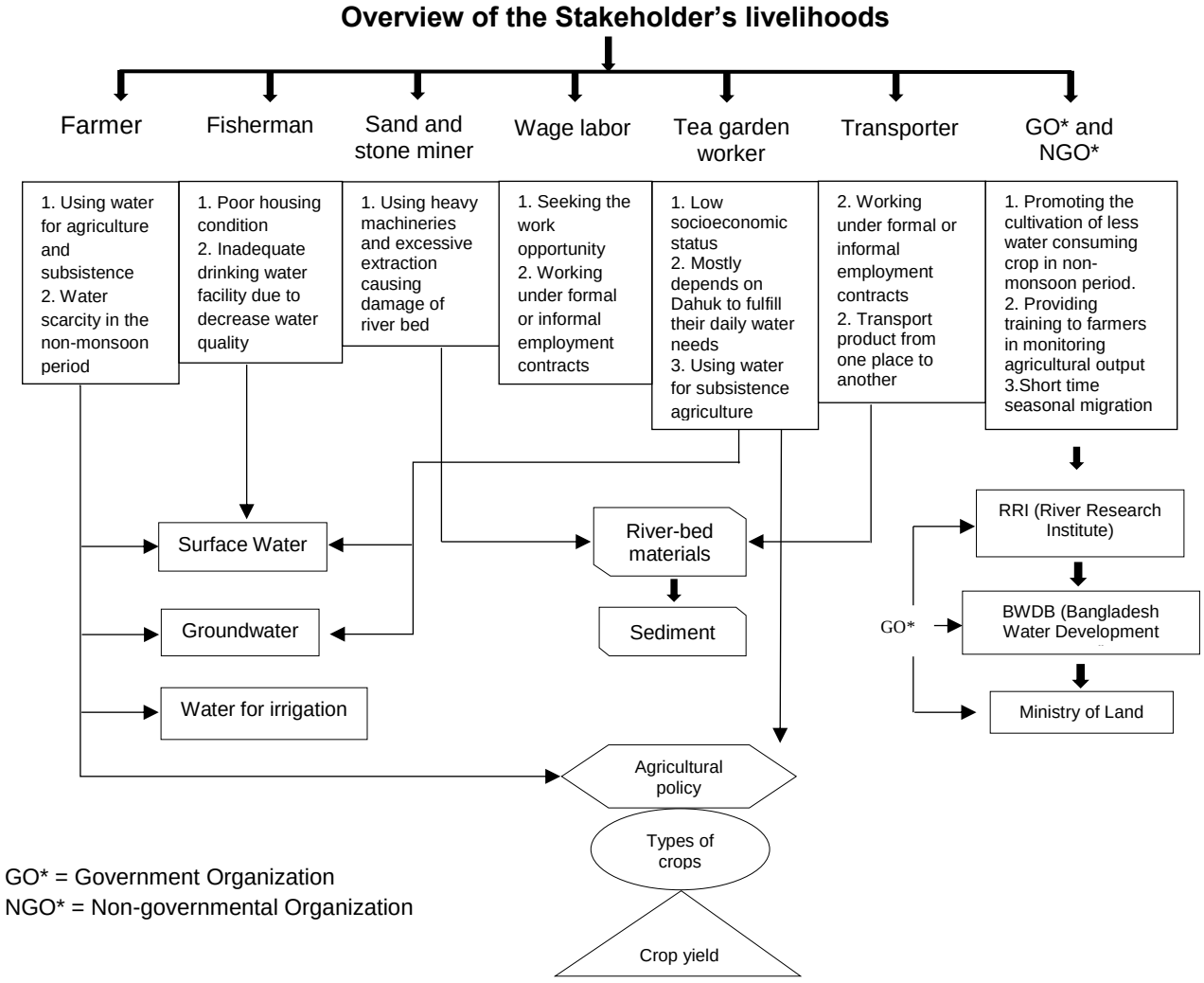

Figure *2*: Overview of the Stakeholder's livelihoods of Dahuk river basin area.
Source: Field Survey (2016)

25% of the respondents are young (20-30 years) and 13% people are in the age group of above 50 years. 38% of the families in the study area are nuclear family. Members of the ordinary families are seen to be tea garden workers and farmers. A very small portion of families consists of members who are working in business and service sectors.

Agriculture assigns about 50% of total labour potential in Bangladesh and contributes about 10% to the GDP (Roy et al., 2014; Rahaman & Shehab, 2017). Similarly, a majority of the residents of the study area mainly depends on agriculture as a source of income for the subsistence. Among the 100 people who were interviewed, 34% of the respondents were farmer. 20% female respondents were tea garden worker. Furthermore, 19% people had been surviving by doing labour work on daily basis. With the seasonal variation, some possibilities of employment are created. A large number of fishermen work in the industry or the agricultural field in the non-monsoon period for their survival when the lack of water in Dahuk river hinders their livelihood based on fishing. In the study area, it is seen that 35% of the people are uneducated. Only 31% and 11% of the respondents have the primary and secondary level of education respectively. Most of the people who are working in the agricultural sector, tea garden, and as day labourer, have no education.

According to the survey, 75% stockholders depend on Dahuk river for their livelihood. People who are working as service holders are more economically solvent. Tea harvesting becomes more challenging due to the low level of water in non-monsoon season resulting in lower wages of tea garden workers (Table 1). In this period, some of them work as a day labor under an informal employment agreement. Moreover, the earnings of farmers rise in the non-monsoon season (Table 1). Farmers mainly depend on river bed area for rice cultivation in the non-monsoon season. Although rice is a high water consuming crop (Rahaman et al., 2016; Rahaman & Shehab, 2017), farmers are more involved in rice harvesting because cultivation of rice is more beneficial compared to other crops. Besides, sand and stone miner's wages is comparatively high in the non-monsoon season (Table 1). Due to the less river water flow in the non-monsoon season, the uprooting of river bed elements is relatively simple for then. In the monsoon period the income of fisherman is quite satisfying compared to the non-monsoon season (Table 1).

The stockholders of Dahuk river basin depend on groundwater to meet their farming and drinking water demands due to seasonal variation of discharge in Dahuk river. For drinking water, 95% people rely on tube well. The surface water is not adequate in the non-monsoon period that increases the dependency on groundwater. More usage of tube well water contributed to decline of the groundwater table day by day. Dahuk river provides 48% of agricultural water requirement and 41% of industrial water requirement. Besides, for the municipal purpose, 32% of stakeholders depend on Dahuk's water. However, the water usability of Dahuk river is declining in current years. Only 22% people use toilets,in the study area. Most of the toilets are located nearby the Dahuk river without proper disposal systems and, consequently, pollute river water, soil, and air. More importantly, bacteria or other contaminants are propagating through infiltration that reduces the groundwater quality. (Ahmed & Rahman, 2000).

3.2 Agriculture practices of Dahuk basin area in Bangladesh

Most of the farmers of Dahuk basin area in Bangladesh are highly involved with rice production. Although Bangladesh has the highest yield of rice production in South Asia (FAOSTAT, 2017; Rahaman & Shehab, 2017), according to the local farmbers, the productivity of rice production is declining in recent year . The lack water availability in Dahuk river and temperature increase could be the reasons for this situation. According to the survey, 75% of the area enclosing the Dahuk river is used for rice cultivation. Farmers have grown rice in the low land area, jute and rice in the medium high land area and various types of daal (lentil) and vegetables in the high land area. As irrigation has an immediate connection to the crop yield, farmers have to supply water to the cultivated land with an interim of five to six days to get a favourable production. However, the unequal discharge of Dahuk river and decline of groundwater table caused to raise the expense of irrigation.

3.3 The discharge variation in Dahuk river

Dahuk is an international cross-border river. The fluctuation of Dahuk river's discharge is significant with the seasonal change. Data from two gauge stations located in Bangladesh (SW 57-Buribari (NTWL) and SW 57-Buribari (NTQ)) have shown a remarkable seasonal discharge variation of water in the Dahuk river over a year (BWDB, 2011). In the monsoon season, more specifically in July to September, the flow of Dahuk river was 48.6 m^3 per second (BWDB, 2011). Furthermore, the river flow was much low during the non-monsoon period particularly in February to April, which was only 0.08 m^3 per second (BWDB, 2011). Hence, the unexpected changes of climate, construction of dams and reservoirs, and other development projects in the upstream could be the cause for the variations of Dahuk river discharge in Bangladesh.

3.4 Possible impacts on the livelihoods

Livelihoods diversification index is used to find out stakeholders income diversification and vulnerability. There are various livelihoods diversification indexes such as Composite Entropy Index, Entropy Index, Modified Entropy Index, Simpson Index, Shannon Wiener Index (Shiyani and Pandya, 1998). In this study, Simpson and Shannon Index are used for recognizing the diversification of earnings in the monsoon and non-monsoon period. The Shannon Index (H) and Simpson Index (D) is represented by**:**

H=-$\sum_{i=1}^{S} \frac{n_i}{N} ln \frac{n_i}{N}$, D= 1-$\frac{\sum_{i=1}^{S} n_i(n_i-1)}{N(N-1)}$; Where N is total number of income, $\boldsymbol{n_i}$ is the individual income ofstakeholders.

Shannon Wiener Index (H) in non-monsoon season is higher than monsoon period, which indicates that the stakeholder's income is more diversified in the non-monsoon season.

Stakeholders	Non-monsoon period (November - May)			Monsoon period (June - October)		
	Income (Current US$)	Shannon wiener Index	Simpson index	Income (Current US$)	Shannon wiener Index	Simpson index
Farmer	1355	-0.35	0.068	409	-0.27	0.02
Fisherman	313	-0.36	0.003	1024	-0.36	0.12
Stone/sand miner	1251	-0.34	0.05	341	-0.25	0.01
Wage labor	651	-0.26	0.01	391	-0.27	0.01
Tea garden labor	782	-0.28	0.02	279	-0.22	0.009
Transporter	810	-0.29	0.02	428	-0.28	0.02
Total	5162	H= 1.89	D= 0.8	2872	H= 1.67	D= 0.78

Source: Data collected from Field Survey (2016)

Based on the standard (no diversification, D<=0.01); low level of diversification, D=0.01-0.25; medium level of diversification, D =0.26-0.50; high level of diversification, D=0.51-0.75; very high level of diversification, D=>0.75) (Ahmed et al., 2015) livelihoods diversification is much higher in the Dahuk basin area (Table 1).

The inadequacy of water is a public concern in Dahuk basin area. During non-monsoon season (November-May), the scarcity of water is extremely high. More importantly, to meet the agricultural water requirement, most of the poor farmers of Dahuk basin area rely on river water. During monsoon season (June to October), Dahuk river fulfils the stakeholder's demand for agricultural, domestic and industrial water requirements but, when water

becomes infrequent in the non-monsoon season, around 33% of people forcefully rely on groundwater for irrigation, thus, creating significant stress on groundwater. Besides, the lack of water availability in Dahuk river in non-monsoon period threaten the ecosystem stability and livelihoods of people that depend on the river.

Drought is another problem in the study area. Around 28% respondents have suffered drought in Dahuk River basin area (Field survey, 2016). In addition, 37% respondents said that extreme sand and stone mining are continually killing the riverbed of the Dahuk river. Setting up grinding stone machine near the river and inappropriate sand and stone mining could be a vital reason for river erosion. 21% respondents are affected directly by the river erosion. In addition, air pollution is a remarkable problem in the study area where emission of CO_2 and CO from several brickfields is a great threat for the vitality of ecological stability. Moreover, Dahuk river has been changed its course with 15 degrees inclined from east to west at "Guccha gram" area (Field survey, 2016). In addition, bad odour is found in river water which is increased in monsoon period though the water level is high at this time. Wetting jute, dumping human and industrial wastes are the main reasons to spread bad odour, and watercolour becomes blackish. 70% respondents are not using river water for drinking and domestic purposes as water is unsafe.

3.5 Sustainable rural livelihoods framework

Livelihoods of rural Bangladesh is dependent on both agricultural and non-agricultural businesses (Ahmed et al., 2015). As an agrarian country, agriculture is the root of the rural livelihoods in Bangladesh. However, a livelihood is sustainable when it can cope with and retrieve from stresses and shocks, keep up or ameliorate its capabilities and assets, while not damaging the natural resources (Smyth & Vanclay, 2017). The study starts with an analysis of people's livelihoods and how these have been changing over time. Social progress like basic human needs, the foundation of well-being and opportunities can contribute to achieve the Sustainable Development Goals related to water (SDGs, 2016). Table 2 has demonstrated the relationship between sustainable goals with the analysis of the research.

Table 2: An approach to change: enhanced capabilities and social life

Sustainable Livelihood Framework				
SDGs Goal No & Name	Goal's targets	The research findings	Possible ways to meet the SDGs	Recommendations
1. End poverty in all its forms everywhere.	1.4 By 2030, ensure that all men and women, in particular the poor and the vulnerable, have equal rights to economic resources, as well as access to basic services, ownership and control over land and other forms of property, inheritance, natural resources, appropriate new technology and financial services, including	Monthly household's income indicates that there has had a higher number of poor compared to per capita income (FAO, 2017).	In the study area, creating equal opportunities could minimize the vulnerable condition (Gerard et al., 2012). Social life and environment could be enriched by enhancing the quality education, health, and other social services (Ali & Zhuang, 2007). Besides, higher agricultural productivity could play a vital role to established	The local and international NGOs and the government should work together for poverty mitigation. Besides, giving microcredit with low-interest rate could be more efficient.

	microfinance.		Sustainable livelihoods framework (Ali & Zhuang, 2007). Activities of the social entrepreneur like the Institute of OneWorld Health (USA) and Sekem (Egypt) could enrich the social structure (Christian & Johanna, 2004).	
2. End hunger, achieve food security and improved nutrition and promote sustainable agriculture.	2.1 By 2030, end hunger and ensure access by all people, in particular the poor and people in vulnerable situations, including infants, to safe, nutritious and sufficient food all year round.	Water scarcity is a significant constraint for adequate food production. Transboundary river conflict is a challenging issue for Bangladesh. Agricultural water demand in the downstream area is affected when the water body is controlled by upstream county (Strasser el al., 2016). Morevoer, farmers claimed that the productivity of rice production is decreasing in recent past (Field survey, 2016).	Rain-fed agriculture and conjunctive use of water could reduce the pressure on groundwater (Rahaman & Shehab, 2017). The rain-fed agricultural practice is more beneficial for poor farmers as it is areound two times more effecient than irrigated agriculture (Seckler, & Amarasinghe, 2000). Besides, high yield varieties crops are grown in rain-fed agriculture, which positively effects food security. Food should be stored in monsoon season for using during drought.	Need to prioritize in some factors for the improvement of food security that includes, implementation of high yield verities crop, reducing yield gap, improvement of irrigation efficiency and ensuring adequate storage facilities for the crop as well as water resources.
3. Ensure healthy lives and promote well-being for at all ages	3.8 Achieve universal health coverage, including financial risk protection, access to quality essential health-care services and access to safe, effective, quality and affordable essential medicines and vaccines for all.	Health facilities are inadequate in study area. In particular, high population growth rate, increasing water demand, and contamination form unplanned waste disposal system have adverse impacts on human health.	Increase investment in the health sector, and the recruitment, development, training, and retention of the health workforce should be encouraged to ensure health amenities.	Usually, rural people live in fresh and contamination free environment but, nowadays, they have affected by several diseases (Saadat, 2010). Health system should improve by investing cost-effective primary health care services including care centers provided by the government and non-government organization.
4. Ensure inclusive and qual¬ity education for all and	4.1 By 2030, ensure that all girls and boys complete free,	Educational qualification among the stakeholders is	The government should take urgent steps for providing primary and secondary education	Providing primary education was the earlier objective of Millennium

promote lifelong learning.	equitable and quality primary and secondary education leading to relevant and effective learning outcomes. 4.3 By 2030, substantially increase the number of youth and adults who have relevant skills, including technical and vocational skills, for employment, decent jobs and entrepreneurship	quite low in Dahuk basin area. Most importantly, farmers have no education and, thus, not able to adopt advanced agricultural technology.	efficiently among all the stakeholders. Moreover, they need to encourage the private sectors for more investment for the development of educational tools, policy, and practice.	Development Goals (MDGs) but providing secondary education and promote lifelong learning is the new target of SDGs which is very aspirational for developing countries to come out from poverty. Without quality education, no sustainable development goal (SDGs, 2017) can be achieved.
6. Ensure availability and sustainable management of water and sanitation for all	6.1 By 2030, achieve universal and equitable access to safe and affordable drinking water for all. 6.2 By 2030, achieve access to adequate and equitable sanitation and hygiene for all and end open defecation, paying special attention to the needs of women and girls and those in vulnerable situations. 6.5 By 2030, implement integrated water resources management at all levels, including through transboundary cooperation as appropriate.	Water scarcity is a common issue in Dahuk river basin area. Decline of groundwater table is caused by the unsustainable extraction of groundwater to fulfill the agricultural demand. Poor sanitation facilities and unplanned waste disposal in Dahuk river have adverse impacts on drinking water. Most of the toilets are built near the riverside and poor operation and maintenance of sanitation results to rapid deterioration of river water (cf. Brikke and Bredero, 2003; Field Survey, 2016). Moreover, function and maintenance of water supply and sanitation system are	Freshwater is a vulnerable and essential resource and should be managed in an integrated manner (Rahaman & Varis, 2005). Water development and management mainly depend on the approach involving users, planners, and policymakers. A nationwide program known as Water Sanitation, and Hygiene (WASH), developed by BRAC aims to enhance the health situation of the poor (Nowreen et al., 2011). It will accommodate safe drinking water for 8.5 million people and sanitation facilities for 17.5 million people in 150 Upazila around the country (Nowreen et al., 2011). Village-level Operation and Maintenance (VOLM) is known as a sustainable technology for operation and maintenance at the community level to ensure long-term	Practices of harvesting less water consuming crops in dry season could reduce the stress on groundwater. The government should establish a proper monitoring system and legislation for using groundwater. Besides non-government organization and the citizens need more closely involved to improve the overall scenario. Most importantly, negotiation needs to be made with the upstream country to solve the transboundary river issues and meet the SDGs.

		neglected by communities as well as the government. However, transboundary river conflict is one of the challenging issues in Bangladesh. Controlling the river body by upstream county results to increase the water insufficiency due to the inadequate flow of surface water during the non-monsoon season.	benefits (Brikke and Bredero, 2003). The following policies stated by EC (2000) and Hall (1998) could be the sustainable approaches for mitigating the adverse impact. • Expanding the scope of water protection. • A strong commitment to pollution prevention by set up a deadline. • A requirement to amplify the advanced technology for waste treatment and disposal. • Need to established guideline of emission and environment-friendly legislation for sustainable development. Increasing the availability of surface water for irrigation during non-monsoon months should be ensured through transboundary water cooperation. Besides, reducing the use of groundwater and increasing irrigation efficiencies should be encouraged. Promoting the conjunctive use of surface and groundwater for irrigation should be promoted (cf. Rahaman & Shehab, 2017).	

4. CONCLUSIONS

This study examines the impacts on the livelihoods of residents due to the variation of Dahuk river's discharge in 'Tetulia' Upazila of 'Panchagarh' district in Bangladesh. In the survey, approximately 100 stakeholders were randomly selected to collect primary data to identify the impacts of the temporal variation of Dahuk river discharge on the livelihoods of the people living in Dahuk river basin area inside Bangladesh. These impacts are summarized below.

45% of the respondents are farmers and majority of them fully depend on Dahuk river's water to fulfil their agricultural water demand. Water scarcity in non-monsoon period is the most concerning issue in the study area. During non-monsoon period (February –April), the discharge of Dahuk river was only 0.08 m^3 per second , and during the monsoon season

(July-September) the discharge increased to 48.6 m^3 per second. Besides, transboundary river conflict is one of the challenging issues in Bangladesh. Controlling the river body by upstream country could results in further increase of the water scarcity due to the inadequate flow of water in Dahuk river during the non-monsoon period. Therefore, the propensity of unsustainable use of groundwater is increasing day by day.

Approximately, 75% respondents directly depend on the Dahuk River for their livelihoods. In terms of economic stability of farmers and fishermen, monsoon season brings more economic benefits for the fisherman in comparison to farmers. Likewise, the monsoon season is also suitable for tea gardening, as it needs much water for cultivation. On the other hand, the non-monsoon season is beneficial for the sand miner, as it is easier to collect stone from the Dahuk River without excavation. However, income and livelihoods diversification index (see Table 1) indicates that the stakeholder's income is more diversified in the non-monsoon season. Many farmers, fishermen, and stone miners have to forcefully change their professions with the seasonal variation of Dahuk's discharge. The river water plays a vital role to fulfil the agricultural, drinking, and industrial water demand. However, unsustainable sanitation practices, lack of industrial waste disposal system, wetting of jute in Dahuk river are the main reasons of decreasing water usability day by day. Already 70% respondents are not using river water for drinking and domestic purposes as water is unsafe.

As the seasonal change of Dahuk river discharge have adverse impacts on agriculture, livelihoods, and well-being of the stakeholders in the study area, a holistic policy approach, presented in table 2, should be considered to enhance the adaptability of local people, minimize the vulnerability and established a sustainable livelihood framework in Dahuk river basin area of Bangladesh in line with the United Nations Sustainable Development Goals.

ACKNOWLEDGEMENTS

The excellent support from the Department of Civil Engineering, University of Asia Pacific, and its staff is greatly appreciated. Thanks to Rony Ahammed and Anamul Karim for their participation during the field study.

REFERENCES

Adel, M. M. (2013). Farakka Barrage, the greatest ever riparian bluff for upstream water piracy. *Academia Journal of Environmental Sciences,* 1 (3), 036-052.

Afroze, S. (2014). Livelihood status of fishing community of the Tetulia River in Barisal district, Bangladesh (Doctoral dissertation), Bangladesh Agricultural University, Mymensingh. (http://dspace.bau.edu.bd)

Ahmed, M. T., Bhandari, H., Gordoncillo, P. U., Quicoy, C. B., & Carnaje, G. P. (2015). Diversification of rural livelihoods in Bangladesh. *Journal of Agricultural Economics and Rural Development*, 2 (2), 32-38.

Allan, C., & Curtis, A. (2002). Participatory rural appraisal. *Natural Resource Management*, 5 (1), 28-34.

Ali, I., and J. Zhuang. (2007). Inclusive Growth toward a Prosperous Asia: Policy Implications. *ERD Working Paper No. 97*. ADB. Manila.

Asadullah, M. N., Amarasuriya, H., Konte, M., Khan, M. R., & Diamint, R. (2016, October 17). Jeffrey Sachs on meeting the Sustainable Development Goals – 'we need a victory of ideas'. *The Conversation*. Retrieved from https://theconversation.com/jeffrey-sachs-on-meeting-the-sustainable-development-goals-we-need-a-victory-of-ideas-66839

Bhaduri, A., & Barbier, E. (2008). *Linking rivers in the Ganges-Brahmaputra River Basin: exploring the transboundary effects*. Strategic Analyses of the National River Linking Project (NRLP) of India Series 2, 373.

BWDB (Bangladesh Water Development Board) (2011). Rivers of Bangladesh, 2nd Edition. Processing and Flood Forecasting Circle, Bangladesh Water Development Board, Tejgaon, Bangladesh.

Christian, S., & Johanna, M. (2004). Social entrepreneurship: Creating new business models to serve the poor. *Business Horizons*, 48 (3), 241-246.
FAO (2017). AQUASTAT database, Food and Agricultural Organization of United Nations. (http://www.fao.org/nr/water/aquastat/data/query/index.html?lang=en)
FAOSTAT (2017). Database for food and agriculture, Food and Agricultural Organization of United Nations. (http://faostat.fao.org/site/291/default.aspx)
Field Survey (2016). Field survey conducted by the respective authors from 19 July 2016 to 23 July 2016.
Gain, A. K., Giupponi, C., & Renaud, F. G. (2012). Climate change adaptation and vulnerability assessment of water resources systems in developing countries: a generalized framework and a feasibility study in Bangladesh. *Water*, 4, 345-366.
Gerard, G., Anita, M., & McGahan, J. P. (2012). Innovation for Inclusive Growth: Towards a Theoretical Framework and a Research Agenda, *Journal of Management Studies*, 49 (4), 661–683.
IUCN (2014). Rivers beyond borders: India-Bangladesh transboundary river atlas, IUCN, Dhaka. (http://www.watermuseum.net/wp-content/uploads/)
Jagerskog, A., & Zeitoun, M. (2009). Getting Transboundary Water Right: Theory and Practice for Effective Cooperation. (Report No. 25). Stockholm: Stockholm International Water Institute, SIWI.
LGED (2016). Official website of Local Government Engineering Department. Ministry of local government rural development and cooperatives. (http://www.lged.gov.bd/ViewMap2).
Peña, H. (2011). *Social Equity and Integrated Water Resources Management*: Volume 15 of TEC background papers. Global Water Partnership, Technical Committee (TEC).
Rahaman, M. M. (2009). Integrated Ganges basin management: conflict and hope for regional development. *Water Policy*, 11, 168–190.
Rahaman, M. M. (2015) Principles of transboundary water resources management and frontier watercourses agreement between Finland and Russia: An analysis, In: Tvedt, T., Mcintyre, O., Woldesadik, T.K. (Eds.) *Sovereignty and International Water Law*, pp. 442-464 (I.B. Tauris, UK). [ISBN: 9781780764481]. DOI: 10.13140/RG.2.1.1163.0240
Rahaman, M. M., & Rahman, M. M. (2017). Impacts of Farakka barrage on hydrological flow of Ganges river and environment in Bangladesh. *Sustainable Water Resources Management*. Doi: 10.1007/s40899-017-0163-y
Rahaman, M. M., Shehab, M. K., & Islam, A. (2016). *Total production and water consumption of major crops in South Asia during 1988-2013*. Proceedings of Conference on Water Security and Climate Change: Challenges and Opportunities in Asia, Asian Institute of Technology, Bangkok, Thailand, November 29 –December 1, 2016.
Rahaman, M. M., & Shehab, M. K. (2017). *Water consumption, land use and production patterns of rice, wheat and potato in South Asia during 1988-2012*. Manuscript submitted for publication.
Rahaman, M. M., & Varis, O. (2009). Integrated Water Management of the Brahmaputra Basin: Perspectives and Hope for Regional Development. *Natural Resources Forum*. 33(1), 60-75. Doi: 10.1111/j.1477-8947.2009.01209.x
Rahaman, M.M. & Varis, O. (2005) Integrated Water Resources Management: Evolution, Prospects and Future Challenges, *Sustainability: Science, Practice and Policy* (USA), 1(1): 15-21.
Reid, W. V., Mooney, H. A., Cropper, A., Capistrano, D., Carpenter, S. R., Chopra, K., … Zurek, M. B. (2005). *Ecosystems and Human Well-Being: Millennium Ecosystem Assessment*. Island Press: Washington, DC, USA, 2005
Roy, R., Chan, N. W., & Rainis, R. (2014). Rice farming sustainability assessment in Bangladesh. *Sustainability Science*, 9, 31-44.
Saadat, A. M. (2010). *Impact of climate change on rural livelihood: a case study*. Institute of Water and Flood Management. Bangladesh University of engineering and technology (BUET), Dhaka.
Seckler, D., & Amarasinghe, U. (2000). *Water supply and demand, 1995 to 2025* (IWMI, Annual Report 1999–2000, 9-17). United Kingdom: University of Sussex, Brighton.
Shiyani, R.L. and Pandya, H.R. (1998). Diversification of agriculture in Gujrat: A spatio-temporal analysis. *Indian Journal Agricultural Economics*, 53(4): 627-639.
Strasser, L. D., Lipponen, A., Howells, M., Stec, S., & Brethaut, C. (2016). A methodology to assess the water energy food ecosystems nexus in transboundary river basins. *Water*, 8(2), 59.
Sustainable Development Goals (SDGs) (2017), United Nations SDGs, New York: United Nation. (http://www.un.org/sustainabledevelopment/hunger/)

Proceedings of the 4th International Conference on Civil Engineering for Sustainable Development (ICCESD-2018), 9~11 February 2018, KUET, Khulna, Bangladesh (ISBN-978-984-34-3502-6)

HYDROLOGICAL CHARACTERISTICS OF PUSSUR RIVER AND ITS NAVIGABILITY

Md. Motiur Rahman[1], and Md. Shahjahan Ali[2]

[1] Executive Engineer, Mongla Port Authority, Bangladesh, e-mail: khan.motiur06@gmail.com
[2] Professor, Department of Civil Engineering, Khulna University of Engineering and Technology, Bangladesh, e-mail: bablu41@yahoo.com

ABSTRACT

Mongla Port is the second gateway of Bangladesh and an eco-friendly seaport of the country situated at the bank of Pussur River about 131 km upstream from the Bay of Bengal. Mongla Port was designed for an average 8.5m draft ship. But after the construction of Jetties at Mongla Port, the depths in several areas of Pussur Channel reduced significantly and regular maintenance dredging is required to provide adequate depth. The objective of the study is to investigate the hydrological characteristics of Pussur river based on available bathometric survey data and hydrographic charts and to study the availability of required draft for navigability of Pussur River. From the longitudinal section of navigation route of Pussur River, it has found that about 16 km river reach called outer bar at the entrance of Pussur river don't have enough draft for 7.5 m draft vessel. From Hiron Point to Harbaria Anchorage, the river has sufficient draft to navigate upto 10.0 m draft vessel. But about 13 km in the base creek area and Port Jetty area called inner bar is suffering for scarcity of sufficient water depth even for 7.0 m draft vessel. The upstream of Harbaria anchorage is shallower and maximum 7.5 m draft vessel can arrive to Mongla Port. At Present, the water depth in upstream area of Mongla Port is about -4.5 m CD. As the channel proceeds from Port Jetty to the proposed power plant jetty at Rampal, the depth further decreases and minimum water depth of this stretch is about 2-3 m, only ordinary inland vessels can negotiate with this depth. Therefore, these areas require proper interventions (dredging and/or structural) to enhence the navigability of the pussur river.

Keywords*: Navigability, Pussur river, Vessel Draft, Hydrographic Chart, Bathometry*.

1. INTRODUCTION

Mongla Port, the second gateway of Bangladesh is the most eco-friendly seaport of the country, situated at the confluence of Pussur River and Mongla Nulla, approximately 71 nautical miles (about 131 km) upstream from the Fairway buoy (approaches to the Pussur River) of the Bay of Bengal. The Port is well protected by the largest mangrove forest known as the Sundarbans, part of which has been declared as "World Heritage" in 1997 by UNESCO. The Port provides facilities and services to the international Shipping lines and other concerned agencies providing shore based facilities like 5 (five) Jetty berths (total length 914m), have a capacity of about 6.5 million tones general cargo/break bulk and 50,000 TEUS. The midstream berth (7 buoys & 14 anchorages) have a capacity of about 6.00 million tones. Total 33 ships can take berth in the Port (in the Jetties, buoys & anchorage) at a time. However, alike other modern port of the world Mongla Port is keen to provide highest port facilities, so that bigger draft ships can enter in to the port channel safely.

Mongla Port was designed for an average 8.5m draft ship. But after the construction of Jetties at Mongla Port, the depths in several areas of Pussur Channel reduced significantly and regular maintenance dredging is required to provide adequate depth alongside the berths, in the approaches to the berths and in the Southern Anchorage areas (ADB, 1996). The main cause of this siltation is empolderment schemes between the Sibsa and Pussur rivers carried out between 1966 and 1974, resulting in reduction in tidal storage and

redistribution of flow, mostly between the Sibsa and the Pussur river, starting in 1959 (DHI, 1993).

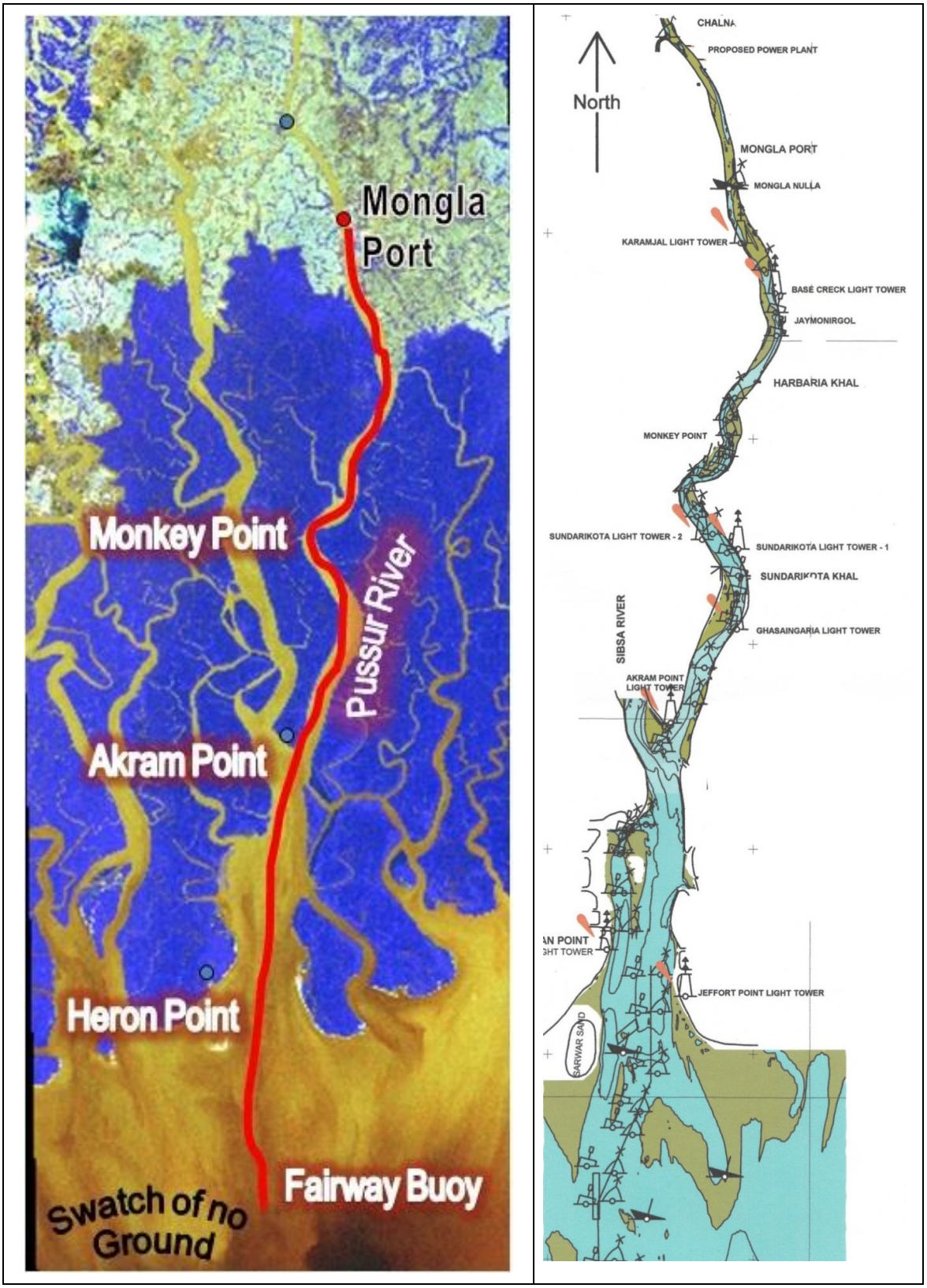

Figure 1: Study reach of Pussur river (IWM, 2013)

Since 1979, several dredging efforts had been made to restore the navigability of the Pussur River. However, because of continued high siltation rates, none of the dredging efforts could sustain a navigable channel and requirement of maintenance dredging has been significant (IWM, 2013). Entrance to the Pussur River is about 6 miles wide at the mouth and has a bar over about 5 miles known as Outer bar where depth is about 6.2m CD (Chart Datum). Ships having draft up to 7.5m can cross the bar in all seasons. The bar is relatively stable with sea bed elevation of -6.4 m CD. With the existing depth in the outer bar, maximum 8.5 m draft vessel can cross the outer bar and enter the port at normal high tide. But the depths over the anchorage area of the channel permit anchoring of 11m draft vessels. Outer bar area is only obstacle for the ships of 11m draft to enter into the anchorage area of Mongla Port.

Moreover Government of the Republics of Bangladesh has undertaken a project to set up a 1320 MW (2 x 660 MW) Coal based Thermal Power Project at Rampal in Bagerhat district of Khulna division, Bangladesh. The power plant is located at approximately at 13 km upstream of Mongla port on the left bank of Pussur River. The power plant is envisaged to be based on super critical technology and fuel envisaged for power generation is imported coal. Around 5.00 Million Tons Per annum (MTPA) of imported coal shall be required for the project which amounts to approximately 15,000 tons of coal movement per day through Pussur river channel. The Power plant authority plans to procure coal from Indonesia or Australia or South Africa or elsewhere. The coal will brought to Bangladesh in partly loaded mother vessels of approximately upto 55,000 DWT, which will berth at Harbaria Anchorage/ Hiron Point Anchorage. But due to non availability of sufficient depth, coal from Harbaria Anchorage/Hiron point will be transshipped to feeder ship having draft approximately 7.50 m. Presently the water depth in upstream area of Mongla Port is about -4.5 m CD. After establishment of power plant, the navigation channel of Mongla Port will be extended another 13 Km.

Mongla Port Authority (MPA) has implemented three capital dredging project between 1990 to 2014. But after every capital dredging the back filling rate is very high and it's becoming a very big challenge for the existence of Port. Therefore it is a very important task to understand the hydrological and morphological characteristics of Pussur River. The overall objective of the study is to investigate the previous studies, available bathometric survey data and hydrographic charts to characterize the Pussur River and availability of required draft for navigability.

2. METHODOLOGY

The study area covers about 145 km navigation route of Pussur River from Fairway Buoy (Bay of Bengal) to Chalna. The Rampal power station is a proposed 1320 megawatt coal-firedpower station located at Rampal Upazila of Bagerhat District and 13 km upstream of Mongla Port. Mongla Port is situated on the east bank of Pussur River about 131 km upstream from the fairway buoy. Figure 1 shows the study reach of Pussur river. Bathymetric data surveyed by Mongla Port Authority (MPA) is the main secondary source of the bathymetric data. MPA bathymetric charts surveyed for different years from Chalna to Fairway buoy have been collected to analyse the bed topography of the Pussur River.

2.1 Topographical Features of Pussur River

The navigation channel as well as the Port limit of MP has started from Fairway Buoy, a deep point in the Bay of Bengal. After fairway to Akram point the wider approach is known as approach to Pussur. At the Akram point it is divided into streams, the eastern one is Pussur and the western one is Sibsha. The main stream of Pussur Channel started from Hiron Point and ended at Chalna. The downstream portion of Hiron Point is actually a part of the sea. Between Mongla Port and the sea, the Pussur River channel is generally straight, with weak

meanders. Only one strong meander is observed at the confluence with Monkey point, 35 km downstream of Mongla. Sinuosity for the whole Pussur Channel from Chalna to Hiron Point has calculated. According to MPA Hydrographic chart no. MPA/HP-CB/12(a)/2008 & MPA/CB-D/12(b)/2008, the areal distance (straight) of Hiron Point to Chalna is 55 km out of the channel length of 91 km. The ratio of straight length to channel length is found as 1:1.65, which implies that the channel is mildly meandering. According to Leopold and Wolman (1957), a river can be considered straight till the sinuosity 1.5. For Pussur river, the sinuosity just crossed the limit.

Based on the MPA Hydrographic charts and available information from hydrographic section of Mongla port, it is observed that the width of the Pussur River varies at different sections between 700 m to 3000 m and approach to the Pussur is about 6000 m. The width and available minimum and maximum depth of those sections are described in Table 1. The minimum depth is found to be varied from 1.4 m to 11.7 m below CD. It can be noted that the lowest depth is found at upstream (Chalna) that gradually increases towards downstream with the highest minimum depth at Mazhar Point to D'Suza Point and again decreases at further downstream near Fairway Buoy. The maximum depth is found to be varied from 7.5m to 29.6 m below CD from upstream to downstream, respectively.

Table 1: Width and Depth of Pussur River at different segments (Source: MPA).

Sl.	River Reach	Length of River Reach (km)	Width of Channel (m)	Min. Width of Navigation Channel (m)	Min. Depth (m Below CD)	Max. Depth (Below CD)
01	Fairway Buoy to Hiron Point	46.30	10,500-6,000	1500	6.2	23
02	Hiron Point to Tinkona Dwip	18.52	7,500 3,750	3500	10.9	22.6
03	Tinkona Dwip to Kagaboga Khal	16.67	4,000-2,500	1800	9.7	19.4
04	Kagaboga Khal to Sundorikota Khal	9.26	2,625-2,125	1000	9.1	22.5
05	Sundorikota Khal to Cheilabogi Khal	9.26	2,150-1,250	900	8.5	29.6
06	Mazhar Point to D'Suza Point	9.26	2250-950	700	11.7	28.0
07	Harbaria to Joymonirgol	9.26	1,800-1,125	550	6.3	23.2
08	Base Creek to Mongla Nulla	9.26	1,750-760	300	5.2	9.8
09	Mongla Nulla to Digraj	9.26	1,500-700	200	5.0	7.5
10	Digraj to Chalna	9.26	1,000-7,00	200	1.4	7.5

2.2 Hydrological Characteristics of Pussur River

The variation of water depth and tidal characteristics in the study area over the years is studied by water level. The water level data analysis shows that the maximum tidal ranges at Mongla during the dry and monsoon period at spring tide in 2015 are about 3.75 m and 3.4 m, respectively. In neap tide the maximum tidal ranges for the dry and monsoon period are 2.0 m and 1.9 m. The seasonal variation at Mongla port between March and September is obtained about 0.9 m. In this study, water level was measured at Chalna for 7 days. The

observed tide data has plotted in Figure 3. The observed data shows that the tidal range is higher at Chalna than Mongla.

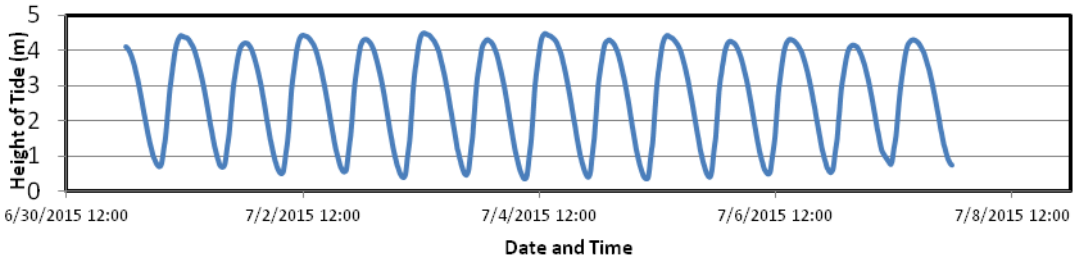

Figure 3: Water level at Chalna (IWM, 2015)

Table 2: Maximum, Minimum and Mean water level and Maximum Tidal range (IWM, 2015).

Location	Duration	Max WL (mPWD)	Min WL (mPWD)	Mean WL (mPWD)	Max Tidal Range (m)
Chalna	07/01/2015 to 07/07/2015	4.518	0.314	2.41	4.204

During weeklong study, the measured water level was found to be varied from 0.314 to 4.518 mPWD (Table 2). Here, the mean water level shows the calculated arithmetic average value of all the measured water level during the measuring period. The tidal range was calculated by the algebraic difference of two consecutive high tide and low tide. Near the Rampal Power Plant at Dacop the tidal range is about 4.204 m.

Semi-diurnal tides with a tidal period of about 12 hours 25 minutes are predominant in the Bay of Bengal. According to the Bangladesh Tide Tables 2015, the mean Tide Levels at Mongla, and Hiron Point along Pussur River are 2.31m and 1.7m in CD respectively (Table 3). The tidal regime is larger at Mongla than at Hiron Point.

Table 3: Tidal levels at Mongla and Hiron Point

Stations	Lowest	Mean	Highest
Mongla (Bangladesh Tide Tables, 2015)	-0.261	2.310	4.882
Hiron Point (Bangladesh Tide Tables, 2015)	-0.256	1.700	3.656

Discharge is an important key factor for the navigability of Pussur Channel. Siltation or scouring of river bed is directly related with the discharge. To understand the hydrology of study area, discharge has measured during spring and neap covering both flood tide and ebb tide. The observed data has plotted in Figure 4 and 5. The summarized observed data has given in Table 4 which shows that the flow in ebb tide is always higher than flood tide at Mongla.

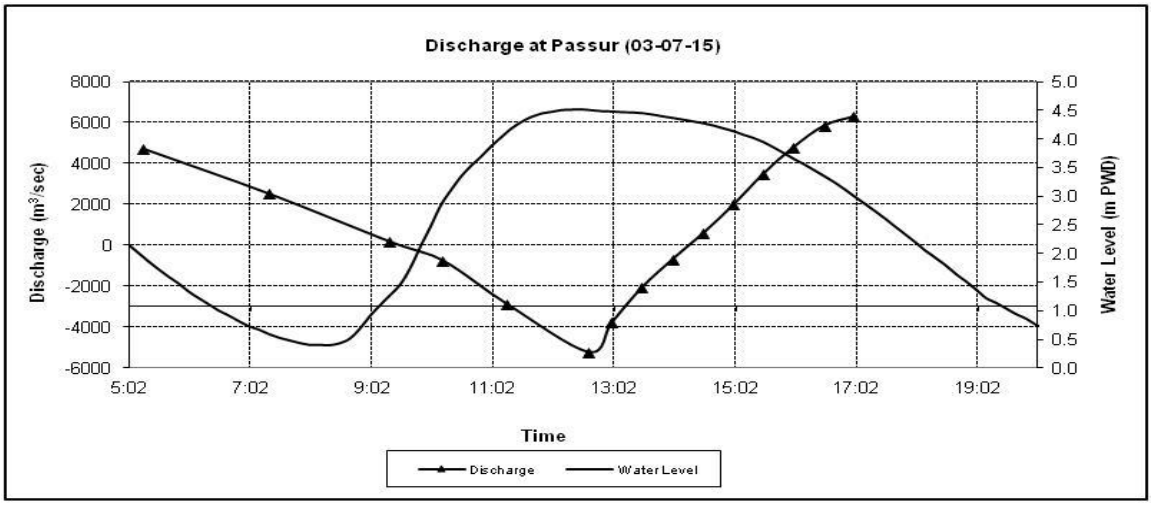

Figure.4: Discharge and water level during spring tide at Mongla (IWM, 2015)

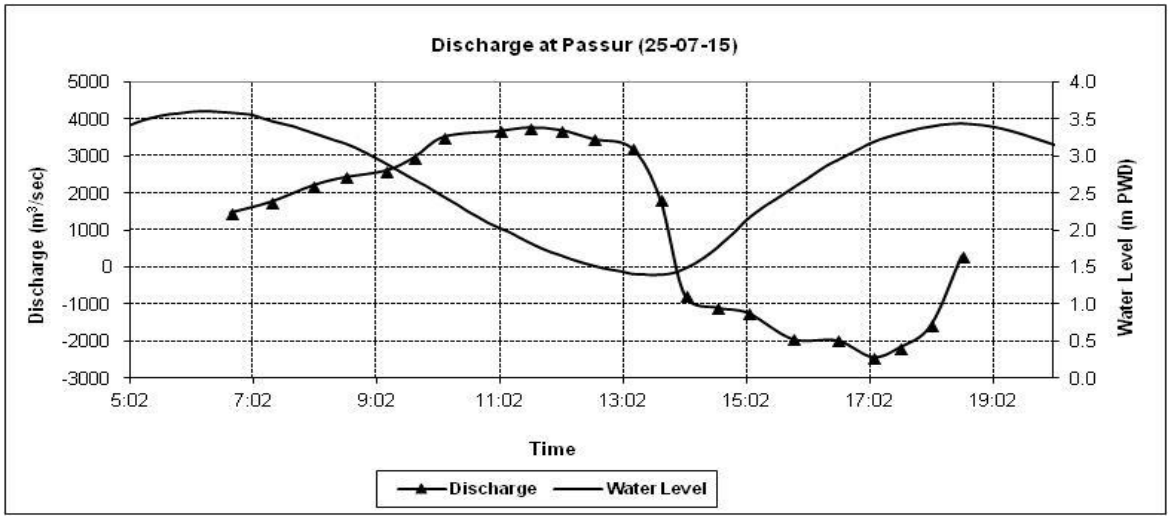

Figure 5: Discharge and water level during neap tide at Mongla (IWM, 2015)

Table 4: Maximum discharge during flood tide and ebb tide (IWM, 2015)

Location	Measurement Period	Type of tide	Max flow during flood tide	Max flow during ebb tide
Mongla	03-07-2015 (half hourly)	Spring	5227	6272
Mongla	25-07-2015 (half hourly)	Neap	2434	3771

3. SEDIMENT TRANSPORT IN THE PUSSUR RIVER

The navigability of Pussur channel is mainly suffering for high sedimentation in the main stream. Sedimentation mainly occurs in dry season when the flow velocity reduces significantly. According to the discussion with the concerned officials of MPA, it was found that the area of tidal prism has reduced significantly after constructions of polders and sluice gates at the mouth of khals of Pussur River. Before those interventions, tidal flow with high sediment volume was allowed to enter into khals and open areas where most of the

sediments were deposited and fresh water returned in the river at ebb tide. But now most of the sediments deposit in the river due to those interventions.

DHI (1993) has collected a large quantity of data on this river, based on which the governing physical processes and the nature of the sediment transport processes in the Pussur River can be understood. From the suspended samples analysis, DHI concluded that the main part of the suspended sediment material consists of silt which is only represented in the bed material by approximately 5 percent. Consequently, the suspended sediment picked up in the measurements for the main part consists of wash load. Silt is generally not found in the bed along the main flow of Pussur River indicates that suspended silt contribute in any significant way to the erosion/deposition processes along the river. The bed material along the main flow areas of the bigger rivers is fine sand. Closer to the banks it is often mainly silt. The suspended fine material does not contribute significantly to erosion/sedimentation processes in the main flow regions of the bigger rivers including the navigation channel of Mongla Port. The transport of bed material is significantly smaller, of the total sediment approximately of one third (DHI, 1993).

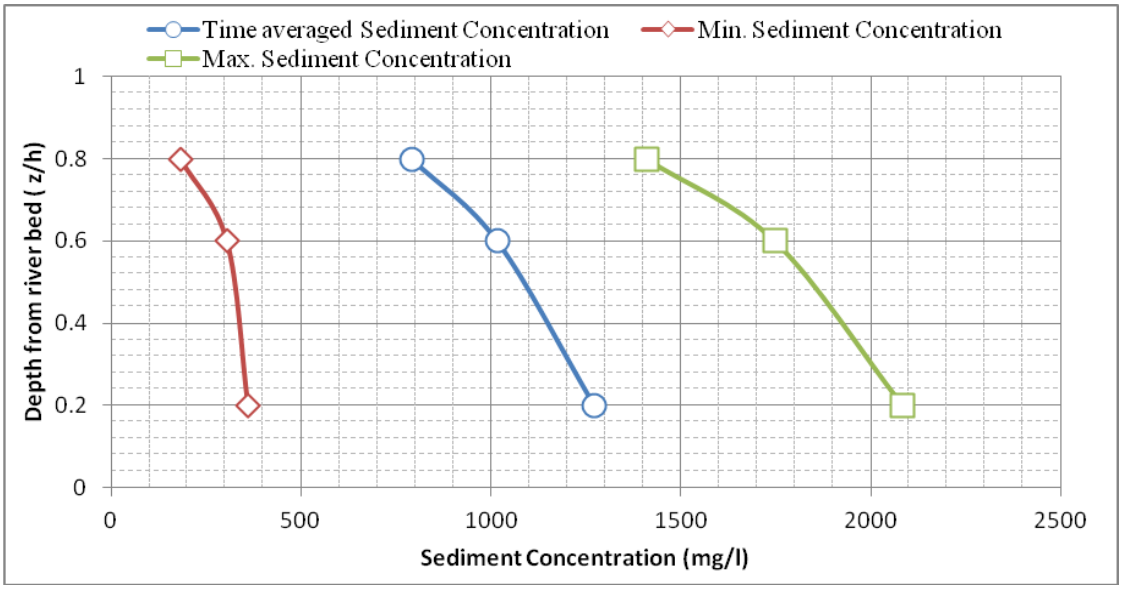

Figure 6: Depth-wise variation of Suspended sediment concentration in the Pussur River at Mongla Port area during spring tide

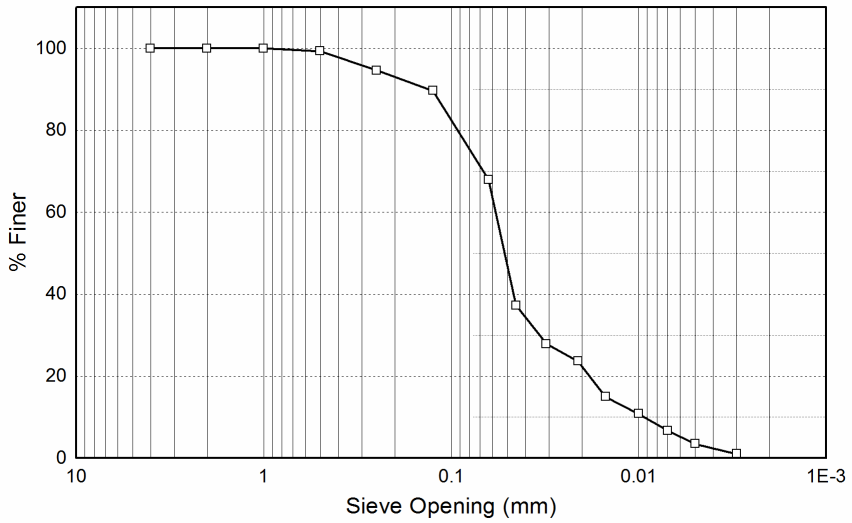

Figure 7: Average grain size distribution of bed material

In this study, suspended sediment concentration at 0.2d, 0.6d and 0.8d (d is the water depth) has been measured during the spring tide for 13 hours. The result shows that, sediment concentration near the river bed (i.e. at 0.8d depth from surface) is always higher than the upper layers at 0.6d and 0.2d from surface. At 0.8d, the concentration varies from 359.65 mg/l to 2096.06 mg/l in flood tide which changes inversely with water level and velocity. At 0.2d, the concentration varies from 153.6 mg/l to 1478.0 mg/l. Figure 6 shows the depth-wise variation of suspended sediment concentration for three scenarios: minimum, maximum and time averaged (12 hrs) sediment concentration profile. It is observed that at low concentration the sediment concentration profile is quite stiff and nearly vertical, means sediment gradient is low. On the other hand, the profile is flatter for higher concentration, and in this case the sediment concentration gradient along the depth is high. In the time averaged profile, the concentration is found as 790 mg/l at 0.2d depth and 1270 mg/l at 0.8d depth. From the time averaged profile, the mean concentration is estimated about 1000 mg/l.

Sediment deposits in the estuaries consist of various proportions of gravel, sand, silt, clay and organic matter. Mc Dowell & O'Corner (1977) reported that gravel and sand are often found at the seaward ends where wave action and residual currents remove the finer fractions, while fine sand, silt, clay and organic matter (often collectively referred to as mud), is found in the upper reaches of an estuary. To investigate the characteristics of river bed material near the Mongla Port area, 4 (four) bed samples were collected and analyzed. Sieve analysis of the bed material shows that the Fineness Modulus (FM) of the collected samples are 0.30, 0.60, 0.48 and 0.49, i.e. the bed material is mostly sandy. Figure 7 shows the average grain size distribution of bed material, where d_{50} is found as 0.052 mm.

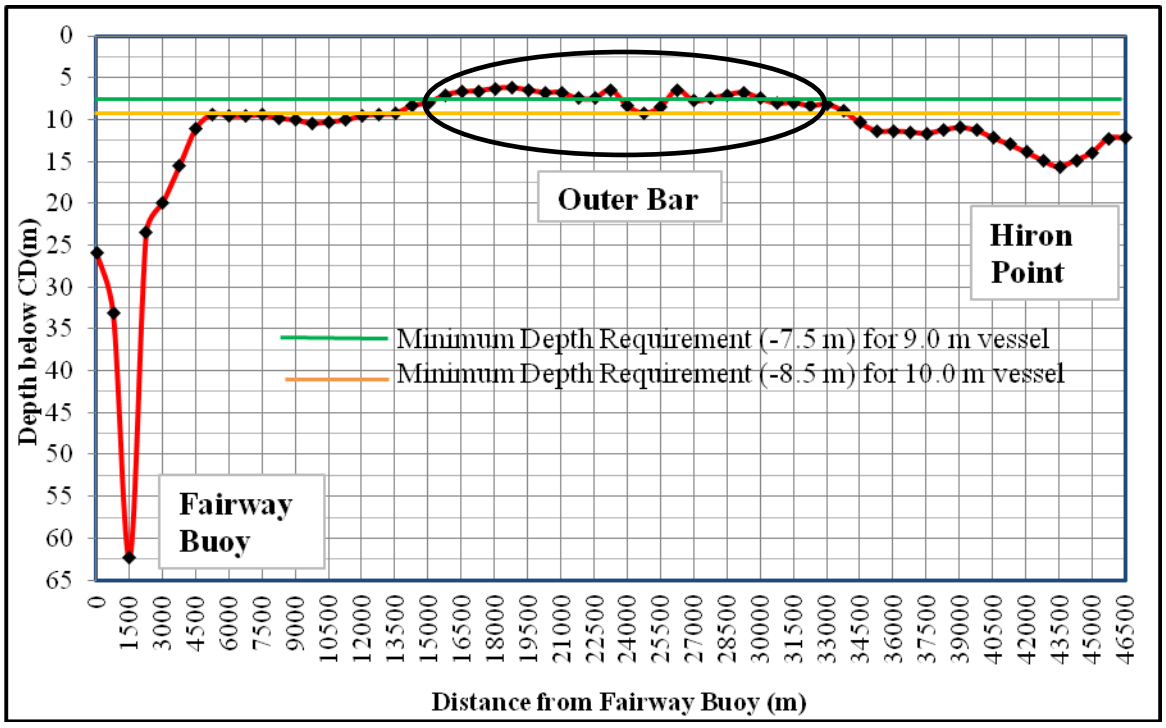

(a) Fairway Buoy to Hiron Point

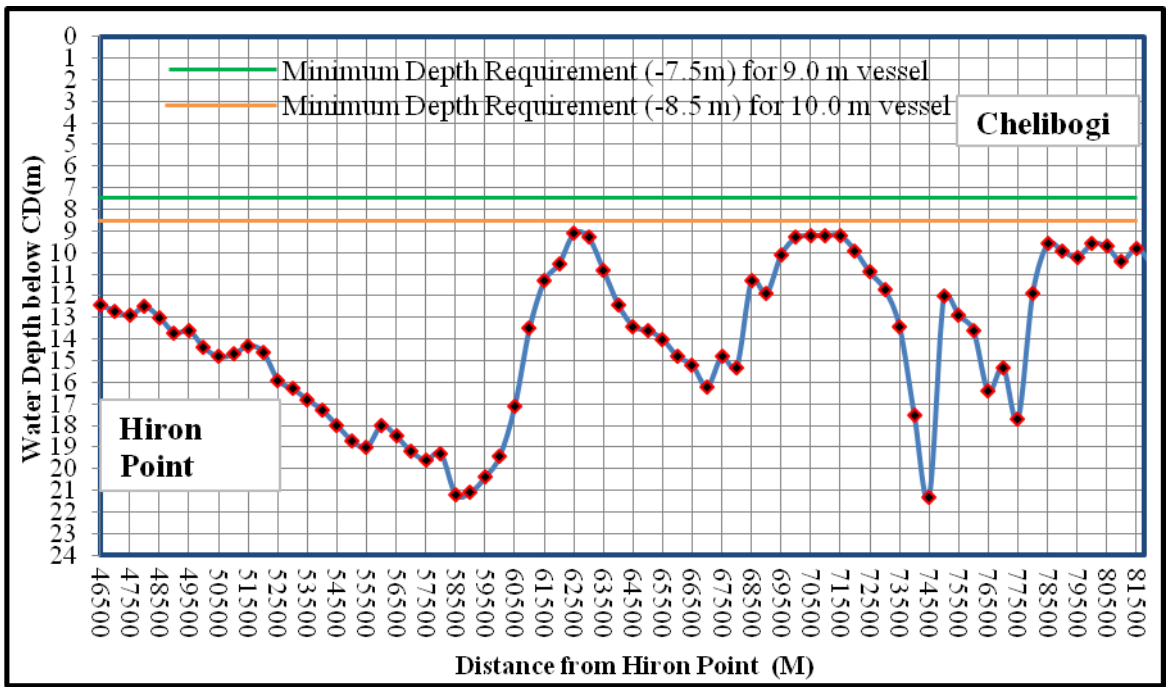

(b) Hiron Point to Chelibogi

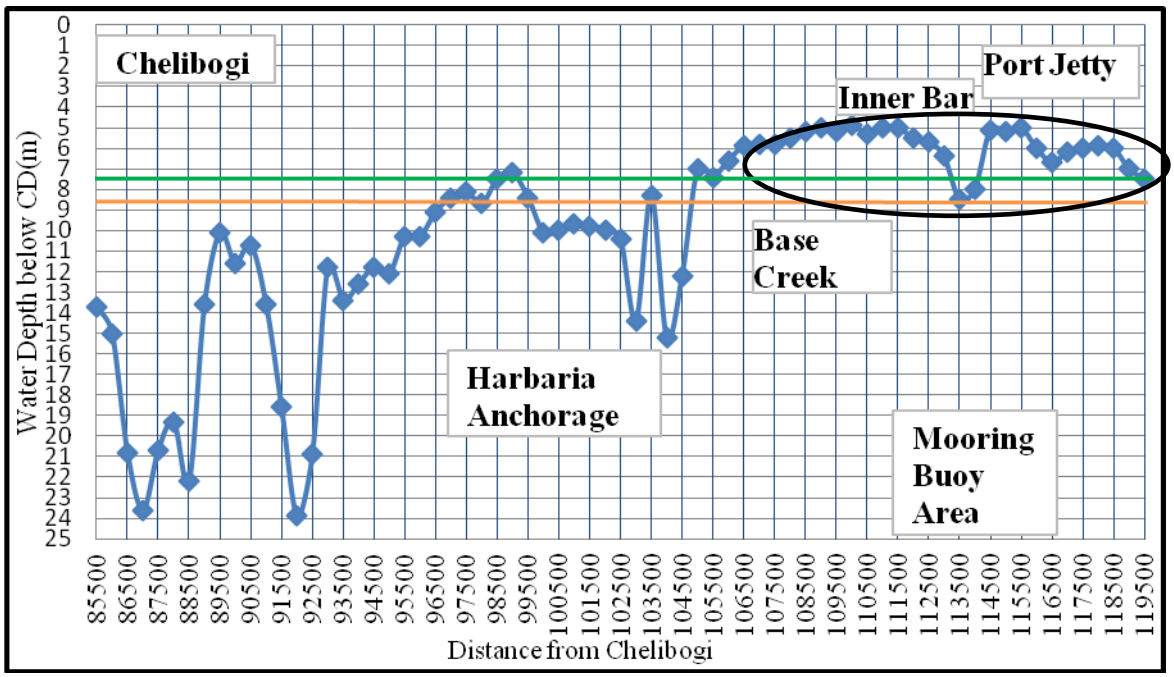

(c) Chelibogi to Mongla Port

Figure 8: Long profile of Pussur River along the navigation line

4. NAVIGATION ROUTE AND ITS NAVIGABILITY

The port limit of MPA started from fairway buoy (in the open sea) and ends at Chalna. Total length of port limit is 149 km. The distance of different important location of Pussur River are given in Table 5.

Table 5: The distance of different important location of Pussur River (Source: MPA)

Important location of Pussur River	Channel Distance
Port Limit (North-South)	149.0 km

PP Jetty - Fairway	131.0 km
PP Jetty - Hiron Point	87.0 km
PP Jetty - Akram Point	68.5 km
Hiron Point - Fairway	44.0 km
Hiron Point - Akram Point	18.5 km
Akram Point - Fairway	62.5 km
PP Jetty - Jhapjhapia River	18.0 km
PP Jetty - Base Creek	13.0 km
PP Jetty - Harbouria Khal	22.0 km
Naval Jetty - Hiron Point	91.0 km

The Bathymetry of the Pussur River has been analysed reach wise from Chalna to Akram Point and also at the Pussur entrance at outer bar area based on the bathymetry charts from 2005 to 2016. The major findings on the navigability of the Pussur river is that, the river has navigation problem for the last two decades mainly from Chalna to Chilla Bazar. After Chilla Bazar, starting from Joymonirgoal, the river shows a more stable navigable reach up to Akram Point and the river is more meandering. Figure 4.9 presents the water depth below CD along the navigation channel from Chalna to Fairway Buoy for the year 2008. From the long section of Pussur River, it has seen that about 16 km river reach called outer bar at the entrance of Pussur river don't have enough draft for 7.5 m draft vessel (Figure 4.9a). From Hiron Point to Harbaria Anchorage, the river has sufficient draft upto 10.0 m draft vessel (Figure 4.9a & 4.9b). Harbaria Anchorage has sufficient draft to handle 10.0 m draft vessel. But about 13 km in the base creek area and Port Jetty area called inner bar is suffering for scarcity of sufficient water depth even for 7.0 m draft vessel (Figure 4.9c). The Pussur River is surveyed by MPA by dividing into 10 segments. However, for navigational purpose, the channel can be divided into following three sections:

Section 1: Fairway Buoy to Akram Point (Downstream to upstream)

The available water depth at Fairway Buoy is above 20-25 m. This depth gradually decreases as ships approach to the river channel due to draft restriction at the outer bar. The shoals along the outer bar in the southern section of 20 km restrict entrance of larger vessel of above 20,000 DWT.

Section 2: Akram Point to Harbaria

The available water depth at Akram Point anchorage ranges from 10 to 15 m. The depth of the channel between Akram Point and Harbaria varies in different stretches. From Akram Point to Kagaboga Khal, it varies from 11 to15 m. After a short patch having 8.00 m to 9.50 m water depth, 10 m up to 21 m depth is available up to D'Souza point. After D'Souza the depth again decreases and up to Harbaria Canal, where the depth is 8 m.

Section 3: Harbaria Anchorage to Chalna

Available water depth at Harbaria Anchorage is 8.5 m~10 m. As the channel proceeds, the depth further decreases from Harbaria to Port Jetty ranging between 5.00 m to 7.50 m. This trend continues up to the proposed power plant jetty at Rampal. Minimum water depth of this stretch is about 2-3 m, only ordinary inland vessels can negotiate with this depth.

5. CONCLUSION

Fresh water flow of Padma Piver and Gorai River is very important for the morphology of Pussur River. Due to low velocity of Pussur River, most of the sediments deposit on river bed which is reducing navigation depth. The most critical sections of this river are: (a) Mongla Port to Rampal power plant, (b) Harbour Area and (c) Outer bar area. Due to depth restriction at outer bar, maximum 8.5 m draft vessel can arrive upto Harbaria anchorage.

The upstream of Harbaria anchorage is shallower and maximum 7.5 m draft vessel can arrive to MP.

ACKNOWLEDGEMENT

The Authors would like to acknowledge the dredging section of Mongla Port Authority for providing necessary data in conducting this research.

REFERENCES

ADB, 1996. Mongla Port Area Development Project, Final Report, Volume I & II, Asian Development Bank-prepared for Mongla Port Authority, Mongla, Bangladesh.

DHI, 1993. Mathematical Model Study of Pussur-Sibsa River System and Karnafuli River Entrance, Final Report, Annex 1 & 2, Bangladesh Water Development Board, Ministry of water resources, Government of Bangladesh.

IWM, 2016. Feasibility study for improvement of navigability at the outer bar area of Pussur channel, Mongla Port Authority, Mongla, Bangladesh

IWM, 2015. Feasibility study of capital dredging in Pussur River from Mongla port to Rampal power plant, Mongla Port Authority, Mongla, Bangladesh,

IWM, 2013. Environmental Impact Assessment of proposed dredging project at Outer Bar Area of Pussur Channel, Mongla Port Authority, Mongla, Bangladesh.

McDowell, D.M. and O'Connor, B.A. 1977. Hydraulic Behaviour of Estuaries, Macmillan Press, Ltd., London, England.

Proceedings of the 4th International Conference on Civil Engineering for Sustainable Development (ICCESD-2018), 9~11 February 2018, KUET, Khulna, Bangladesh (ISBN-978-984-34-3502-6)

POTENTIAL CAUSES OF NAVIGATION PROBLEM IN PUSSUR RIVER AND INTERVENTIONS FOR NAVIGATION ENHANCEMENT

Md. Motiur Rahman[1], and Md. Shahjahan Ali[2]

[1]Executive Engineer, Mongla Port Authority, Bagerhat, Bangladesh, e-mail: khan.motiur06@gmail.com*
[2]Professor, Department of Civil Engineering, Khulna University of Engineering and Technology, Bangladesh, e-mail: bablu41@yahoo.com

ABSTRACT

In this study, historical and recent hydrographic survey charts of the navigation routes in Pussur river were collected from Mongla Port Authority (MPA) and analyzed to assess the trends of morphological changes at the potential sites over the years. It is found that the navigation route in MPA jetty area and its approaches is slightly scouring where the upstream i.e Chalna to Digraj is being silted up (rate approx. 0.22 to 0.95 m/yr). Downstream of mooring buoy is also slightly silted in last few years. The channel is quite stable in Joymonirgol to Hiron point. The current navigational channel at outer bar has siltation pattern (rate approx. 0.35 m/yr) where the west channel is scouring. High backfilling rate is found after dredging (upto 1.3 m/year) in the Sabur Beacon to Joymonirgol area. Channel bed siltation, nmerous wrecks at different positions and humen disturbences are found to be the main cause behind the navigational problems in the river route. The main humen interventions that causing siltation are reducing the upland flow after construction of Farakka barrage and construction of polders around the Pussur River. Approximately 52 wrecks including the sunken ships and sunken barges loaded with cement, billets, jute and jute goods at the bottom of the Pussur River also caused siltation and deterioration of draft. These sunken barges are acting as dangerous silt traps. In this research, some site specific potential measures (purpose based) are suggested including capital dredging and structural interventions to enhance the navigability.

1. INTRODUCTION

Southwestern region of Bangladesh is bounded by the Ganges and the Lower Meghna in the east and by the Indian Border in the west and by the Bay of Bengal in the south. The coastal region of Bangladesh and the rivers in this region shows a continuing process of siltation progressing generally from northwest to southeast. The significant source of upstream freshwater at South-west Bangladesh is the flow of Ganges through Gorai to Pussur. Pussur River is situated in South Western part of Bangladesh and Mongla Port is established on left bank of this river. The Port is the second gateway of Bangladesh situated at the confluence of Pussur River and Mongla Nulla, approximately 71 nautical miles (about 131 km) upstream from the Fairway buoy (approaches to the Pussur River) of the Bay of Bengal. The Port provides facilities and services to the international Shipping lines and other concerned agencies providing shore based facilities like 5 (five) Jetty berths (total length 914m), have a capacity of about 6.5 million tones general cargo/break bulk and 50,000 TEUS. The midstream berth (7 buoys & 14 anchorages) have a capacity of about 6.00 million tones. Total 33 ships can take berth in the Port (in the Jetties, buoys and anchorage) at a time. However, alike other modern port of the world Mongla Port is keen to provide highest port facilities, so that bigger draft ships can enter in to the port channel safely.

Many estuarine and coastal areas around the globe are found to be significantly influenced by human activities. Such activities includes harbor construction, reclamation, dredging and disposal, coastal protection schemes, poldering, dam or barrage construction, commercial fishing, etc. Sediment transport and river morphology of rivers can also be changed significantly due to human activities (Walling, 2006). The vulnerability of many large deltas in the world are increasing due to such disturbances (Syvitski and Saito, 2007; Syvitski et al.,

2009). The empolderment schemes in the Pussur basin, harbor and jetty operation of Mongla port, dredging and disposal, fish farming, etc. affected the morphology and ecology of Pussur river significantly. Mongla Port was designed for an average 8.5m draft ship. But after the construction of Jetties at Mongla Port, the depths in several areas of Pussur Channel reduced significantly and regular maintenance dredging is required to provide adequate depth alongside the berths, in the approaches to the berths and in the Southern Anchorage areas (IWM, 2004). The main cause of this siltation is empolderment schemes between the Sibsa and Pussur rivers carried out between 1966 and 1974, resulting in reduction in tidal storage and redistribution of flow, mostly between the Sibsa and the Pussur river, starting in 1959 (DHI, 1993; Farleigh, 1981; Farleigh,1984). Since 1979, several dredging efforts had been made to restore the navigability of the Pussur River. However, because of continued high siltation rates, none of the dredging efforts could sustain a navigable channel and requirement of maintenance dredging has been significant (Malek and Ashraf, 2004). Entrance to the Pussur River is about 6 miles wide at the mouth and has a bar over about 5 miles known as Outer bar where depth is about 6.2m CD (Chart Datum). Ships having draft up to 7.5m can cross the bar in all seasons. The bar is relatively stable with sea bed elevation of -6.4 m CD. With the existing depth in the outer bar, maximum 8.5 m draft vessel can cross the outer bar and enter the port at normal high tide (IWM, 2013). But the depths over the anchorage area of the channel permit anchoring of 11m draft vessels. Outer bar area is only obstacle for the ships of 11m draft to enter into the anchorage area of Mongla Port.

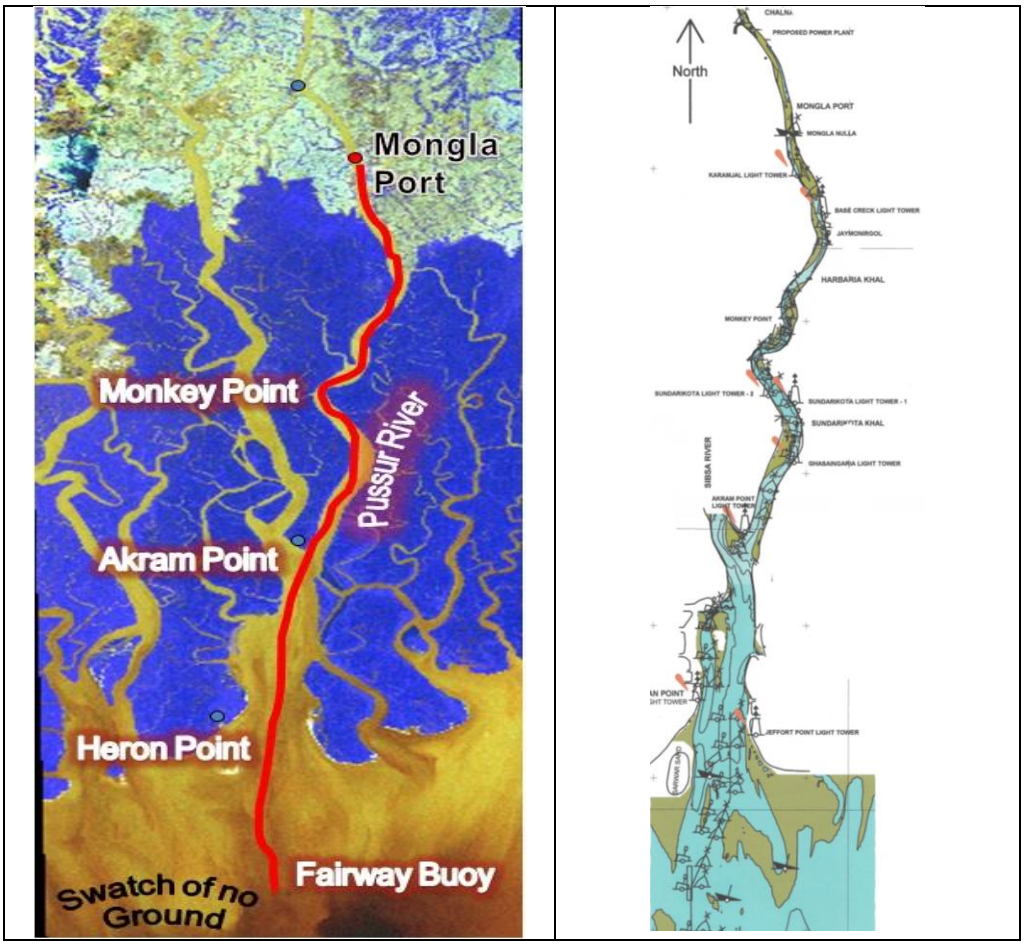

Figure 1: Study reach of Pussur river (IWM, 2013)

Being an important water course for Bangladesh, Gorai River has drawn attention of different national and international researchers (Islam and Karim, 2001; Clijncke, 2001; Sarker, 2002;

Islam and Gnauck, 2012; Shamsad et al. 2014). However, the studies regarding the morphology of Pussur river are very few and those are mainly concentrated on the navigability required for the activities of Mongla port. The overall objective of the study is to investigate the previous bathometric survey data and available hydrographic charts to characterize the change in morphological behavior of Pussur River. The causes of navigation problem, previous intervention and future plan of MPA to improve navigability, dredging history of the river and effectiveness of dredging are discussed. Some potential measures to enhance navigability are also suggested.

2. METHODOLOGY

The study area covers about 145 km navigation route of Pussur River from Fairway Buoy (Bay of Bengal) to Chalna. The Rampal power station is a proposed 1320 megawatt coal-firedpower station located at Rampal Upazila of Bagerhat District and 13 km upstream of Mongla Port. Mongla Port is situated on the east bank of Pussur River about 131 km upstream from the fairway buoy. Figure 1 shows the study reach of Pussur river. Bathymetric data surveyed by Mongla Port Authority (MPA) is the main secondary source of the bathymetric data. MPA bathymetric charts surveyed for different years from Chalna to Fairway buoy have been collected to analyse the past changes in the morphology of the Pussur River. MPA historical and recent hydrographic surveys of the navigation routes in Pussur river was analyzed to assess the trends of morphological changes at the potential sites over the years. Based on the availability of the hydrographic charts, erosion/ deposition scenarios will be assessed for different years. The port limit of MPA started from fairway buoy (in the open sea) and ends at chalna. Total length of port limit is 149 km. Between Mongla Port and the sea, the Pussur River channel is generally straight, with weak meanders. One strong meander of importance for navigation at the confluence with Monkey point, 35 km downstream of Mongla. The width of the channel increase from 1000 m at Mongla, 1500 m at downstream of Monkey point; 3000 m at downstream of Akram Point (Sibsa River confluence); and some 6000 m wide at Hiron Point.

3. POTENTIAL CAUSES OF NAVIGATION PROBLEM IN PUSSUR RIVER

During the establishment of MP at present location, there was sufficient depth for berthing of 8.5 m draft vessel. Siltation started at Jetty area and its approaches after 1980 (MacDonald, M., 1998). One of the main reasons of siltation is reducing the upland flow after construction of Farakka barrage (Mirza and Hossain, 2000; Ali et al, 2012; Kowser and Samad, 2016) and construction of polders around the Pussur River (Dusgupta et al. 2014; Islam and Gnauck, 2008). Another threat for navigability is the wrecks at different position of Pussur River.

3.1 Channel Bed Siltation

Siltation in Pussur River mainly happens in three segments which are: (a) Chalna to Digraj-upstream of MP (b) Mongla Port to Base Creek Khal- Harbour area and (c) Downstream of Hiron Point- Outer Bar. The rate and amount of siltation/ scouring in those three areas has identified in various study and which are summarized below:

3.1.1 Chalna to Digraj- upstream of MP

In the feasibility study for capital dredging of Pussur River from Mongla port to Rampal power plant, IWM (2015) pointed the sedimentation and scouring in 05 dredging areas as Table 1. It is observed that the channel is aggrading type with yearly rising of bed level varies from 0.21 to 0.97 m.

Table 1: Sedimentation in different segments between Mongla jetty to Chalna (considering changes between years 2013-2015)

Location of navigation channel segment	Average Siltation depth (m/year)
Power Plant Turning Ground (600 m × 300 m segment)	0.97
Power Plant Jetty Front (500 m × 200 m segment)	0.43
Maidara - Jetty Front (2400 m × 200 m segment)	0.45
Digraj – Maidara (3140 m × 200 m segment)	0.21
Sabur Beacon – Digraj (3000 m × 200 m segment)	0.21

3.1.2 Harbour Area

Table 2 shows the natural siltation/scouring rate at harbor area calculated from hydrographic chart comparing the data of 2013 with 2008. Note that within this period no dredging was performed in the channel. It is observed that the channel is slightly degrading type with yearly lowering of bed level varies from 0.12 to 0.32 m. However, in this area, the high backfilling rate after capital/maintenance dredging is the main problem to get sufficient draft. Figure 2 shows the longitudinal bed profile from Digraj to Mongla showing backfilling within one year after dredging the channel in the year of 2014. After completion of Harbour Area Dredging project, the monitoring consultant IWM carried out monitoring survey and develop mathematical model to access the backfilling rate of dredging. According to their opinion backfilling rate was 50-80% of capital dredging per year.

Table 2: Natural siltation/scouring rate at harbor area calculated from hydrographic chart.

Sl.	Sections	Bed Level (m below CD)		Siltation (+)/ Scouring (-) rate (m/yr.)
		2008	2013	
01	Kleenheat LPG Jetty	4.9	6.1	-0.24
02	Middle of MPA jetty-09	4.2	5.8	-0.32
03	North Side of MPA Jetty-05	4.2	4.9	-0.14
04	MPA Vessel Berth	4.4	5.4	-0.20
05	Wreck Pavlina	3.8	4.4	-0.12

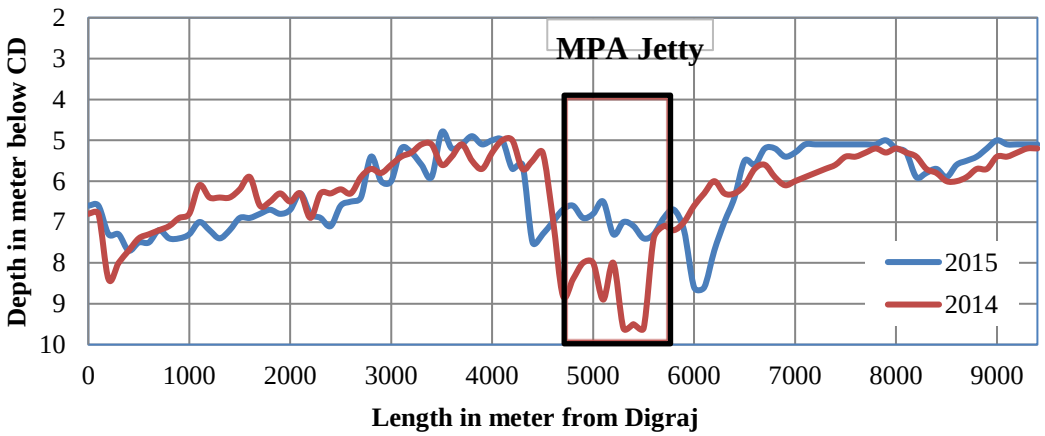

Figure 2: Longitudinal bed profile From Digraj to Mongla showing backfilling within one year (2014 is the dredging year).

3.1.3 Outer Bar Area

Table 3 shows the natural siltation/scouring rate at Outer bar area calculated from hydrographic chart comparing the data of 2009 to 2016. At outer bar area presently shipping channel is on the eastern side of wreck ocean wave. But this channel is being silted up and the shallow portion is extending towards east side day by day. Note that within this period no dredging was performed in the channel. In the downstream of buoy 14, the bar is found to be gradually raised up, where the sedimentation rate at two points are found to be about 0.35 m/year.

Table 3: Sedimentation and scouring in Outer Bar

Longitudinal position	Transverse distance from west bank (m)	Siltation (m/year)
Wreck Ocean Wave	750	1.1
	2250	0.13
Buoy 14	5250	0.38
	6375	0.33

3.2 Obstacle due to Wrecks

During the liberation war and thereafter, some local and foreign ships, (13 local and 5 foreign) sank at different reaches in the Pussur channel. MPA has taken steps several times to remove the wrecks. Top portion of some wrecks have been removed but the bottom and sides of these wrecks still remain in the channel. MPA has difficulty in removing all the portion of wrecks fully. Detail information of foreign wrecks are available in MPA. But information's of local wrecks are not available. MPA only have the location of those local wrecks.

For instance, one of the wrecks in the outer bar area (wreck ocean wave) causes siltation at its downstream. Thus the existing navigation route at the downstream east side of the wreck is narrowing and swallowing and causes threat to the existence of the route. MPA is planning to shift/relocate the route to the west side channel after performing the required dredging.

Table 4: List of foreign and local ship (Wreck) sunk in Pussur Channel (Source: MPA)

Sl.	Name of Ship	Length (m)	Width (m)	GRT (MT)	NRT (MT)	Location	Year
Foreign Wrecks							
01	MV Ocean Wave	174.09	22.90	15,684	6,539	About 2 km west of buoy B-16 at the entrance of Pussur	1999
02	MV Cheri Lazu	135.43	16.00	3,776	2,119	About 6.7 km west of Fairway Buoy	1984
03	Unknown	-	-	-	-	About 3.4 km east of buoy B-7 at the entrance of Pussur	-
04	Unknown	-	-	-	-	About 13 km south of Dublar Char	-
05	MV Pavlina-1	143.66	20.65	9,627.56	4,900	At the confluence of Mongla Nulla and Pussur river (West Side)	1994
Local Wrecks							
01	Barge President-1	-	-	-	-	Mongla Anchorage Area	1993

02	Barge NSC -8/E	-	-	-	-		1995
03	MV Shah ali	42.79	8.81	344.00	-		1997
04	Barge KSY-508	28.15	7.31	-	-		2000
05	Unknown	-	-	-	-		-
06	Unknown	-	-	-	-		-
07	Unknown	-	-	-	-	Mongla Nullah	-
08	Unknown	-	-	-	-		-
09	Unknown	-	-	-	-		-
10	Unknown	-	-	-	-		-
11	Barge Akash Prodip-5	-	-	-	-	Joymonirgol	2005
12	Unknown	-	-	-	-		2010
13	Unknown	-	-	-	-		2012

3.3 Human Disturbances

The navigability of Pussur River also suffered a lot due to human activities along with the natural reasons. After construction of MPA jetty at present location depth around jetty area started to reduce. The main reason of siltation is reducing the tidal prism in surrounding Pussur River. To maintain the Pussur with sufficient draft required for navigation, it is most significant to keep the volume of the tidal prism unchanged, or at least not decrease it.

According to the observations of MPA officials, the human interventions mainly responsible for changing the morphology of Pussur River are:

- Construction of polders and coastal embankments, which prevents tidal water to spread over the land which has decreased the tidal prism considerably in the river.
- Excavation of Mongla-Ghasiakhali link channel, which diverted a great volume of tidal water from its original course
- Restriction of upland flow due to less discharge of water from Padma to Modhumati and Nabaganga, Kobadak Bhairab and ultimately to Pussur due to Farakka withdrawal of Ganges water.
- Less availability of fresh water in the system increased the salinity of water. This increased salinity, which in turn, is causing more siltation in the estuary by flocculation processes.

The sunken ships and sunken barges loaded with cement, billets, jute and jute goods at the bottom of the Pussur River also caused siltation and deterioration of draught. Approximately 52 wrecks are lying at Joymanirgol to Bajua. These sunken barges are acting as dangerous silt traps.

4. MPA INTERVENTIONS TO ENHANCE NAVIGABILITY

4.1 Maintenance Dredging

Mongla Port was designed for berthing ships having 8.50 m draft. Upto 1980 there was not any siltation problem either in Jetty front or Channel area. But after 1980 siltation started in Jetty front Area. From that time regular maintenance dredging was performed in jetty front area. In the meantime it was seen that siltation has started in Harbour Area (About 13 km downstream from Port Jetty). For regular maintenance dredging, Mongla Port Authority has 02 nos 18" dia Cutter Suction Dredger. From the establishment of the Port, the quantity of maintenance dredging are listed in Table 5.

4.2 Capital Dredging

In spite of above maintenance dredging, to remove the siltation, 03 capital dredging projects have been implemented in the year of 1991 - 1992, 2000 - 2004 & 2013-2014. The most recent capital Dredging project titled "Harbour Area Dredging" has completed in the year 2014. After completion of this project, ships having draft of 7.50 m can easily take berth at Mongla Port. The details of 03 Capital Dredging Project are described in Table 6.

Table 5: Details of Maintenance Dredging performed by MPA in Pussur Channel to increase the navigation depth.

Dredging period	Dredger Authority	Dredging Area	Dredging Quantity (Mil. cu.m)	Dredger Type
1979-1981	BWDB	Jetty front (J5-J9)	0.325	CSD
1983-1987	BIWTA	Jetty front (J5-J9)	0.695	CSD
1988-1990	BWDB	Jetty front (J5-J9) & Confluence	0.523	CSD
1993-1996	Khanak dredger of CPA (TSHD)	Southern Anchorage confluence & Sabur Beacon	0.226	TSHD
1994-2001	BWDB	Jetty front (J5-J9)	0.813	CSD
2003-2004	BWDB	Jetty no- 8 & 9	0.069	CSD
2004-2005	Basic dredging Co.	Jetty no- 8 & 9	0.054	CSD
2005-2006	BWDB	Jetty no- 8 & 9	0.069	CSD
2007-2008	BWDB	Jetty no- 8 & 9	0.108	CSD
2009-2010	BWDB	Jetty no- 8 & 9	0.071	CSD
2012-2013	MPA's own Dredger	Jetty no- 8 & 9	0.017	CSD
2015-2016	AZ dredging Company Ltd	Approach and Pontoon front of Nil Komol	0.155	CSD
Total			3.125	

Table 6: Details of Capital Dredging performed in Pussur Channel to increase the navigation depth.

Dredging period	Dredging Company	Dredging Area	Dredging Quantity (Million cu.m)	Dredger Type
1991-1992	China Harbour Engineering Company, China	Harbour Area	3.551	CSD
2000-2004	PT. Rukindo- Basic Dredging Partnership (a joint venture of Indonesia and Bangladesh).	Harbour Area	2.79	CSD & TSHD
2013-2014	China Harbour Engineering Company, China	Harbour Area	3.406	CSD
Total			9.747	

The total volume dredged over the period 1979 to 2016 is about 12.872 Mm^3, which is equivalent to an average of 3,47,000 m^3 per year. Out of 37 years record, around 3.0 Mm^3 dredging was done in the Jetty Front to maintain the berthing pocket alongside the jetty. This is a localized dredging requirement is a continuous problem and the practice has been for maintenance dredging using Cutter suction dredger. The dredging operations at the jetty front area were required mainly to clean up very shallow patches just along the berths. This

sediment deposition is formed by the sliding down of sediment that accumulates due to the cluster of piles under the apron. This is considered the main reason of quickly filled up of the dredged areas alongside the jetties to natural river bed level.

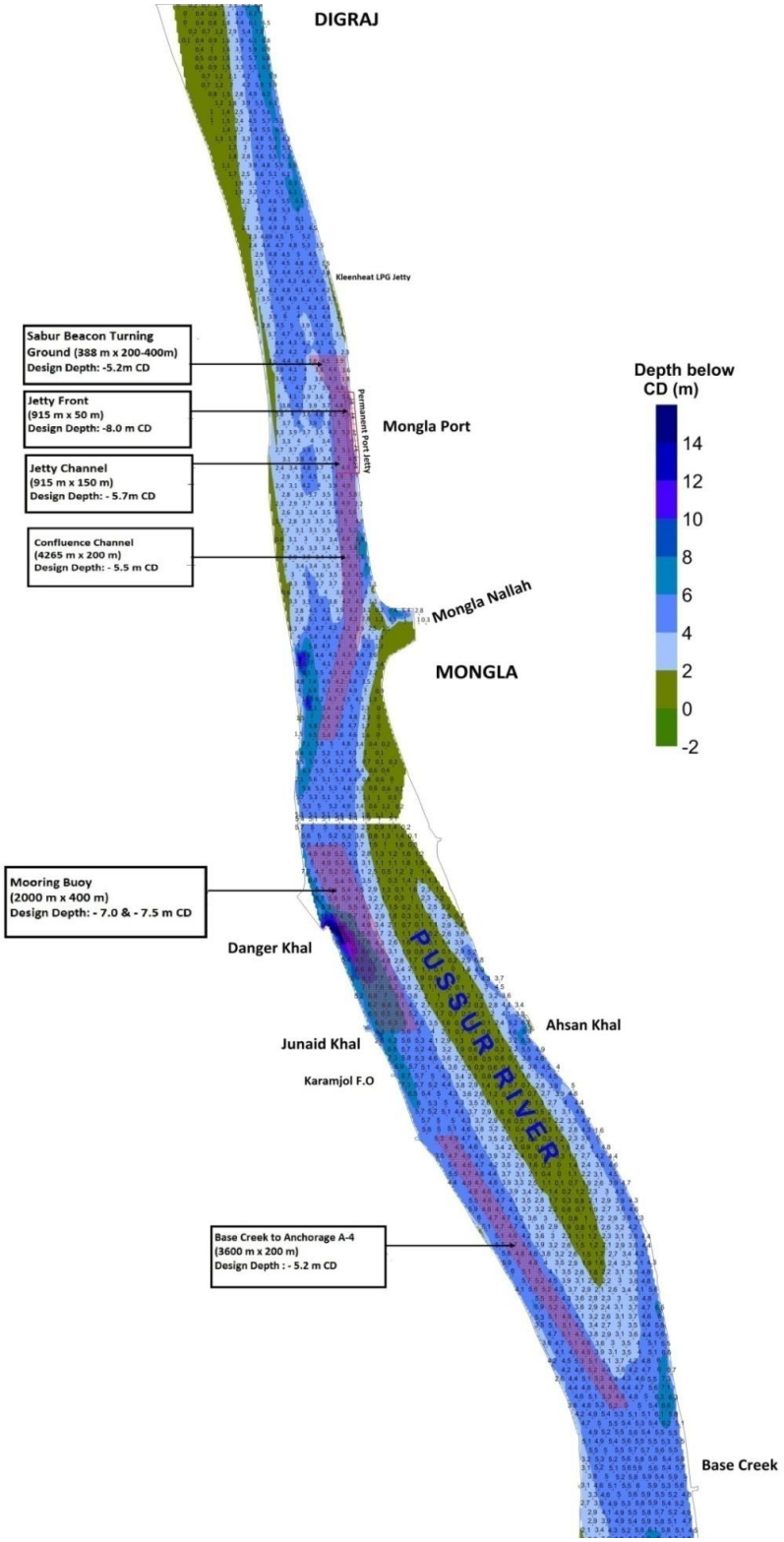

Figure 3: Location and alignment of dredging Segments at Harbour Area (Source: MPA)

5. BACK-FILLING RATE AND EFFECTIVENESS OF DREDGING

Upto now MPA has considered the dredging as the only option to improve the navigability. The dredging already completed by MPA and their future plan was presented above. However, the positive impact of dredging on navigability of Pussur channel is not found so significant due to the high backfilling rate. In this section, the backfilling rate is analyzed comparing the bed profile before and after dredging in several sections of Pussur channel. For this, the capital dredging in the year of 2014 in different segments of Pussur navigation route is considered. That time, Harbour Area (Base creek to MPA Jetty) was dredged upto 8.0 m at Jetty front, 7.0 to 7.5 m at Mooring Buoy and 5.5 m at other areas. Total 3.506 million cubic meter deposited silt was dredged at a cost of 112.0 crore taka. Figure 3 shows the location and alignment of the dredging in Harbour area of Pussur channel. The backfilling rate of those capital dredgings are presented below.

5.1 MPA Jetty Area

MPA has 5 nos Jetty having total length of 915 m. The jetty area is situated at concave end of a small mender. Ships berth here in both high and low tide and for that minimum 8.0 m draft required at 50 m wide are in front of Jetties. For movement of other vessels another 150 m required more than 5.0 m draft which called Jetty channel. In the year 2013, depth at MPA jetty front & Jetty Channel was reduced to -5.50 m & -4.0 m CD which was increased to more than -8.0 m & -5.5 m CD accordingly in the year 2014. After one year the depth at jetty front & Jetty channel has reduced to -7.50 m and -5.2 m CD respectively. But in the same time the west side of channel has deepened about 0.8 m. This implies that the concave end (East side) has silted up more than 1.0 m and convex end (West Side) scoured 0.8 m within one year. Jetty area has silted due to sliding of loose material underneath the jetty. Moreover this area was dredged like a pocket which is also a reason of quick siltation. A comparative bed profile of the year 2013, 2014 & 2015 has presented in Figure 4.

5.2 Confluence Channel

Approach at the confluence of Mongla Nullah and Pussur is known as confluence Channel. Merchant ships entered into port only in high tide and for that minimum 5.0 m draft required in this area. In the year 2013, at front of MPA vessel berth and along wreck pavlina was reduced to -4.2 m CD which was increased to more than -5.5 m CD in the year 2014.

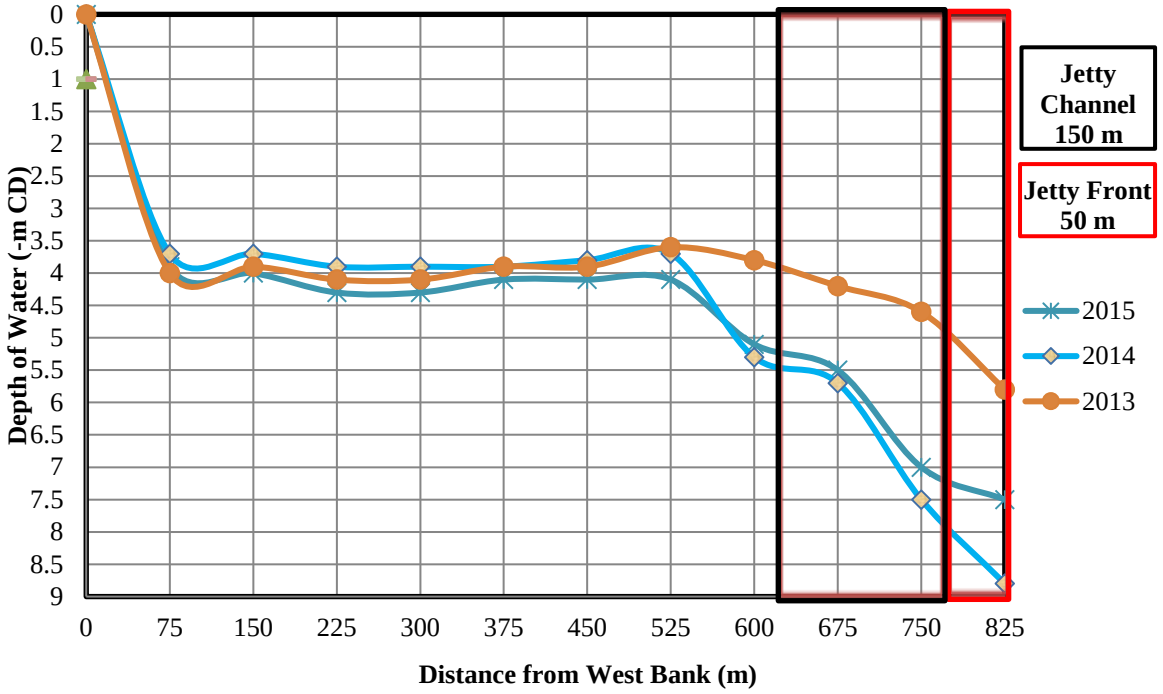

Figure 4: Cross section at Jetty Front before and after dredging (Dredging: 2014)

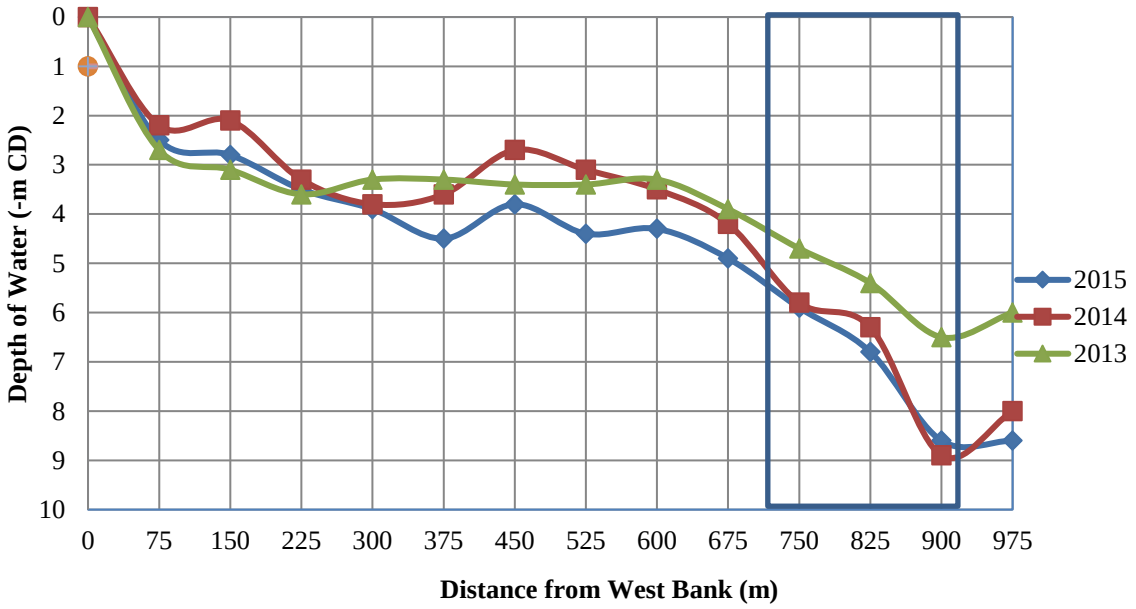

Figure 5: Cross section at Confluence Channel before and after dredging (Dredging: 2014).

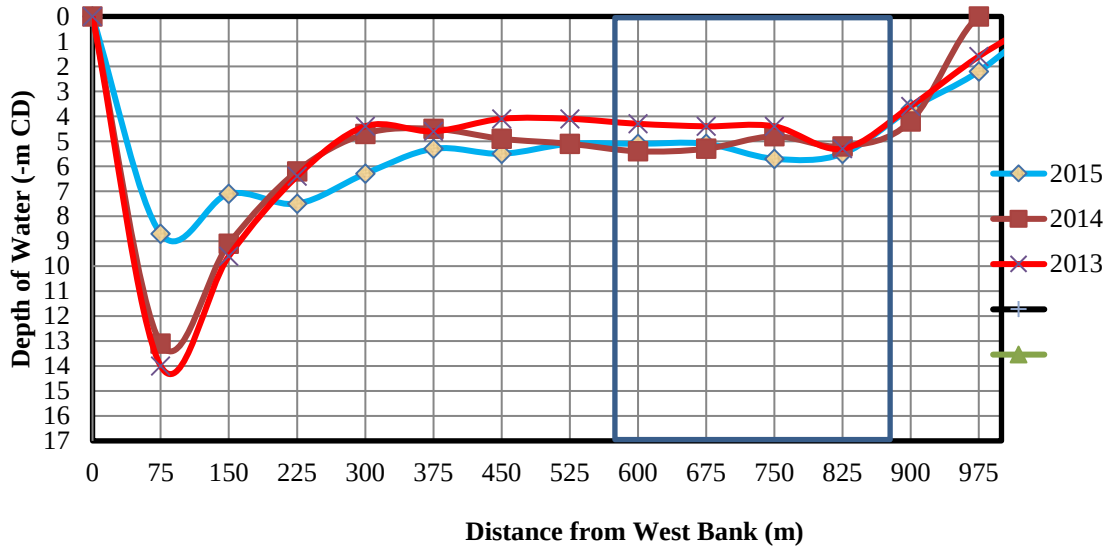

Figure 6: Cross section at Confluence Channel before and after dredging (Dredging: 2014).

After one year the depth at MPA vessel berth and along wreck pavlina has increased to near 6.0. But in the same time the west side of channel has silted up. This implies that the concave end (East side) has scoured and convex end (West Side) has silted. A comparative bed profile of the year 2013, 2014 & 2015 has presented in Figure 6. After the confluence channel, the navigation route is shifted from east bank to west bank side.

5.3 Mooring Buoy Area

At this section, the river is braided with two channels having the main navigation route near the west bank of the river and a small channel near the east bank with a shoal in between. In 2013, the depth at mooring buoy area was reduced to - 4.0m CD. Ships anchor in this area for unloading and for that minimum -7.5 m CD depth required. This area was dredged to more than -7.5 m CD in the year 2014 which has decreased to -6.0 m CD within one year. This area has silted mostly because of creating a deep pocket like jetty front (west side). Siltation happens along the full segment here. A comparative bed profile of the year 2013, 2014 & 2015 has presented in Figure 7.

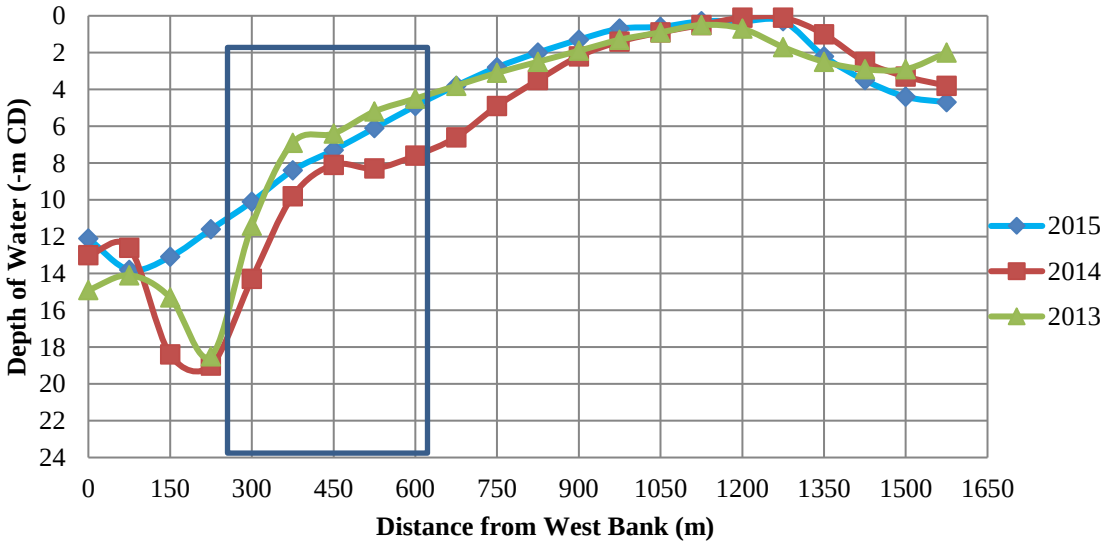

Figure 7: Cross section at Mooring Buoy Area before and after dredging (Dredging: 2014).

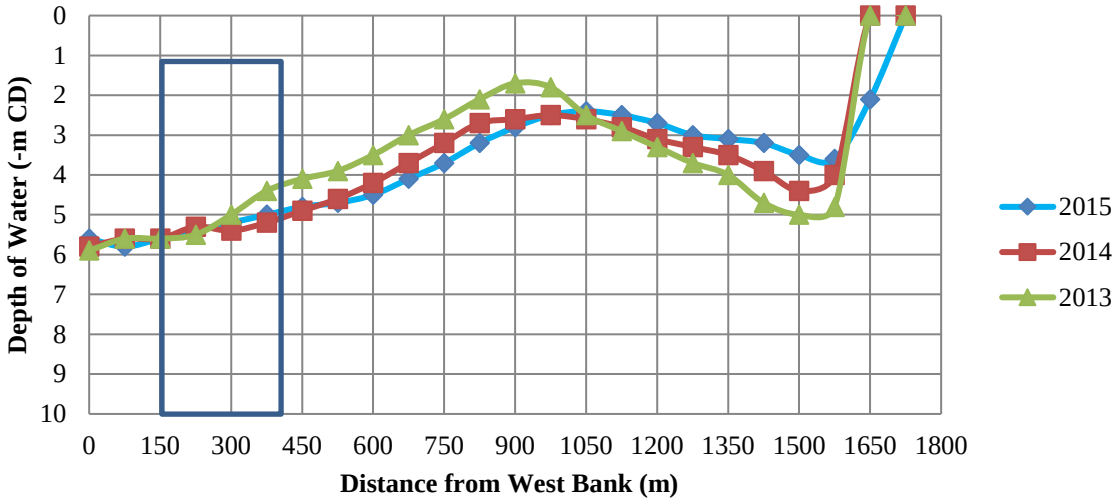

Figure 8: Cross section at Base Creek Area before and after dredging (Dredging: 2014).

5.4 Base Creek Area

Braided condition with two channels is continued up to this section having the main navigation route near the west bank of the river and a small channel near the east bank with a shoal in between. Before the capital dredging in the west side navigation channel, the depth in this area was reduced to -4.5 m CD. Ships only pass this area during the high tide and considering that base creek area was dredged upto -5.2 m CD. After one year of dredging the main navigation channel hasn't changed significantly. But the East side of this channel (Convex side) has deepened about 0.8 m naturally. A comparative bed profile of the year 2013, 2014 & 2015 has presented in Figure 8. The channel near the east bank of the river is found to be silted up by about 0.5 m in 2014 and about 1.0 m in 2015 compared to previous years.

The rate of backfilling after dredging measured in the field by MPA is given in Table 7. The backfilling rate is found to be very high for jetty front (1.0 m) and Mooring Buoy area (1.5 m).

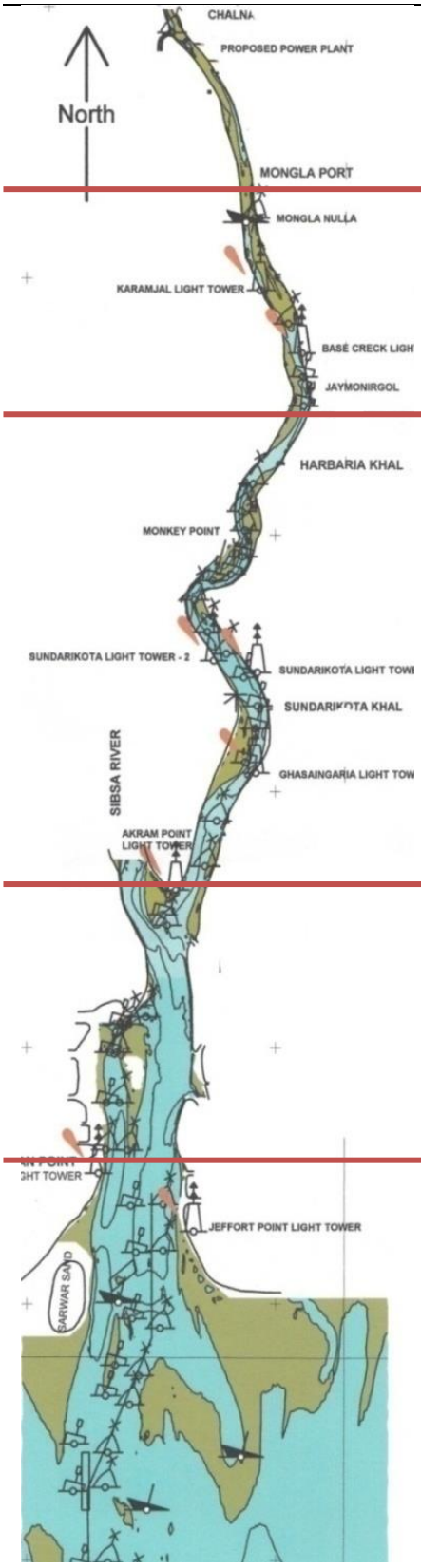

Chalna to Sabur Beacon

- Very shallow depth (-1 to -5 m CD)
- High siltation rate (0.22 to 0.95 m/yr)
- Capital dredging is required to get required draft for navigation

Sabur Beacon to Joymonirgol

- Shallow depth (>-6 m CD)
- Mildly scour prone (scour rate 0.20 m/yr)
- High backfilling rate after dredging (upto 1.3 m/year)
- Maintenance dredging and structural intervention are required

Joymonirgol to Akram Point

- Depth is more than -9m CD
- Quite stable
- Slightly scour prone (scour rate 0.06 m/yr)
- No dredging is required
- Structural intervention can be done to channelize the flow and increase the draft.

Akram Point to Hiron Point

- Depth > -9m CD
- Quite stable
- No dredging is required

Hiron Point to Fairway Buoy

- Outer bar area relatively shallow (Depth < -7.5m CD)
- Obstacled by Wreck
- High siltation rate (0.35 m/yr.) at downstream of wreck
- Capital dredging and shifting of navigation route is required

Figure 9: Segment-wise characterization for navigability and geomorphic features of Pussur River

Table 7: Backfilling rate in the dredged navigation route of harbor area (Source: MPA)

Area/ Section	**Field Measurement of backfilling rate (m/year)**
Jetty Front	1.00
Jetty Channel	0.30
Confluence Channel	-0.50
Mooring Buoy	1.50
Base Creek to Anchorage A-4	No Change after dredging

6. PROPOSALS FOR ENHANCEMENT OF NAVIGABILITY

From the analysis of result, the summary on the geomorphic characteristics, navigability and required interventions are presented in Figure 9 classifying the segments of Pussur channel having similar nature. It is found that the MPA jetty area and its approaches is mildly scouring where the upstream i.e Chalna to Digraj is being silted up. Downstream of mooring buoy is also slightly silted in last few years. The channel is quite stable in Joymonirgol to Hiron point. The current navigational channel at outer bar has siltation pattern where the west channel is scouring. To enhance the navigability of Pussur channel following interventions are proposed.

- Capital dredging is required to get required draft for navigation from Sabour Beacon to Rampal Power Plant and for outer bar area to remove the sediment in the existing route or fix up a new route in the nearby area.
- To improve the berthing pocket depth in front of the jetty, in addition to maintenance dredging, sheet piling could be proposed as a solution. The rapid siltation rate in front of the jetty is due to the sliding of the sediment from the jetty underneath.
- The main reason of siltation is low velocity of flood and ebb flow. If the velocity of flow could be increased in vulnerable sections such as MPA Jetty area and danger khal area, then the bed could be scoured naturally.
- Velocity could be increased by contracting the channel using structural interventions. For the canalization effect near the jetty area, spur dykes/groins/ guide bund opposite to jetty may also require as a structural intervention. The deflected flow due to the structural intervention in east bank may cause bank erosion at the upstream of the jetty area, a bank revetment may propose to prevent this.
- For the canalization of the Mooring Buoy area, structural measures can be proposed to close the eastern channel along the inner bar. For more effective result, a bank revetment at the western bank, opposite to inner bar may be required.

However, these structural measures require in depth study to establish the effectiveness.

7. CONCLUSION

Channel bed siltation (upto 0.95 m/year), High backfilling rate after dredging (upto 1.5 m/year), numerous wrecks at different locations of navigation route (approximately 52 wrecks including the sunken ships and sunken barges) and humen disturbences (including the Farakka barrage at upstream and construction of polders around the Pussur River) are found to be the main causes behind the navigational problems in the river route. In this regard, some site specific potential measures (purpose based) are suggested including capital dredging and structural interventions to enhance the navigability.

ACKNOWLEDGEMENT

The Authors would like to acknowledge the dredging section of Mongla Port Authority (MPA) for providing necessary data in conducting this research.

REFERENCES

Ali M. S., Mahzabin T. and Hosoda T. 2012, Impact of Climate Change on Temporal Variation of Floods in Bangladesh, Proceedings of the International Conference on Environmental Technology and Construction Engineering for Sustainable Development (ICETCESD), SUST, Bangladesh. pp. 235-248.

Clijncke A. 2001, Morphological response to dredging of the upper Gorai river, Masters thesis, Faculty of Civil Engineering and Geosciences, TU Delft.

Dasgupta, S., Kamal, FA, Khan, ZH, Choudhury S and Nishat, A. 2014. "River salinity and climate change: Evidence from coastal Bangladesh." Policy Research Working Paper 6817. World Bank, Washington, DC.

DHI, 1993. Mathematical Model Study of Pussur-Sibsa River System and Karnafuli River Entrance, Final Report, Annex 1 & 2, Bangladesh Water Development Board, Ministry of water resources, Government of Bangladesh.

Farleigh, D.R.P., 1984a. Report on Mathematical Model Studies, prepared for Port of Chalna Authority, Mongla, Bangladesh.

Farleigh, D.R.P., 1984b. Pussur River Study Phase II, Final Report prepared for Port of Chalna Authority, Mongla, Bangladesh.

Islam, S. N. and Gnauck, A., 2008. Mangrove wetland ecosystems in Ganges-Brahmaputra delta in Bangladesh. Front Earth Sci. China, 2(4), 439–448.

Islam G.M. T, Karim M.R (2005) " Predicting downstream hydraulic geometry of the Gorai river", Journal of Civil Engineering (IEB), 33 (2) 55-63.

IWM, 2015. Feasibility study of capital dredging in Pussur River from Mongla port to Rampal power plant, Mongla Port Authority, Mongla, Bangladesh.

IWM, 2013. Environmental Impact Assessment of proposed dredging project at Outer Bar Area of Pussur Channel, Mongla Port Authority, Mongla, Bangladesh.

IWM, 2004. Feasibility Study for Improvement of Navigability of Mongla Port, Mongla Port Authority, Mongla, Bagerhat, Bangladesh

Kowser, MA, and Samad, MA. 2016, Political history of Farakka Barrage and its effects on environment in Bangladesh, Bandung J of Global South 3:16, DOI 10.1186/s40728-015-0027-5.

MacDonald, M., 1998. Final Report, Ports Upgrading Project, Asian Development Bank, Government of the People's Republic of Bangladesh.

Malek, A. and Ashraf, J., 2004. Improvement of Navigation of Mongla Port, B. Sc. Engg. Thesis-2010, Department of Water Resources Engineering, BUET, Bangladesh.

Mirza, M., and M. Hossian. 2000. Adverse effects on agriculture in the Ganges basin in Bangladesh. In The Ganges water diversion: environmental effects and implications, ed. M.Q. Mirza. Netherlands: Kluwer Academic Publishers.

Sarker M.H, Kamal M.M and Hassan K. 1999, The Morphological Changes of a distributary of Ganges inresponse to the Declining Flow using Remote Sensing, Proceedings of the 20th Asian Conference on RemoteSensing,Vol.1.

Shamsad S.Z.K.M, Islam K.Z and Mahmud M.S, 2014, Surface Water Quality of Gorai River ofBangladesh, Journal of Water Resources and Ocean Science, 3(1):10-16.

Syvitski, J.P.M., Saito, Y. 2007, Morphodynamics of deltas under the influence of humans, Global Planet. Change, 57, pp. 261-282

Syvitski J.P.M., Kettner A.J., Overeem I., Hutton E.W.H., Hannon M.T., Brakenridge G.R., Day J., Vorosmarty C., Saito Y., Giosan L., Nicholls R.J. 2009, Sinking deltas due to human activities, Nat. Geosci., 2 , pp. 681-686

Walling D.E. 2006. Human impact on land-ocean sediment transfer by the world's rivers, Geomorphology, 79, pp. 192-216

Proceedings of the 4th International Conference on Civil Engineering for Sustainable Development (ICCESD 2018), 9~11 February 2018, KUET, Khulna, Bangladesh (ISBN-978-984-34-3502-6)

STUDY OF LAND SURFACE TEMPERATURE CHANGES IN SELECTED DRAINAGE BASIN OF ATAI-BHAIRAB-RUPSHA RIVER BASED ON NDVI AND NDWI ANALYSIS

Chandan Mondal[1] and Md. Jahir Uddin[2]

[1] Post Graduate Student, Khulna University of Engineering & Technology, Khulna, Bangladesh,e-mail: chandance2k7@gmail.com
[2] Associate Professor, Khulna University of Engineering & Technology, Khulna, Bangladesh, e-mail: jahiruddin@ce.kuet.ac.bd

ABSTRACT

Land Surface Temperature (LST) is one of the key parameters in the physics of land surface processes from local through global scales. It has a great influence on life cycle of plants and living organisms which play an important role to keep environment livable. One should be careful about the changes of LST and regular observation is necessary. LST largely depends on vegetation, especially healthy vegetation and water body. In this study, satellite image analysis technique has been demonstrated to understand the LST changes in 20 years time span. The study area is the drainage basin of Atai-Bhairab-Rupsha river confluence which is an important place both for agriculture and trade in the south-western part of Bangladesh. Normalized Difference Vegetation Index (NDVI) and Normalized Difference Water Index (NDWI) analyses are used to observe the effect of healthy vegetation and water body on LST. NDVI, NDWI and LST maps have been created for the year 1995, 2006 and 2015 at end of the dry season in mid-February, when there is no influence of rainfall effect on vegetation, water body and soil surface temperature. From the analysis, it is found that the highest and lowest values of NDVI are 0.96 and -0.94 respectively in the year 1995, which means the study area was covered by both healthy vegetation and bare soil. As well the highest and lowest values of NDWI ranges from 0.93 and -0.94 respectively which represent both for effective water body, marsh and bare soil area. At that time period the highest and lowest values of LST are observed 36.48^{0}C and 15.96^{0}C respectively. It is observed during the year 2006 that the difference of the highest and lowest values of NDVI and NDWI decreases considerably, which indicates healthy vegetation was significantly replaced by shrub and grassland, means destruction of healthy vegetation and water body. During the year 2015, the changes of the difference between highest and lowest values of NDVI and NDWI are quite same as compared to 2006.

Keywords: *NDVI, NDWI, LST, water body, vegetation*

1. INTRODUCTION

Urbanization and transformation of the earth surface to urban application illustrate huge changes in global usage of the land and provide considerable influence on the environment (Weng & Yang, 2004). The population in global urban areas has risen quickly from 13% in 1900 up to 46% in 2000, and it is believed that it can go up to 69% by 2050. The influence of climate change is foreseeable in the shape of altering weather patterns and extreme weather events, like heavy rainfall, flood, windstorm, heat waves and windstorms (IPCC 2007). One of the main reasons for his type extreme weather condition occurring so frequently is global warming. Rapid urbanization, deforestation, filling up water body is some of the causes of global warming. Land Surface Temperature (LST) is a popular indicator of global warming, which is largely depends on vegetation, amount of water body and mostly urbanization. The Land Surface Temperature (LST) is the radiative skin temperature of the land surface, as measured in the direction of the remote sensor. It is estimated from Top-of-Atmosphere brightness temperatures from the infrared spectral channels of a constellation of geostationary satellites. Its estimation further depends on the albedo, the vegetation cover and the soil moisture. LST is a mixture of vegetation and bare soil temperatures.

The Multi Spectral Remote Sensing images are very efficient for obtaining a better understanding of the earth environment (Ahmadi & Nusrath, 2010). It is the Science and Art of acquiring information and extracting the features in form of Spectral, Spatial and Temporal about some objects, area or phenomenon, such as vegetation, land cover classification, urban area, agriculture land and water resources without coming into physical contact of these objects (Karaburun, 2010). Certain pigments in plant leave strongly absorb wavelengths of visible (red) light. The leaves themselves strongly reflect wavelengths of near-infrared light, which is invisible to human eyes. As a plant canopy changes from early spring growth to late-season maturity and senescence, these reflectance properties also change. Many sensors carried aboard satellites measure red and near-infrared light waves reflected by land surfaces. Using mathematical formulas (algorithms), scientists transform raw satellite data about these light waves into vegetation indices. A vegetation index is an indicator that describes the greenness, the relative density and health of vegetation, for each picture element, or pixel, in a satellite image. Although there are several vegetation indices, one of the most widely used is the Normalized Difference Vegetation Index (NDVI) ranges from +1.0 to -1.0 (Remote Sensing Phenology 2015).

Drought is caused by long-term lack of soil water content which would affect agriculture, ecology and socio-economy; it is particularly harmful to food production (Zhang & Huai-Liang 2016).Plants experience water stress either when the water supply to their roots becomes limiting or when the transpiration rate becomes intense. Water stress is primarily caused by the water deficit, i.e. drought or high soil salinity (Lisar et al. 2012). The Normalized Difference Water Index (NDWI) is known to be strongly related to the plant water content. It is therefore a very good proxy for plant water stress. It is real-time retrieval of soil moisture, which has high retrieval accuracy (Gao, 1995).

Is this study, we have figured out some relation among LST, NDVI and NDWI, where NDVI is an indicator of vegetation presence and NDWI mainly stands for a very good proxy for plant water stress which mainly denotes availability of water sources, for instance water body and soil moisture.

2. STUDY AREA

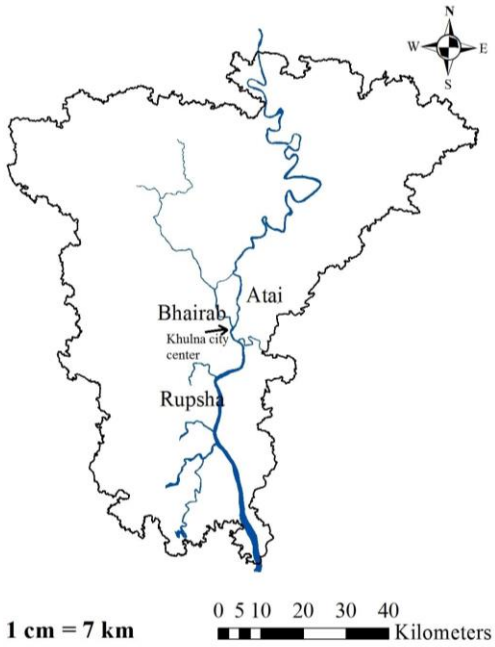

Figure 1: Atai-Bhairab-Rupsha drainage basin

The study area is the drainage basin of Atai-Bhairab-Rupsha river confluence which is an important place both for agriculture and trade in the south-western part of Bangladesh (Figure 1). The study area covers mainly Khulna district and some portion of Barisal division. Mainly the center of the Khulna city is situated at the confluence area.

3. RESOURCES AND TECHNIQUES

In this study for image analysis, different tools from ArcMap, which is the central application of ArcGIS software have been used. The version of this software is ArcGIS 10.4.1. Total 20 years' time span is considered for study. Satellite images of the years 1995, 2006 and 2015 are downloaded from the website https://glovis.usgs.gov/. Landsat-5 TM images for years 1995, 2006 and Landsat-8 OLI/TIRS images for year 2015 of UTM zone 46 are downloaded. Landsat-7 ETM+ images are not considered because on May 31, 2003 the Scan Line Corrector (SLC) in the ETM+ instrument failed, so the image data type is erroneous. Whereas there are some techniques to improve the quality of the image, but here completely error free space born images are consider. SRTM 1 Arc-Second Global DEM is downloaded from the website https://earthexplorer.usgs.gov/ to select the drainage basin.

3.1 Calculation of NDVI and NDWI

Governing equations for analyzing the space-born data are given below. NDVI and NDWI is calculated from the following equations

$$NDVI = \frac{NIR - VISR}{NIR + VISR} \tag{1}$$

$$NDWI = \frac{VISG - NIR}{VISG + NIR} \tag{2}$$

Where,
$NDVI =$ Normalized Difference Vegetation Index
$NDWI =$ Normalized difference water index
$NIR =$ Spectral reflectance measurements acquired in the near infra-red regions
$VISR =$ Spectral reflectance measurements acquired in the visible red regions
$VISG =$ Spectral reflectance measurements acquired in the visible green regions
Here, in case of Landsat-5 TM Band 2, Band 3, Band 4 stand for visible green regions, visible red regions, near infra-red regions respectively and in case of Landsat-8 OLI/TIRS Band 3, Band 4, Band 5 stand for visible green regions, visible red regions, near infra-red regions respectively.

3.2 Calculation of LST

Conversion of digital number to radiance can be performed by the equation given below. For Landsat-5 TM, during 1G-product rendering, image pixels are converted to units of absolute radiance using 32 bit floating-point calculations. Pixel value are then scaled to byte values prior to media output. The following equation (Landsat 7) is used to convert DN's in a 1G product back to radiance units

$$L_\lambda = \left(\frac{LMAX_\lambda - LMIN_\lambda}{QCALMAX - QCALMIN} \right) * (QCAL - QCALMIN) + LMIN_\lambda \tag{3}$$

Where,
$L_\lambda =$ Spectral Radiance in watts/ (m^2*ster*μm)

$QCAL$ = The quantized calibrated pixel value in DN
$LMIN_\lambda$ = The spectral radiance that is scaled to $QCALMIN$ in watts/ (meter squared*ster*μm)
$LMAX_\lambda$ = The spectral radiance that is scaled to $QCALMAX$ in watts/ (meter squared*ster*μm)
$QCALMIN$ = The minimum quantized calibrated pixel value (corresponding to $LMIN_\lambda$) in DN
$QCALMAX$ = The maximum quantized calibrated pixel value (corresponding to $LMAX_\lambda$) in DN

For Landsat-8 OLI/TIRS, images are processed in units of absolute radiance using 32-bit floating-point calculation. These values are then converted to 16-bit integer values in the finished Level 1 product. These values are converted to spectral radiance using the radiance scaling factors provided in the metadata file by using the following equation (Landsat 8)

$$L_\lambda = M_L Q_{cal} + A_L \tag{4}$$

Where,
L_λ = Spectral Radiance in watts/ (m^2*ster*μm)
M_L = Radiance multiplicative scaling factor for the band (from metadata)
A_L = Radiance additive scaling factor for the band (from metadata)
Q_{cal} = Level 1 pixel value in DN

Radiance is converted to satellite temperature by following equation

$$T = K2 / \ln\left((K1 / L_\lambda) + 1\right) \tag{5}$$

T = TOA Brightness Temperature (K)
$K2$ = Calibration constant 2 (1260.56 K) for Landsat-5 TM
=Thermal conversion constant for the band (K2_CONSTANT_BAND_n from metadata) For Landsat-8 OLI/TIRS
$K1$ = Calibration constant 1 (607.76 watts/ (m^2*ster*μm))
= Thermal conversion constant for the band (K1_CONSTANT_BAND_n from metadata) For Landsat-8 OLI/TIRS

Proportion of vegetation is determined by following equation

$$P_v = \left(\frac{NDVI - NDVI_{MIN}}{NDVI_{MAX} - NDVI_{MIN}} \right)^2 \tag{6}$$

Where,
P_v = Proportion of vegetation

Land surface emissivity is determined by following equation

$$e = 0.004 P_v + 0.986 \tag{7}$$

Where,
e = Land surface emissivity

Land surface temperature is determined by following equation

$$LST = T / (1 + (wT / p) \times \ln(e)) \tag{8}$$

Where,
$LST =$ Land Surface Temperature (K)
$w =$ Wavelength of emitted radiance (μm)
$p = hc / s = 1.438 \times 10^{-2}$ (mK)
$h =$ Panck's constant (6.626×10^{-34} Js)
$s =$ Boltzmann constant (1.38×10^{-23} J/K)
$c =$ Velocity of light (2.998×10^{-8} m/s)

Landsat-5 TM has only one thermal band (Band 6), whereas Landsat-8 OLI/TIRS has two thermal bands (Band 10 and Band 11). So in case of Landsat-8 OLI/TIRS, LST is calculated individually both for Band 10 and Band 11 and then average is calculated. These values are calculated in Kelvin scale which is finally converted to Degree Celsius scale by the following equation

$$LST(^0C) = LST(K) - 273.15 \quad (9)$$

4. RESULTS AND DISCUSSION

The values of NDVI, NDWI and LST of mid-February for the years 1995, 2006 and 2015 are shown in the Figure 2. NDVI values range from +1.0 to -1.0. Values close to zero (-0.1 to 0.1) generally correspond to barren areas of rock, sand, or snow. Lastly, low, positive values represent shrub and grassland (approximately 0.2 to 0.4), high NDVI values (approximately 0.6 to 0.9) correspond to dense vegetation such as that found in temperate and tropical forests or crops at their peak growth stage. While The NDWI index is most appropriate for water body mapping. The water body has strong absorbability and low radiation in the range from visible to infrared wavelengths. The index uses the green and Near Infra-red bands of remote sensing images based on this phenomenon. The NDWI can enhance the water information effectively in most cases. It is sensitive to built-up land and often results in over-estimated water bodies. Values of water bodies are larger than 0.5. Vegetation has much smaller values, which results in distinguishing vegetation from water bodies easier. Values -1 to 0 represents Bright surface with no vegetation or water content (Uysal & Polat, 2015).

The values of NDVI, NDWI and LST of mid-February of the years 1995, 2006 and 2015 are shortened in the Table 1 from Figure 2. Data of 2006 is analysed instead of 2005, as Landsat-5 TM satellite image data of 2005 is not suitable for analysis. Because during mid-February 2005 all the images of study area are covered with cloud that brings erroneous result.

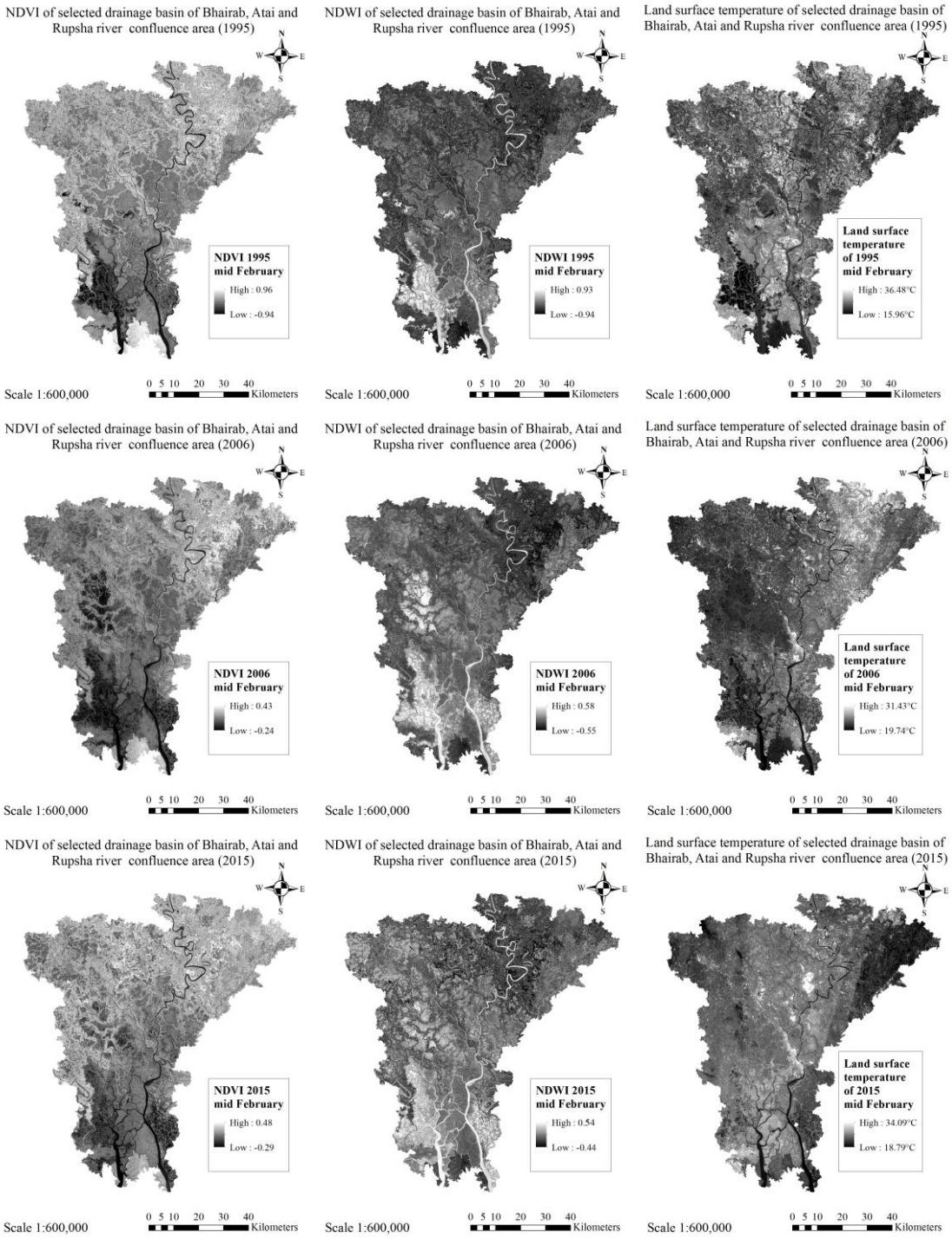

Figure 2: NDVI, NDWI and LST of years 1995, 2006 and 2015 of study area

Table 1: List of NDVI, NDWI and LST values from figure 2 for different years

Year		1995	2006	2015
NDVI	Highest	0.96	0.43	0.48
	Lowest	-0.94	-0.24	-0.29
NDWI	Highest	0.93	0.58	0.54
	Lowest	-0.94	-0.55	-0.44
LST(^{0}C)	Highest	36.48	31.43	34.09
	Lowest	15.96	19.74	18.79

It is observed from Table 1, that the highest and lowest values of NDVI are 0.96 and -0.94 respectively during mid-February 1995, which means this study area was covered by both healthy vegetation and bare soil. As well highest and lowest values of NDWI range from 0.93 and -0.94 respectively which represent both for effective water body, marsh and bare soil area. At that time highest LST was 36.48^0C and lowest was 15.96^0C. This temperature variation is possible because of areas of both dense vegetation cover, good number of water body and also bare land surface area. Because vegetation cover and water body both have a great influence to keep local weather condition in a reasonable state. Whereas empty land area without minimum vegetation cover act like desert area which is much warmer in day time and colder at night.

Also from the Table 1, it is observed detail scenario of the study area during 2006 mid-February. Both the differences of highest and lowest values of NDVI and NDWI decrease significantly. These indicate healthy vegetation was significantly replaced by shrub and grassland, means destruction of healthy vegetation and water body. The lowest values of NDVI and NDWI represent not only barren soil but some human activities like cultivation or civilization. During this time, the highest LST is 31.43^0C and lowest is 19.74^0C. It shows that highest temperature decreases and lowest temperature increases. It indicates barren soil seems like covered with minimum vegetation so desert like symptom decreases like high day time temperature. Also as healthy vegetation and water body decrease, local temperature also affected as they have high impact on local environment so lowest LST also increased.

Further it is seen from the Table 1, during mid-February 2015, the change of the difference between highest and lowest are NDVI and NDWI are quite same as compared 2006. Lowest LST was quite same as 2006, nearly 1^0C difference while above 2^0C increment is observed than 2006's highest LST. This means gradual destruction of water body and shrinkage of healthy vegetation also the barren soil, healthy vegetation and marsh area are replaced by cultivable land and urban area. The NDVI and NDWI values also represent the same scenario.

5. CONCLUSIONS

Vegetation and water body play an important role to keep local environment suitable for living. In this study, it is easily understand that during 1995 due to some barren soil area, highest temperature was greater and in 2006 and 2015 the highest temperature was lower than 1995 but lowest temperature of these two years also increased. In a comparison between the year 2006 and 2015, a sign of temperature increase is observed. This means, whatever the barren soil area is replaced by urban and cultivable area, increase of temperature is continuing in a holistic level.

REFERENCES

Ahmadi, H., & Nusrath, A. (2010). Vegetation change detection of Neka River in Iran by using remote-sensing and GIS. Journal of geography and geology, 2(1), 58.

Gao, B. C. (1995, June). Normalized difference water index for remote sensing of vegetation liquid water from space. In Imaging Spectrometry (Vol. 2480, pp. 225-237). International Society for Optics and Photonics.

IPCC. (2007). Fourth assessment report. Cambridge, Retrieved from https://www.ipcc.ch/publications_and_data/publications_and_data_reports.shtml

Karaburun, A. (2010). Estimation of C factor for soil erosion modeling using NDVI in Buyukcekmece watershed. Ozean Journal of applied sciences, 3(1), 77-85.

Landsat, N. A. S. A. (7). Science Data Users Handbook. *2011-03-11]. http://landsathandbook. gsfc. nasa. gov/inst_cal/prog_sectS_2. html*.

Landsat, N. A. S. A. (8). Science Data Users Handbook. *2016-03-29]. https://landsat.usgs.gov/sites/default/files/documents/Landsat8DataUsersHandbook.pdf*

Lisar, S. Y., Motafakkerazad, R., Hossain, M. M., & Rahman, I. M. (2012). Water stress in plants: causes, effects and responses. In *Water stress*. InTech.

Remote Sensing Phenology (2015), https:// Environmental study/Remote Sensing Phenology.html

Uysal, M., & Polat, N. (2015). An investigation of the relationship between land surface temperatures and biophysical indices retrieved from Landsat TM in Afyonkarahisar (Turkey)/Ispitivanje odnosa izmedu temperatura na povrsini zemlje i biofizickih pokazatelja dobivenih zemljinim satelitom Landsat TM u Afyonkarahisaru (Turska). *Tehnicki Vjesnik-Technical Gazette*, *22*(1), 177-182.

Weng, Q., & Yang, S. (2004). Managing the adverse thermal effects of urban development in a densely populated Chinese city. *Journal of Environmental Management*, *70*(2), 145-156.

Zhang, H. W., & Huai-Liang, C. H. E. N. (2016). The Application of Modified Normalized Difference Water Index by Leaf Area Index in the Retrieval of Regional Drought Monitoring. DEStech Transactions on Engineering and Technology Research, (sste).

Proceedings of the 4th International Conference on Civil Engineering for Sustainable Development (ICCESD 2018), 9~11 February 2018, KUET, Khulna, Bangladesh (ISBN-978-984-34-3502-6)

INTERPOLATION METHODS FOR GROUNDWATER LOWERING PREDICTION

Linkon Bhattacharjee[1], Aysha Akter[2] and Md. Misbah Uddin Mahin[1]

[1] Department of Civil Engineering, Chittagong University of Engineering and Technology, Bangladesh, e-mail: lkbcharya@gmail.com; misbah.mahin@gmail.com
[2] Professor, Department of Civil Engineering, Chittagong University of Engineering and Technology, Bangladesh, e-mail: aysha_akter@yahoo.com; http://aakter.weebly.com

ABSTRACT

Experiences around the world showed low water availability in many regions directly linked to reduced forest cover, soil degradation and on the other hand urbanization drastically affects local aquifer systems. Although, a major portion of the rapid urbanizing Chittagong city requirements are achieved through ground water extraction, however, due to lack of observation well and proper database there is no published record on possibilities of groundwater lowering in Chittagong city. Absence of continuous dataset on groundwater level, different interpolation methods are usually applied by researchers for prediction and those are inverse distance weighted (IDW), Spline and Kriging method of interpolation. In this study, the sum of least squares method under the time series regression analysis was used to compute groundwater level trend. Then Kriging method was used in GIS environment for interpolation of data and visual representation. This study conducted over 22 wells during 2009 to 2013, thus, the calculated water level lowering rate in the studied area was found as 0.12- 7.92 m reasonably matched with measure values. With propoer dataset, this method envisaged to provide necessary information to the decision support system.

Keywords: *Lowering; Chittagong City; Kriging method*

1. INTRODUCTION

Ground water is a precise and the most widely distributed resource of the earth. Ground water plays a vital role for drinking, irrigation, industrial purpose. Rapid increase of population is pushing usage of ground water into a limit. At present nearly one fifth of all the water used in the world is obtained from groundwater resources (Raghunath, 1987; Lee, Kim & Oh, 2012). Exploitation and over consumption of groundwater has increased in past years which causes decreased in groundwater levels and deterioration of water quality (Magesh, Chandrasekar & Soundranayagam, 2012). This study proposes to quantitatively evaluate and map the regional groundwater depletion in recent years. Chittagong is the second largest city in Bangladesh having the main sea port of the country. The total area of Chittagong and sub-urban areas is around 550 km^2. The industrialized city of Chittagong is growing rapidly and the population in the City Corporation area has been estimated to be about 4.2 million. At present the demand for water supply within the city area is about 500 million liters per day (MLD). But, Chittagong Water Supply & Sewerage Authority (CWASA) has present capacity of supply about 210 MLD through its transmission and distribution pipelines. Out of The 210 MLD production capacity, 120 MLD productions are abstracted from groundwater and by local supply from some deep wells. Despite the abundance of water resources, there is a serious shortage of treated water supply to the city. The present shortfall of water supply is about 60% (CWASA, 2014).

Involvements of geostatistics is a useful tool for analyzing groundwater level depletion. Statistical methods for trend analysis vary from simple linear regression to more advanced parametric and non parametric methods (Helsel, Hirsch, 2002). To estimate the trend of groundwater level and the water level fluctuation, time series regression analysis was adopted using Microsoft office Excel 2007 (Shalini, Pandey & Nathawat, 2012). Previously

an attempt was made for Dhaka city using 17 years (1988-2004) information aimed to assess the water level fluctuation and predicting its trend using the MAKESENS computer model (Sarkar and Ali, 2009). Linear regression method was used to analyse the water level fluctuation in Kutahya – Cavdarhisar plain in Turkey (Nuri, 1988). Similar method and study was done in Kushtia district in Bangladesh (Adhikary, Chaki, Rahman & Gupta, 2012). Various characteristics controlling groundwater lowering can be presented and analyzed by using geographic information system (GIS). GIS technology is effective spatial tools widely used for the prediction, monitoring, management, and visual representation of geographic information (Lee, Kim & Oh, 2012; Oh, Kim, Choi, Park & Lee, 2011; Magesh, Chandrasekar & Soundranayagam, 2012; Shalini, Pandey & Nathawat, 2012). The Geographic Information System (GIS) presents an important tool in the effective management of groundwater resources (Shalini, Pandey & Nathawat, 2012). Different interpolation methods were adopted for surface interpolation (Shalini, Pandey & Nathawat, 2012, Gong, Mattevada & O'Bryant, 2014). Kriging method of Interpolation was used in mapping global solar radiation over southern Spain global solar radiation over southern Spain (Alsamamra, Arias, Vázquez & Pescador, 2009), estimating groundwater arsenic concentrations in Texas (Gong, Mattevada & O'Bryant, 2014), mapping liquefaction potential over alluvial ground (Pokhrel, Kuwano & Tachibana, 2013). In this study, the sum of least squares method under the time series regression analysis was used to compute groundwater level trend. Then Kriging method was used in GIS for interpolation of data and visual representation.

2. METHODOLOGY

2.1 Study area

The study area lies between 22°18'0 ″ to 22°24'0 ″ N latitude and 91° 46'0 ″ to 91° 51'0 ″ E longitude (Figure 1). Spatial distribution of Chittagong Sadar area reveals that thick prolific medium and coarse sand aquifer exist around the study area whose sediment formation is composed of medium to coarse sand. This aquifer is not laterally extended around the study area.

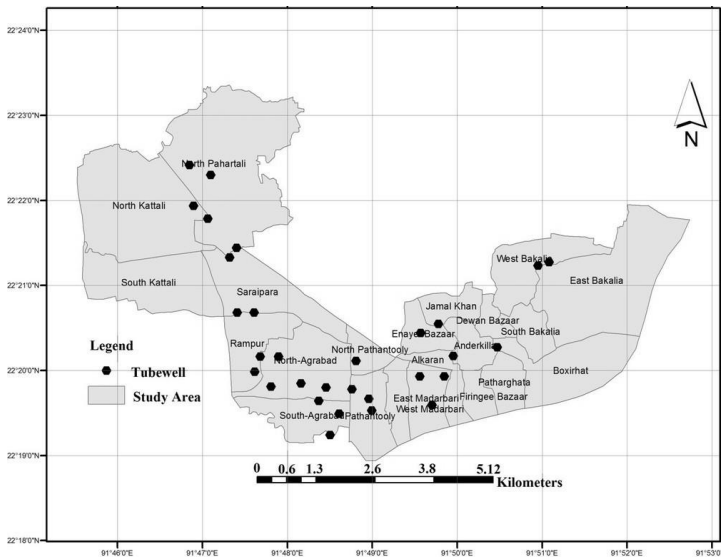

Figure 1: Study area and the selected well locations

Fine and medium sand aquifer also present around the study area. Aquifers in the Chittagong city are divided in to two separate zones, i.e., zone 1: Quaternary sediments form the aquifer in which the vertical recharge in deep aquifer is prohibited by the presence of

thick sequence of clay layer and rather horizontal recharge in dominant. But the zone 2 belongs to the higher elevated hills and valleys of exposed Tertiary sediments. Vertical recharge through percolation of rainwater is high in this area as the exposed areas are sandstone dominant. Apart from vertical recharge, horizontal recharge from the higher elevation to lower elevation may be responsible for recharging the groundwater in Zone 1. (Hossain, Bashar & Ahmed, 2008, CWASA, 2014).

Tertiary Aquifer System belongs to the northern part of the city area. Tertiary sediments are mainly exposed at surface and the ground level is very high with respect to the mean sea level. This part of the study area is the southern end of Sitakund anticline and staratigraphic layer of this part are dipping in east and west direction. Three distinct aquifers are mainly observed in all the area of this zone. But their thickness is highly variable latterly. Among the three aquifers, first or shallow aquifer is exposed at the surface and the average thickness of this aquifer is 23m and the maximum thickness is about 50m. Second aquifer situated at a depth of 140-150m and the average thickness is 27m. Third or deep aquifer is a good quality aquifer whose average thickness is about 35m. The strainer positions of all the production wells of this zone are situated in this aquifer and most of them are single screen. Fine to medium sand exist within the depth location ranges from 217 m to 266 m and finer materials that is clay exist from 266 m to 364 m (CWASA, 2014). Specific yield of these mentioned layers varies from 0.030 to 0.132, 0.030 to 0.132 and 0.030 in the study area. Up to 215m depth three aquifer layers have already been identified. These aquifer layers are semi-confined to confine in nature. The average range depth location and transmissivity value of these aquifer layers are presented below:

Table 1: Aquifer layer location and transmissivity value

Aquifer Layer	Depth Location	Transmissivity Value
First Aquifer	45m to 80m	148m^2 / day to 420m^2 / day
Second Aquifer	105m to 135m	308m^2 / day to 748m^2 / day
Third Aquifer	140m to 215m	697m^2 / day to 1040m^2 / day

2.2 Rainfall

Chittagong City is located in the tropical zone, which is subject to tropical climate. It is characterized by high temperature, and heavy rainfall with often-excessive humidity. There are three distinct seasons. The hot season continues from March to May but has some wet days. The monsoon season begins in June and continues usually to September with maximum temperature. The monsoon season generally comes and ends with cyclones. The cold and dry season begins in November and extends to February. Annual rainfall in the city ranges from 259.98 mm to 2540.8 mm in past nine years since 2004. Average annual rainfall is 2,557 mm (Table 2). Monthly average rainfall is very low during cold and dry season ranging from 9.7 mm to 57.4mm. Reversely, remaining seasons of hot and monsoon have comparatively abundant rainfall of from 87 mm to 594 mm per month on an average.

Table 2: Monthly Average Rainfall (mm) in Chittagong for the Period from January 2004 to January 2013 (Bangladesh Meteorological Department)

Month	2009	2010	2011	2012	2013
Jan					
Feb		7.87		17.27	0.5
March		154.18	109.72	13.46	3.3
April	75.95	31.49	49.28	226.31	60.19
May	374.39	373.63	299.46	228.34	759.96
June	431.81	648.46	456.43	754.38	572.52
July	1248.2	295.39	583.96	741.44	343.16
Aug	580.64	460.01	807.47	283.47	258.32
Sep	281.18	116.82	764.79	206.24	183.64
Oct	299.72	320.81	23.87		359.16
Nov	17.27	37.59		3.55	
Dec		19.05			
Total	3309.1	2465.3	3095	2474.5	2540.8

2.3 Well Flow Rates

Available bore log and flow details of 30 tube wells were collected from CWASA. Discharge rate is decreasing year by year and hence water level is increasing (Figure 2a and 2b).

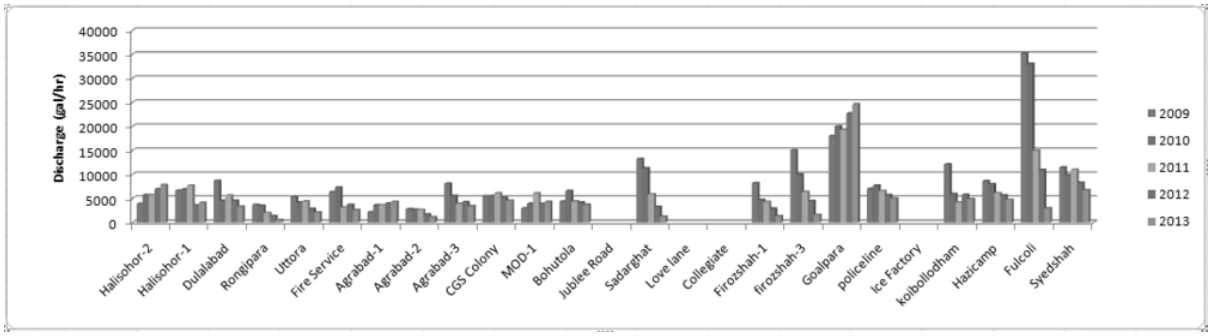

Figure 2 a: Locationwise discharge variation

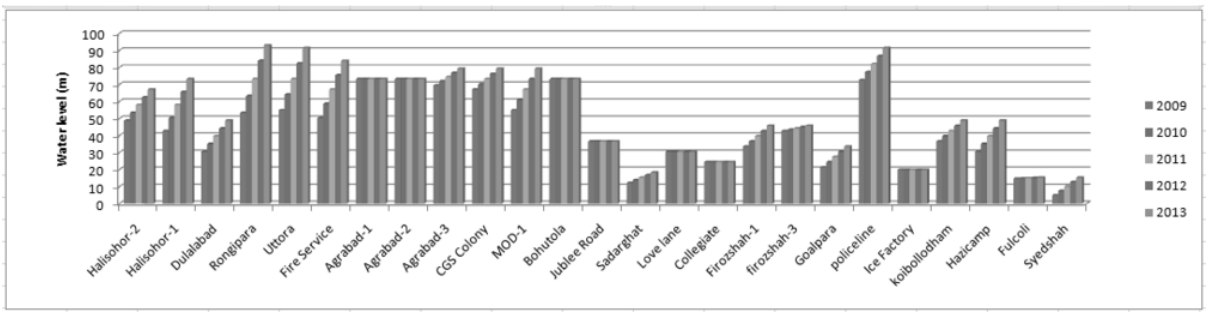

Figure 2 b: Locationwise water level variation

Geographic Information System (GIS). GIS technology is effective spatial tools widely used for the prediction, monitoring, management, and visual representation of geographic information. Different interpolation methods were adopted for surface interpolation (Shalini, Pandey & Nathawat, 2012; Gong, Mattevada & O'Bryant, 2014). Among them three methods of interpolation are widely use. The Inverse Distance Weighted (IDW) considers the concept

of spatial autocorrelation literally. This assumes that the unknown value of a point is influenced more by nearby control points than those further away. The nearer sample point provides information to the cell whose value is to be estimated, the more closely the cell's value will resemble the sample point's value. IDW performs reasonable with phenomena whose distribution depends on more complex sets of variables as this account only for the effects of distance. There is possibility to improve the accuracy of an IDW surface by using line layers as barriers. On elevation surfaces, barriers can represent abrupt changes in elevation, such as cliffs. Thin plate Splines creates surface that passes through control points and has the least possible change in slope at all points (Franke, 1982). In other words, thin-plate splines fit the control points with a minimum-curvature surface. Spline interpolation method fits a flexible surface, as if it were stretching a rubber sheet across all the known point values. The Spline method of interpolation estimates unknown values by bending a surface through known values. An advantage of the Spline interpolator is that it can make estimates outside the range of input sample points (Shalini, Pandey & Nathawat, 2012). Kriging method of Interpolation was used in mapping global solar radiation over southern Spain global solar radiation over southern Spain (Alsamamra, Arias, Vázquez & Pescador, 2009), estimating groundwater arsenic concentrations in Texas (Gong, Mattevada & O'Bryant, 2014), mapping liquefaction potential over alluvial ground (Pokhrel, Kuwano & Tachibana, 2013). In this study, the sum of least squares method under the time series regression analysis was used to compute groundwater level trend. Then Kriging method was used in GIS for interpolation of data and visual representation (Figure 3).

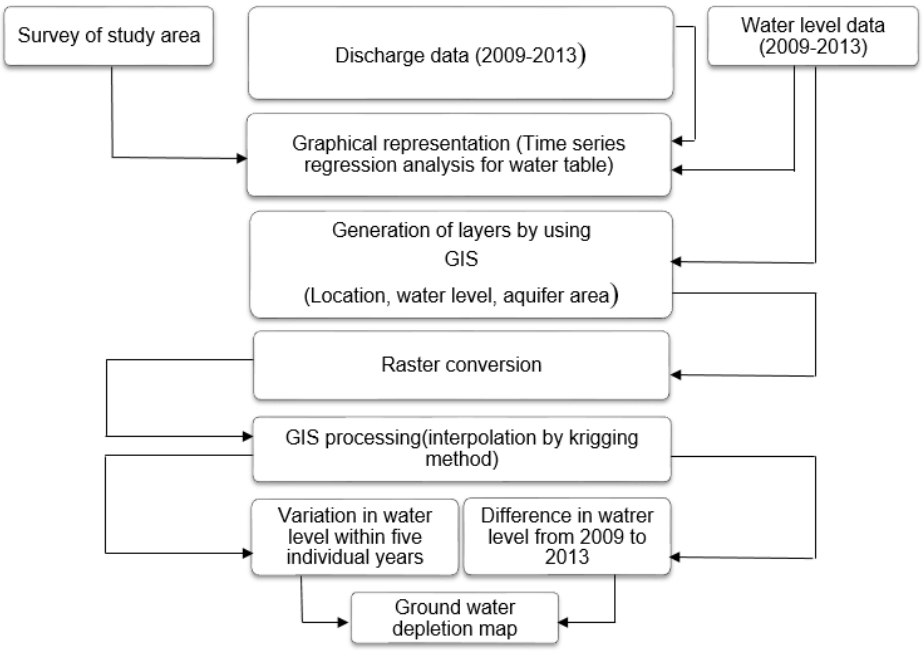

Figure 3: Adopted methodology

2.4 KRIGING

The basic idea of Kriging is to predict the value of a function at a given point by computing a weighted average of the known values of a function in the neighbourhood of the point. The method is mathematically closely related to regression analysis. Kriging refers to a family of least-square linear regression algorithms that attempts to predict values of a variable at locations of inadequate data. The description of kriging theory and its application are given in detail by Delhomme (1978). Ordinary kriging is the only technique that considers two sources of information regarding the attribute, the variation and the distance between points (Webster & Oliver, 2001; Alsamamra, Arias, Vázquez & Pescador, 2009). This is a single

method of incorporating characteristic irregular, small-scale variations into the construction of a contour map is to model the concentration field as a Spatial Random Field (SRF). The mathematics of SRFs is formidable. However, under certain simplifying assumptions, they produce classical linear estimators with very simple properties, allowing easy implementation for prediction purposes. These estimators, primarily ordinary kriging (OK), give both a prediction and a standard error of prediction at unsampled locations. This allows the construction of a map of both predicted values and level of uncertainty about the predicted values. Denote the SRF by Z(r), $r \in D \subset R^2$ .The following model for Z(r) is assumed:

$$Z(r) = \mu + \varepsilon(r) \quad (1)$$

Here, μ is the fixed, unknown mean of the process, and ε(r) is a zero mean SRF representing the variation around the mean. In most practical applications, an additional assumption is required in order to estimate the covariance C_z of the Z(r) process. This assumption is second-order stationarity:

$$C_2(r_1, r_2) = E[\varepsilon(r_1)\, \varepsilon(r_2)] = C_2(r_1 - r_2) \quad (2)$$

This requirement can be relaxed slightly when you are using the semivariogram instead of the covariance. In this case, second-order stationarity is required of the differences $\varepsilon(r_1) - \varepsilon(r_2)$ rather than ε(r) :

$$\gamma z(r_1, r_2) = 1/2E[\varepsilon(r_1) - \varepsilon(r_2)]^2 = \gamma z(r_1 - r_2) \quad (3)$$

By performing local kriging, the spatial processes represented by the previous equation for Z(r) are more general than they appear. In local kriging, at an unsampled location r_0, a separate model is fit using only data in a neighbourhood of r_0. This has the effect of fitting a separate mean μ at each point. Given the N measurements $Z(r_1)$, ... , $Z(r_N)$ at known locations r_1, ... ,r_N, you want to obtain an estimate $\hat{Z}$ of Z at an unsampled location r_0. When the following three requirements are imposed on the estimator $\hat{Z}$, the OK estimator is obtained.

(i) $\hat{Z}$ is linear in $Z(r_1), \ldots, Z(r_N)$.

(ii) $\hat{Z}$ is unbiased.

(ii)$\hat{Z}$ minimizes the mean-square prediction error. $E(Z(r_0) - \hat{Z}(r_0))^2$
Linearity requires the following form for $\hat{Z}$ (r0):

$$\hat{Z}(r_0) = \sum_{i=1}^{N} \lambda_i Z(r_i)$$

Applying the unbiasedness condition to the preceding equation yields

$$E\hat{Z}(r_0) = \mu \Rightarrow \mu = = \sum_{i=1}^{N} \lambda_i E Z(r_i) \Rightarrow$$

$$\sum_{i=1}^{N} \lambda_i \mu = \mu \Rightarrow \sum_{i=1}^{N} \lambda_i = 1 \quad (4)$$

Finally, the third condition requires a constrained linear optimization involving $\boldsymbol{\lambda}_1, \ldots, \boldsymbol{\lambda}_N$ and a Lagrange parameter 2m. This constrained linear optimization can be expressed in terms of the function $L(\boldsymbol{\lambda}_1, \ldots, \boldsymbol{\lambda}_N, m)$ given by

$$L = E(Z(r0) - \sum_{i=1}^{N} \lambda_i Z(r_i))^2 - 2m \sum_{i=1}^{N} \lambda_i - 1) \quad (5)$$

Define the N ×1 column vector by

$\boldsymbol{\lambda} = (\lambda_1, \ldots, N)^T$

and the (N+1) ×1 column vector $\boldsymbol{\lambda}_0$ by

$\boldsymbol{\lambda}_0 = (\lambda_1, \ldots, N, m)^T = \begin{pmatrix} \lambda \\ m \end{pmatrix}$

The optimization is performed by solving

$$\frac{\partial L}{\partial \boldsymbol{\lambda}_0} = 0$$

in terms of $\boldsymbol{\lambda}_1, \ldots, \boldsymbol{\lambda}_N$ and m.

The resulting matrix equation can be expressed in terms of either the covariance Cz(r) or semivariogram $\gamma_2(r)$. In terms of the covariance, the preceding equation results in the following matrix equation:

$C\boldsymbol{\lambda}_0 = C_0$

Using this solution for and m, the ordinary Kriging estimate at r_0 is
$\hat{Z}(r_0) = \boldsymbol{\lambda}_1 Z(r_1) + \ldots + \boldsymbol{\lambda}_N Z(r_N)$

with associated prediction error. Where c_0 is C_0 with the 1 in the last row removed, making it an N ×1 vector.

3. OUTCOMES

Kriging of groundwater levels was applied in this study. The measure of the degree of spatial dependence among the sampled known points is the semi variance that can be fitted with a mathematical function or a model such as spherical, circular, exponential, linear, and Gaussian. These three methods are applied in this study for interpolation and then the errors were calculated (Table 3). This is evident that water table is declining per year in selected areas (Figure 4 and Table 4). In this study adopted interpolation method worked based on the collected details from the CWASA during 2009 to 2013. This study conducted over 22 wells during 2009 to 2013, thus, the simulated water level lowering rate in the studied area was found as 0.12- 7.92 m reasonably matched with measure values.

Table 3: Comparison of interpolation errors

Interpolation methods	Values in meter	Actual value	Error (%)
IDW	50.3	50.29	0.02
Spline	50.14	50.29	-0.29
Kriging (Ordinary)	50.13	50.29	-0.3.

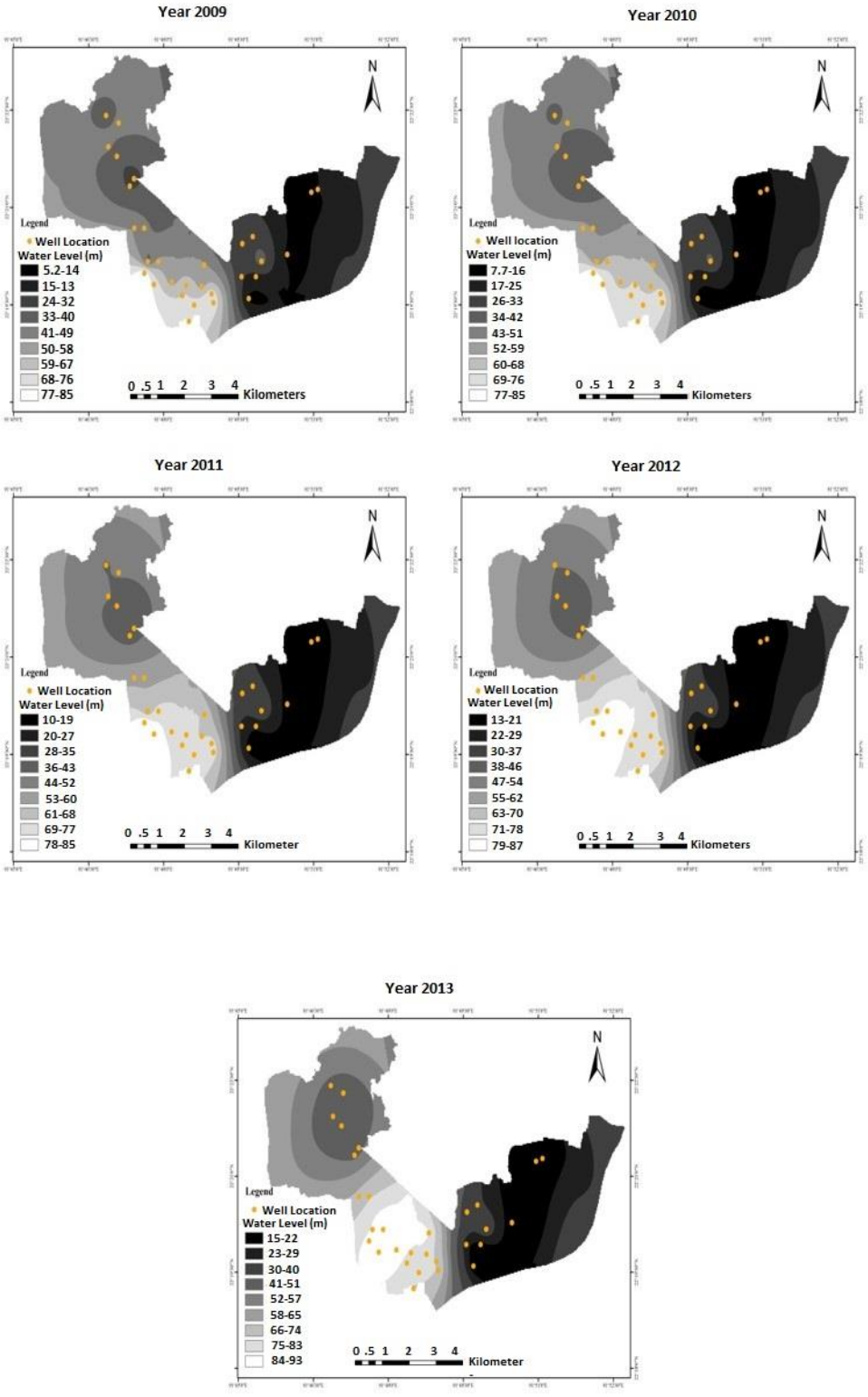

Figure 4: Map showing variation in water table in selected wells from 2009 to 2013.

Table 4: Water level declining rate in selected wells

Pump Name	Decline rate per year	Pump Name	Decline rate per year
Halisohor-2	3.656	**Sadarghat**	1.218
Halisohor-1	6.094	**Love lane**	0
Dulalabad	3.656	**Collegiate**	0
Rongipara	7.922	**Firozshah-1**	2.436
Uttora	7.312	**firozshah-3**	0.608
Fire Service	6.704	**Goalpara**	2.438
Agrabad-1	0	**policeline**	3.776
Agrabad-2	0	**Ice Factory**	0
Agrabad-3	1.948	**koibollodham**	2.436
CGS Colony	2.436	**Hazicamp**	3.656
MOD-1	4.874	**Fulcoli**	0.122
Bohutola	0	**Syedshah**	2.072
Jublee Road	0		

4. CONCLUSIONS

This study comprises of an interpolation method to predict ground watre lowering in the selected wells in Chittagong city. In this connection only few available wells were studied due to lack of observation information. The prediction showed on an average the lowering rate in the study area extends 0.12- 7.92 m to mimic the measured values.The prediction reasobly matches the observed data. With intensive field study, this is expected to provide reasonable information for the planners, policy makers, researchers to take necessary actions to ensure the optimum level of ground water table.

ACKNOWLEDGEMENTS

The authors would like to express their appreciation and gratitude to Chittagong Water Supply and Sewerage Authority, for their kind help. Humble gratitude expressed to Muhammad Shahabuddin, CWASA, Bangladesh, for his support by providing useful documents.

REFERENCES

Alsamamra H., Arias-R J. A., Vázquez D. P., Pescador J.T., (2009). A comparative study of ordinary and residual kriging techniques for mapping global solar radiation over southern Spain. *Agricultural and Forest Meteorology*, Volume 149, Issue 8, Pages 1343-1357.

Adhikary S. K, Chaki T, Rahman M. M and Gupta A D. (2012). Estimating groundwater recharge into a shallow unconfined aquifer in Bangladesh. *Journal of Engineering Science* 04(1), 2013 11-22

Chittagong water supply and sewerage authority (CWASA), (2014). Emergency Water Supply &DTW Rehabilitation Project.Hydrogeological Report.Institute of water modeling.

Delhomme, J.P., (1978). Kriging in the hydrosciences. Adv. Water Resource 1, 251– 266.

Franke, R. (1982). Smooth Interpolation of Scattered Data by Local Thin Plate Splines. Computers and Mathematics with Applications 8: 273-281.

Ganapuram, S., Kumar, G. T. V., Krishna, I. V. M., Kahya, E. & DemireL, M. C. (2009). Mapping of groundwater potential zones in the Musi basin using remote sensing data and GIS. *Advances in Engineering Software,* 40**,** 506-518.

Gong G, Mattevada S, O'Bryant S. E. (2014). Comparison of the accuracy of kriging and IDW interpolations in estimating groundwater arsenic concentrations in Texas. Environmental Research 130 59–69.

H. M. RAGHUNATH. Ground Water, 2nd Edition.

Helsel D.R. & Hirsch R.M. (2002). Statistical Methods in Water Resources U.S. Geological Survey. Chapter 2. Graphical Data Analysis.

Hossain S., Bashar K & Ahmed N. (2008). An Approach to Hydrological Zonation: A case Study for the Chittagong City. *Bangladesh Geoscience journal*, VOL. 14, P. 33-35.

Lee, S., Kim, Y.-S. & Oh, H.-J. (2012). Application of a weights-of-evidence method and GIS to regional groundwater productivity potential mapping. *Journal of Environmental Management,* 96**,** 91-105.

Magesh, N. S., Chandrasekar, N. & Soundranayagam, J. P. (2012). Delineation of groundwater potential zones in Theni district, Tamil Nadu, using remote sensing, GIS and MIF techniques. *Geoscience Frontiers,* 3**,** 189-196.

McGuire V.L., Lund K. D., & Densmore B. K. (2009). Saturated Thickness and Water in Storage in the High Plains Aquifer and Water-Level Changes and Changes in Water in Storage in the High Plains Aquifer, 1980 to 1995, 1995 to 2000, 2000 to 2005, and 2005 to 2009.

Nampak, H., Pradhan, B. & Manap, M. A. (2014). Application of GIS based data driven evidential belief function model to predict groundwater potential zonation. *Journal of Hydrology,* 513**,** 283-300.

Nuri K. (1988) The Estimation of Groundwater Recharge From Water Level and Precipitation Data. *Journal of Islamic Academy of Sciences*, 1:2, 87-93.

Oh, H.-J., Kim, Y.-S., Choi, J.-K., Park, E. & Lee, S. (2011). GIS mapping of regional probabilistic groundwater potential in the area of Pohang City, Korea. *Journal of Hydrology,* 399**,** 158-172.

Pokhrel R. M, Kuwano J, Tachibana S. (2013). A kriging method of interpolation used to map liquefaction potential over alluvial ground. Engineering Geology. Volume 152, Issue 1, 18 January 2013, Pages 26-37.

Shalini T. A. I, PandeyA.C. & Nathawat M.S. (2012). Groundwater Level and Rainfall Variability Trend analysis using GIS in parts of Jharkhand state (India) for Sustainable Management of Water Resources. *International Research Journal of Environment Sciences*, Vol. 1(4), 24-31.

Sarkar A.A. and Ali M.H., (2009). Water level dynamics of Dhaka city and its long-term trend analysis using the “MAKESENS” model, Water Int., 34(3), 373-382.

Webster, R., Oliver, M.A., (2001). Geostatistics for Environmental Scientist. John Wiley and Sons, Chichester, England, p. 149.

Proceedings of the 4th International Conference on Civil Engineering for Sustainable Development (ICCESD 2018), 9~11 February 2018, KUET, Khulna, Bangladesh (ISBN-978-984-34-3502-6)

HYDRO-MORPHOLOGICAL ASSESSMENT OF THE RIVER JAMUNA AND OLD DHALESHWARI OFFTAKE

Tasmiah Ahsan*[1] and M. A. Matin[2]

[1] *Lecturer, Department of Civil Engineering, Stamford University, Bangladesh, e-mail: tasmiahahsan@ymail.com*
[2] *Professor, Department of WRE, BUET, Bangladesh, e-mail: mamatin@wre.buet.ac.bd*

ABSTRACT

The offtakes are important links between the main rivers and the distributaries. An example is the Jamuna and Old Dhaleshwari offtake. The mouth of the river at offtake is not stable. At present, serious deposition has taken place at the mouth. This paper presents the hydro-morphological analysis of the Jamuna and Old Dhaleshwari offtake of Bangladesh to predict its sustainability. The present study has been undertaken to assess the hydraulic behavior of the Old Dhaleshwari River based on its flow carrying capacity. Satellite images, old maps and hydro-morphological data have been used to understand the morphology and planform of the river. From conveyance analysis rating curves have been developed for the cross sections in the vicinity of offtake for both Jamuna and Old Dhaleshwari. Analysis of historical hydrometric data and satellite images near the offtake has been carried out.

Keywords: *River offtake, River morphology, Rating curve, Conveyance analysis*

1. INTRODUCTION

The Old Dhaleshwari River is a distributary, 160 km long, of the Jamuna River in central Bangladesh. It starts off the Jamuna near the northwestern tip of Tangail District (BWDB, 2011).

The distribution of discharge and sediment transport at river offtake is a key factor for the long term morphological development of the main rivers (FAP24, 1996a). The dynamics of such offtakes have undoubtedly been of great significance during channel avulsion, such as: the occupation of the current Jamuna channel and Old Dhaleshwari channel. At present, serious deposition has taken place at the mouth, induced by intense char movement. The large discharges and heavy sediment loads carried by these rivers results in highly variable and dynamic channel morphologies characterized by rapid adjustments to the cross-sectional geometry, bankline positions and planform attributes (Noor, 2013).

The sediment transport distribution, in addition, may be influenced by the local planform and bathymetry at the offtake, which on the other hand are dependent on the planform and sediment transport conditions of the main river (FAP24, 1996a). A bar in front of the offtake may partly block the inflow to the distributary. For the development of the distributaries the offtakes are the crucial elements. At an offtake the flow and the sediment transport entering into the distributary are determined by the downstream conveyances, the local geometry of the offtake becomes less important. If more sediment is entering into the offtake than can be transported over a longer period, the distributary will start to aggraded. As a consequence less water is entering and hence this may start a self-accelerating process. It has been found that most offtakes are unstable: either the distributary start to die or gradually the distributary takes the function of the main river. They start to function only during higher stages. Any change in the stages in the main river will affect the flow (and sediment transport) entering into the distributary (Noor, 2013).

2. METHODOLOGY

Flow chart outlining the fundamental steps in the methodology is shown in Figure 1.

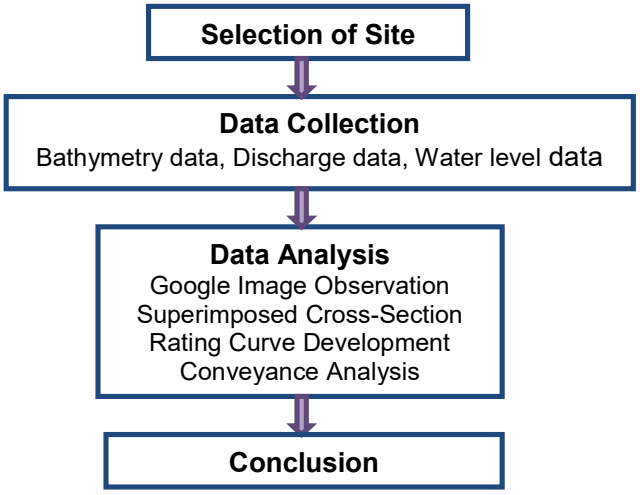

Figure 1: Fundamental steps of methodology

The study area in the Jamuna-Old Dhaleshwari offtake as shown in Figures 2 & 3. Data collected for cross-sections at the locations near offtake such as Tangail, Sirajganj, Manikganj. Data list is shown in Table 1.

Figure 2: Google Earth image of study area (Jamuna-Old Dhaleshwari Offtake)

Figure 3: Image of Jamuna-Old Dhaleshwari Offtake during 2016 (18th March)

Table 1: List of collected data (Source: BWDB)

Type of Data	Location	Station	Available Time Period
Bathymetry Data	Jamuna	RMJ 6.1 to RMJ 2	2005, 2006, 2008 & 2010 to 2014
	Old Dhaleshwari	RMD 1 to RMD 12	2003, 2008, 2013
Discharge Data	Jamuna	SW 46.9	2006 to 2014
	Old Dhaleshwari	SW 68.5	2006 to 2015
Water-level Data	Jamuna	SW 46.9	2006 to 2015
	Old Dhaleshwari	SW 50, SW68, SW68.5	2006 to 2014 (seasonal)

3. ANALYSIS

3.1 Present State of Old Dhaleshwari River

Due to the construction and associated river bank protection works of Jamuna Multipurpose Bridge on Jamuna River at Bangladesh, water flow through the Old Dhaleswari River was reduced significantly. The river remains usually dead during the dry season. The river feeds a little to its distributaries. As a result, the downstream rivers also remain dead at the dry season. Erosion of the river causes a great problem for the people surrounding the area. The actual river is lost for various man-made reasons. There are various industries near the banks of the river which dump untreated waste in the river. As a result, the river water quality is deteriorating day by day. Polluted water of Old Dhaleshwari is posing serious threats to public life as it is unfit for human use (Doza, 2013).

3.2 Morphological Analysis

3.2.1 Plan form analysis using satellite images

Satellite images of Old Dhaleshwari River for the years 2008, 2011, 2012, 2013 and 2016 have been extracted from the Google Earth. The years were chosen on the basis of availability of imagery. For the purpose of desk analyses, a reach from near the mouth to near Maddhapara is selected (Figure 4).

In order to analyze the plan form changes, bank line conditions are superimposed (Figure 5) for the above years. ArcGIS 10.2.2 software has been used for the purpose. The reach shows moderate bends.

Figure 4: Google Image of Old Dhaleshwari Planform

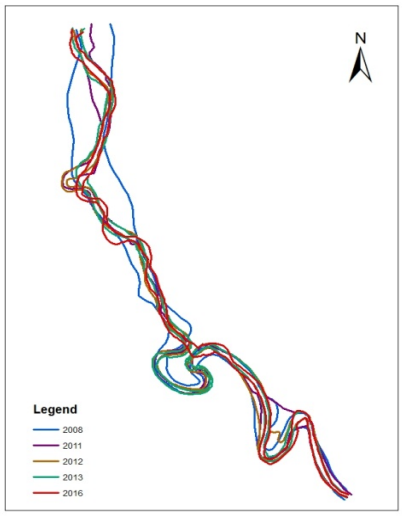

Figure 5: Superimposition of Old Dhaleshwari Planform of Selected Reach

3.2.2 Change in bed elevation

A change in bed elevation is, however, a useful indicator that channel characteristics are responding to a change in sediment load (Lisle, 1982). Superimposed cross-section plot shows aggradations and degradations over years. In case of Old Dhaleshwari River, main channel and bank has shifted greatly from 2003 to 2008. The channel has become narrower

but deeper. But the carrying capacity has decreased over years. It is evident from the Figures 6 & 7 that cross-section near the offtake has changed more than cross-section relatively far from the offtake.

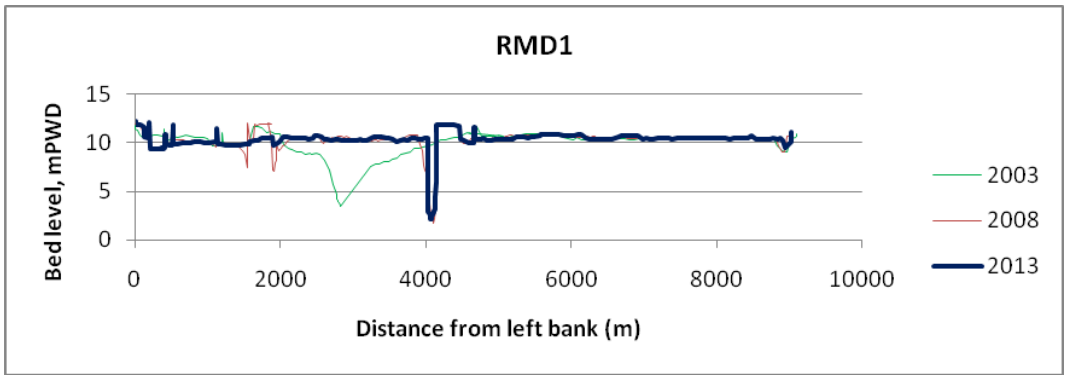

Figure 6: Superimposition of cross section near offtake (RMD1) in different years

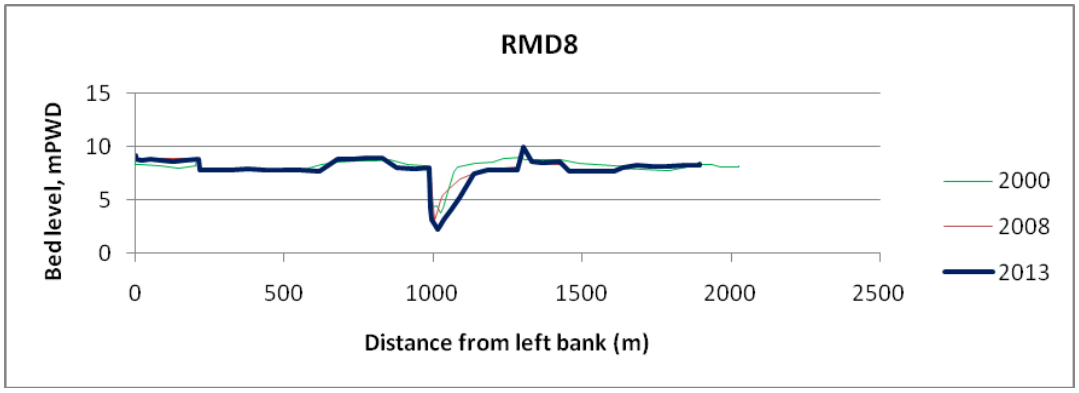

Figure 7: Superimposition of cross section relatively far from offtake (RMD8) in different years

3.3 Discharge and Water Level

Mean daily water level (MDWL) variation from year 2005 to 2015 at Tilli (SW68) of Old Dhaleshwari River is shown graphically in Figure 8. According to the Figure 9 water level is decreasing throughout the years in Old Dhaleshwari River.

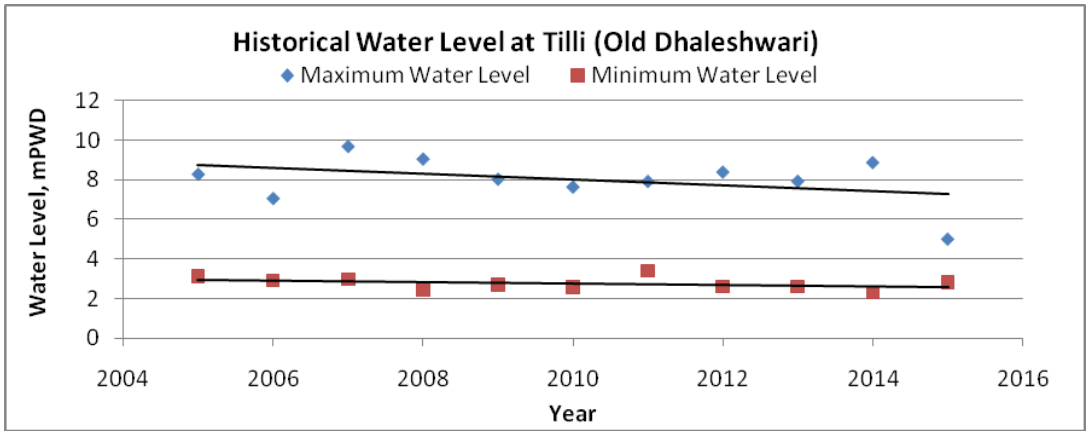

Figure 8: Maximum and Minimum MDWL variation from year 2005 to 2015 at Tilli

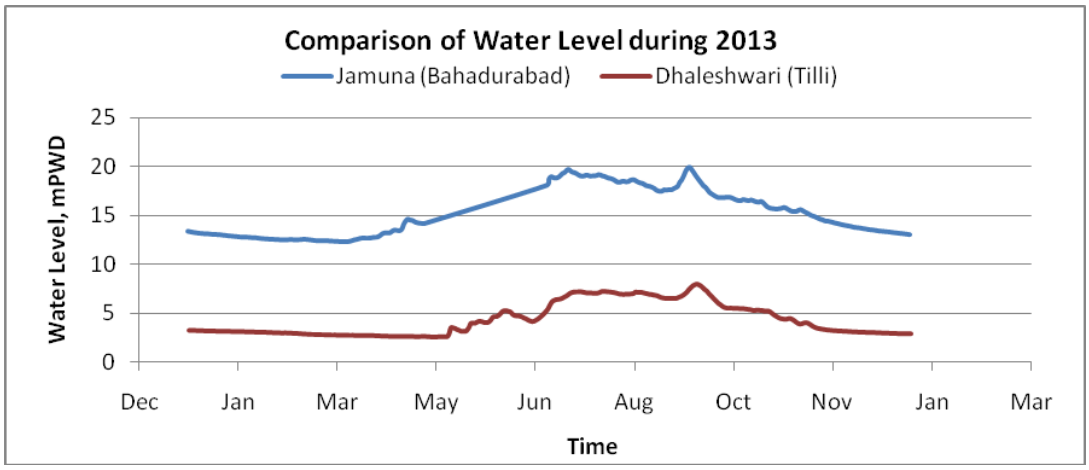

Figure 9: Comparison of Water Level at Jamuna and Old Dhaleshwari Rivers

3.4 Observations from Plotting of Mouth Sections of Jamuna-Old Dhaleshwari Offtake

The Old Dhaleshwari River starts off from a place between RMJ4 at upstream and RMJ4.1 at downstream of the Jamuna River. The flow continues through RMD1 and RMD2 of Old Dhaleshwari River near the mouth.

The cross-sectional area and depth of Old Dhaleshwari River is much less than that of Jamuna River. Figure 10 shows that the width of Old Dhaleshwari channel is very small compared to that of Jamuna. Hence the discharge carrying capacity is significantly low for Old Dhaleshwari River.

The dash lines in the figure indicate levels of water from datum. Water levels equal to 2m, 4m, 6m, 8m, 10m and 12m are shown in the figure. In case of lower water level such as 2m; the discharge cannot contribute to the Old Dhaleshwari channel. Old Dhaleshwari River will have no flow and will become dry. Though RMD2 has the elevation to permit flow even for this low water level case it won't be utilized. The bottom elevation of RMD1 cannot support the low flow.

The Highest water level such as 12m may cause flooding in Old Dhaleshwari River and areas adjacent to the river. The carrying capacity of Old Dhaleshwari River is not enough to accommodate this high level of flow.

The nearest cross-section to the offtake on Old Dhaleshwari River is RMD1. The next one is RMD2. RMD1 has its bottom elevation higher than RMD2. This elevation may be a sign of siltation near the offtake.

RMD1 has a smaller cross-section than RMD2. RMD1 also has its bottom elevation higher than the downstream section RMD2. Discharge from Jamuna River can only enter the Old Dhaleshwari river channel up to the highest capacity of RMD1. Larger cross sections present along the channel may not be utilized fully if the nearest section to mouth, RMD1 is not large enough.

RMJ4 at downstream of the offtake provides a larger cross-sectional area that that of RMD1. It increases the probability of less discharge entering the Old Dhaleshwari channel.

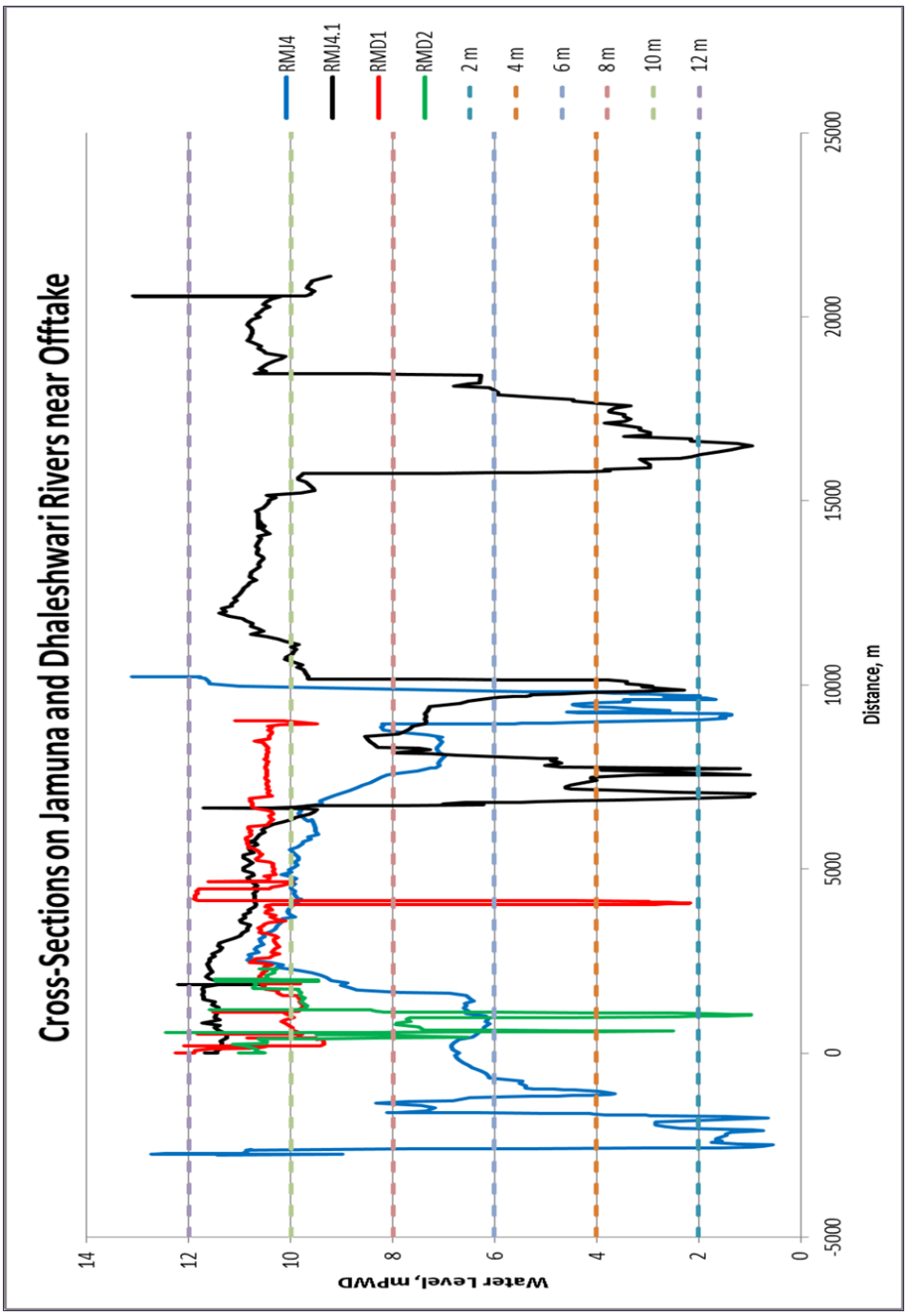

Figure 10: Cross-Sections of Jamuna River and Old Dhaleshwari River Near Offtake

4. DEVELOPMENT OF RATING CURVE

4.1 Using Collected Data

In hydrology, rating curve is a graph of discharge vs. stage (water level) for a given point/station on a stream/river, usually at gauging stations, where the stream discharge is measured across the stream channel with a flow meter/ADCP.

Rating curves have been developed for recent years for Bahadurabad station (SW 46.9) on Jamuna River (Figure 11) and Jagir station (SW 68.5) on Old Dhaleshwari River (Figure 12).

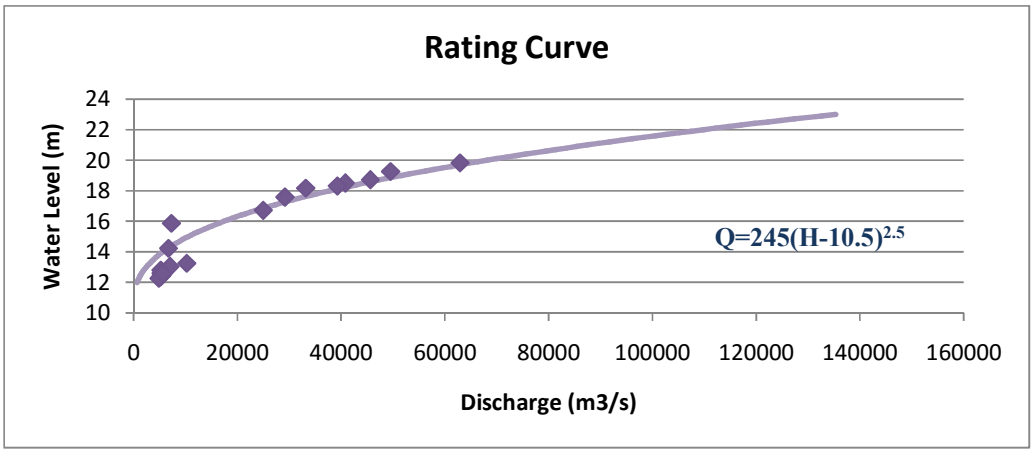

Figure 11: Rating curve for Bahadurabad Station on Jamuna River

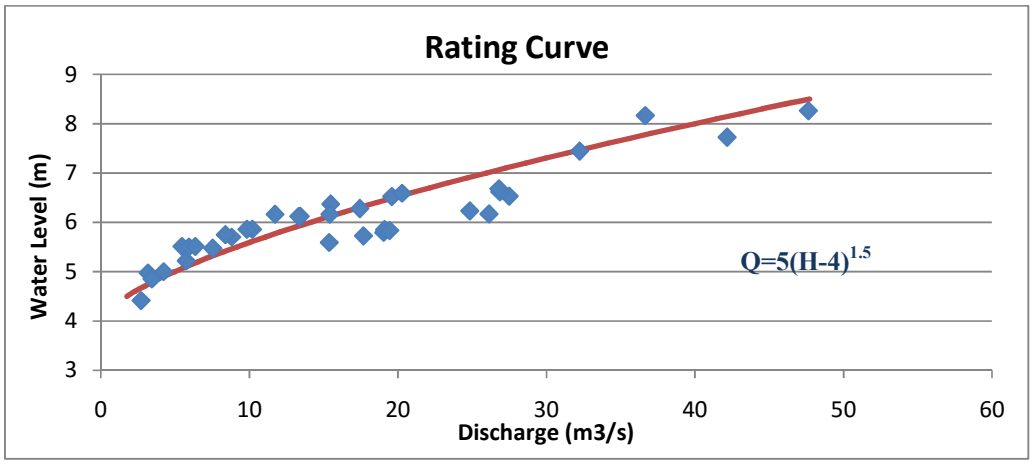

Figure 12: Rating curve for Jagir Station on Old Dhaleshwari River

4.2 Using Conveyance Analysis

Conveyance, $K = (AR^{2/3})/n$ where n is Manning's roughness coefficient. The discharge becomes $Q = K\sqrt{S}$. The Manning's roughness value of 0.025 and 0.018 is assumed for Jamuna and Dhaleshwari Rivers respectively from previous studies (Islam, 2016). Area and perimeter for the section near offtake on Jamuna River and Old Dhaleshwari River are computed by AutoCAD.

For computing the slope of the channel thalweg for both Jamuna River and Old Dhaleshwari River are plotted as shown in Figures 13 & 14 respectively. The trendline of the plot gives a close value for the slope of the channel. The longitudinal slope for Jamuna River is assessed to be 0.00015 m/m and 0.00004 m/m for Old Dhaleshwari River. The slope of the Old Dhaleshwari River is milder than that of the Jamuna River. Less discharge enters the Old Dhaleshwari River due to the slope disadvantage. Rating curves developed from conveyance analysis are compared in Figure 15 and obtained equations for the curves are shown in Table 2..

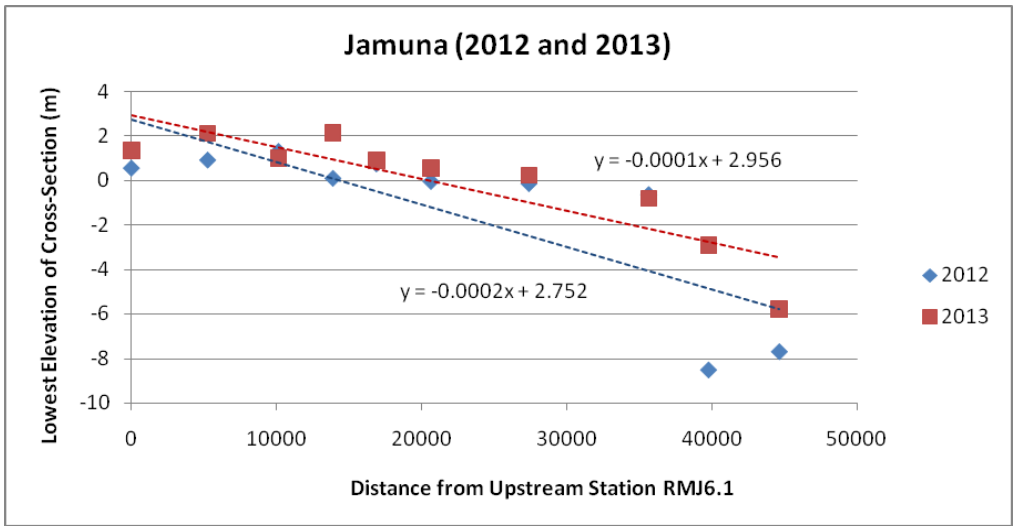

Figure 13: Thalweg from Station RMJ6.1 to Station RMJ2 on Jamuna River (2012 & 2013)

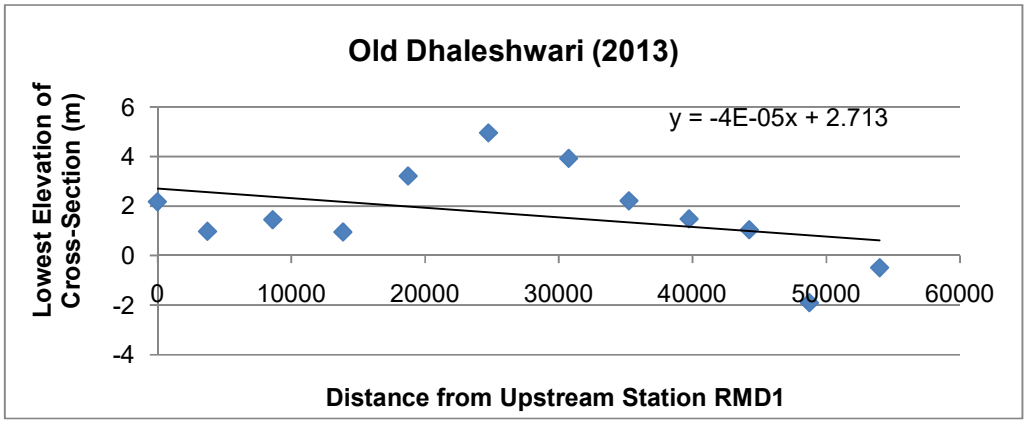

Figure 14: Thalweg from Station RMD1 to Station RMD12 on Old Dhaleshwari River (2013)

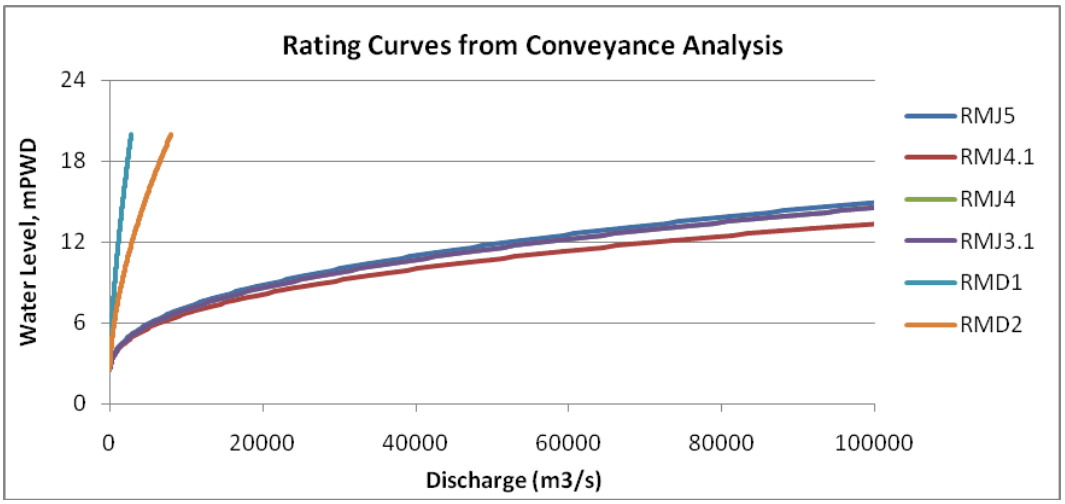

Figure 15: Comparison of Rating Curves Using Conveyance Analysis for Jamuna (RMJ5, RMJ4.1, RMJ4, RMJ3.1) and Old Dhaleshwari (RMD1, RMD2) Rivers

Table 2: Obtained equations of rating curve from conveyance analysis

Section	Equation for Rating Curve
RMJ5	$Q=166(H-2)^{2.5}$
RMJ4.1	$Q=180(H-2)^{2.6}$
RMJ4	$Q=180(H-2)^{2.5}$
RMJ3.1	$Q=180(H-2)^{2.5}$
RMD1	$Q=35(H-2)^{1.52}$
RMD2	$Q=56(H-2)^{1.72}$

5. CONCLUSIONS

The analysis includes planform analyses by using Google Earth image, superimposition of cross-sections, development of rating curves and conveyance analysis. Analysis of primary data shows that there is no flow in the Old Dhaleshwari River during dry period. The minimum depth of the river is about 1.0m which is almost static. The upper reach of the river has lower velocity compared to the lower part of the river reach. Therefore, the upper reach will face more siltation problem. It reveals that sedimentation has been occurring which leads to formation of sand bars. Prominent bank shifting is evident from the planform analysis. Natural cutoff has developed in recent years. From conveyance analysis rating curves have been developed for the cross sections in the vicinity of offtake for both Jamuna and Old Dhaleshwari. For the Old Dhaleshwari maximum discharge is obtained as 900 m^3/s and minimum discharge is obtained as 80 m^3/s (for Least Available Depth=1.5m) for cross section no.1 of Old Dhaleshwari that is RMD1. In reality the flow in Old Dhaleshwari River is not justified to ots full capacity. The developed rating curves also show the same. The assessments are made to define the boundary condition for setting up a HEC-RAC 4.1.0 model for the Old Dhaleswari River. The scope of further improvement remains for detailed analysis.

REFERENCES

BWDB. (2011). *Rivers of Bangladesh; North-Central Zone*. Bangladesh Water Development Board, Dhaka, Bangladesh.

Doza, B. (2013). *State of the Dhaleswari River*. Retrieved from https://www.scribd.com/document/234961350/State-of-Dhaleswari-River

FAP24. (1996a). *River Survey Project, Morphological Process of Jamuna River*. Special Report 24, GoB/FPCO, Prepared for Water Resources Planning Organization, Dhaka, Bangladesh.

Islam, M. R. (2016). *Hydrodynamic Modeling of Old Dhaleshwari River for Dry Period Flow Augmentation* (Bachelor's thesis). WRE, Bangladesh University of Engineering and Technology, Dhaka, Bangladesh.

Lisle, T. E. (1982). *Effects of Aggradations and Degradations on Riffle-Pool Morphology in Natural Gravel Channels, Northwester California*, 18(6), 1643-1651.
doi:10.1029/WR018i006p01643

Noor, F. (2013). *Morphological Study of Old Brahmaputra Offtake Using 2D Mathematical Model* (Master's thesis). WRE, Bangladesh University of Engineering and Technology, Dhaka, Bangladesh.